
**An investigation into the development of an advanced
ship performance monitoring and analysis system**

Thijs Willem Frederik Hasselaar

A thesis submitted for the degree of Doctor of Philosophy (Ph.D) at Newcastle University



December 2010

School of Marine Science and Technology
Faculty of Science, Agriculture and Engineering
Newcastle University
Newcastle upon Tyne, UK

ABSTRACT

The complete ban on TBT in marine antifouling coatings in 2008, rocketing fuel prices over the past six years, environmental concern and upcoming energy efficiency indices for ships have resulted in a strong interest of the shipping industry to monitor, evaluate and optimise ship performance. Furthermore, the complete ban on TBT in anti-fouling coatings resulted in new types of foul-release hull-coatings, based on silicon, whose effectiveness and performance still needs to be evaluated. Because of the difficulty of measuring coating roughness in service and the large effect of marine bio-fouling on ship performance, a research project was setup at Newcastle University in collaboration with a major paint company to investigate the ways to evaluate hull coating through ship performance monitoring.

This thesis describes the details of this project which aimed to investigate the feasibility of a real-time ship performance monitoring and analysis (PM&A) system by implementation and evaluation onboard a 16m research vessel and 300.000dwt VLCC. The thesis starts with a review of the state of art of PM&A systems. The main weaknesses of existing PM&A systems is that often abstract logbook data is used as input and that too little attention is paid to data quality. Furthermore, the systems often act as a black box, showing little insight in data analysis, harming the reliability and trustworthiness of output indicators. Additionally, there are large differences in the way that performance data is corrected to standard conditions, resulting in contradicting and unreliable performance indicators. The thesis focuses therefore on theoretically sound, transparent data analysis and improved data collection. In the thesis, all performance affecting environmental and operational conditions have been reviewed including sensor characteristics and data acquisition aspects. Based on the experience from the analysis of the data collected from both vessels, it reveals that automatic, real-time data collection and rational filtering for periods of acceleration, deceleration, course deviation, drift, shallow water and ship motion is the way forward for accurate performance monitoring.

Performance analysis is highly sensitive to errors in shaft torque and ship speed through water. A frequently calibrated/validated shaft torque & RPM sensor and Doppler speed log are therefore the most important sensors for performance monitoring. Speed logs are

affected by many environmental conditions and cannot be used directly for performance monitoring. Other ways to determine ship speed through water, e.g. using the propeller inflow speed, are however affected by hull fouling and loading deviations unless corrected for accordingly. Corrections using full scale trials are then necessary to avoid overestimation of the effects of hull fouling on ship performance. To avoid these errors, a method is described to use the speed log by evaluating its reliability and utilise its reading for performance analysis only in periods where it can be considered reliable.

A new transparent analysis method is described to analyse ship performance based on conversion of torque and rpm at constant ship speed. The method differentiates between the hull and propeller performance by empirically correcting the propeller open water diagram for roughness (periodically measured by divers). Evaluation of the proposed PM&A system on both vessels indicates that reliable performance indicators can be calculated but that fluctuations in performance indicators of $\pm 12\%$ remain unavoidable due to inaccurate wave observations and errors from the speed log. Trials on the research vessel furthermore show that the system is able to identify fouling, but sensor accuracy requires further research so that fouling can be defined with less performance data and higher reliability. This thesis demonstrates for the first time in open literature that the design and implementation of a transparent and fully automatic, real-time, shipboard PM&A system is perfectly viable and can be installed on any ship with the use of reliable sensors.

ACKNOWLEDGEMENTS

The work behind this thesis was carried out at Newcastle University over the period 2005 – 2010. During this period, I was fortunate to receive support from a great number of people. The first word of appreciation goes to my supervisors Ehsan Mesbahi and Mehmet Atlar, who provided the encouragement, discussion, and support when needed.

The installation of the performance monitoring system onboard the *RV Bernicia*, on which much of the fundamental research was done, could not be succeeded without the help and support of the entire crew, in particular Alistair Simpson, for who I am ever so thankful. OSG Ship Management provided the opportunity to develop and evaluate a performance monitoring onboard the *MT Overseas Tanabe*, and I would like to thank them for their support.

Without the funding and support from International Paint, this project would not be possible in the first place. My special thanks goes out to Dr. Colin Anderson, who provided invaluable information of real-life problems of performance analysis in industry. Furthermore, my gratitude goes out to Dimitrios Gaganatsios who executed model tests for the validation of wave resistance predictions on the *Bernicia*. Also, I would like to thank Henk van den Boom for giving me flexibility towards me needing time to finish my thesis while working at MARIN.

Last but not least, I would like to thank my friends and family for their support and encouragement over the past five years.

TABLE OF CONTENTS

ABSTRACT	I
ACKNOWLEDGEMENTS	III
TABLE OF CONTENTS	IV
LIST OF TABLES	VIII
LIST OF FIGURES	IX
NOMENCLATURE	XIII
1 INTRODUCTION	1
1.1 OVERVIEW	1
1.2 BACKGROUND.....	2
1.2.1 <i>Economical drivers for performance monitoring</i>	2
1.2.2 <i>Environmental regulations and directives</i>	4
1.2.3 <i>TBT ban & fouling</i>	6
1.3 SHIP PERFORMANCE ASSESSMENT	9
1.4 BENEFITS OF PERFORMANCE MONITORING.....	11
1.5 MOTIVATION OF THESIS	13
1.6 AIM AND OBJECTIVES OF THE THESIS	15
1.7 THESIS LAYOUT.....	16
1.8 SUMMARY	18
2 STATE OF ART OF PERFORMANCE MONITORING AND ANALYSIS	19
2.1 INTRODUCTION.....	19
2.2 DATA COLLECTION METHODS.....	20
2.2.1 <i>Manual data logging</i>	20
2.2.2 <i>Automatic data logging</i>	22
2.2.3 <i>State of art of data logging</i>	24
2.3 PERFORMANCE ANALYSIS METHODS.....	25
2.3.1 <i>Trend analysis</i>	25
2.3.2 <i>Statistical analysis</i>	31
2.3.3 <i>Deterministic performance analysis</i>	32

2.3.4	<i>System identification</i>	41
2.3.5	<i>Selection of analysis method</i>	42
2.4	PERFORMANCE INDICATORS.....	43
2.4.1	<i>KPIs based on fuel consumption versus time</i>	45
2.4.2	<i>KPIs based on ship speed against time</i>	50
2.4.3	<i>KPIs based on RPM or power against time</i>	51
2.4.4	<i>KPIs based on ship or engine characteristics</i>	52
2.4.5	<i>Other KPIs</i>	55
2.5	CONCLUSIONS	56
3	DATA DESCRIPTION	58
3.1	INTRODUCTION.....	58
3.2	SHIP'S ENVIRONMENT.....	59
3.2.1	<i>Waves</i>	59
3.2.2	<i>Current</i>	62
3.2.3	<i>Atmosphere</i>	63
3.2.4	<i>Water density and viscosity</i>	65
3.2.5	<i>Fouling</i>	67
3.2.6	<i>Local conclusions regarding ship environment</i>	71
3.3	SHIP BEHAVIOUR IN SERVICE CONDITIONS	71
3.3.1	<i>Manoeuvring</i>	71
3.3.2	<i>Acceleration</i>	72
3.3.3	<i>Wake fraction</i>	73
3.3.4	<i>Thrust deduction fraction</i>	76
3.3.5	<i>Propeller characteristics</i>	77
3.3.6	<i>Draft, trim and Squat</i>	83
3.3.7	<i>Shallow water effects</i>	86
3.3.8	<i>Seakeeping characteristics</i>	87
3.3.9	<i>Windage, yawing and rudder resistance</i>	88
3.3.10	<i>Engine performance</i>	89
3.3.11	<i>Local conclusions regarding data acquisition requirements</i>	92
3.4	SENSORS AND MEASUREMENT CHARACTERISTICS	94
3.4.1	<i>Ship speed</i>	94

3.4.2	<i>Shaft torque</i>	113
3.4.3	<i>Fuel consumption and LCV</i>	117
3.4.4	<i>Shaft revolutions</i>	120
3.4.5	<i>Course & Heading</i>	120
3.4.6	<i>Draft and trim</i>	121
3.4.7	<i>Wind speed and direction</i>	121
3.4.8	<i>Air density</i>	124
3.4.9	<i>Wave characteristics</i>	125
3.4.10	<i>Water depth</i>	130
3.4.11	<i>Water density and viscosity</i>	131
3.4.12	<i>Ship motion</i>	131
3.4.13	<i>Rudder angle</i>	131
3.4.14	<i>Thrust</i>	132
3.4.15	<i>Propeller roughness</i>	134
3.5	DATA CONDITIONING.....	138
3.5.1	<i>Identification of outliers</i>	138
3.5.2	<i>Transients filter</i>	139
3.5.3	<i>Smoothing</i>	142
3.5.4	<i>Data conditioning system design</i>	143
3.6	CONCLUSIONS	145
4	MODELLING OF PERFORMANCE ANALYSIS SYSTEM	148
4.1	INTRODUCTION.....	148
4.2	CORRECTION METHODOLOGY.....	150
4.2.1	<i>Mathematical model for correction to standard conditions</i>	150
4.2.2	<i>Effect of propeller roughness</i>	155
4.2.3	<i>Wake calibration for hull fouling</i>	156
4.2.4	<i>Wind resistance</i>	157
4.2.5	<i>Added wave resistance</i>	162
4.2.6	<i>Shallow water resistance</i>	163
4.2.7	<i>Frictional resistance due to viscosity variations</i>	163
4.2.8	<i>Changes in draft and trim</i>	164
4.3	PERFORMANCE INDICATORS.....	166

4.3.1	<i>Real-time performance indicators</i>	167
4.3.2	<i>Semi real-time performance indicator</i>	168
4.3.3	<i>Long-term condition monitoring indicators</i>	171
4.4	SENSITIVITY ANALYSIS	174
4.5	PERFORMANCE MONITORING SYSTEM STRUCTURE	182
4.6	CONCLUSIONS	189
5	SYSTEM EVALUATION.....	191
5.1	INTRODUCTION.....	191
5.2	PM&A SYSTEM IMPLEMENTATION ONBOARD RV BERNICIA	192
5.2.1	<i>Vessel characteristics</i>	192
5.2.2	<i>Installation of sensors & data acquisition system</i>	194
5.2.3	<i>PM&A software and User Interface</i>	198
5.2.4	<i>Data collection</i>	204
5.2.5	<i>Data conditioning</i>	208
5.2.6	<i>Data analysis</i>	218
5.2.7	<i>Concluding remarks of PM&A on Bernicia</i>	228
5.3	PM&A SYSTEM IMPLEMENTATION ONBOARD MT OVERSEAS TANABE.....	230
5.3.1	<i>Vessel characteristics</i>	230
5.3.2	<i>Installation of sensors & data acquisition system</i>	231
5.3.3	<i>PM&A software and User Interface</i>	234
5.3.4	<i>Data collection</i>	240
5.3.5	<i>Data conditioning</i>	247
5.3.6	<i>Data analysis</i>	253
5.3.7	<i>Concluding remarks on PM&A on Overseas Tanabe</i>	263
5.4	CONCLUSIONS	265
6	CONCLUSIONS & RECOMMENDATIONS.....	267
6.1	INTRODUCTION.....	267
6.2	REVIEW OF THESIS	267
6.3	MAIN CONCLUSIONS	273
6.4	RECOMMENDATIONS FOR FUTURE WORK	275
	REFERENCES	277

LIST OF TABLES

Table 1.1: Definition of standard conditions	11
Table 2.1: VDR & SVDR requirements	23
Table 2.2: Frequently used Key Performance Indicators for ship performance	44
Table 3.1: Factors influencing sinkage and dynamic trim	85
Table 3.2: Speed log characteristics	99
Table 3.3: Douglas Sea scale	127
Table 3.4: Douglas Swell scale	127
Table 3.5: Musker's characteristic roughness measure of Rubert Gauge surface.....	137
Table 3.6: Weights for calculating Average Propeller Roughness APR	137
Table 3.7: Parameters required for ship performance monitoring	147
Table 4.1: Sensitivity and uncertainty analysis for the Bernicia.....	178
Table 4.2: Sensitivity analysis for the Bernicia for Method 1 and Method 2 ^{GPD}	179
Table 4.3: Sensitivity and uncertainty analysis for a container vessel at 21.6kn	180
Table 4.4: Sensitivity and uncertainty analysis for a laden VLCC at 15.7kn	181
Table 5.1: Main particulars RV Bernicia.....	192
Table 5.2: Main particulars MT Overseas Tanabe	230
Table 5.3: Sensitivity analysis wake fraction calculation for the Overseas Tanabe.....	253
Table 5.4: Draft correction factors	254
Table A-1: Variables required for PM&A, in order of importance.....	296
Table B-1: Description of performance logs 'Raw data XXX.xls'	299
Table B-2: Description of performance logs 'Data in Units XXX.xls'	300
Table C-1: Description performance logs 'Raw data XXX.xls'	313

LIST OF FIGURES

Figure 1.1: Inflation adjusted crude oil prices 1946 – 2009	3
Figure 1.2: Laser profilogram of a SPC (left) and foul-release coated plate (right)	8
Figure 1.3: Sankey diagram for a container vessel at 24 knots.....	9
Figure 2.1: Example abstract deck log of an LNG tanker	20
Figure 2.2: Admiralty coefficient, RPM loss and ship speed through water	27
Figure 2.3: Fuel flow vs. ship speed for a 74.000dwt container ship	30
Figure 2.4: Generalised Power Diagram relating power, ship speed, RPM and slip	33
Figure 2.5: Differences in correction of ship performance of two methods	40
Figure 2.6: Specific fuel consumption vs. Engine load.....	46
Figure 2.7: Performance curves with constant SFC curves	47
Figure 2.8: Increase in SFC with increase in propeller roughness	48
Figure 2.9: Empirical relationship between hull roughness, power & SFC	49
Figure 3.1: Three typical North Atlantic sea spectra.....	60
Figure 3.2: Ocean current profile for wave buoy station 42014	63
Figure 3.3: Wind gradients for strong (n = 10) and light winds (n = 5) at open seas.....	64
Figure 3.4: Relationship between temperature, salinity and density at atmospheric pressure.....	66
Figure 3.5: Potential density ($\rho - 1000 \text{ kg/m}^3$) at 10m	66
Figure 3.6: Slime on Bernicia	69
Figure 3.7: Weed fouling on a rough hull.....	69
Figure 3.8: Barnacles on Overseas Tanabe.....	70
Figure 3.9: Severe weed & shell fouling	70
Figure 3.10: Torque and rpm during acceleration of a laden 300.000t VLCC	73
Figure 3.11: Propeller characteristics in still water with varying propeller immersion.....	78
Figure 3.12: Propeller open water tests for with different propeller blade roughness.....	81
Figure 3.13: Speed-power curves for a 2400TEU container vessel	84
Figure 3.14: Ship speed velocity vectors.....	95
Figure 3.15: Doppler log switching from water track to bottom track.....	101
Figure 3.16: 24h Performance log of the Overseas Tanabe in deep water	102
Figure 3.17: 24h Performance log of the Overseas Tanabe in deep water	103
Figure 3.18: Open water diagram with sea trial performance data from the Bernicia	107
Figure 3.19: Definition of wake fraction using open water diagram.....	110
Figure 3.20: Effect of propeller roughness on the definition of wake fraction	110
Figure 3.21: Principal components of a shaft torque sensor	115

Figure 3.22: The general flow pattern above the bridge of a generic tanker/bulk carrier.....	122
Figure 3.23: Airflow distortion over the stern of a typical tanker.....	123
Figure 3.24: Wind speed and significant wave height relationship.....	126
Figure 3.25: Example of a wave record.....	128
Figure 3.26: Nautical radar image, showing back scatter from surface waves.....	130
Figure 3.27: Full Wheatstone bridges for thrust and torque measurement.....	133
Figure 3.28: Rubert Propeller Roughness Comparator Scale.....	135
Figure 3.29: Propeller roughness measurement locations.....	136
Figure 3.30: Example of simplified transients filter on Bernicia.....	140
Figure 3.31: Identification of transients using RPM and torque.....	141
Figure 3.32: Data acquisition system for ship performance monitoring.....	143
Figure 3.33: Effect of transients filter and smoothing for sea trials on the Bernicia.....	144
Figure 4.1: Flow diagram of proposed ship performance correction methodology.....	151
Figure 4.2: Longitudinal wind force coefficient for tankers.....	160
Figure 4.3: Variation in bow configuration.....	161
Figure 4.4: Real-time performance indicator for direct feedback on ship operation.....	168
Figure 4.5: Example of a Semi-realtime performance indicator.....	170
Figure 4.6: Hull Roughness versus power loss for different types of roughness.....	172
Figure 4.7: Effects of a $\pm 2\%$ measurement error in shaft torque.....	175
Figure 4.8: Effects of a $\pm 2\%$ measurement error in shaft torque on $\Delta P_{D,corr}$	176
Figure 4.9: System architecture of the proposed PM&A system.....	184
Figure 4.10: Correction of ship performance to standard conditions.....	187
Figure 4.11: Effect of corrections to standard conditions.....	187
Figure 4.12: Histogram of the corrected and uncorrected ΔPD for a sea trial on the Bernicia....	188
Figure 5.1: General Arrangement and body plan of the RV Bernicia.....	193
Figure 5.2: Anemometer and wind vane of the Bernicia.....	195
Figure 5.3: DGPS receiver of the Bernicia.....	195
Figure 5.4: EM Speed log of the Bernicia.....	195
Figure 5.5: Fuel flow sensor of the Bernicia.....	195
Figure 5.6: Rudder angle sensor of the Bernicia.....	195
Figure 5.7: Torque sensor of the Bernicia.....	195
Figure 5.8: Draft (pressure) sensor of the Bernicia.....	195
Figure 5.9: Echo sounder of the Bernicia.....	195
Figure 5.10: RPM sensor of the Bernicia.....	195
Figure 5.11: Centralised, tailor-made data acquisition system installed on the Bernicia.....	196
Figure 5.12: Software architecture of the PM&A system.....	198

Figure 5.13: Main user interface of the PM&A system on the Bernicia	199
Figure 5.14: ‘Serial data input’ interface.....	200
Figure 5.15: ‘Conversion to units’ interface for fuel flow.....	201
Figure 5.16: ‘Signal conditioning’ interface of apparent Wind	202
Figure 5.17: ‘Correction to standard conditions’ interface.....	203
Figure 5.18: Typical track of sea trials on the Bernicia.....	204
Figure 5.19: Conditioned dataset of ship speed during speed trials on Bernicia	206
Figure 5.20: Apparent and true wind speed & direction during speed trials	207
Figure 5.21: Transients filter user interface of PM&A system on Bernicia	210
Figure 5.22: Propeller open water diagrams for Bernicia.....	212
Figure 5.23: SOG and GPD speed calculated using different KQ curves	213
Figure 5.24: Measured torque coefficients of the Bernicia.....	214
Figure 5.25: Resistance – speed curve from model tests and calculations	215
Figure 5.26: Measured and computer modelled K_T – curves for Bercia	217
Figure 5.27: Above water profile of Bernicia and ship model RES0201BN.....	219
Figure 5.28: Corrected ship performance for 12 trials on the Bernicia	220
Figure 5.29: Slime fouling on the Bernicia in April 2007.	222
Figure 5.30: Slime fouling on starboard side of Bernicia.....	222
Figure 5.31: Slime on test patch no.6 starboard side.....	223
Figure 5.32: Speed trial results before and after hull cleaning	224
Figure 5.33: GPD- P_D relationship during trials while dragging loads	226
Figure 5.34: ΔP_D and $\Delta P_{D,corr}$ for trials while dragging loads.....	227
Figure 5.35: General arrangement MT Overseas Tanabe.....	231
Figure 5.36: (D)GPS receiver of Overseas Tanabe.....	233
Figure 5.37: Dual axis Doppler log indicator of Overseas Tanabe	233
Figure 5.38: Torque & RPM sensor on propeller shaft of Overseas Tanabe.....	233
Figure 5.39: Anemometer of Overseas Tanabe.....	233
Figure 5.40: Gear fuel flow sensor of Overseas Tanabe	233
Figure 5.41: Pneumatically operated draft indicators of Overseas Tanabe	233
Figure 5.42: Main user interface of the PM&A system on the Overseas Tanabe	235
Figure 5.43: ‘Serial data collection’ interface.....	236
Figure 5.44: ‘Torque data conditioning’ interface	237
Figure 5.45: Manual input of wave parameters user interface.....	238
Figure 5.46: Draft gauges on the Overseas Tanabe.....	239
Figure 5.47: ‘Ship’s Draft’ user interface.....	239
Figure 5.48: Torque measurement by means of angular deflection measurement.....	241

Figure 5.49: Torque sensor on the Overseas Tanabe	241
Figure 5.50: Damage on one of the forks of the torque sensor on the Overseas Tanabe	242
Figure 5.51: Torque and RPM recorded by the torque.....	243
Figure 5.52: Relative torque deviation from propeller design load curve versus time.....	244
Figure 5.53: Deviation of measured torque from Power - Fuel consumption relationship.....	245
Figure 5.54: Measured power and predicted power based on fuel consumption	246
Figure 5.55: Data conditioning for Overseas Tanabe.....	248
Figure 5.56: Example of STW filter on Overseas Tanabe performance data	250
Figure 5.57: Wake fraction as function of ship speed	251
Figure 5.58: Wake fraction as function of torque coefficient K_Q	251
Figure 5.59: Deviation in wake fraction before and after correction for propeller loading.....	252
Figure 5.60: Longitudinal wind force coefficient for Overseas Tanabe.....	255
Figure 5.61: Corrected and uncorrected ship performance for 106 data points	256
Figure 5.62: Corrected and uncorrected ship performance versus time	257
Figure 5.63: Corrected and uncorrected ship performance versus time	258
Figure 5.64: Sailing track Overseas Tanabe between 04-07 May 2008	259
Figure 5.65: Ship performance Overseas Tanabe while sailing along African coast.....	260
Figure B-1: Example of unconditioned and conditioned shaft torque.....	302
Figure B-2: Main interface panel of PM&A system Bernicia	303
Figure B-3: Example of source code PM&A system Bernicia	304
Figure B-4: Interface panels for data collection on PM&A system Bernicia	306
Figure B-5: Interface panels ‘conversion to units’ on PM&A system Bernicia	307
Figure B-6: Interface panels on PM&A system Bernicia	308
Figure B-7: Interface panels of data conditioning on PM&A system Bernicia	309
Figure B-8: Interface panels for data conditioning on PM&A Bernicia.....	310
Figure B-9: Interface panels for calculation of standard performance	311
Figure C-1: Data acquisitioning system installed on the bridge of the Overseas Tanabe	312
Figure C-2: Performance monitoring system on the bridge of the Overseas Tanabe.....	312
Figure C-3: Main interface panel of PM&A system Overseas Tanabe.....	315
Figure C-4: Interface panels for data collection on PM&A system Overseas Tanabe	316
Figure C-5: Interface panels for ‘data conditioning’ on PM&A system Overseas Tanabe	317
Figure C-6: Interface panels for ‘data conditioning’ on PM&A system Overseas Tanabe	318
Figure C-7: Interface panels for manual data entry on PM&A system Overseas Tanabe	319
Figure C-8: Interface panels for manual data entry on PM&A system Overseas Tanabe	320

NOMENCLATURE

Symbols

Roman

A_L, A_F	[m ²]	Lateral or Frontal projected above-water area of the ship
A_M	[m ²]	Midship section area
B	[m]	Hull width at shoulders
c	[m]	Section cord length at 0.7 of the propeller radius in meters
c_1, c_2, c_3	[-]	Polynomial regression coefficients
C_{DRAFT}	[-]	Draft power correction factor
C_F	[-]	Frictional resistance coefficient
C_R	[-]	Residuary resistance coefficient (wave and eddy resistance)
C_T	[-]	Total resistance coefficient
$C_{W-DRAFT}$	[-]	Wake fraction correction
C_X	[-]	Wind loading coefficient for longitudinal wind force
D	[m]	Propeller diameter, Distance of keel to deck
FC	[l/h]	the Fuel Consumption
Fn	[-]	Froude number
g	[ms ⁻²]	Acceleration due to gravity (9.81ms ⁻²)
h	[-]	Water depth
h'	[-]	Musker's roughness parameter
J	[-]	Propeller advance coefficient
k	[-]	Form factor from model tests
K_Q	[-]	Propeller torque coefficient
K_T	[-]	Propeller thrust coefficient
L	[m]	Ship length at water length
L_{pp}	[m]	Ship's length between perpendiculars
N, n	[min ⁻¹ ,sec ⁻¹], [-]	Propeller speed or rotation, wind gradient
p	[Pa]	Barometric pressure
P/D	[-]	Propeller Pitch to Diameter ratio
ΔP_D	[-]	Relative power loss at constant speed
$\Delta P_{D,corr}$	[-]	Relative power loss at constant speed, corrected to standard conditions
Q	[Nm]	Propeller shaft torque

q	[L/h]	Measured fuel flow
Q_{loss}	[Nm]	Propeller shaft torque losses
\dot{Q}	[kg/h]	Corrected fuel flow
R	[N], [m]	Resistance, propeller radius
R_{ADD}	[N]	Added resistance components from wind, wave, shallow water, viscosity and draft deviations
Re	[-]	Reynolds number
R_F	[N]	Frictional resistance
R_{SFC}	[-]	Specific fuel consumption ratio
R_{std}	[N]	Resistance corrected to ‘standard conditions’
S	[m ²]	Wetted surface area of the hull
T	[N], [degC]	Propeller thrust, Temperature, Dry-air temperature in Kelvin
t	[-]	Thrust deduction fraction
T_O	[m]	Propeller immersion depth; propeller centre to water level
$\bar{u}(z)$	[ms ⁻¹]	wind at height z above water level
U, u	[ms ⁻¹]	Apparent wind speed
\bar{u}_h	[ms ⁻¹]	the wind speed at reference height h (100m)
V_a	[ms ⁻¹]	Speed of advance
V_S	[ms ⁻¹]	Ship speed through water
V_{std}	[ms ⁻¹]	Ship speed through water in standard conditions
w	[-]	Taylor wake fraction
x_s, x_{H_2O}, x_{Ash}	[-]	Sulphur, water and Ash content in % Mass
z	[m]	Height of anemometer above sealevel

Greek

Δ	[m ³]	Ship’s displacement
f	[Hz]	characteristic wave frequency
ν_{Σ}	[m ² /s]	Kinematic viscosity
ρ_{51}	[kgm ⁻³]	fuel density at 15°C
ε	[deg]	Wind direction relative to bow
η_D	[-]	Propulsive efficiency
η_O	[-]	Propeller open water efficiency
η_R	[-]	Relative rotative efficiency
η_S	[-]	Shaft efficiency
θ	[deg]	Wave direction relative to bow

Θ	[°C]	Fuel temperature
ρ	[kgm ⁻³]	Seawater density
ρ_{corr}	[kgm ⁻³]	Corrected density for temperature
τ	[-]	Propeller loading coefficient

Abbreviations

AC	Acoustic Correlation
AFC	Anti Fouling Convention
AFS	International Convention on the Control of Harmful Antifouling Systems on Ships, set by the IMO
AHR	Average hull roughness
APR	Average Propeller Roughness
BF	Beaufort number
CO ₂	Carbon Dioxide
COG	Course Over Ground
DAQ	Data Acquisition
EC	European Commission
EM	Electro Magnetic
GHG	Green house gas
GPD	Generalised Power Diagram
GPD speed	Ship speed through water determined using propeller characteristics and the measurement of shaft torque, RPM and wake fraction
gt	Gross tonnage
IMO	International Maritime Organisation
IMO	International Maritime Organisation
JONSWAP	Joint North Sea Wave Project
KPI	Key Performance Indicator
LCV	Fuel Lower Calorific Value or Net Specific Energy
MARPOL	Maritime Pollution convention
MCR	Maximum continuous rating of a diesel engine
NO _x	Nitrogen Oxide
o.w.d.	Propeller Open Water Diagram
PM	Particulate matter
PM&A	Performance Monitoring and Analysis
PPI	Plan Position Indicator
RAO's	Response Amplitude Operators
RPM	Propeller speed of rotation (Revolutions Per Minute)
SAR	Satellite synthetic Aperture Radars

SFC	Specific Fuel Consumption [g/kWh]
SHP	Shaft power
SM	Service Margin
SOG	Ship speed over ground
SOLAS	Safety Of Life At Sea
SO _x	Sulphur Oxides
SPC	Self-Polishing Copolymer
STW	Ship speed through water
SVDR	Simplified Voyage Data Recorder
TBT	Tributyltin
ULCC	Ultra Large Crude oi Carrier
VDR	Voyage Data Recorder
VLCC	Very Large Crude oil Carrier

1 INTRODUCTION

1.1 Overview

Ever since the steam engine has been used for ship propulsion, there has been an interest in monitoring the performance of a vessel. With fuel prices quadrupled between 2004 – 2009 (McMahon 2009) and emission pollution becoming a conversational topic in the marine industry, the urge to increase engine and propulsive efficiency has never been higher. Recent engine developments have focused on improvements in the combustion process (with thermal efficiencies reaching up to 52%), waste heat recovery systems and emission reduction technologies (Ferreira 1998; Jensen 2009). The propulsive efficiency can be improved significantly by reducing hull roughness. Frictional resistance forms about 70-90% of the total resistance of a ship for bulk carriers and tankers (approx. 50% for cruise liners and container vessels (MAN-Diesel 2008)) and is directly affected by hull roughness, which in turn is affected by fouling. Keeping the hull and propeller smooth and free from fouling is therefore essential.

Fouling has traditionally been combated by toxic antifouling coatings for example Tributyltin (TBT) based SPC systems. The complete ban on TBT in marine antifouling systems in 2008 resulted in an increased use of biocide free foul-release coatings. Because these foul-release coatings are relatively newcomers and differ considerably from traditional antifouling systems, no widespread experience in their effectiveness and performance exists yet in terms of frictional resistance and fouling in service. The effectiveness of the coatings can be assessed by monitoring the ship performance over a long period and comparing speed and power capabilities with clean-hull performance.

Experience has taught that the current practice of ship performance monitoring, using standard abstract logbooks for data collection and simple statistical methods for analysis, results in a large scatter in Key Performance Indicators (KPIs). There is therefore a need

to clarify the aspects that are involved with performance monitoring and to identify more reliable ways to analyse ship performance. As a response to this need, a research project was initiated in 2004 at the School of Marine Science and Technology, Newcastle University, in collaboration with International Paint[®], with the aim of developing a methodology to assess ship performance with higher accuracy. The analysed ship performance indicators should allow coating performance to be assessed and aid in the reduction of fuel consumption and environmental pollution of ships.

This chapter gives a background to ship performance in general and the motivation and structure of the thesis. The reasons for performance optimisation and assessment are described in detail and an overview is given of the most commonly known obstacles in benchmarking and assessing ship performance. Based on this review, the aims and objectives of the thesis are laid-out. Finally, each chapter is introduced to give a clear overview of the contents of the thesis.

1.2 Background

The interest in ship performance monitoring can be attributed to economical, environmental and technical drivers. The desire to gain insight in the operational performance of a ship is directly related to fuel price and environmental pollution. Many performance monitoring systems, vessel operation strategies and energy saving devices were developed in the 1980s just after the oil recession in the late 1970s. Over the past five years, the interest in energy saving and performance monitoring has gained interest again due to the high oil prices and environmental concern.

1.2.1 Economical drivers for performance monitoring

Figure 1.1 shows price of crude oil from 1946 to 2009. The causes of the oil recession over the last decade can be attributed to a rapid increase in demand, reduction in production, political instability and speculations and war in Iraq. Oil industry leaders acknowledge that new sources of oil are becoming increasingly difficult to find and more

costly to exploit. In 2002, the world used four times more oil than was found from new sources. Since about 80% of the oil, that will be necessary to meet the projected needs in 10 years time, is not currently in production (ODAC 2008), unprecedented levels of investment and yet-to-be-achieved technological advances will be required to balance supply with future demand. From now to 2020, world oil consumption will rise by about 60% (IAGS 2008), with India and China the two largest growing users. The high costs of exploiting oil and higher demand than future supply put pressure on the market and make the cost per barrel to rise (IAGS 2008).

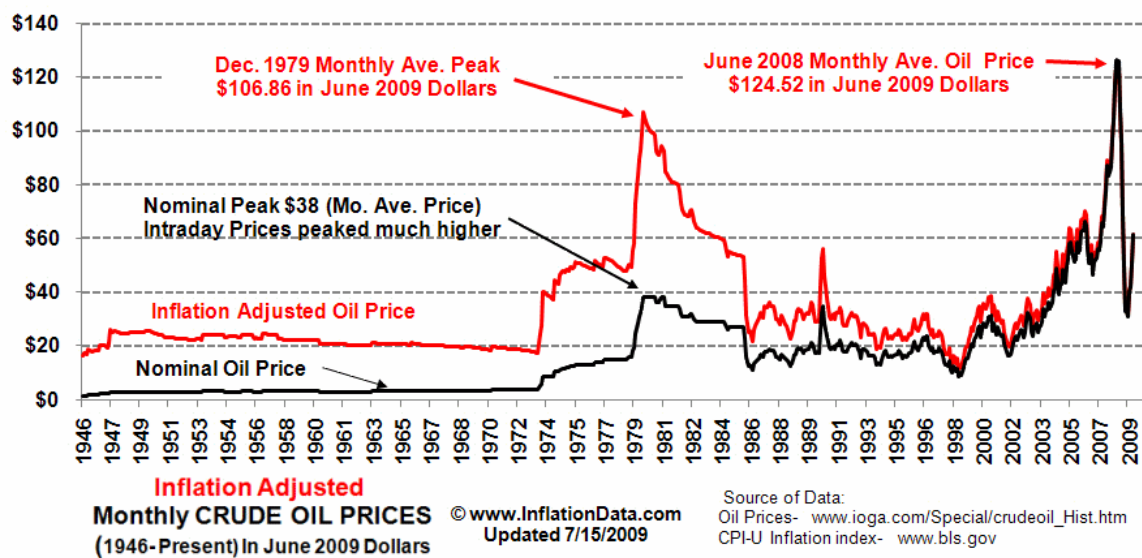


Figure 1.1: Inflation adjusted crude oil prices 1946 – 2009 (McMahon 2009)

As a result of the rapidly rising oil prices, the fuel costs as percentage of the ship's total operational costs have increased from 20% to 50% in the last few years (Zin 2008). In order to reduce fuel costs, operators slow down their ships where ever possible (Orton-Jones 2007). Slowing down ships is only a limited possibility, as ships operate below their most optimal operating point resulting in additional engine wear. Ship owners are therefore pushed to operate more efficient ships and look at their current practice of ship management for optimal operation strategies.

1.2.2 Environmental regulations and directives

Apart from fuel costs, raising concerns on environmental pollution over the past decade have urged shipping companies to operate their fleets more environmentally friendly. In the 1960s, the most serious environmental problem was oil spillages in the seas, through accidents or poor operating practices. This resulted in 1973 in the International Convention for the Prevention of Pollution from Ships, known globally as MARPOL. This deals with the prevention of pollution from ships by oil, noxious liquid substances carried in bulk, and harmful substances. In 1997 a new MARPOL regulation known as 'Annex VI' was adopted which covered the prevention of air pollution from ships. These regulations set limits on sulphur oxide (SO_x) and nitrogen oxide (NO_x) emissions from ship exhausts, prohibited deliberate emissions of ozone-depleting substances, and put a global cap on the sulphur content of fuel oil. In April 2008, the IMO amended the MARPOL Annex VI regulations with a new three-tier structure to reduce NO_x emission even further. The current limits of MARPOL (Tier I) will be replaced by Tier II for diesel engines installed from 1 January 2011. Tier II restricts NO_x emission levels to maximum 14.4g/kWh (a 15-25% reduction compared to Tier I). The reductions in emissions can be accomplished by in-engine technology. Tier III states an 80% reduction compared to Tier I, such that NO_x emission levels for engines installed from 1 January 2016 are not to exceed 3.4g/kWh when sailing in a Designated Emission Control Area. In order to obtain the 80% reduction, different after-treatment techniques can be used such as Selective Catalytic Reduction, Humid Air Motor or Exhaust Gas Recirculation (IMO 2008).

Apart from amendments to the regulations on NO_x, the regulations regarding Sulphur Oxides and Particulate Matter (described in regulation 14 of MARPOL Annex VI) are also amended. The current global cap on the sulphur emission from ships is to be reduced from the current 4.5% to 3.5% from 1 January 2012 and 0.5% from 1 January 2020. The sulphur limit applicable in Emission Control Areas will be reduced from the current 1.5% to 1.0% from 1 March 2010 down to to 0.1% from 1 January 2015 (IMO 2008).

MARPOL Annex VI, which entered into force in 2005, has gained an exceptionally high profile as a direct result of the politically charged global debate on the impact of Green House Gas emissions (GHGs) on climate change. Since 2005, the Kyoto Protocol, an

international effort setup in 1997 to prevent global warming caused by GHGs including CO₂, legally binds participating industrialised nations to reduce GHG emissions by at least 5% between 2008 and 2012. The shipping industry currently forms a smaller contribution (3.5%) to the total volume of GHG emissions than road vehicles, aviation and land based industry (Ambrogi 2008). However, there are predictions that approximately 50% of Europe's air pollution will come from shipping by 2020 if no action is undertaken. The European Union aims to reduce CO₂ emissions by 20% by 2020 and 80% by 2050, and shipping will therefore play an important role in achieving these targets (Barnes 2008). Since ocean shipping activities cover the entire world, the Kyoto Protocol has given the IMO Authority to limit and reduce GHG emissions from merchant vessels. In response, the IMO assigned a Maritime Environmental Protection Committee (MEPC) to develop a calculation method for GHG emissions from vessels plying international waters. This resulted in the introduction of an energy efficiency design index (EEDI), energy efficiency operational index (EEOI) and ship emissions management plan. The current plan is to make the EEDI mandatory for all new-buildings once it is finalised and adopted, while keeping the operational index voluntary. For the EEDI all new-buildings will be given an index figure which will be benchmarked against an industry baseline for one of seven ship types. The EEDI will work by a target being set below the base line to which all vessel designs must be under. The target is then tightened over time (LloydsList 2009). In parallel to the indexes, industry experts came up with the ship energy efficiency management plan. This can be thought of as an environmental version of the international safety management code. It would include guidelines to plan, implement, record and monitor efficiencies on board and to then improve them over time. The EEDI is still under review in order to identify and analyse potential risks or difficulties resulting from the use the EEDI as during the development of the formula various concerns were raised.

In the meantime, the EU is preparing its own mandatory policy options as a precaution. These include bringing shipping into emissions trading schemes, variable harbour dues based on greenhouse gas emissions, bunker levies, and binding CO₂ index limits for ships visiting EU ports (Barnes 2008).

In the future, restrictions to the use of heavy fuel oil and caps on CO₂ emissions and emission trading schemes are likely to be introduced (IMO 2009). As the amount of CO₂

emitted from a ship is directly related to the consumption of fuel oil, fuel efficiency has become an important item for shipping companies. Furthermore, fuel saving directly results in lower SO_x, NO_x and Particulate Matter emissions.

1.2.3 TBT ban & fouling

Another new environmental regulation that affects the marine industry relates to hull coating. For decades anti fouling coatings were dominated by paints containing the toxic TBT (Tributyltin) as their principal biocide. The IMO ban of TBT for new applications from 1 January 2003, and a complete ban from September 17, 2008 (AFS Convention and EC regulation No. 782/2003 (IMO 2007)) has resulted in the use of new alternatives, based on the less toxic biocide copper, and non-biocidal, silicon based foul-release coatings. Further environmental concern is pushing towards a ban to all toxic biocides, already in place in certain coastal stretches in Europe. The new types of foul release coatings have had varying degrees of success and, because of the large number of new developed coatings, no widespread long-term experience in the performance of biocide free coatings exists yet. Since frictional resistance of slow steaming ships forms about 70-85% of the total hull resistance (Carlton 1994), keeping the roughness of the hull as low as possible is perhaps the most effective way to reduce speed and power penalties and unnecessary increases in fuel consumption and CO₂ emission.

Hull roughness develops as a result of damage, corrosion, coating deterioration and bio-fouling. The rate of increase depends on the quality of hull fabrication, surface preparation, application and type of coating, and vessel operating profile and age. Coating damage mostly occurs during ship handling within harbour and during anchorage, for example from the nosing of tugs, fender damage and bottom abrasions. Other causes of roughness increase from coating are coating build-up and paint system failures (e.g. detachment, cracking or blistering). In a survey of 272 vessels, Townsin (Townsin et al. 1981) found that the amount of mechanical damage varied between 3.6 and 7.3% of the total area (depending on ship type), whereas paint failure damage was fairly independent of ship type and covered about 2% of the total area. Corrosion is generally only a minor source of roughness.

Bio-fouling contributes to a larger extent to the increase in frictional resistance compared to hull roughness. It manifests in slime, weed and shell (barnacles, tubeworms etc) fouling from light to heavy grades and can contribute to up to 40% of the total resistance of a ship, depending on its extent and type of coating (Townsin 2003). Hull maintenance for fouling control is therefore a relatively easy way to significantly reduce fuel consumption, emitted CO₂, SO_x and NO_x. It is therefore important to monitor and assess the performance of the coating in its ability to remain free of fouling and other types of deterioration.

Traditionally, hull roughness could be characterised using a stylus instrument such as the Hull Roughness Analyser (BMT-SeaTech 2005). By measuring at 100 locations around the underwater hull the maximum peak to lowest trough height (R_{t50} , expressed in microns) over a sampling length of 50mm, the Average Hull Roughness (AHR) could be estimated. Using the AHR and power loss from a large number of ships, a relationship could be derived to predict the power loss for any measure of AHR (e.g. Deltaplan from International Paint (International 2004) or (Townsin et al. 1986)). The relationship between power loss and hull roughness can be made as long as roughness can be accurately measured. The new type of TBT free, silicon based foul-release coatings can however not be accurately measured using the hull roughness analyser. When dry, the coatings feel like rubber to the finger, causing the stylus tip of the analyser to judder when moved over the surface. When wet, the coatings are fish slippery, causing the drive wheel of the instrument to slip (Townsin 2002). More importantly, roughness expresses in amplitude as well as texture. Silicon based foul-release coatings differ significantly in texture and amplitude which causes different resistance characteristics (Candies et al. 2001). Figure 1.2 shows the surface profile of a traditional self-polishing co-copolymer (SPC) and a silicon based foul-release coating. The foul release coating displays a much smoother micro-surface, with an 'open' texture, whereas the SPC antifouling micro-surface exhibits much steeper and closely packed roughness peaks and valleys, which can be described as a 'closed' texture.

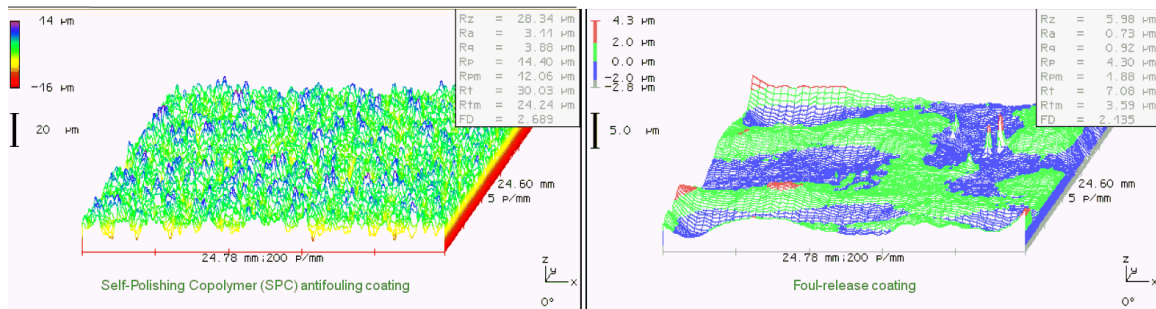


Figure 1.2: Laser profilogram of a SPC (left) and foul-release coated plate (right) (Candies et al. 2001)

Musker (Musker 1977) introduced a parameter to characterise a surface roughness by means of one parameter taking both the amplitude and texture of the roughness into account. Although the parameter proved extremely useful, it can only be determined accurately using advanced measurement techniques in laboratory conditions. At the moment of writing there is still no accepted instrument available to measure hull roughness for silicon based foul release coatings on site. It has therefore become difficult to relate the hull roughness to added resistance in a practical applicable way, especially after the introduction of the TBT ban and the extensive use of foul-release coatings. Tests in towing tanks with flat plates with different types of coating may be done (e.g. (Candries 2001), but it is relatively difficult to develop the same type of fouling, and the distribution of fouling and the three dimensional boundary layer due to the hull form can not be taken into account. Moreover, the shipping industry is reluctant to rely on experimental results only. Assessing the effect of roughness and fouling on a ship therefore requires a radically different way of measurement; through indirect measurement of the overall performance of the ship and its environment.

1.3 Ship performance assessment

In order to assess and optimise a ship's performance in the areas of hull, propeller, engine and operational efficiency, ship performance should be compared to a benchmark condition. For land based trials, e.g. engine shop tests, all factors affecting performance can be accurately controlled. For ships in service, engine, propeller and hull performance are all interconnected and affected differently by environmental, loading and operational conditions. Simply measuring speed and fuel consumption, for example, do not result in any usable data for comparison. It is therefore important to understand the energy distribution of a ship. In Figure 1.3, an example of such an energy distribution is shown for a container ship sailing at 24kn.

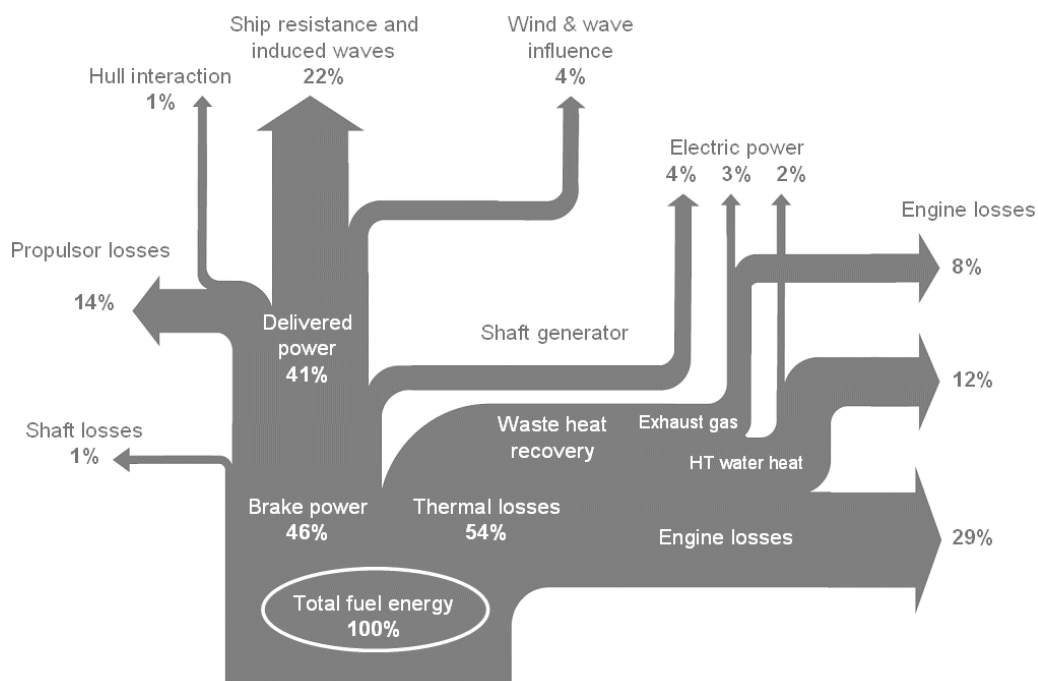


Figure 1.3: Sankey diagram for a container vessel at 24 knots (Miemois 2006)

Only a small percentage of the fuel energy is converted into mechanical power, from which a significant part is used to overcome losses in the propulsion system (shaft losses, propeller losses, hull interaction). Environmental forces result in additional losses. In adverse weather conditions, they can become significant, leaving less energy available to maintain a certain ship speed. For ship performance monitoring, the energy used to propel the ship at a certain speed (in Figure 1.3 referred to as the 'Ship resistance and

induced waves'), the propeller losses and the fuel consumption relative to brake power (engine performance) is of interest.

Because of the difficulties in separating the energy losses and effects of changing environmental conditions, optimisation strategies are often based on computer simulations. Full-scale tests are however still necessary to validate the computer or model scale predictions. Full-scale evaluation of ship performance requires carefully planned sea trials in constant, calm weather conditions. Because of the high costs of sea trials, they cannot be done frequently. Moreover, the effectiveness of hull, propeller and engine maintenance strategies and weather routing systems can only be assessed by monitoring ship performance over a longer time frame in service conditions. Performance data from in-service conditions is affected by varying environmental and loading conditions. In order to separate the performance changes from environment and loading from the tested performance improving solution, it is necessary to monitor all parameters that affect ship performance and correct the measured performance so that it represents sailing in a pre-defined reference condition.

The reference baseline condition is often related to calm weather with no wind and waves and sailing at design draft. The standard condition should be defined corresponding to the field of interest. For example, if the effect of fouling is to be identified, the definition of the standard condition should include information about the initial state of the hull and propeller (e.g. clean, only light slime etc.). Table 1.1 lists the condition often used as benchmark, or 'standard' condition for ship performance monitoring. The conditions listed in Table 1.1 are used throughout the analysis in this thesis.

Table 1.1: Definition of standard conditions

Definition of ‘standard conditions’
<ul style="list-style-type: none">• No acceleration• No course deviations, no drift• No wind• No waves• No pitch, roll, heave, yaw• Deep, open water• Pre-defined draft & trim• Pre-defined water density & viscosity• Pre-defined air density• Pre-defined fuel quality (calorific value, temperature, density)• Calibrated sensors

1.4 Benefits of Performance Monitoring

Knowledge and understanding of the capabilities of the vessel in terms of ship speed and power and her behaviours in service (speed and power loss in different environmental and loading conditions) is useful both in terms of economical and environmental aspects. The following benefits from this knowledge and understanding can be listed:

- Assessment of hull condition

When the capabilities of a vessel are known (speed that can be obtained with a set power) at different stages of hull roughness, the quality of any anti-fouling system can be assessed. The economically optimum intervals for hull cleaning or dry-docking for example can be defined and economic penalties and delays due to fouling can be identified for improved voyage planning.

- Assessment of engine condition

With an instantaneous figure of engine efficiency such as specific fuel consumption, the effects of any adjustments in the timing of the main engine can be made visible. An example of these adjustments are valve timing changes or important engine faults such as broken piston rings, faulty injection, burned valves, fouled turbochargers, air filters, air coolers etc.

- Evaluation for ship design

When the true performance of the ship in service is known, and the degradation after a number of years is monitored, the correct service and engine margins can be estimated for definition of design point definition of propeller-engine matching and propeller design.

- Refinement of charter party agreements

The current speed and fuel consumption warranties in charter party agreements are imprecise in engineering terms and reflect the evidential difficulties that arise in dispute when it is not known whether inefficient ship performance is caused by adverse weather conditions or a badly maintained ship. When the ship's capabilities and ship performance can be determined irrespective of environmental or loading conditions and with higher precision, agreements can be defined more precisely.

- Optimising sailing performance

If all performance affecting parameters are measured simultaneously at frequent intervals, a large database becomes available which can be used to design an optimisation system. Trim, draft, autopilot and engine settings in different environmental conditions are examples of areas that can be optimised. Moreover, with the availability of an accurate speed-fuel consumption curve that represents the actual capabilities of a vessel, the most optimum service speed can be determined based on the total expenditure. Also, with the availability of prompt and reliable information of the vessel's sailing performance, the ship's crew would be able to obtain an immediate understanding of the impact of their actions.

- Environmental assessment

As a response to global pressures caused by environmental concerns on ship operators, classification societies have introduced notations (green certificates) concerning ship efficiency and pollution. Examples are DNV's 'clean' notation (DNV 2009), the 'Green star' standard from RINA (RINA 2007), the 'Environmental Passport' from GL (GL 2007) or the 'Environmental Protection' notation from LR (LR 2007). To be able to achieve an environmental notation, the quantity of emission gasses must be known. Fuel consumption efficiency for a ship in calm waters may diverge by 10% from its efficiency in normal service conditions (Tsuda 2008). Shipbuilders deliver their newly built vessels following their trials on the basis of calm waters and reference is therefore often made to empirical correction factors to include service conditions. The availability of a continuous performance monitoring system allows better assessment and evaluation of emissions and environmental impact, and helps in obtaining an environmental notation. The introduction of CO₂ indexing schemes such as the Energy Efficiency Operational Index (IMO 2009) for ships also requires continuous performance monitoring to accurately index a ship on a scale.

1.5 Motivation of thesis

A bad understanding of the aspects involved in ship performance monitoring is the main problem of poor quality performance monitoring results. Performance monitoring starts with the acquisition of accurate and reliable data. Often, inaccurate and incomplete abstract logbooks are used as input to performance analysis algorithms, regardless of the fact that the requirements and purpose of abstract logbooks are different from those for performance monitoring. The Author has been involved with performance analysis using abstract logbooks for containerships and LNG carriers (Atlar et al. 2006) (Hasselaar 2006). Different data analysis methods have used on data sets; trend analysis techniques (Hasselaar 2005a), multiple regression analysis (Hasselaar 2005b) and deterministic methods (Ata et al. 2006). Although some scatter could be reduced in the performance indicators, the results remained unsatisfactory. The principle cause of the scatter is the poor quality of data. In many cases for example, the draft was not included in the performance logs; only the speed-made-good (averaged speed over ground) was given;

no reliable speed through water; the shaft power was not given or data was inconsistent (differences between SOG and STW > 9kn, wind speeds exceeding 91kn etc. (Ata et al. 2006)). If the logging protocol of the abstract logbooks are not crystal clear to the personnel in terms of the log duration, sampling rate, averaging method, calibration, accuracy etc., an averaged data in abstract logs does not make much sense for the person (or institution) analysing them remotely after some time. The main problems of data collection can be summarised as:

- Inconsistent performance logs resulting from spot measurements of ship performance in a constantly changing environment
- Unreliable readings due to inconsistent use of instrumentation for performance logging, caused by unclear data collection protocols
- Errors in data entry, due to human errors
- Insufficient provision of training to collect performance data accurately and following the right procedures, e.g. for wave observations.
- Incorrect data collection protocols, unsuitable for performance monitoring (missing parameters, too few details etc.)

Performance analysis, the process of converting a large number of performance parameters into a limited number of KPIs for the assessment of ship, propeller or engine performance, is often done ashore because it requires a large database of historical data and specialised skills. When data is analysed onshore however, the quality and characteristics of the data logged are unknown to the data analyst. This may lead to ill-defined assumptions harming the reliability and accuracy of the performance analysis. Vice-versa, unless clearly documented, the data collection protocol may not be known to the crew onboard, causing misinterpretation of the quality of the data by the data analyst. Assumptions and subjective decisions regarding the accuracy must be reported carefully to avoid misinterpretation in the analysis and KPIs. Analysis should therefore preferably be done completely automatic without human influence, to avoid misinterpretations and subjective decisions affecting KPIs. Moreover, because it is not possible to have experts constantly available for performance analysis, the analysis is done periodically when a sufficient large number of voyage data has been collected. As a result, data logs and KPIs can only be used for long-term performance analysis. Instantaneous feedback to vessel

operation, which allows officers to obtain a deeper understanding of vessel behaviour and capabilities, so that they can optimise vessel operation, is not possible.

Finally, the right selection and interpretation of performance indicators is important. Because of the many KPIs in use for the assessment of long-term and short-term vessel performance, their physical meaning is often not well understood or described. It is often found (Ata et al. 2006; Hasselaar 2005a) that KPIs show contradicting trends due to different characteristics and sensitivity to the used input parameters or because of the fact that they include the combined efficiency of hull, propeller and engine while others are only affected by e.g. propeller and hull performance. Furthermore, if for ‘clarity’ purposes data points are removed and only trend lines are indicated, the accuracy and the significance of the regression analysis is often overestimated and conclusions based on incorrect results. The correct selection, description and availability of KPIs are therefore important characteristics for the usability and credibility of any performance analysis system.

1.6 Aim and Objectives of the thesis

Following the background and motivation of the thesis mentioned before, the aim of the thesis is to investigate the feasibility of developing an advanced (on-line) ship performance monitoring and analysis system for typical merchant ships in order to assess ship performance with high accuracy. The analysed data should allow coating performance to be assessed and aid in the reduction of fuel consumption and environmental pollution of ships. Within the framework of this aim, the specific objectives of the thesis are set to:

- review the state of art of performance monitoring and analysis
- identify factors that influence ship performance and data acquisition
- develop a methodology to convert performance to ‘standard’ conditions
- develop an online ship performance monitoring and analysis system
- evaluate the developed system and methodology on two types of vessels

In order to achieve these specific objectives, accurate performance data has been collected from two ships in service conditions by equipping the ships with a range of sensors and a tailor made data acquisition system. The two ships are different in type and size; the *RV Bernicia*, a 16m research vessel from Newcastle University, and the *MT Overseas Tanabe*, a 330m VLCC from OSG Ship Management Ltd. The large database of data collected from these ships has formed the basis and platform to validate the conclusions and algorithms described in this thesis. All installation work, development of hardware and software as well as the implementation onboard have been done by the Author himself.

1.7 Thesis layout

Having presented an overall introduction to the research study presented in the thesis in Chapter 1, Chapter 2 reviews the current state of art of performance monitoring (PM) and analysis (A) by breaking PM&A systems down in three parts: data collection; data analysis; and performance indication. This chapter concludes with a list of shortcomings from which general requirements for the development and implementation of a PM&A system is derived.

Chapter 3 focuses on the ways to collect accurate performance data. In Section 3.2 the environment in which ships sail is reviewed in order to understand the characteristics of the external forces and parameters that influence ship performance. In Section 3.3, operational factors that affect ship performance are discussed, and the effect changes in environmental conditions have on ship performance is described. From this review, the requirements for data acquisition for ship performance monitoring are defined. In Section 3.4, the environment and physical characteristics of the sensors that are required for performance monitoring, are described. For many parameters, the limitations regarding accuracy are determined by the environment of the sensor rather than the sensor limitations. Readings should therefore be averaged over a time frame to be meaningful. The accuracy and reliability of readings can furthermore be improved by signal validation and filtering. In Section 3.5, these methods are described.

In Chapter 4 the proposed performance analysis system is described. The methodology to convert performance data to standard conditions is presented (Section 4.2), and key performance indicators are proposed for the visualisation of ship performance for different purposes and end-users. The impact of uncertainties in data on the long-term performance indicators has been evaluated using a sensitivity analysis (Section 4.4). Based on this sensitivity analysis, the system architecture of an online ship performance monitoring and analysis system is developed and described (Section 4.5).

The development of the PM&A system is based on the extensive data collection on two vessels; a 16m research vessel for fundamental research and development of the model, and a 330m VLCC for the evaluation of the system on a merchant vessel. In Chapter 5, a description is given of the installation and implementation of the PM&A system on each of these vessels. In Section 5.2, the installation and implementation on the RV *Bernicia* is described. The ability of the PM&A to identify fouling is given and considerations given for the development of a PM&A system for performance on small craft. Section 5.3 describes the implementation of a data acquisition system on the MT *Overseas Tanabe* and discusses the limitations of long-term KPIs that result from speed through water measurement errors.

Finally, in Chapter 6 conclusions are given with respect to the aims and objectives of the project. Fields of further research are discussed and a checklist for the design and implementation of the proposed PM&A system on ships is given.

The appendix section includes a checklist for the design of a PM&A system (Appendix A) and details of the PM&A system and data collected on the RV *Bernicia* and MT *Overseas Tanabe* (Appendix B and C respectively).

1.8 Summary

This chapter presents the background and motivation of the thesis which established the aims and specific objectives of the thesis. A brief layout of the thesis is also presented in achieving these aims and specific objectives in this chapter.

2 STATE OF ART OF PERFORMANCE MONITORING AND ANALYSIS

2.1 Introduction

From the earliest days of steam ships there has been a recurrence of the need to know the speed and power relationship of ships as they are performing in service. Performance analysis has historically been done by analysing the all-in fuel consumption from bunkering data and log abstracts periodically over a period of time or sailing. The earliest mathematical analysis methods to evaluate ship performance were addressed by Telfer in 1926 (Telfer 1926).

In this chapter a review is given on the types and characteristics of different performance monitoring and analysis systems with the aim to ascertain the required improvements for the design of an advanced PM&A system. The review is based on published papers and information from commercially available PM&A systems, and is separated in three parts: in section 2.2 a review is given on two kinds of data collection methods; manual data collection using abstract logs and automatic data collection using a dedicated data acquisition interface. A list is included of modern commercial PM&A systems indicating the state of art. In section 2.3 four methodologies to correct ship performance to standard conditions are reviewed: trend analysis; multiple regression analysis; deterministic analysis; and analysis based on system identification. Section 2.4 reviews a number of performance indicators used for vessel performance analysis. Finally, Section 2.5 concludes on the requirements for the design of an automatic, autonomous online ship performance monitoring system.

2.2 Data collection methods

2.2.1 Manual data logging

Onboard most merchant ships, a daily logbook system is used to monitor for engine performance, navigation and loading. Engine-logs are mainly of interest to engine maintenance specialists and provide technical data to assess the condition of the engine and machinery. Deck- or navigation logbooks are used for voyage planning, insurance/safety and ship performance analysis, while loading logbooks are used for stability assessment, cargo planning etc. Engine and deck logbooks are traditionally filled-in either once a day (noon-noon logs) or every watch (4 hours) and averaged over 24 hours to form so-called ‘abstract logs’. The number of variables that are logged depends on the requirements from the shipping company, the available instrumentation and the motivation and training of the crew. A typical deck log contains information about the ship’s position, speed, propeller revolutions, slip, draft, and sea state. Figure 2.1 shows an example of a deck/engine log abstract.

DECK/ENGINE ABSTRACT

VOYAGE NUMBER 001

FAOP: PORT RA'S LAFFAN DATE 96/12/23 TIME 1555 AT POSITION LAT 25-55N LONG 51-42E

EOSP: PORT (KAWAGOE) DATE 97/01/10 TIME 0300 AT POSITION LAT 34-09N LONG 137-15E

DATE	NOON POSN.		DIST		STMG LOG	SPEED OBS	WIND		SEA		AV.		FO		LNG		DO USED	GO USED	TIME ZONE	REMARKS	
	LAT N	LONG E	OBS	ENG			DIRN	SPEED	DIRN	STATE	RPM	SLIP	NORM	OTHER	M3	FO. EQ					
1 96/12/23	RA'S LAFFAN																			1455LT DEP. RA'S LAFFAN	
2 96/12/24	25-31N	57-09E	346	364	344	20-05	17.23	NNW	4	NNW	3	75.6	+4.8	66.66	-	67.04	32.45	-	-	+03:00	
3 96/12/25	21-25N	62-08E	374	391	382	23-15	16.09	NORTH	5	NORTH	4	70.2	+4.3	66.84	-	71.99	34.84	-	-	+03:45	TIME CORR. AH'D 45'
4 96/12/26	17-17N	66-52E	365	381	368	23-15	15.70	NE	5	NE	4	68.4	+4.2	54.43	-	90.71	43.90	-	-	+04:15	TIME CORR. AH'D 45'
5 96/12/27	13-08N	71-34E	369	394	376	23-15	15.87	NNE	6	NNE	5	70.8	+6.4	50.83	-	108.64	52.58	-	-	+05:00	TIME CORR. AH'D 45'
6 96/12/28	8-39N	75-36E	361	378	364	23-15	15.53	NE	4	NE	3	67.8	+4.4	59.96	-	78.93	38.20	-	-	+05:45	TIME CORR. AH'D 45'
7 96/12/29	5-39N	80-38E	355	384	357	23-30	15.11	ENE	7	ENE	6	68.3	+7.6	35.34	-	132.29	64.03	-	-	+06:30	TIME CORR. AH'D 30'
8 96/12/30	5-40N	86-16E	336	386	357	23-30	14.30	NE	5	NE	4	68.6	+13.0	32.85	-	129.70	62.77	-	-	+07:00	TIME CORR. AH'D 30'
9 96/12/31	5-59N	92-31E	374	410	379	23-30	15.91	NE	5	NE	4	72.8	+8.7	31.93	-	142.78	69.11	0.50	-	+07:30	TIME CORR. AH'D 30'
10 97/01/01	4-37N	98-48E	403	446	417	23-30	17.15	ENE	6	ENE	5	79.2	+9.6	35.58	-	169.01	81.80	-	-	+08:00	TIME CORR. AH'D 30'
11 97/01/02	1-17N	104-17E	406	422	405	24-00	16.92	NNE	6	NNE	5	73.5	+3.9	40.89	-	140.96	68.22	-	-	-	-
12 97/01/03	7-01N	108-15E	425	472	423	24-00	17.71	NORTH	6	NORTH	5	82.1	+9.9	28.65	-	218.09	105.56	-	-	-	-
13 97/01/04	12-17N	112-45E	413	447	411	24-00	17.21	NNE	5	NNE	4	77.8	+7.6	00.00	-	242.65	117.44	-	-	-	-
14 97/01/05	17-28N	117-06E	401	428	396	24-00	16.71	NNE	5	NNE	4	74.4	+6.2	00.00	-	221.45	107.18	-	-	-	-
15 97/01/06	20-46N	120-53E	292	391	298	24-00	12.17	NE	9	NE	8	68.0	+25.3	00.00	-	198.10	95.88	-	-	-	-
16 97/01/07	24-13N	125-30E	330	409	323	23-30	14.04	NNE	8	NNE	7	72.7	+19.4	00.00	-	215.13	104.12	0.30	-	+08:30	TIME CORR. AH'D 30'
17 97/01/08	28-11N	130-10E	352	388	344	23-30	14.98	NW	7	NW	6	68.9	+9.2	4.86	-	177.23	85.78	-	-	+09:00	TIME CORR. AH'D 30'
18 97/01/09	32-13N	134-54E	345	399	336	24-00	14.38	NORTH	8	NORTH	7	69.4	+13.5	67.31	-	83.21	40.27	0.17	-	-	-

↑
*1/07 DO (0.30 NT) :TO INCINERATOR DO TANK

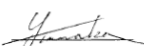

CHIEF ENGINEER  MASTER 

Figure 2.1: Example abstract deck log of an LNG tanker

Because logbooks are used on all ships, they are often used for performance monitoring. Ship performance monitoring requires however a higher level of accuracy than abstract logbooks can provide. The following shortcomings of manual data logging can be named:

- **Uncertainty in the used instrumentation.** To increase redundancy, critical sensors for ship performance are often duplicated. Experience indicates however that duplicate instruments often show differences. Unless well described, this causes confusion in which instrument indicates the best true representation and should be used for performance monitoring. Furthermore if the source of the instrument is unknown (e.g. for draft, whether it is calculated, measured by draft gauges or read-off from draft markings on the hull), the reliability of the logged data is low
- **Wrong data collection protocol.** A time lag of an hour in sampled data may represent two completely different performance conditions if environmental or sailing conditions have changed in this period. Most parameters, such as torque, are affected by even the smallest change in environment, and require therefore that all parameters are logged at the same time
- **Insufficient training.** If parameters cannot be measured using dedicated instruments, for example wave characteristics, visual observations must be made. They can be accurate, if done by highly experienced officers, but change of shifts and quick changing vessel crew causes inconsistent observations
- **Inaccurate data collection.** Certain parameters (wind, speed, torque etc) must be averaged over a time period to be meaningful. Spot measurements result therefore in errors. Furthermore, it is normal practice for officers to enter higher sea states than actually experienced if the vessel experiences delays (due to engine problems, strong currents, course alterations etc.). This is done to avoid claims from the charterer on the vessel's capabilities.
- **Limited logging frequency.** The high workload of the officer on duty limits the logging frequency for performance monitoring. With the recent increase in legislations, the number of administrative tasks and safety checks has increased dramatically with many officers complaining that there is little time left for watch keeping and ship operation.

- **Errors in data entry.** Experience indicates that abstract logbooks frequently contain data inconsistencies, e.g. wind, water and ground speeds are mixed up, unrealistically high or low parameters are entered or relative wind instead of true wind speed is logged. The errors may be the result of unclear logging protocols, inaccurate sensors or insufficient training. Because copies are only periodically send ashore, error tracking is difficult.

With the developments in satellite communication and email, electronic logbooks have emerged and accepted by many flag states (MarineNorway 2008). They replace paper abstract logbooks and enable logs to be send via email to shore, allowing ship performance to be analysed on a daily basis. Furthermore, anomalies can be identified directly at the source and, if applicable, daily feedback of the ship's operation can be send back to the vessel. The data however still represents manual spot measurements.

2.2.2 Automatic data logging

With the introduction of electronic logbooks and wireless data transmission from ships, it is now possible to collect many ship performance parameters electronically. A central data acquisitioning system interconnected to all necessary instrumentation can monitor and store data for either instantaneous or offline analysis. The automation of data collection contributes significantly to the improvement of data quality:

- Continuous monitoring allows signal validation, filtering and averaging for increased accuracy and reliability
- The source and characteristics of each sensor can be described and documented accurately, which reduces the uncertainty and errors in data entry
- Automatic data collection allows real-time data analysis, which can be used for monitoring for alarm in extreme operating conditions or real time feedback on vessel operation

Examples of automatic data logging systems are Voyage Data Recorders (VDR) and diesel engine condition monitoring systems. A VDR is an automatic data logging system for accident investigation collecting information concerning the position, speed, physical status, command and control of a vessel over the period leading up to and following an

incident. Every passenger vessel and other ship, which have a capacity of greater than 3,000gt and constructed on or after 1 July 2002, is required to carry a Voyage Data Recorder (IMO 2007). Cargo ships larger than 20.000gt constructed before 1 July 2002 are required to carry at least a Simplified (S) VDR before 1 July 2009 (cargo ships 3,000-20,000gt before 1 July 2010). A simplified VDR differs from a normal VDR in that it is not required to include data from echo sounder, main alarms, rudder order and response, engine order and response, watertight and fire door status (if applicable) and wind speed and direction (IMO 2007). The minimal logging requirements for a VDR and S-VDR listed in Table 2.1.

Table 2.1: VDR & SVDR requirements

S-VDR requirements	VDR, in addition to S-VDR:
<ul style="list-style-type: none"> • Date and Time • Ship's Position • Speed • Heading • Bridge Audio • Communications Audio • Radar Data 	<ul style="list-style-type: none"> • Echo Sounder • Main Alarms • Rudder Order and Response • Engine Order and Response • Hull Openings (doors) status • Watertight and fire door status • Accelerations and Hull Stresses • Wind Speed and Direction

Many parameters logged by a VDR are required for performance monitoring. However, the use of the VDR for performance monitoring is limited since data is stored only a limited period of time and difficult to access. Furthermore, as standard the system does not log engine power, sea characteristics or draft and trim and the system is not suitable for manual data entry. Yet, the infrastructure of the VDR (cabling etc.) can be used for the installation of a PM&A system when the PM&A system is installed in collaboration with the VDR manufacturer.

2.2.3 State of art of data logging

Over the past 6 years many advances have been made in commercial PM&A systems regarding data collection. Some solutions already utilise automatic data acquisition systems for onboard analysis. However, most systems use manually entered data for performance monitoring. Since most commercial PM&A systems are black boxes, whereby even the ship owner can not get full insight in how data is collected, conditioned or analysed, it is difficult to comment on the characteristics of their data conditioning and analysis algorithms and reliability of KPIs. As a result, many shipping companies still use their own methodologies for data collection and performance monitoring. The following list includes a number of commercially available PM&A systems. The list is alphabetically ordered and is by no means complete. Only those systems are included that make allowances for wind, wave and draft variations. Systems that only collect fuel flow, torque, rpm and GPS and calculate the specific fuel consumption or fuel/mile travelled have not been included

- *CASPER* from Propulsion Dynamics Inc (Munk 2006b) - Onshore analysis of daily ship logbooks. Periodical performance reports are send to the customer. Correction for wind, waves and displacement variations.
- *Kyma Ship Performance* from Kyma AS (KYMA 2006) – Onboard real-time data collection and analysis
- *Performance Monitoring* by Ocean Systems Inc (OSI 2010) – Onboard data analysis by periodical input of abstract logbook sheets or data from VDR
- *Seatrend* from Force Technology (Force-Technology 2008) – Onboard manual data collection, analysis onshore with corrections for wind, wave and displacement variations
- *SMART^{POWER}* from BMT Seatech Ltd (BMT-SeaTech 2004) – Onboard real-time data collection, analysis and performance analysis. Both instantaneous and long-term performance feedback is given
- *SOPRANwebTM* from MARINTEK (MARINTEK 2005) – Onshore analysis of daily abstract logbooks for both operational feedback as well as long-term condition monitoring
- *TOMAS* from Mitsui OSK lines (MOL 2003) – Onshore analysis of daily abstract logbooks via regression analysis

- ...

It can be concluded that although most systems use onboard computers for data collection, data is still often entered manually once a day. This does not improve the quality of data and still insufficient data is collected for advanced condition monitoring and data validation.

2.3 Performance analysis methods

There are many published methods for analysing ship performance. They can be divided in four types; (1) Methods using regression analysis over time (Trend analysis); (2) Statistical methods using more sophisticated regression techniques to account for variations in weather conditions (Statistical methods); (3) Deterministic methods using hydrodynamic relationships and (4) System identification techniques. In this section, a review is given over these four types of analysis.

2.3.1 Trend analysis

Long-term performance analysis by deriving trend curves is the simplest form of performance analysis. It does not require much knowledge of ship behaviour in different weather conditions, quality of input data or detailed hydrodynamic and hydrostatic ship characteristics which are often difficult to obtain. It is therefore still a popular method, used by many shipping companies (examples can be found in (Carlton and Parsons 1989), (Wallentin 2004), (MOL 2003), (KYMA 2006)). Trend analysis relies however on the availability of large amounts of data, collected consistently over a period of several months or years, during which the ship sailed at one particular speed. Trend analysis, without corrections for wind, wave or draft variations etc. is based on the assumption that changes in performance from wind and waves may be ignored if analysed over a year. The large scatter in ship performance caused by varying environmental loads, changes in displacement, voluntary speed deviations etc., makes trend identification however extremely difficult and unreliable. Scatter in performance parameters may result in large

uncertainty margins in derived trends and, unless they are carefully reported, it can be easily misinterpreted by non-experts in the fields of statistics.

A simple way to reduce part of the scatter is to filter performance data for severe weather conditions (e.g. do not consider sea state > Beaufort 4) and separate loaded and ballast conditions. Other techniques to reduce scatter is by converting ship performance directly into carefully selected Key Performance Indicators (KPIs), such as the Admiralty Coefficient, which takes speed and displacement deviations into account. Other examples of KPIs are slip, sea margin or RPM loss (MOL 2003).

An example of the difficulty of interpreting un-analysed, but thoroughly filtered performance data is shown in Figure 2.2. It shows three frequently used KPIs for trend analysis for a 72,500dwt LNG carrier: Admiralty coefficient, RPM loss and ship speed. The displayed data are obtained from deck abstract logs over a period of 8 years after the building of the vessel and filtered for the following conditions:

- Heavy weather (wind force Beaufort 4 or above)
- Wind direction relative to the bow within 112 degrees port or starboard side
- Laden conditions only: displacement >93% of design displacement
- Engine loading higher than 50% MCR
- Avoiding shallow water effects as much as possible by taking out days of arrival and departure in port

Dry docking dates, when the hull was cleaned and/or recoated, are indicated by three vertical lines on the abscissa.

The large scatter in Figure 2.2 makes the trend analysis difficult. If regardless the scatter trend lines are drawn, one would see contradicting trends, e.g. a reduction in RPM loss with an increase in speed. Moreover, in many cases the effect of dry-docking cannot be determined without the dry-docking dates.

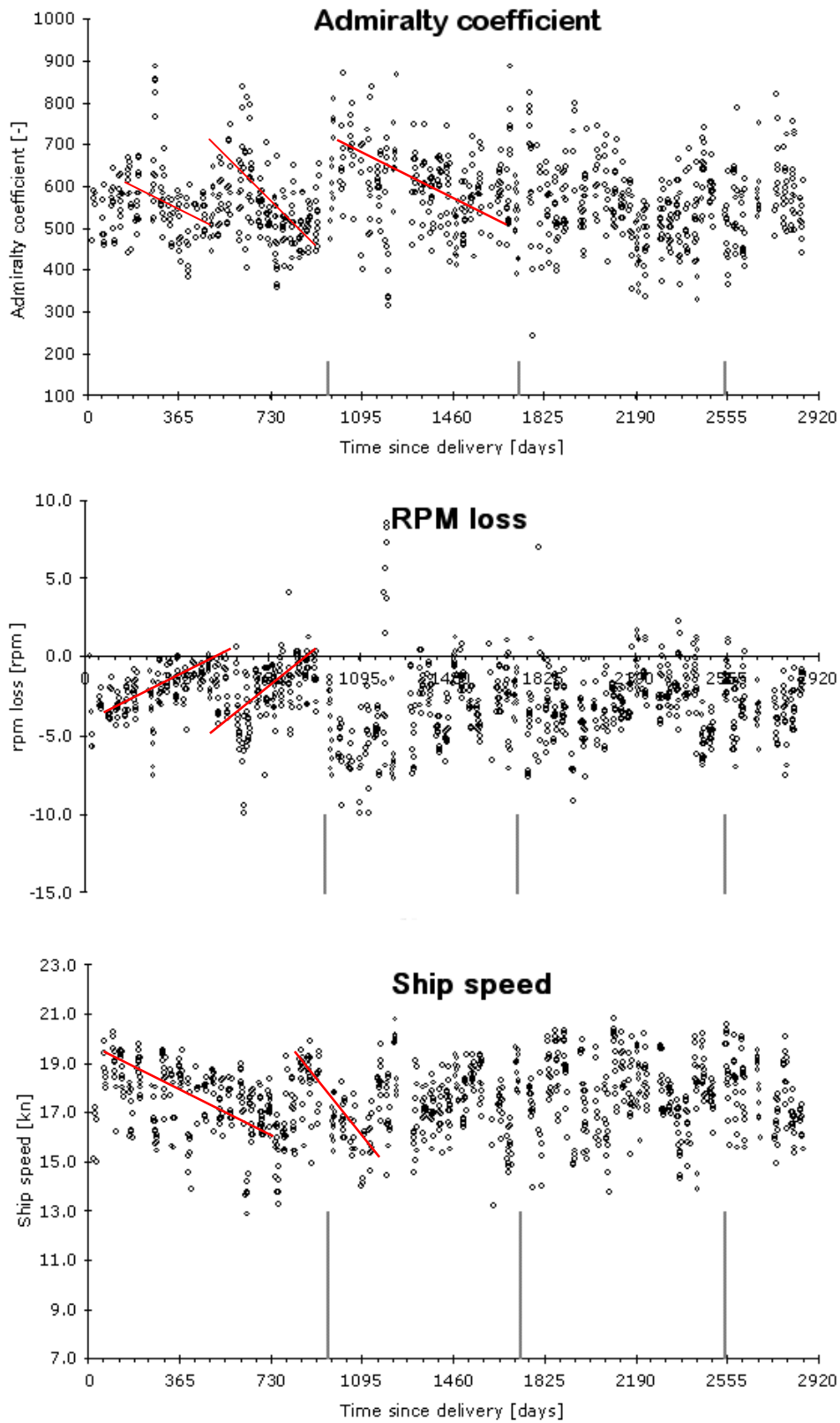


Figure 2.2: Admiralty coefficient, RPM loss and ship speed through water versus days since maiden voyage of an LNG carrier. Vertical lines on the abscissa indicate dry-docking dates (source confidential)

The effect of hull cleaning in dry dock can not be identified in many cases without information of dry-docking dates. The characteristics of the Admiralty Coefficient, RPM-loss and ship speed as KPI are discussed in detail in section 2.4. Only a brief overview is given here to illustrate the difficulties in using regression analysis techniques for performance analysis.

Admiralty Coefficient

The admiralty coefficient relates displacement (Δ), ship speed (V_s) and power (P_S). It is therefore independent of small variations of speed and loading. The admiralty coefficient is defined as:

$$A_C = \frac{\Delta^{2/3} V_s^3}{P_S} \quad (2.1)$$

An increase in hull fouling or roughness can be identified by a gradual decrease in admiralty coefficient. In Figure 2.2, after the first dry-docking, a temporary increase in admiralty coefficient can be noticed. However, during the other dry-docking periods, in which the hull was cleaned and re-coated, no clear change in performance can be observed using this KPI, due to the large scatter.

RPM-loss

The middle diagram in Figure 2.2 shows the RPM-loss which relates the measured output power and engine speed $n(P_S)$ to the trial ship speed at the same output power $n_{Trial}(P_S)$:

$$RPM_{LOSS} = n_{Trial}(P_S) - n(P_S) \quad (2.2)$$

Negative values can be regarded as the propeller margin, while positive values indicate the engine running in the torque-rich (heavily loaded) region. Fouling expresses as an increase in RPM-loss (towards zero or higher). The middle figure in Figure 2.2 shows in the first period before dry-docking two clear trends, which cannot be identified in the other two graphs. In the period after the first dry-docking, large scatter makes the derivation of regression curves difficult. If regardless the large scatter, regression curves are plotted, their shapes do not match the expected changes from hull and propeller cleaning during dry-docking and contradict trends from the other plotted KPIs.

Ship speed

The bottom plot in Figure 2.2 shows the uncorrected STW over time. The KPI ship speed relies on the assumption that the ship sails normally at one set engine speed. With increasing hull roughness, ship speed reduces. Speed logs have a high error margin in the order of knots which makes trend analysis difficult. Due to the uncertainty in trend analysis, incorrect trends are easily made. For example, in the period before the first dry-docking, the ship speed seems to indicate initially a decrease. Around day 800, an increase in ship speed can be seen, suggesting the hull has been cleaned in dry-dock. However, the real dry-docking happens only 200days later.

The three KPIs show the problems faced with performance analysis based on simple trend analysis. If no rigorous performance correction is applied, deviations are large and identify contradicting trends. Each parameter has its own sensitivities and uncertainties, and comparison of KPIs is therefore difficult. Furthermore, if data is not collected consistently or filtered for certain conditions, the data may not be equally distributed in time. This causes errors in trend analysis. Figure 2.3 shows the relationship between the daily logged main engine fuel consumption and average ship speed for an LNG ship. The data has been filtered out for sea states corresponding to wind speed $BF > 4$ and a correction is made for differences in displacement using the admiralty coefficient. A regression curve is drawn for the ship's performance before and after dry-dock..

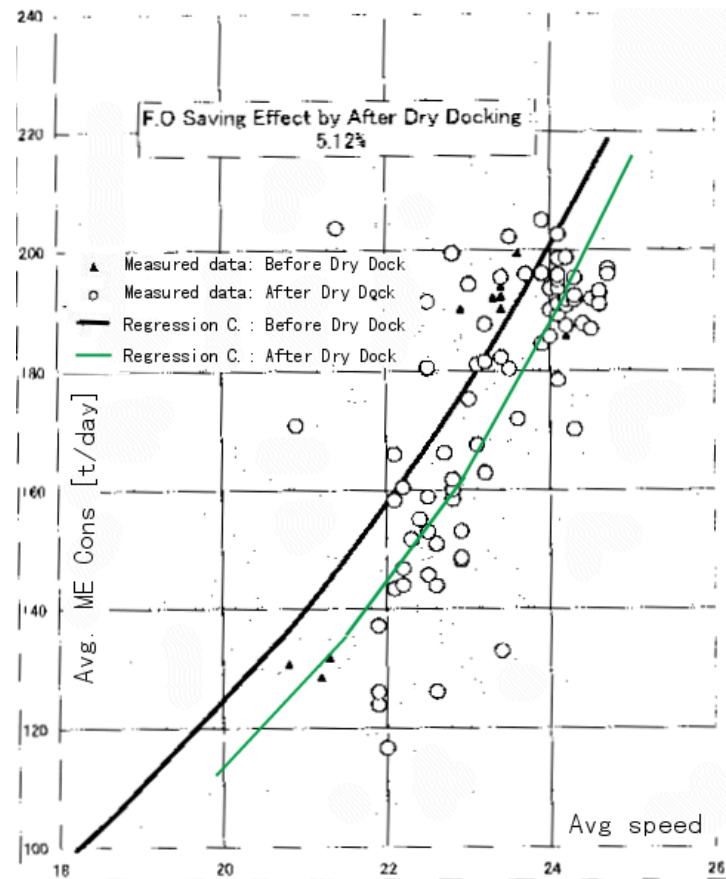


Figure 2.3: Fuel flow vs. ship speed for a 74.000dwt container ship (source confidential)

Figure 2.3 has been taken from a report used to prove the effect of a fuel saving device installed on a container vessel after a dry-docking period (source confidential). The fuel saving after the installation of the device in dry-dock, based on the derived regression curves, was estimated as 5.12%. However, the large scatter and the uneven number of data points before and after dry-dock (3 months of data before dry-docking, against 8 months after dry-docking) indicates that the derived regression curves have a large standard error. The large scatter makes the regression analysis highly sensitive to outliers and number of included data points. If the same amount of scatter can be expected before dry-docking as indicated in the period after dry-docking, the regression curve before dry-docking will most likely shift. Simple trend analysis without paying attention to data quality is therefore prone to errors. Unless uncertainties in the data points is reduced, and the possible causes of changes in performance are reduced, no claims can be made with respect to the effect of fuel saving devices.

2.3.2 Statistical analysis

One of the most commonly used parameters for the identification of fouling is ship speed through water (STW). At a set power, ship speed can vary however strongly due to variations in displacement, wind, waves etc. Logan et al showed that many variations can be reduced by using multiple regression techniques (Logan et al. 1980; Scott 1971; Thomson 1978). The advantage of multiple regression analysis techniques is that no reference has to be made to physical parameters, such as propeller characteristics or hull form data which introduce additional uncertainties and may be difficult to obtain. However, drawbacks for real-time on-line performance analysis are:

- The relationships derived are strictly valid for the vessel analysed and the conditions that were met. Therefore, extensive development time is required each time new ship performance data is available or other vessels are to be analysed
- The input data cannot be validated using physical relationships to identify outliers and errors
- Analysis relies on the availability of a large set of voyage data containing a wide range of environmental conditions. It is therefore difficult to determine degradation in ship performance as and when it occurs
- The ability to take non-linear multivariate relationships into account using standard statistical methods is limited, which affects the quality of the analysis
- The use of statistical method requires specialist knowledge. The methodology is therefore difficult to understand or validate by third parties

Examples of commercial performance monitoring systems based on statistical analysis are (MICAD 2008), (NCS 2008) and (InCoreTec 2005).

2.3.3 Deterministic performance analysis

Performance analysis by using hydrodynamic relationships to account for changes in environmental and ship's loading conditions was first introduced in 1926 by Telfer (Telfer 1926). Since then, many other methods have been derived. A review of six methods to correct sea trial data to standard conditions, based on propeller open-water characteristics and the speed-power curve can be found in (ITTC 2002c). Performance analysis of measured mile speed trials is however easier than analysis of service performance data. During normal service conditions, ship speed cannot be determined using measured mile trials but must be obtained from the speed log, which lacks accuracy in service conditions (Munk 2006a). The uncertainties in ship speed cause large errors in performance analysis. The problem with the measurement of ship speed has been long understood. As stated by Townsin *'Correction to standard conditions of power, displacement and weather may alter the general level of speed data and alter the error sequence, but does little to reduce the scatter. It may be concluded that it is the measurement of speed itself which is the principal source of error in ship performance data'* (Townsin et al. 1975).

To address this problem, the 'Generalised Power Diagram' can be used, originally derived by Telfer (Telfer 1926). A 'Generalised Power Diagram' (GPD) relates power, ship speed of advance and propeller revolutions for a particular wake fraction in one diagram. Knowledge of any two of these values enables the calculation of the third. The relationship holds for any weather or load condition, as long as the propeller characteristics do not change. It holds for fixed pitch propellers, where the propeller characteristics can be defined accurately. For controllable pitch propellers, the GPD should be developed for each pitch setting, which may be practically difficult to determine. The use of ship speed and delivered power implies that it is dependent on the correct selection of wake fraction. Wake fraction is subject to continuous change due to fouling, hull roughness, draft and ship motion, although the latter doesn't affect wake significantly. The GPD must therefore be 'calibrated' periodically by determining an appropriate wake fraction which will cause the calculated speed values to closely match observed values. Use can be made for example of data from the previous voyage for this

purpose (Townsin et al. 1975). In higher sea states, where waves and ship motion affect the wake fraction, the GPD cannot be used.

The generalised power diagram can be derived either from speed trials (Garg 1972; Telfer 1926) or propeller open-water characteristics from model tests (Garg 1972; Townsin et al. 1975). As discussed by Scott (Scott 1971), the use of trial results receives preference since no reliance has to be made on model results and the accompanying scaling errors. Figure 2.4 shows an example of a GPD for a cargo liner for shaft power, slip, ship speed and propeller revolutions for a wake fraction of 0.22.

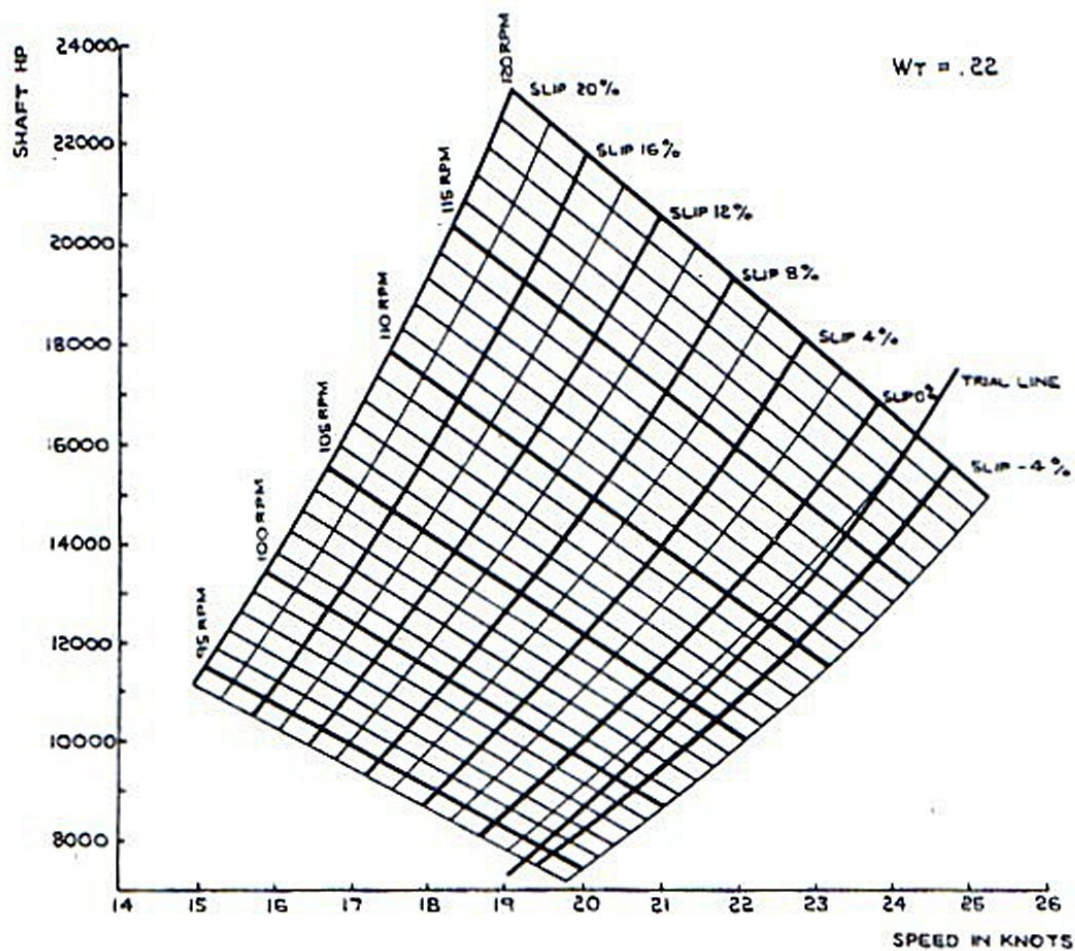


Figure 2.4: Generalised Power Diagram relating power, ship speed, RPM and slip ((Townsin et al. 1975) fig. 7)

Apart from using the GPD to calculate ship speed, it can also be used to convert performance data to a single pre-defined design speed or power. By entering the diagram

with power and revolutions and by moving along the same apparent slip line, the standard power or speed can be obtained (Garg 1972).

Significant improvements in performance estimation can be made by only correcting the ship speed through water and measuring performance in good weather conditions, as shown by (Toki 2005; Townsin et al. 1975; Townsin and Svensen 1980).

As an alternative to correcting ship speed and keeping power constant, variations in measured performance can be accounted for by correcting power. It is hereby assumed that the measured ship speed is reliable, which is debatable. The operating condition in standard conditions can then be calculated by separately calculating the added resistance from wind, wave, changes in displacement etc, and deducing this from the measured shaft power. A value for propulsive efficiency is hereby required to convert from shaft power to resistance. This can either be assumed, obtained from sea trials or calculated using the propeller open-water diagram. Many performance analysis methods use the same hydrodynamic principles to correct ship performance. Examples may be found in (Guedes Soares et al. 1998), (Andersen et al. 2005), (Kim et al. 2001), (Journée et al. 1987), (Grossman and Kloster 1993), (Toki 2005) and (Logan et al. 1980). The main difference between the methods is the basis to which ship performance is corrected; constant revolutions or constant ship speed, and how the propulsive efficiency is taken into account. The differences in calculated performance can be large. The correct selection is therefore important. Both differences are here discussed.

2.3.3.1 Deterministic analysis using constant propulsive efficiency, constant speed

Performance analysis using constant propeller efficiency and constant ship speed has been used widely and is described by e.g. (Aertssen and Sluys 1972; Andersen et al. 2005; SNAME 1989a). The correction to standard conditions relies on the calculation of the resistance from wind, wave, draft deviations, shallow water etc. The measured shaft power must therefore be converted to resistance. Using the measured shaft power P_D , ship speed V_s and an assumed propulsive efficiency η_D , the total resistance to be overcome by the propeller can be calculated by:

$$R_T = \frac{P_D \eta_D}{V_S} \quad (2.3)$$

The total added resistance from (windage, waves etc.), R_{ADD} , can then be deduced and the corrected power at the same ship speed can be calculated by:

$$P_{corr} = \frac{(R_T - R_{ADD})V_S}{\eta_D} \quad (2.4)$$

The correction for changes in draft and trim from the reference condition can be estimated from model test results, and is often expressed as percentage change in power per unit change in draft (e.g. every 10cm) over a range of speeds.

The assumption that the total propulsive efficiency remains constant during rough weather conditions and calm water conditions is however not correct. The total propulsive efficiency η_D is defined as:

$$\eta_D = \eta_O \eta_H \eta_R \eta_S \quad (2.5)$$

Where:

η_O = open-water propeller efficiency

η_H = hull efficiency = $(1-t)/(1-w)$

η_R = relative rotative efficiency

η_S = shafting efficiency

The efficiency varies as an effect of the varying wake fraction, thrust deduction and propeller loading. Hull fouling increases the wake fraction, and environmental conditions, such as wind and waves, influence the propeller open-water efficiency.

Added resistance results in a higher propeller load which decreases propeller efficiency. For example, if a 229m VLCC (details in (ISO15016 2002)) sails against the wind resulting in an added resistance of 10% of the total resistance, and this would be used to calculate the performance in standard conditions, the calculated power to obtain the same ship speed would be only 7% lower than the measured power. Three percent is gained by

the higher propeller efficiency in standard conditions. For 20% added resistance, the gain would become 6%. If a constant propeller efficiency would be used, the standard performance would be estimated too low.

2.3.3.2 Deterministic analysis using calculated propulsive efficiency, constant revolutions

By using the propeller open-water diagram to convert the performance to standard conditions, the change in propeller efficiency can be taken into account correctly. The correction to standard conditions can be done by measuring the delivered power, engine RPM and ship speed and using the well-known laws of propeller action. At any given shaft speed and a given speed of advance a propeller delivers a definite amount of thrust and absorbs a definite amount of power (Schoenherr 1931). This relationship is often expressed in the form of the thrust and torque coefficient K_T and K_Q . The correction to standard conditions using the propeller characteristics is done by the following steps:

- With the measurement of torque and RPM, the torque coefficient can be calculated:

$$K_Q = \frac{Q}{\rho N^2 D^5} \quad (2.6)$$

- The torque coefficient can be intersected with the propeller open-water diagram to get the advance coefficient J and the thrust coefficient K_T . Assuming the thrust deduction fraction is known and can be assumed equal to the model thrust deduction coefficient, the resistance to be overcome by the propeller action can be calculated:

$$R = (1 - t) K_T \rho N^2 D^4 \quad (2.7)$$

- When the added resistance components (wind, wave etc.) are known, the measured propeller thrust can be corrected by deducing added resistance components.

$$R_{std} = R - R_{ADD} \quad (2.8)$$

- Using a constant propeller speed of revolution, the thrust coefficient in the calm weather condition can be calculated:

$$K_T' = \frac{R_{std}}{(1-t)\rho N^2 D^4} \quad (2.9)$$

- By intersecting the K_Q curve from the open-water diagram with K_T' , the corrected power can be calculated:

$$Q_1 = K_Q \rho N^2 D^5 \quad (2.10)$$

$$P_1 = 2\pi N Q_1 \quad (2.11)$$

- With the intersection of K_T' with the propeller open water diagram, the new advance coefficient J_1 can be obtained. Assuming the wake fraction remains the same for the two conditions, the ship speed in standard conditions, V_{std} , can be calculated as follows:

$$V_{std} = \frac{J_1 N D}{(1-w)} \quad (2.12)$$

The new power and speed represents the power as if the vessel would operate in standard conditions at the same propeller revolution. This method is widely used for speed trial analysis and during the trials engine speed is kept constant for up- and downstream runs (Grossman and Kloster 1993; Guedes Soares et al. 1998; Journée et al. 1987; Schoenherr 1931; Toki 2005; Townsin and Svensen 1980). This correction method allows weather

and loading conditions to be taken into account, on the condition that information about open-water diagram and wake fraction is available.

2.3.3.3 Deterministic analysis using calculated propulsive efficiency, constant ship speed

According to the previous method, it is assumed that the difference in torque between the performance in service conditions (with a certain wind and wave) and calm water (no-wind and wave) conditions is a result of wind and added wave resistance only. However, another change in resistance takes place: the reduction in ship speed changes the hull resistance (frictional, form and wave) as well. In the previous described correction method, this is not taken into account (Taniguchi and Tamura 1966). The effect of the reduced ship speed on hull resistance, in terms of propeller torque is in the same order or even larger than the torque difference due to wind and wave and must not be ignored.

A method to take these effects into account was developed by (Taniguchi and Tamura 1966) summarised in the following. By using a load coefficient τ , the added resistance can be deduced from the measured performance in such a way that the ship speed remains constant. Hence, changes in hull resistance from speed reductions as the effect of wind or wave are avoided. The calculation method continues:

- With the measurement of torque and RPM, the torque coefficient can be calculated:

$$K_Q = \frac{Q}{\rho N^2 D^5} \quad (2.13)$$

- The torque coefficient can be intersected with the propeller open-water diagram to get the advance coefficient J and the thrust coefficient K_T . The propeller loading coefficient τ can be defined as:

$$\tau = \frac{K_T}{J^2} = \frac{T/\rho}{V_a^2 D^2} \quad (2.14)$$

- The decrement of τ due to the correction of wind and wave resistance component ΔR from the total resistance of the hull can be defined as:

$$\Delta\tau = \frac{\Delta R}{\rho(1-t)V_a^2 D^2} \quad (2.15)$$

$$\tau_1 = \tau - \Delta\tau \quad (2.16)$$

- The new propeller load coefficient τ_1 can be intersected with the τ - J propeller open-water curve to obtain the torque and advance coefficient in the standard conditions (indicated with subscript $_1$). The propeller absorbed torque and revolutions in the new condition can then be calculated using the K_Q - J curve and using:

$$Q_1 = K_{Q1}\rho N^2 D^5 \quad (2.17)$$

$$N_1 = N \frac{J}{J_1} \quad (2.18)$$

$$P_1 = 2\pi N_1 Q_1 \quad (2.19)$$

This method is based on the assumption that wake fraction for service- and calm water conditions is equal. A derivation of similar methods can be found in (ISO15016 2002; Kim et al. 2001; Taniguchi and Tamura 1966; Thomson 1978).

2.3.3.4 Discussion on the comparison the constant RPM and constant ship speed method

The difference between the constant ship speed and constant revolution method becomes especially apparent when the added resistance corrections are large. The previous method (constant revolution) takes the added resistance corrections more rigorously into account compared to the method using the constant ship speed.

Figure 2.5 shows an example of the differences in correction between the above two methods using measured data of the *Bernicia* which was used as one of the test vessels in this study. The performance of a ship is corrected to standard conditions using added

resistance R_{ADD} . The aim of the corrections is to get a smooth performance curve, in this case the RPM – torque curve. Any deviations from this curve identify the added resistance.

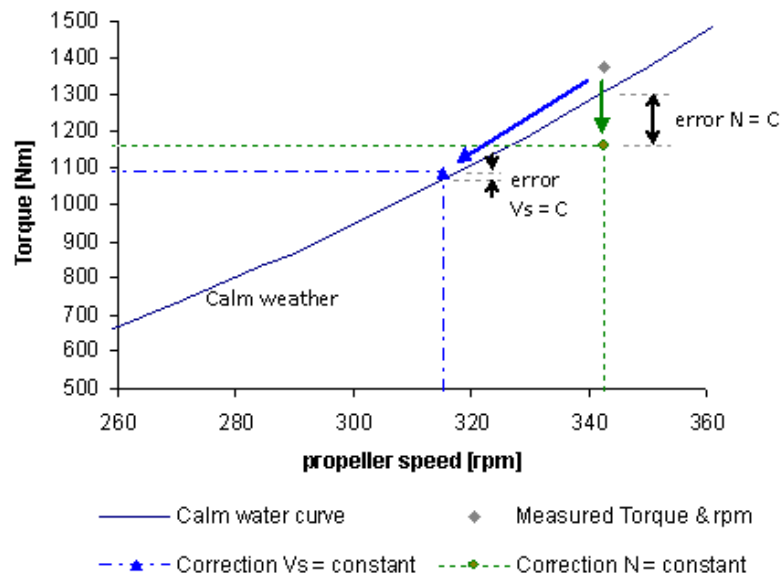


Figure 2.5: Differences in correction of ship performance of two methods

Method 1, based on the constant RPM approach, over-predicts the performance and predicts the resistance in calm weather lower than it should be, as indicated by ‘*error N = C*’. Method 2, based on the constant speed approach, corrects both speed and RPM, resulting in a much smaller error than Method 1. When Method 1 is used, it seems that the calculations for added resistance are approximately three times larger than expected. However, when Method 2 is used to assess the accuracy of the added resistance calculations, the correction seems accurate. The selection of the right methodology is therefore of significant importance for performance analysis.

Both methods described above rely on the availability of a complete set of ship hydrostatic data. The propeller open-water diagram, wind resistance coefficients, wave response resistance coefficients, wake fraction and thrust deduction fraction are parameters that must be known with great accuracy. Although all these coefficients have

been derived and known in the design stage of the vessel, practical experience indicates that they are often difficult to obtain by the ship owner or ship charterer. This has direct consequences to the accuracy and hence reliability of the analysed results based on the assumptions.

2.3.4 System identification

A radically different way of performance analysis is to conduct special periodic manoeuvres to determine the capabilities of the vessel, which are comparable with conducting trial runs. The runs consist of acceleration and deceleration manoeuvres whereby the performance is carefully logged. By using system identification techniques based on first principles of physics, the calm water resistance of a ship can be obtained without the need for any predefined propulsive characteristics. The fact that no model tests are required reduces a considerable amount of uncertainty from scaling errors, especially for full bodied ships (Abkowitz 1989). The calculated propulsion coefficients represent the full scale performance and all hull-propeller interactions are being treated implicitly.

In spite of their potential attraction, system identification techniques have not raised practical interest in the shipbuilding community, possibly due to the following shortcomings:

- There are no yardsticks or reference points available other than consistency checks to validate the methods and used axioms, since most hydrodynamic relationships can only be determined in model scale conditions using conventional methods
- Special manoeuvres are required, which makes it not suitable for use on a day-to-day basis (manoeuvres require additional attention and hinder the normal operation of the vessel). Therefore it can only be used for long-term trend/performance analysis
- The methods are still in development and are not in use by large ship builders or design companies. To recognise and accept the methodology's outcomes, methods can therefore only be used in parallel with traditional systems

- The methods rely on the measurement of thrust, which is practically difficult to measure with long-term stability
- The system identification techniques, described by Schmiechen and Abkowitz, predict the resistance lower than the traditional techniques (Abkowitz 1980; Abkowitz 1988; Abkowitz 1989; Schmiechen 1991a; Schmiechen 1998). Shipping companies are therefore more reluctant to use system identification techniques. Traditional techniques already incorporate a higher safety factor to account for calculation of manufacturing errors which seem to be necessary. At first sight, an even lower prediction of resistance does not seem to be correct.

2.3.5 Selection of analysis method

The analysis of ship performance can be done ashore or onboard, which has implications on the selection of the correction methodology and the use of the data. The thesis focuses on real-time, onboard data collection, monitoring and analysis so that performance indicators can be used directly as feedback for ship operation. This requires a transparent and deterministic correction method. System identification or statistical regression analysis techniques are here not suitable, as they require specialists to interpret the data and large datasets to develop regression coefficients. The most rigorous and usable method to correct performance real-time is based on the conversion of delivered power to thrust using propeller characteristics, from where the added resistance from wind, waves, draft etc. (calculated using empirical calculations) is deduced, as discussed in Section 2.3.3. Deterministic data analysis is therefore used in this thesis for performance analysis.

2.4 Performance Indicators

The way that ship performance is represented using meaningful indicators can be done in numerous ways. Performance indicators may be characterised by the following aspects:

- The principal components they describe; hull, propeller and / or engine condition
- The ability of the indicator to account for changes in speed, environmental conditions, displacement etc.
- The sensitivity of the indicator to errors in data; certain parameters rely for example on an accurate speed log, while others are based on an accurate torque sensor
- The physical representation of the indicator; certain parameters are more intuitive and easy to interpret than others
- Ability to identify slow time varying performance changes, e.g. due to fouling

Due to the many criteria, none of two indicators is the same or can be compared. To avoid misinterpretation, it is therefore important that the characteristics and applicability of a Key Performance Indicator (KPI) are accurately known, and that uncertainty bands are included.

Most KPIs are based on the indication of either one of speed, power, fuel consumption or a combination hereof. Table 2.2 shows a number of frequently used KPIs for performance monitoring. They differ in the way they exclude the engine, propeller or hull condition, sensitivity to voluntary changes in engine speed and sensitivities to input parameters (such as speed or torque). The following sections describe the listed indicators.

Table 2.2: Frequently used Key Performance Indicators for ship performance

Indicator	Principal component (<u>E</u> ngine, <u>P</u> ropeller, <u>H</u> ull)	Affected by voluntary speed deviations
Based on Fuel consumption vs. time		
- Fuel consumption	<i>E, P, H</i>	<i>yes</i>
- Specific Fuel Consumption	<i>E, P, H</i>	<i>To limited extend</i>
- Specific Fuel Consumption ratio	<i>E, P, H</i>	<i>no</i>
Based on ship speed vs. time		
- Ship speed through water	<i>P, H</i>	<i>yes</i>
- Apparent Slip	<i>P, H</i>	<i>To limited extend</i>
- Speed or power loss	<i>P, H</i>	<i>no</i>
Based on RPM or power vs. time		
- RPM loss	<i>P, H</i>	<i>no</i>
- Torque loss (relative or absolute)	<i>P, H</i>	<i>no</i>
- Engine service margin	<i>P, H</i>	<i>yes</i>
Based on ship speed & torque or RPM		
- Admiralty coefficient	<i>E, P, H</i>	<i>Tolimited extend</i>
- Admiralty coefficient vs. slip	<i>E, P, H</i>	<i>no</i>
- Effective wake fraction	<i>P, H</i>	<i>no</i>
- Ship speed vs. fuel consumption	<i>E, P, H</i>	<i>no</i>
- Ship speed vs. delivered power	<i>P, H</i>	<i>no</i>
- RPM vs. torque	<i>P, H</i>	<i>no</i>

2.4.1 KPIs based on fuel consumption versus time

Fuel consumption gives an indication of the overall ship performance, as it is affected by the following conditions:

- Engine efficiency (maintenance, wear, engine timing settings, inlet air temperature and humidity, cooling water temperature)
- Method of engine control (engine speed, pitch or fuel rack)
- Fuel characteristics (density, calorific value, water content)
- Propeller loading (which is a function of environment, speed, draft, trim, hull condition etc)
- Propeller condition (roughness, fouling, damage)
- Load demand from shaft generators (if applicable)

Apart from the physical causes of changes in fuel consumption, the characteristics and accuracy of the fuel measurement directly influence the KPI fuel consumption versus time. The way fuel is measured (e.g. by tanks soundings, using a flow meter or estimated based on fuel rack etc.) and whether it represents total fuel consumed or fuel burned by the main engine alone has large implications on accuracy and precision on fuel consumption readings. Considering the many parameters that influence fuel consumption, for ship performance monitoring it is a rather blunt indicator.

By relating fuel consumption to output power, an indication of engine efficiency (Specific Fuel Consumption ‘SFC’) can be obtained. Most marine diesel engines are designed to run with the highest efficiency between 70-90% of their Maximum Continuous Rating (MCR). Deviation from this rating causes a drop in efficiency and hence increases the SFC. Figure 2.6 shows an example of two SFC curves for large slow-speed diesel engines.

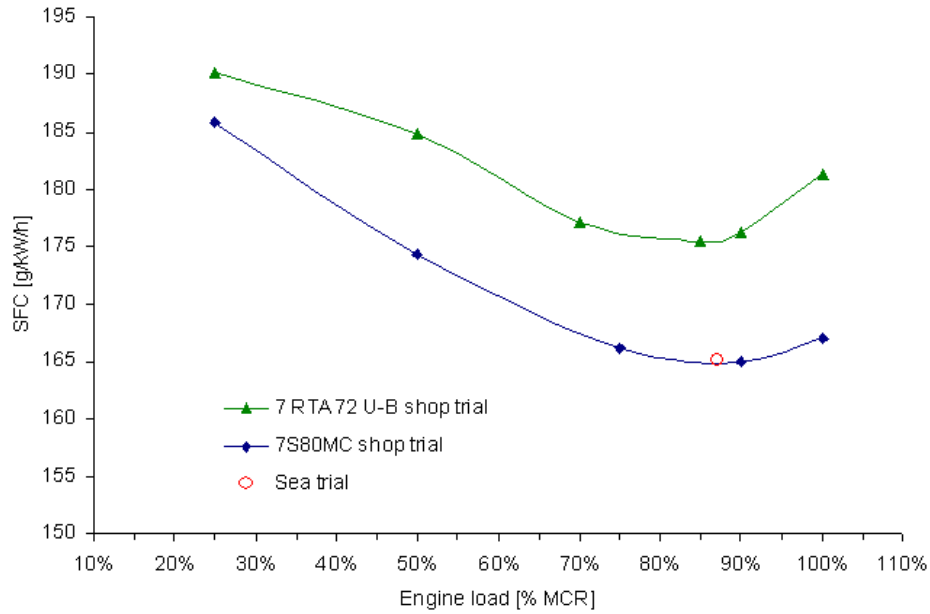


Figure 2.6: Specific fuel consumption vs. Engine load for a container ship (upper) (Wärtsilä 2004) and VLCC (lower curve) (Hitachi-Zosen 2001)

Because of this load dependency, the SFC can not be plotted directly against speed. However, by dividing the measured SFC by the SFC obtained during speed trials at the same power, a single parameter is obtained that can be plotted against time. The SFC as a percentage deviation from a benchmark condition is easier to interpret than absolute numbers and is valid for the complete power range. The SFC ratio R_{SFC} can be defined as:

$$R_{SFC} = \frac{SFC(P_S)}{SFC_{TRIAL}(P_S)} \quad (2.20)$$

Where $SFC(P_S)$ is the measured specific fuel consumption at shaft power P_S and $SFC_{TRIAL}(P_S)$ is the specific fuel consumption at sea trials at the measured shaft power P_S . It is important that the relationship SFC_{TRIAL} vs. P_S relates to sea trials and not to the shop tests. Engine shop trials may be done with different load characteristics (applied torque at set RPM) than the load characteristics of the propeller during sea trials, which influences the SFC.

Apart from output power, specific fuel consumption is also dependant upon the load balance (absorbed torque at set RPM) of the propeller. Figure 2.7 shows the engine performance diagrams in terms of constant SFC curves of a *MAN K8SZ 90/160-B* and *K8SZ 90/160-BL* slow speed marine diesel engine. For the *KSZ-BL*, two propeller curves are plotted. The lower curve represents design conditions, while the blue curve represents a high loaded propeller, e.g. due to hull and propeller fouling or rough weather. When the engine runs in design conditions, around 70-90% MCR and at its highest efficiency, it may be seen from Figure 2.7 that with increasing propeller loading, the SFC increases.

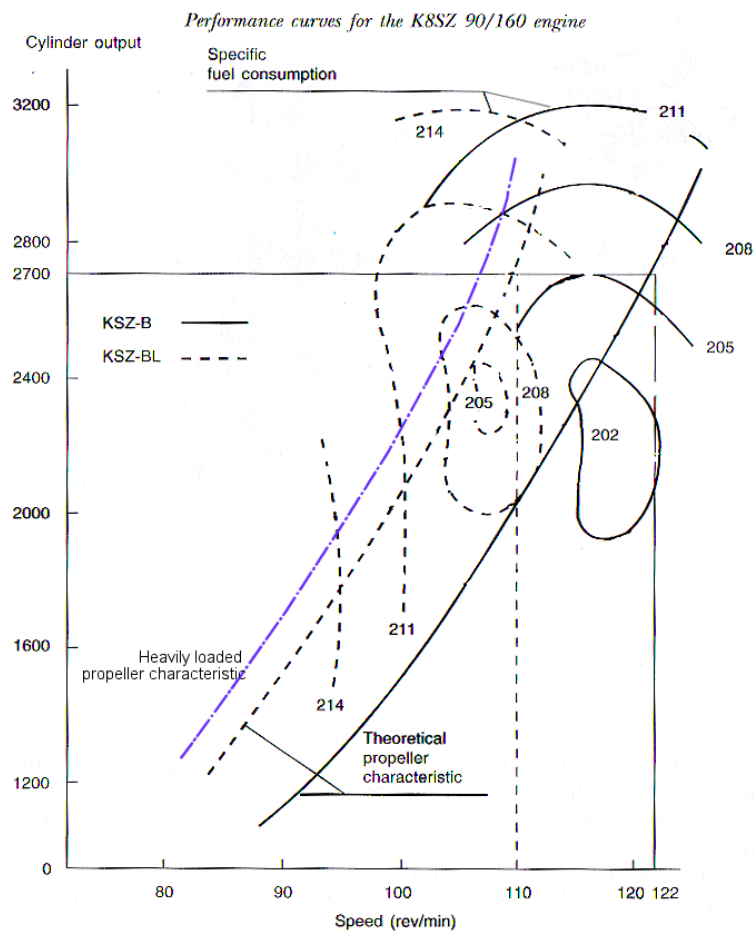


Figure 2.7: Performance curves with constant SFC curves for a *MAN K8SZ 90/160* engine. A normal and heavily loaded propeller characteristic is included. ((Woodyard 1998) fig. 17.4)

Because the engine efficiency is dependent on propeller load, the relationship SFC versus output power, as shown in Figure 2.6, cannot be used to indicate engine efficiency on its own. Ostojic illustrated the effect of propeller fouling and hull fouling on the SFC increase of a diesel engine (Ostojic 1990). Based on data collected from over 30 vessels and empirical calculations, he related roughness to power and SFC increment to maintain ship speed (Figure 2.8 and Figure 2.9).

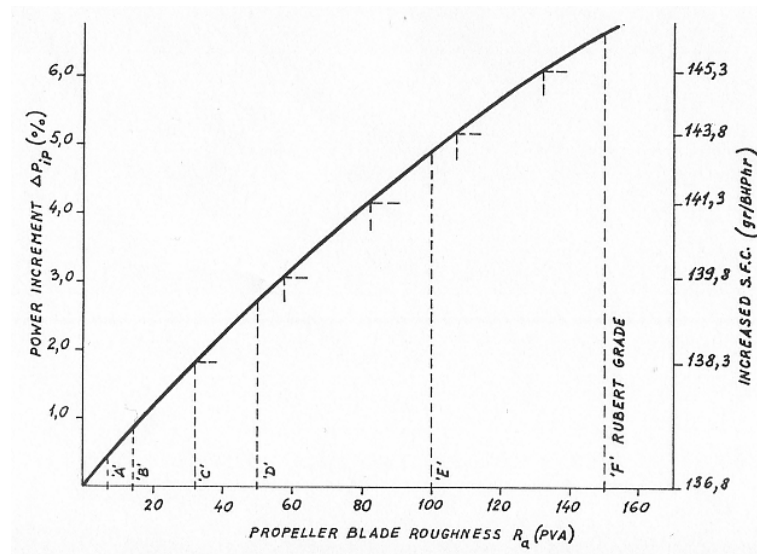


Figure 2.8: Increase in SFC with increase in propeller roughness (Ostojic 1990)

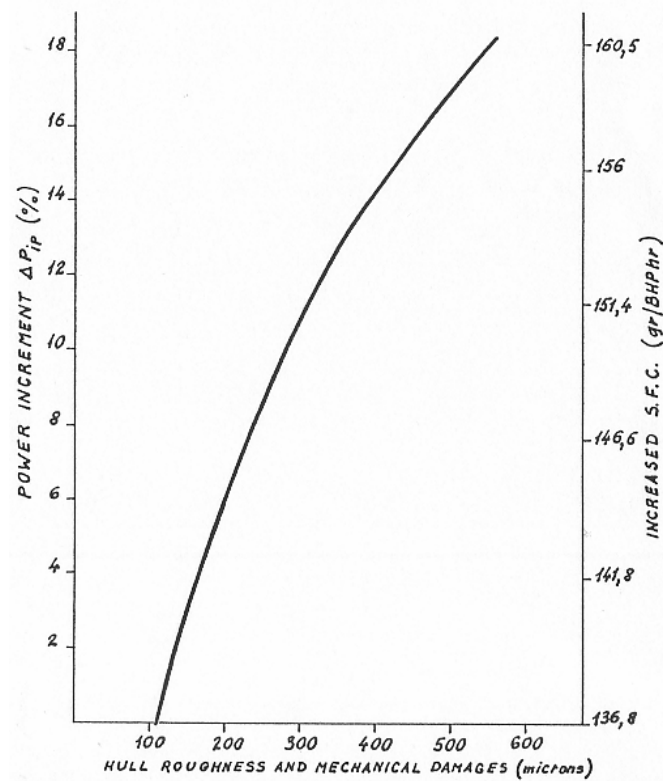


Figure 2.9: Empirical relationship between hull roughness, power & SFC to maintain ship speed (Ostojic 1990)

Although electronic engine speed control systems have reduced the efficiency drop for increases in loading at constant RPM, the effects illustrated in Figure 2.8 and Figure 2.9 may still be apparent and should be considered.

It may be concluded that specific fuel consumption as indicator for performance monitoring can only be used as a rough indicator of the engine's performance. To be able to compare engine performance changes between different engines or ships, a complete performance check of the initial engine condition must be made so that corrective measures can be taken. This includes the logging of combustion conditions, engine balance, load, and outside influences.

2.4.2 KPIs based on ship speed against time

Ship speed through water (STW) is a frequently used parameter for performance monitoring. It describes propeller and hull efficiency. If directly plotted against time, with the assumption that the ship sails at a constant RPM, it is affected by the physical measurement of ship speed using the speed log, (calibration errors, unsteady currents under the ship, water characteristics, hull fouling etc.) and environmental and loading conditions. Especially the physical measurement causes most of the fluctuations.

Ship speed (STW) is often confused with ship speed over ground (SOG), or speed made good measured by GPS using the distance and time taken to travel between two points. The speed over ground includes the direct effects of currents and gives therefore not much useful information of the performance of a ship.

Slip is defined as the difference between the distance a boat actually travels through the water and the theoretical distance it would travel if it advanced the full pitch length of the propeller. When the ship speed reduces, the propeller loading and consequently the slip ratio increases. By comparing the slip with a benchmark slip, obtained during sea trials, the changes in performance can be obtained. Voluntary changes in engine speed affect slip ratio only little. However, slip is still influenced by environmental and loading conditions and relatively difficult to interpret.

Within the context of ship speed a better and easy to interpret KPI is ‘speed loss’, defined as:

$$\text{Speed-Loss} = V_{STrial}(SHP) - V_{SM}(SHP) \quad (2.21)$$

Where:

$V_{SM}(SHP)$ = measured ship speed through water at power SHP

$V_{STrial}(SHP)$ = ship speed obtained during sea trials at the same shaft power

This KPI accounts for voluntary speed changes and indicates a direct usable parameter that can be used for voyage planning and navigation. It is however influenced by the power measurement, and introduces therefore additional uncertainties.

2.4.3 KPIs based on RPM or power against time

Most marine diesel engines are speed controlled. In certain cases, maximum power is required and the governor is overruled to obtain maximum fuel flow, whereby power fluctuations cause swings in engine speed. If it is assumed that this condition rarely applies, it can be said that, within limits, the engine RPM will remain constant for a constant telegraph setting on ships. The indicator RPM versus time gives therefore no information about ship performance. However, if it is related to power output, such as ‘RPM-loss’, it provides an easy to interpret indicator, independent of voluntary speed changes. RPM loss can be calculated by:

$$RPM - loss = n_{Trial}(P_S) - n_M(P_S) \quad (2.22)$$

where $n_{Trial}(P_S)$ is the propeller speed that was obtained at power P_S during sea trials at the maiden voyage, and $n_M(P_S)$ the measured propeller speed at P_S . It is affected by sensor drift and calibration errors in the power measurement. Torque loss can be calculated in similar manner, by comparing the measured torque with the torque obtained at the same RPM in trial conditions. The big advantage is that this KPI is speed corrected, but without the measurement of ship speed. However, both RPM and torque loss are relatively weak indicators for hull fouling. Frictional resistance is a function of ship speed, and has therefore little to do with RPM and torque. Only when wake fraction is known, can the RPM and torque be related to ship speed. The increase in RPM or torque loss due to fouling is therefore less than when e.g. speed loss is used.

RPM or torque loss gives a measure of propeller and hull efficiency only. It is independent of engine condition, since the propeller can be considered a torque absorber, unaffected by engine output.

Another KPI sometimes found to be used is Service Margin. Service Margin (SM) is calculated by dividing output power (P_S) by the engine’s maximum continuous service rating (MCR) and can be used when RPM remains constant:

$$SM = \frac{P_S}{MCR} \quad (2.23)$$

As the propeller absorbed power increases, service margin reduces. Apart from the difficulty in interpretation (as it is related to a condition that cannot be reached even in new conditions), it is affected by operational, environmental and loading conditions and the physical errors in power measurement. It will therefore lead to considerable scatter.

2.4.4 KPIs based on ship or engine characteristics

Admiralty coefficient

The definition of Admiralty coefficient has been given earlier by the following relationship:

$$A_c = \frac{\Delta^{2/3} V_s^3}{P_s} \quad (2.24)$$

where Δ is displacement, V_s is STW and P_s the shaft power.

The use of the Admiralty coefficient has been the basis of many service performance analysis programs used by ship owners and paint manufacturers (see e.g (Carlton and Parsons 1989; Wallentin 2004)). In section 2.3.1 an example was given of the Admiralty coefficient for a container ship over a period of 8 years. A large scatter was observed. Some of the scatter may be contributed to the characteristics of the coefficient.

Since the admiralty coefficient was derived around 1850, assumptions in the derivation of the relationship are not always valid anymore. For example, the majority of merchant ship forms nowadays appear to have been selected so that at their design speeds their power is varying as the 4th power of the speed, instead of the 3rd. Furthermore, it is always found that when a vessel is being used at smaller draft than the designed loaded draft, the admiralty constant is lower than in the designed loaded condition (Telfer 1972). One reason for this lies in the fact that for a given vessel the wetted surface does not vary as the two-thirds power of the displacement, but, theoretically at least, as the square root of the displacement (Telfer 1972).

Regardless the improvement in performance indication over simply plotting vessel speed or fuel consumption, it is furthermore subject to interpretation problems. Admiralty coefficient is a relatively abstract parameter with little physical meaning. It combines engine, propeller and hull performance and the inherent amount of scatter make it difficult to use. Attempts have been made to reduce the variations in Admiralty coefficient by relating it to apparent slip. By plotting the admiralty coefficient versus slip, typically a linear curve can be plotted over the range of interest for difference weather conditions and loading conditions (Carlton 1994). However, difficulties with interpretation still remain.

Wake fraction

Effective wake fraction is a more robust performance indicator. It is calculated by means of the measured torque, RPM and ship speed through water and the propeller open-water diagram. It is only little affected by speed and propeller loading, but deviates depending on draft and fouling. The fact that wake is only little influenced by fluctuations in environmental conditions and voluntary speed reductions, and is not affected by engine performance make it a strong indicator for ship performance (Carlton 1994). Because the wake fraction relies on the measurement of ship speed through water, it is affected by the physical errors in measurement from the speed log. Furthermore, it is sensitive to errors of the torque sensor. Because the wake has no physical meaning, it is difficult to interpret without in-depth knowledge. For online performance analysis onboard, it is therefore not directly suitable.

Speed versus Power

KPIs that show the relationship between two physical parameters have the advantage that regression curves can be derived based on sound hydrodynamic relationships, model tests or trial data, which can be extrapolated to wider speed or power ranges. The relationship can however not be plotted versus time out of dock. For the indication of slowly developing changes in performance, such as fouling, this may cause inaccuracies. The selection of a data period used to derive a regression curve is important. If one year of

data is selected to derive a regression curve, performance in the beginning of the year, where the ship is little fouled, is mixed with data in the end of the year, where the ship is more fouled. The regression curve will therefore indicate the mean performance, and not represent the actual performance of the vessel at the end of the year. A shorter period is therefore necessary. The length of the period is however difficult to define. There should be sufficient data to reduce the influence of outliers and random variables, but short enough to avoid performance of different engine, propeller or hull conditions to be mixed. One way to avoid this problem is by using the KPI speed loss, as described before.

Ship speed versus power is a common used relationship throughout the design of a vessel. It can be directly related to resistance and hull fouling and is easy to interpret. The disadvantage of the speed-power relationship is the steep gradient (4th-5th order) that the curve typically has. As a result, at high speeds the power becomes extremely sensitive to ship speed. Because the speed log has typically a large random error, in the order of knots, the speed – power plot typically has a large clutter.

RPM versus Torque

As with the relationship speed-power, the KPI RPM-torque cannot be plotted directly against time out of dock. The selection of the period for regression analysis must therefore be chosen with care. The resistance of a ship is related to ship speed and therefore manifests itself less well by changes in torque or rpm. Changes in propeller performance on the other hand, for example increase in blade roughness, reflects itself as an increase in torque at constant rpm, and is only marginally affected by ship speed. The relationship RPM-torque is therefore suitable for propeller performance monitoring when no measure of delivered thrust is available. As with all KPIs based on a measure of power or torque, it is sensitive to calibration errors of the torque sensor (as discussed in section 3.4.2). Engine speed on the other hand can be regarded as the most accurate to measure parameter on ships. Because the RPM-torque relationship can be approximated by a 2nd order polynomial, based on the wake fraction and the propeller characteristics, outliers or inconsistencies can be identified easily (MOL 2003).

2.4.5 Other KPIs

Real-time indicators for operational feedback

Apart from performance indicators that can be used to indicate long-term developments, a number of indicators can be used more specifically for voyage analysis, either for real-time feedback on vessel operation or for voyage planning, for example:

- Real-time indication of the energy distribution; which percentage of the developed power is spend to overcome ship resistance, wind resistance, wave resistance, shallow water resistance etc.
- Speed or fuel loss over a period of time due to weather, fouling, sea condition etc.
- Time loss due to weather, fouling, manoeuvring etc.

Indicators based on added resistance are dependent on the accuracy of the empirical predictions, which are difficult to estimate. Speed, fuel or time loss may be calculated based on a pre-defined reference condition and are therefore more accurate to indicate.

Ship energy-performance rating

Ship energy benchmarking/rating can be used to assess the performance of a vessel against best-in-class equivalents. Furthermore, it can be used as a policy tool. For example, the CO₂ production per mile of cars is currently used by the UK government as the basis of setting the road tax in order to encourage the use of energy efficient and environmental friendly cars. With the expanding application of Green House Gas emission control protocols, approval of the IMO CO₂ index for voluntary application (IMO 2005), and forthcoming emission trading schemes, similar policy tools are introduced within the shipping industry. The following energy rating KPIs may be used for this purpose (Bazari 2006):

1. Fuel consumption index (fuel consumed / weight carried / distance travelled)
 - Ship Energy Intensity (energy consumed / weight carried / distance travelled)
 - Propulsion Energy Intensity (propulsive power / weight carried / ship speed)
 - CO₂ Intensity (CO₂ produced / weight carried / distance travelled).

2.5 Conclusions

In this chapter a review is given on the types and characteristics of different ship performance monitoring & analysis systems. PM&A systems have been broken down in data collection, analysis and performance indication and reviewed separately. It is concluded that:

- Many PM&A systems focus on analysis, and rely on the quality of the data collected in manual log books such as abstract logbooks, which cannot provide the required accuracy and reliability needed for performance analysis. The only way to improve the accuracy and reliability of any KPIs is to collect more reliable and accurate data through the use of a dedicated, automatic data acquisition system
- Data analysis is often based on simple linear regression of data filtered for bad weather and speed deviations. This causes large uncertainties and results in unreliable and sometimes contradicting results. More advanced analysis systems do not provide insight in data analysis, which reduces the usability and trustworthiness of these systems
- A more rational and deterministic approach to correct ship performance to standard conditions is to calculate added resistance from wind, wave and displacement variations, and use the propeller characteristics to deduce the resistance from the thrust generated from the propeller. This correction should be done based on the correction of torque and rpm with constant ship speed
- Ship speed through water is difficult to measure but it is one of the most important parameters for performance analysis. Ship speed can be validated using a ‘Generalised Power Diagram’ (GPD) which is based on the accurate measurement of torque and wake fraction. However, this requires the use of a fixed pitch propeller
- The suitability of indicators for ship performance depends on its use and the type of performance analysis that has been used. The performance of the engine, propeller and hull should be separated through correct selection of the KPI. Furthermore, differences in sensitivity of KPIs to input parameters, e.g. speed, torque or rpm and speed variations should be considered.

- In order to create a trustworthy system, data collection and analysis should be done transparently and presented using easy to interpret and well described KPIs
- The combination of real-time automatic data collection, focussing on data validation and direct automatic data analysis and display of results onboard is the way forward for any PM&A system. In the following chapters, all aspects related to the design and evaluation of such a system and its implementation onboard of two full-scale vessels are described.

3

DATA DESCRIPTION

3.1 Introduction

In the previous chapter it has become clear that accurate performance data, obtained automatically with a high rate of data acquisition is one of the most important requirements for performance monitoring. The quality of the collected data depends on the data conditioning characteristics, sensor characteristics, environment of the sensor, and the behaviour of the ship. The main objective of this chapter is therefore to review the ship's environment and operation and the way it affects ship performance and sensor operation, and to design a practical, reliable and accurate data acquisition system suitable for performance monitoring and analysis.

To address the above objective, this chapter is divided into 4 sections. Section 3.2 describes the marine environment in order to understand the characteristics of the physical phenomena that affect ship performance and that should be measured. Section 3.3 describes the ship's behaviour in operational (speed, draft, acceleration, manoeuvring etc.) and environmental conditions (ocean, wind, waves, fouling). From this review, the parameters that must be logged for correcting ship performance to the standard performance conditions are identified. The sensitivities and uncertainties with the measurement of the parameters identified are described in Section 3.4. Finally, in Section 3.5, the signal conditioning that is required to improve the data collection is described.

As stated in the first chapter, in this thesis the review of the ship behaviour in different operational and environmental conditions, and the data conditioning requirements have been determined based on real-time data collected on two test vessels; the RV *Bernicia*, a 16m trawler type research vessel of Newcastle University, and the MT *Overseas Tanabe*, a 333m, 300.000dwt VLCC from OSG Ship Management. Both vessels were equipped

with a range of sensors and a tailor made data acquisition system by the Author. Details regarding the installation of the sensors, a full description of the data acquisition system and experience with data collection on both vessels is further discussed in Chapter 5. However, some relevant data collected on these vessels are used in this chapter to support some of the discussions of this chapter.

3.2 Ship's environment

The ship's environment consists of the sea which is affected by waves, current, water depth, viscosity and density, and the atmosphere surrounding the ship including the effect of wind, temperature & density. Furthermore, marine bio-fouling can also be considered as part of the marine environment. The environment affects the way a ship behaves in service conditions, the way environmental parameters can be measured and the uncertainties that are present when logging them. A thorough understanding is therefore important. In this section, a review is given of the relevant characteristics of the marine environment.

3.2.1 Waves

Ocean waves can be separated in wind generated gravity waves and swell. They are affected by wind speed and duration, water depth, fetch, currents etc. Most waves appear confused and completely irregular. Their severity can therefore not be described visually and can only be described in terms of a wave amplitude energy density spectrum. Figure 3.1 shows an example of four energy spectra for the North Atlantic Ocean.

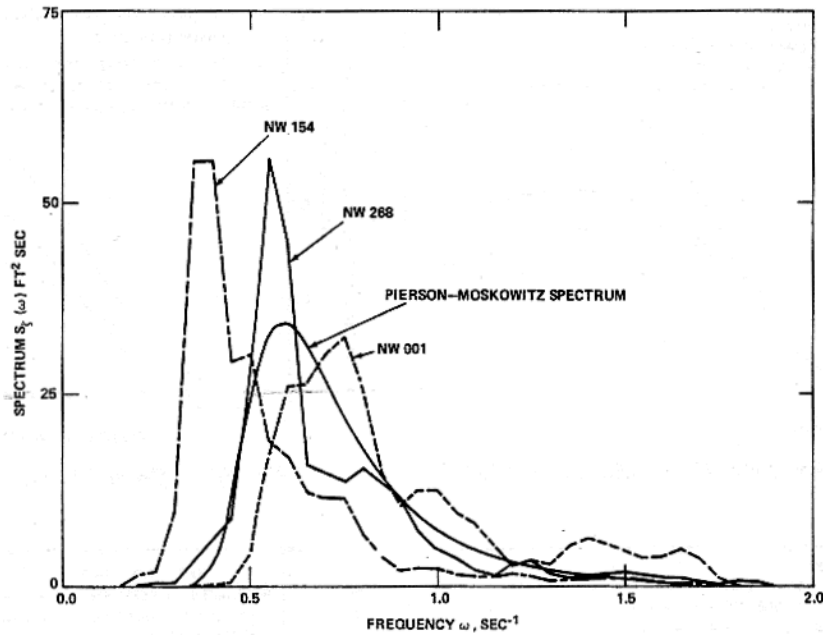


Figure 3.1: Three typical North Atlantic sea spectra compared with Pierson-Moskowitz spectrum ((Strom-Tejsen et al. 1973) Fig. 21)

Mathematical models enable a spectrum to be expressed as some functional form, usually in terms of frequency or frequency and direction. Perhaps the simplest spectrum model is that proposed by Pierson and Moskowitz (Pierson and Moskowitz 1964). They assumed that if the wind blew steadily for a long time over a large area, the waves would come into equilibrium with the wind to form a ‘fully developed sea’. Using accelerations from British weather ships in the North Atlantic Ocean in waves, they derived the following equation to describe the observed wave spectra:

$$S(\omega) = \frac{\alpha g^2}{\omega^5} \exp \left[-\beta \left(\frac{\omega_0}{\omega} \right)^4 \right] \quad (3.1)$$

Where $\omega = 2\pi f$, f is the characteristic wave frequency in Hz, $\alpha = 8.1 \times 10^{-3}$, $\beta = 0.74$, $\omega_0 = g / U_{19.5}$ and $U_{19.5}$ the wind speed at the height of the anemometers on the weather ships, 19.5 m above sea surface.

The assumption that any sea can be described by a spectrum model based on the wind speed alone is however inaccurate. Gulev (Gulev and Hasse 1998) indicated using wave measurements from the Northeast Atlantic Ocean that most of the wind generated waves are not fully developed. The relation between wind speed and wave height becomes therefore irregular and unusable. However, even when significant wave height is used to characterise a sea spectrum, the variations in possible spectrum shape for any wave height is still extremely large. The three sea spectra in Figure 3.1 for example are plotted for the same wave height, but differ in energy density and characteristic period. Record NW 154 shows a decaying sea state, whereby the major energy is concentrated at the lower frequencies, indicating swell. NW001 is an example of a developing sea, while NW 268 represents a spectrum that is fully developed. The Pierson-Moskowitz spectrum represents in principle a fully developed sea. The variations in spectrum shape and characteristic wave periods represented by these examples will produce radically different values of added resistance for a given response curve even through all spectra have nearly the same significant wave height. The added resistance might differ for as much as a factor 3 (Strom-Tejsen et al. 1973).

In order to make a distinction between different wavelengths, the wave period should therefore be included. Furthermore, since about 25% of all spectra from open ocean and coastal areas is double peaked due to swell (Rodriguez et al. 2002), corrections should be made for swell. An overview of frequently used wave spectra models, can be found in (ITTC 2002b).

Apart from the uni-directional sea spectrum, the directional spreading of the sea must be accounted for as well. Irregular seas are formed by waves from different directions to form a directional wave spectrum. In fully developed seas, this can be approximated by the product of the wave energy spectrum and an uni-modal angular distribution with mean direction approximately equal to that of the wind direction (Mitsuyasu and Mizuno 1976). Many forms exist in representing the spreading. For practical purposes the following spectrum can be used for fully developed seas: (Yoshino and Matsumura 1997):

$$G(\theta, \omega) = \frac{2}{\pi} \left| \cos(\theta - \bar{\theta}) \right|^2 \quad (3.2)$$

For swell, the JONSWAP spectrum can be used in combination with the following directional distribution:

$$G(\theta) = 2 \left| \cos\left(\frac{\theta - \bar{\theta}}{2}\right) \right|^{100} \quad (3.3)$$

3.2.2 Current

Sea currents are a function of many environmental, geographical and physical parameters. Especially in coastal areas, current speed may vary considerably with depth and depend on tidal & global currents and wind and wave stresses. Figure 3.2 shows a current profile for an offshore buoy on the West coast of Florida, USA. It shows that current velocity can vary considerably over depth and time. In this particular example, differences of up to 0.4kn over the first 18m of the ocean surface are apparent. The large variations in current over the first 20m of the sea surface make the definition of the mean current the ship's underwater hull experiences difficult. A speed log installed on the bottom of a ship, measuring the speed of the water relative to the bottom of the hull, does therefore not necessarily indicate the actual speed experienced by the ship, resulting in erroneous speed figures. Furthermore, Figure 3.2 indicates that sea surface current measurement techniques (e.g. wave radars) cannot accurately be used to determine current speed and direction. One solution would be e.g. to install different logs along the hull at different water depths.

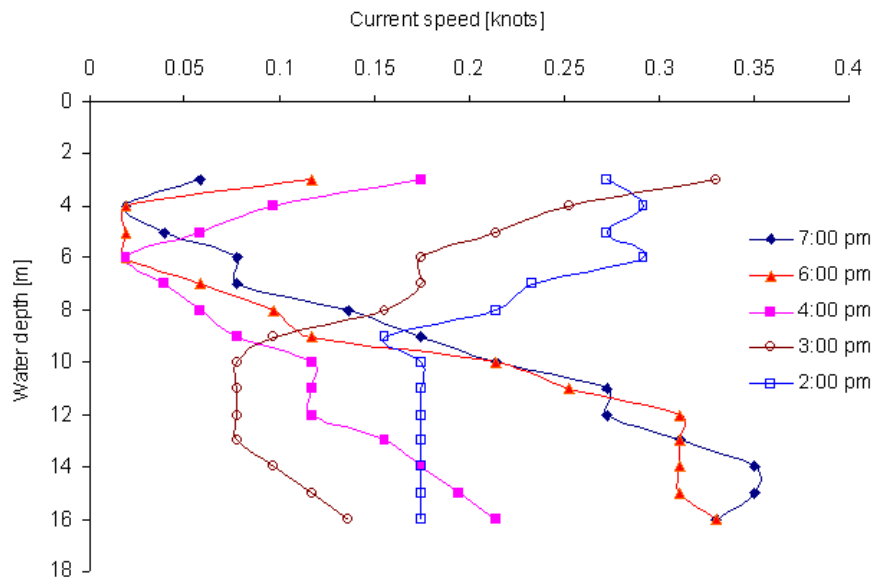


Figure 3.2: Ocean current profile for wave buoy station 42014 West Florida South East Atlantic coastal system at 19-4-2005 (NDBC 2005)

3.2.3 Atmosphere

Wind has a highly fluctuating nature. The relevance of the fluctuations for ship operation is limited to mainly the longitudinal high energy wind turbulences that have relatively long time periods and dimensions, so that it can be assumed that the whole ship is affected. For the measurement of wind speed, short wind fluctuations should therefore be filtered out. Apart from the turbulences, the wind close to the sea surface has a different speed compared to the wind at higher levels. The surface of the sea causes a frictional drag on the wind slowing down the wind close to the sea surface. The dynamic head experienced by the vessel close to the sea surface is therefore less than the dynamic head higher up on the superstructure. The mean head may be calculated at the vessel's mean head calculated by $z = A_L / L_{OA}$ with A_L the lateral-plane area and L_{OA} length over all. The wind speed at this height can be described by (Blendermann 1996):

$$\bar{u}(z) = u_h \left(\frac{z}{h} \right)^{\frac{1}{n}} \quad (3.4)$$

Where $\bar{u}(z)$ is the wind at height z above water level and \bar{u}_h the wind speed at reference height h (100m). For strong winds $\bar{u}_{10} > \sim 6$ m/s, for which constant atmospheric conditions are met at sea, $n \cong 8$ to 12 may be assumed. A suitable mean value is $n = 10$. For light winds or winds over open harbour areas the atmosphere is generally unstable. The wind profile is then less full and is better approximated by $n \cong 5$ to 6 (Brix 1990). Figure 3.3 shows two wind gradients for $n = 5$ and 10.

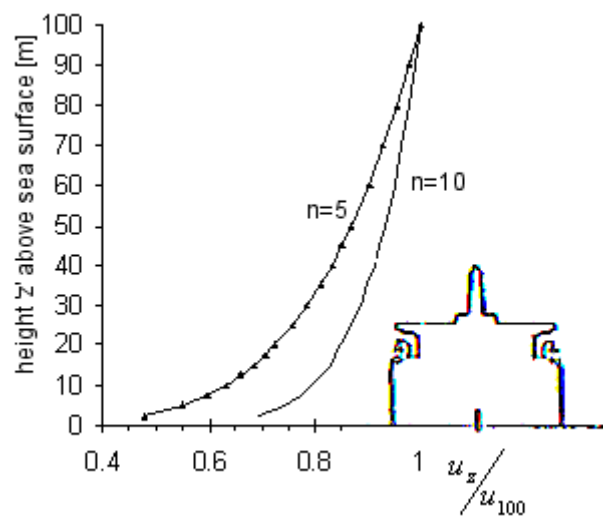


Figure 3.3: Wind gradients for strong ($n = 10$) and light winds ($n = 5$) at open seas displayed as function the ratio wind speed at height z to free wind speed at 100m.

The wind force fluctuations above the sea surface can be estimated by means of a Gaussian energy distribution spectrum, which changes as a function of ship speed (Brix 1990). For winds at open seas, well away from any coastal areas, the wind turbulence is relatively small compared to the mean wind speed (for a typical turbulence intensity at sea, about 2/3 of all fluctuations fall between $\pm 0.1 \cdot \bar{u}$). For marine applications the wind speed can be therefore be calculated using a 10 minute average (Brix 1990; Taylor et al. 1994).

Air density

The impact of wind on a surface is directly related to density, which is a function of pressure, temperature and humidity. An increase in air humidity and temperature causes a

reduction in density, while an increase in pressure results in an increase in air density. As a result of continuously changing environmental conditions (depending on location, time of day, season etc.), a ship in transit is subject to continuously changing air density. For example, when sailing in Northern regions where air temperature is 0°C, pressure 1050mBar and humidity 5%, the density of air is 1.337 kg/m³, while in hot climates with 35°C, 900mbar and 90% relative humidity, the density is as low as 0.9947 kg/m³, a difference of 25%. Pressure and temperature are hereby the main contributors to the density differences; a change in relative humidity of 20-90% contributes to a difference of 0.0054 kg/m³ at 15°C, while a pressure change between 900 – 1100mb gives a difference in pressure at 15°C of 0.24 kg/m³ (1.205±10%). However, in rain, the effect of wind forces on the hull increases. Kubo (Kubo et al. 1997) indicated a 15% increase in wind loading when rainfall was present.

3.2.4 Water density and viscosity

Seawater density varies nonlinearly with temperature, pressure and salinity. Figure 3.4 shows the relationship between salinity, density and temperature. With an increase in temperature, the density decreases, while with an increase in salinity the density increases. Figure 3.5 shows the distribution of the annual average of the seawater density at 10m water depth. From this figure it can be seen that a vessel trading world-wide may encounter waters with a density between 1022 - 1027 kg/m³ in a single voyage. The effect upon changes in resistance (draft variations) and propulsive characteristics is however rather small (a difference of 1025 ± 0.3%).

The effect of changing temperature, salinity and density has a large effect on the speed of sound through water. For Doppler speed logs, which are based on the measurement of speed of sound through water, this variation should be accounted for.

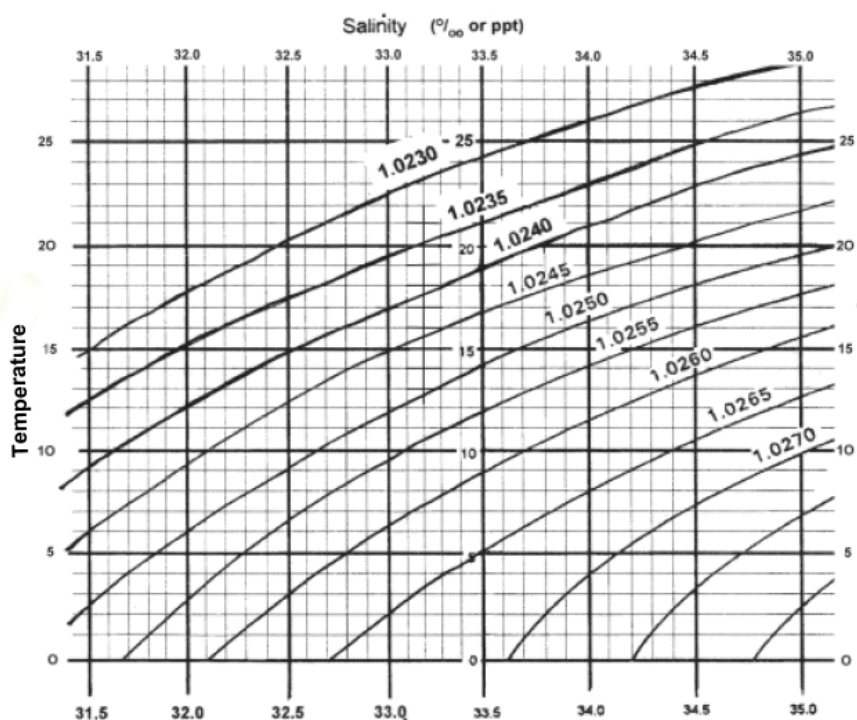


Figure 3.4: Relationship between temperature, salinity and density at atmospheric pressure (UCLA 2008)

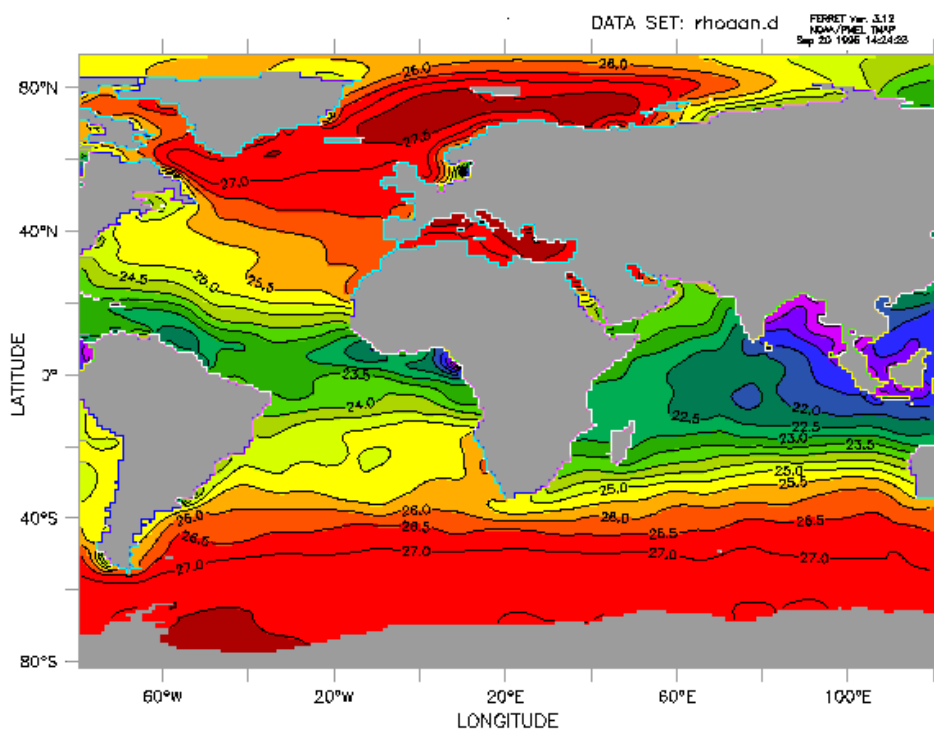


Figure 3.5: Potential density ($\rho - 1000 \text{ kg/m}^3$) at 10m annual average 1996 (NOAA 2008a)

Viscosity

Viscosity, often referred to as kinematic viscosity by dividing by density, affects the resistance of the ship's hull and propeller. It is influenced by temperature. For a ship making a world-wide voyage, the variation in temperature that will be encountered may be large, resulting in significant changes in kinematic viscosity. Assuming salinity is constant, the viscosity difference between waters of e.g. 5°C in Europe and 31°C in Asia is for example approx. 0.74 mm²/s or $\nu = 1.118 \pm 35\%$. Contrary to density, viscosity is therefore an important factor affecting ship performance. For a tanker, a 35% change in viscosity expresses in a change in frictional resistance of about 4%.

Kinematic viscosity may be calculated using the following equation:

$$\nu = a + bT_w + cT_w^2 + dT_w^3 + eT_w^4 \quad (3.5)$$

Where:

ν = kinematic viscosity in m²/s

	Fresh water (0% salinity)	3.5% Salinity
a	1.786170×10^{-6}	$1,827788 \times 10^{-6}$
b	-6.071739×10^{-8}	$-6,020031 \times 10^{-8}$
c	1.507093×10^{-9}	$1,528715 \times 10^{-9}$
d	$-2.552462 \times 10^{-11}$	$-2,741868 \times 10^{-11}$
e	2.087519×10^{-13}	$2,3718711 \times 10^{-13}$

T_w = Seawater temperature in °C

Linear interpolation may be used for salinity in between 0 and 3.5% (ISO15016 2002).

3.2.5 Fouling

Fouling starts from the moment a ship is immersed in seawater. Within seconds dissolved organic matter and molecules such as polysaccharides and proteins in the sea water attach to the hull. This conditioning process can be regarded as the first stage of fouling, and sets the scene for later fouling stages. When a conditioning film has been formed, bacteria and unicellular organisms settle, and form a microbial film, referred to as 'slime'

(Candries et al. 2003). This slime film eases the way for macrofouling settlement (such as weeds or barnacles). Slime comes in different grades and thicknesses and can trap considerable amounts of inorganic particles such as silt and clay minerals. Figure 3.6 shows an example of a developed slime layer on the test vessel *Bernicia*.

The effect of slime on ships in service is difficult to determine. Experiments by (Conn et al. 1953) on a steamer, report an increase in frictional resistance of 5%, while Watanabe et al (Watanabe et al. 1969) report a 11-18% increase in frictional resistance on a 9 meter model of a tanker. A set of full-scale trials on a frigate where after 22 months the mature slime layer was removed in dry-dock reported indicated an 8-18% decrease in total propulsive power in power trials (Bohlander 1991). Lewthwaite et al (Lewthwaite et al. 1985) reported a 25% increase in the local frictional resistance from a slime layer 'too thin to measure but detectable by touch' on a 23m fleet tender hull. More recently, Schultz (Schultz 2007) predicted for an 124.4 m, 3779dwt frigate at a speed of 15 knots an increase in resistance of 9% for light slime and 18% for heavy slime at constant speed.

In the past, calcareous or 'hard' fouling organisms such as barnacles were considered most problematic. At present, the duty cycles of modern merchant ships, marked by short periods in port and in larvae-rich coastal areas, favour the settlement and growth of algae. The most common macro algae found is the filamentous green alga 'Enteromorpha'. It has a nearly global distribution, grows fast and can survive in wide ranges of temperature and salinity, because it requires only inorganic nutrients and light to grow. A characteristic of the green weed is that it can adhere strongly to surfaces and is essentially unaffected by the speed of the ship (Gangadharan et al. 2001) (Figure 3.7).



Figure 3.6: Slime on Bernicia

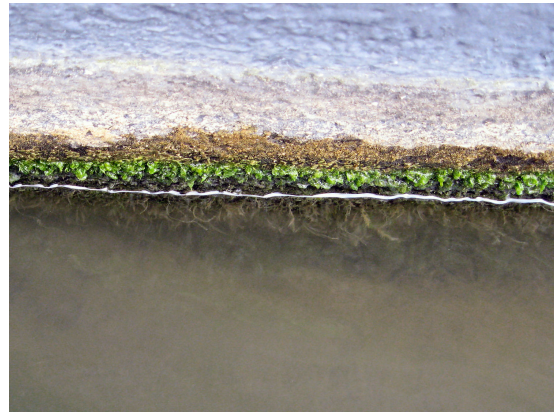


Figure 3.7: Weed fouling on a rough hull

The estimation of drag forces of weed fouling on its own is difficult, as a hull fouled with weed fouling also has areas with slime fouling. Underwater measurements of fouling on several VLCCs and ULCCs by Tokyo Tanker Co., Ltd in the period 1977 – 1979, showed that the rate of power increase due to slime and weed fouling is about 30% per year in case underwater cleaning is not carried out. The rate of power increase is reduced to 10 - 15% per year if macro fouling is removed every two months using underwater cleaning (Baba and Tokunga 1980). International Paint (International 2005) reports that if the vertical sides of a vessel are 100% covered with grass weed, at least a 10% fuel penalty can occur. Predictions of the resistance increase on a frigate by Schultz (Schultz 2007) based on towing tests of a fouled flat plate with ‘calcareous or weed fouling’ showed a 32% increase in R_T at 15 knots (21% at 30kn) compared to clean conditions. Regardless the fact that the power increase in these cases was estimated by the analysis of logbooks or from extrapolation of model tests, it shows that weed fouling can have a significant contribution to the total resistance of a ship.

Calcareous fouling in the form of barnacles, tube worms or mussels (Figure 3.8) develops when ships are in port, as water currents inhibit the attachment and growth. The development of fouling in general is dependent on the hull finish (type of hull coating, roughness), the vessel’s trading pattern (water salinity, light, temperature, pollution and nutrient availability in the water) and operational profile (ship speed and activity).



Figure 3.8: Barnacles on Overseas Tanabe



Figure 3.9: Severe weed & shell fouling

The drag penalty for a shell fouling on a hull depends strongly on the extent and location. Kempf (Kempf 1937) found that the maximum drag increase on a pontoon test occurs when the shell fouling covers 75% of the wetted surface, with a shell height of 14mm. However, even with only 5% of the wetted area covered, the drag increase was 66% of the maximum. From this empirical data he was able to calculate the increased resistance of a 120m vessel. With 75% coverage with shell of 4.5mm height he calculated that the skin friction resistance would increase with 85% (Townsin 2003). Schultz predicts the effect on resistance of ‘medium calcareous fouling’ and ‘heavy calcareous fouling’ from flat plate towing tank tests extrapolated to a 124m frigate to be 50 and 78% for 15kn respectively and 32 and 51% for 30kn respectively.

The location of hull roughness on the hull (stern, bow, side, bottom) influences the contribution of the roughness to the ship’s total frictional resistance. Frictional resistance depends on speed and pressure; the higher the speed, the more frictional resistance. The first quarter from the bow of the underwater hull contributes most to the overall friction drag and the contribution progressively diminishes fore to aft. Details can be found in (Baba and Tokunga 1980; Kim and Lewkowicz 1992; Townsin et al. 1984)

Propeller fouling

Propeller fouling manifests itself primarily by fouling of the animal type, such as acorn barnacles, tubeworms and calcium deposits as can be seen in Figure 3.8. In spite of most propeller materials contain more than 70% copper, most alloys are either designed to resist solution in seawater, or are deliberately made cathodic to the hull by cathodic

protection. The copper is therefore not active and available as toxicant to the fouling organisms. As such, they have no antifouling properties (Townsin et al. 1981).

3.2.6 Local conclusions regarding ship environment

It may be concluded that the marine environment is highly dynamic and irregular. Waves are highly irregular and cannot be described with an instantaneous figure but must be expressed using statistical formulations. Furthermore, sea characteristics are different throughout the world, depending on location, time of year and time of day, and water depth. Wind is highly variable and cannot be described by speed and direction alone, as gustiness and density are important aspects affecting windage. Finally, marine bio-fouling is a phenomena affected by many parameters. It is therefore extremely difficult to predict, and due to its irregular nature, complex to quantify. The measurement of the environment, necessary to correct ship performance in service to standard conditions, requires therefore care and should preferably be logged continuously.

3.3 Ship behaviour in service conditions

In the previous section, the marine environment in which the ship operates was discussed. Ship performance varies not only because of its environment; also ship operation, such as acceleration, deceleration, course deviations and loading has a strong effect on the ship performance. This section describes the main factors that affect performance, in order to understand which variables should be logged, for which conditions service performance should be corrected for, and under which conditions performance should not be used for analysis purposes. These data logging requirements are summarised in section 3.3.11.

3.3.1 Manoeuvring

During course alteration the resistance of the hull increases as a result of an induced drag from the rudder as well as the hull drift. This results in a decrease in ship speed.

Furthermore, due to the sideways movement of the ship's stern section and the interaction of the rudder induced currents, the wake field becomes irregular resulting in a change in propeller loading. During manoeuvring, the data logged should therefore be disregarded for performance analysis.

3.3.2 Acceleration

The rate of increase in ship speed as a result of an increase of engine speed is dependent on engine & propeller characteristics and the ship's inertia. Acceleration can be described in a number of phases. Firstly, propeller speed increases due to a change in demand. As a response, the propeller-absorbed torque rapidly increases. Due to the mass inertia of the vessel, the advance speed of the water into the propeller plane is initially low, causing a high propeller load. As the ship speed increases, the propeller load reduces until the ship has stopped accelerating. To avoid the initial increase in torque causing engine overload on large vessels, the increase of engine speed is slow such that the absorbed propeller torque stays within limits. Figure 3.10 shows the acceleration of the *Overseas Tanabe* in laden condition from 52 to 62 RPM, collected by the data acquisition system developed by the Author. Even though the engine speed is increased over a period of approximately 100 seconds to avoid engine overload, the ship cannot accelerate enough to avoid overshoot in torque. It takes approximately 23 minutes before the ship has stopped accelerating and the delivered power is constant.

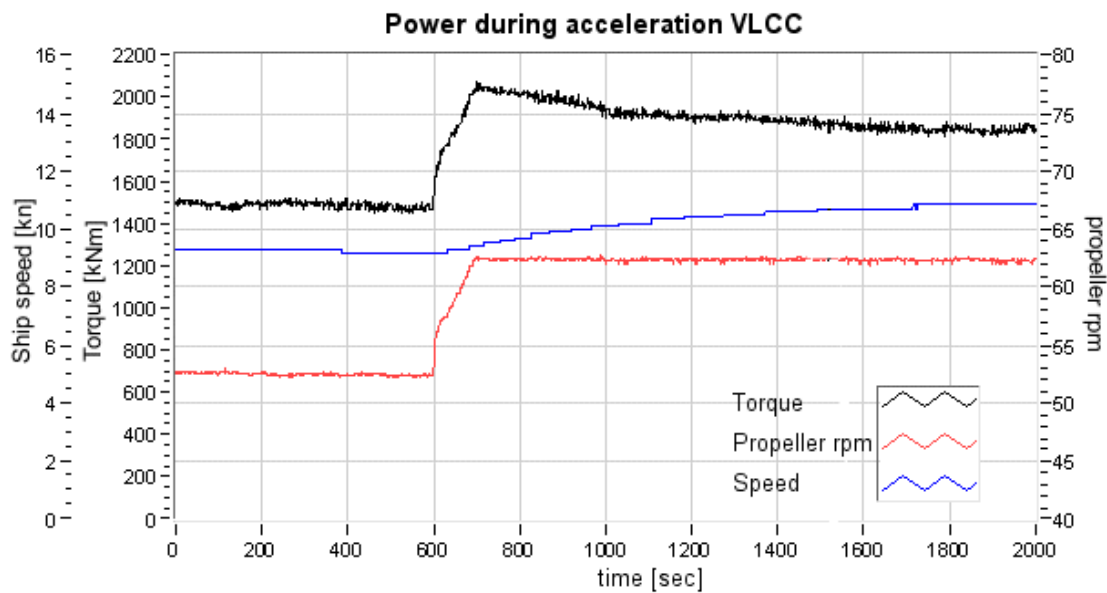


Figure 3.10: Torque and rpm during acceleration of a laden 300.000t VLCC (Overseas Tanabe)

Deceleration works in a similar fashion. To avoid engine over-speed when the propeller is being propelled by the water rather than from the engine ('wind milling'), engine speed is reduced in slow steps.

The acceleration and deceleration behaviour of a vessel depend mainly on the loading condition, propeller and engine characteristics (including engine load-computer settings) and ship speed. Because of the inertia effects of the ship, ship performance in these transient conditions differs significantly from normal sailing conditions. The data logged during these transient events should therefore be discarded for the performance analysis purposes.

3.3.3 Wake fraction

The wake of a ship is not a physical representation or action of a ship. It is a parameter that is used for performance analysis describing the relative difference between the velocity of the ship (V_s) and the velocity with which the water flows into the propeller plane, advance velocity (V_a). The wake fraction changes constantly in service conditions. It is therefore important to understand its physics. The effective wake fraction can be split

into four components; potential, friction, wave and apparent alteration of the wake due to the change of the rotation in the propeller race and to other alternations in the inflow conditions. Changes in draft and trim, water depth, drift, waves, rudder action and hull fouling also have an influence on these factors, as described below:

- Draft and trim: The underwater hull shape affects the flow around the hull. Changes in draft and trim, which alter the underwater hull shape, have therefore a direct effect on the wake fraction. The changes can be estimated by model tests and trials at different draft conditions.
- Water depth: The bottom interaction with the ship causes changes in the wake distribution due to a change in stern wave, sinkage and a reduced pressure field under the ship. The change in wake can be preceded using empirical relationships (e.g. (Harvald 1983)), but since propeller and thrust deduction are affected as well, the reduction in accuracy must be considered.
- Drift: Quartering or beam winds give rise to drift and consequently rudder must be applied to keep the ship on a desired course. Drift results in an asymmetric wake field causing changes in propeller characteristics. Corrections have been discussed by e.g. (Abramowski 1999; Jorgensen and Prohaska 1966; Kuiper et al. 2002) but due to the complexity of the relationships, no practical applicable methods are available. The effects can be considerable; Jorgensen et al (Jorgensen and Prohaska 1966) showed a 21% deviation in wake fraction on a 7m model Mariner type vessel for a drift angle of 4 degrees
- Waves: In general, the propeller loading has little influence on the nominal wake fraction (Harvald 1983). Wave induced ship motion however does affect wake fraction. Pitch motion of is the major reason to the increase in wake velocities, caused by a drop in mean pressure from the middle of the ship towards the stern, resulting in a increased flow and smaller boundary layer (Faltinsen et al. 1980). The amount of change of wake depends on hull and seakeeping characteristics and wave characteristics (wave length, height, spectrum, direction) and is therefore difficult to predict. It is most pronounced in regular wave conditions around the natural period of pitch (Nakamura and Naito 1977)
- Speed: When the speed of the ship is altered, the stern wave and therefore the potential part of the wake changes. Furthermore, the frictional wake changes with

speed. Investigations by Harvald (Harvald 1950) show that for ships with small propellers, which are more affected by wake, the wake fraction *falls* at rising speed, while ships with relatively large propellers (tugs, pilot boats etc.) have a very small *increase* in w at increasing speed. The question with model tests remains whether the variation found experimentally will be confirmed in the actual ship, especially regarding the frictional contribution. Full scale measurements of the effective wake fraction for a range of ship speeds are therefore necessary to estimate the relationship between wake and speed.

- **Rudder:** Rudder action has a large impact on the wake. A rudder action increases the potential flow aft of the propeller and the change in the rotation in the propeller race alters the effective wake coefficient registered by the propeller (Harvald 1983)
- **Fouling:** Hull fouling mainly affects frictional wake, which is often the largest of the wake components (Harvald 1983). Due to the slow but irregular increase over time, it is the most difficult to deal with. Many different relationships have been derived to relate roughness to the wake increment (ITTC 1978; Kresic and Haskell 1983). For example, the difference in wake for a VLCC between a clean hull with an Average Hull Roughness of $125\mu\text{m}$ and a fouled hull with an roughness equivalent to an AHR of $750\mu\text{m}$ causes a change in effective wake from 0.340 to 0.366, a change of 7% (Svensen 1983). The same increase in roughness on an Ore, Bulk & Oil carrier indicated an 11% increase by (Kresic and Haskell 1983). The difficulty to quantify hull roughness and fouling, especially with the introduction of modern silicon based foul-release coatings, has made the use of the traditional relationships inaccurate and unusable.

It can be concluded that during sailing in extreme shallow water, strong off head or stern winds when the ship experiences drift, heavy sea states and manoeuvring, the wake fraction is not constant and is difficult to predict. During these conditions, ship performance should be disregarded for the analysis task. Self-propulsion model tests or full scale measurements can be used to account for changes in wake fraction in off-design loading conditions. To account for changes in wake from hull fouling, the wake fraction should be periodically measured in service conditions to monitor the increase in wake

fraction over time. In order to identify these changes, water depth, wind direction and speed, motion, rate of turn and ship speed through water should be monitored continuously.

3.3.4 Thrust deduction fraction

The thrust deduction fraction is another mathematical definition that cannot be measured in service, but is used in the correction of service performance to standard performance. It is influenced by a number of conditions that change during the normal operation of ships. The thrust deduction factor describes the influence of the propeller on the resistance of a ship due to the increased velocity of the flow created by the propeller action over the hull surface and reduced local pressure field over the after part of the hull surface. It is build-up from potential, frictional and wave components and is affected by the same parameters as the wake fraction, i.e. the vessel's aft end immersion (draft & trim), speed of advance, propeller loading and water depth, as discussed below.

- Propeller loading: The thrust deduction decreases with increase in loading to about 0.03-0.05 in bollard condition. In the normal field of variation of propeller loading, the variation of the thrust deduction fraction is rather small (Harvald 1983) and may be ignored
- Shallow water: The effects of shallow water on the thrust deduction become apparent in water depth smaller than approximately twice the draft of the ship. Increases in the thrust deduction fraction of up to 40% may be expected for a depth of 1.25 times the ship's draft (Harvald 1983)
- Hull fouling: Thrust deduction describes the increase in flow over the hull surface, and is therefore in theory affected by hull fouling. Yet, tests by (Kan et al. 1958) on a roughened scale model indicate that the thrust deduction coefficient retains a nearly constant value for a wide range of hull surface roughness in spite of the remarkable increases of wake fraction due to roughness. They conclude that the thrust deduction coefficient depends mainly on the potential wake and not much on the frictional wake
- Waves & ship motion: when wave height (and ship motion) increases, the trust deduction fraction decreases. A minimum will be found around the natural period

and pitch of the ship (Faltinsen et al. 1980; Nakamura and Naito 1977). Yet, no general applicable relationships have been derived so far

- Ship speed: The relationship between thrust deduction and ship speed depends on hull and propeller characteristics. However, because of the large dependency of propeller-hull characteristics, no general applicable conclusions can be made.

Based on the above review, it may be concluded that during shallow water and heavy weather conditions, the prediction of resistance overcome by the propeller to propel the ship is uncertain. Furthermore, draft variations have a direct effect on the thrust deduction fraction, and appropriate corrective measures have to be used when analysing ship performance in different loading conditions. No corrections have to be made for changes in hull roughness.

3.3.5 Propeller characteristics

Torque and thrust characteristics of a propeller are normally estimated from open water model tests. The model test results are then corrected to full scale using appropriate correction factors on the thrust and torque coefficient K_T and K_Q from the model-testing institute (e.g. ITTC'78 corrections (ITTC 1978)). To account for the difference in power absorbed by the propeller when working in a uniform flow field at a given speed and that absorbed when working in a mixed wake field having the same mean velocity, the 'relative rotative efficiency' correction factor is applied. This single correction factor is however not sufficient for all service conditions. During the service operation of a ship, the propeller characteristics differ from the scaled-up calm water model tests by changes in the wake fraction and in the following factors:

- Propeller submergence
- Blade roughness and fouling
- Drift
- Water density and viscosity

3.3.5.1 Propeller submergence

In shallow drafts, the propeller sets up a steady wave motion when it is working close to the free surface. If the loading on the propeller increases, the surface in front of the propeller is lowered and eventually the air is sucked down, forming a dead water or air region on the suction side of the propeller blades. This will lead to a reduction in the propeller thrust, which is a function of the propeller loading and Froude number (Lee 1983). Figure 3.11 shows typical propeller performances at various water depths, whereby T_0 the immersion depth of the propeller shaft is and R the propeller radius.

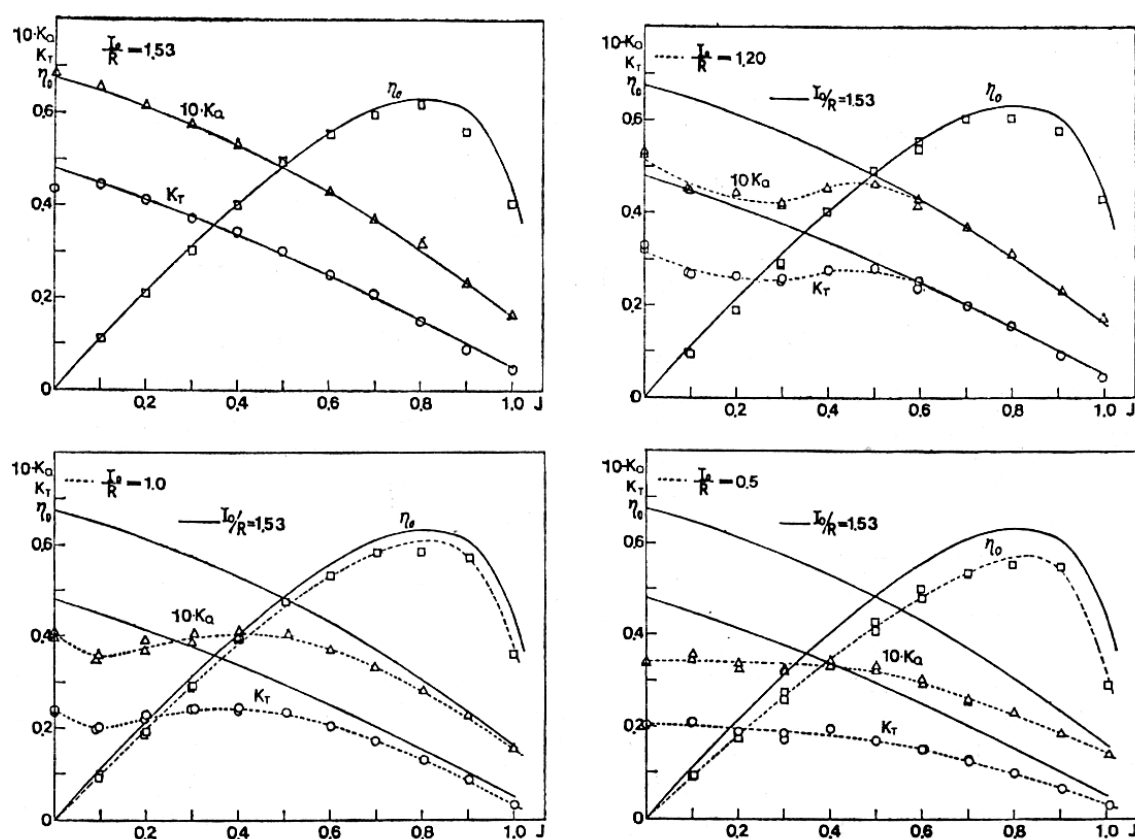


Figure 3.11: Propeller characteristics in still water with varying propeller immersion ((Lee 1983) fig. 2)

The reduction in torque and thrust can be significant, especially at high propeller loads. By ballasting, the propeller immersion depth is normally kept outside the range $T_0 / R < 1.5$. However, when a ship sails in ballast under the influence of waves, the propeller may well be oscillating periodically in instantaneous positions where $1 < T_0 / R < 1.5$.

Torque reductions of 10-15% may be expected in these conditions (Faltinsen and Minsaas 1984; Takahishi et al. 1984).

The change in immersion depth has furthermore effect on the wake fraction, and consequently the propeller absorbed torque. Kyrtatos et al (Kyrtatos et al. 2000; Xiros and Kyrtatos 2000) attempted to predict the variations in torque and thrust at full scale based propeller immersion during ship motion, but because of the complications and uncertainty in the prediction, it is questionable whether correction factors provide sufficient reliability and accuracy to improve power measurements. Periods where torque fluctuations are large due to excessive ship motion should therefore not be used for performance monitoring.

3.3.5.2 Blade roughness and fouling

An increase in blade roughness causes an increase in frictional resistance, which results in a decrease in propeller efficiency. A range of numerical methods have been derived each relating different types of roughness to propeller performance. For moderate values of blade roughness, the decrease in propeller efficiency may be described as an increase in section drag and a reduction of lift, caused by a reduction in circulation around the propeller blade. Lerbs' equivalent profile method can then be used to convert the enhanced section drag into a power penalty (Townsin et al. 1985). It shows that an increase in section drag increases the torque, while the decrease in lift causes a slight reduction in thrust. Yet, for moderate values of blade surface roughness, the reduction in thrust is small and may be assumed negligible (Atlar et al. 2002a; Svensen and Medhurst 1984).

The effect on performance from macro bio-fouling may be described by assuming a change in blade section by the boundary layer displacement thickness, expressed by the change of chamber curve and blade thickness. Using numerical boundary layer theory, the propeller performance can be calculated using the propeller with apparently deformed blades by use of the vortex lattice model (Wan et al. 2002). A number of model and full scale experiments have been done to validate the empirically derived relationships for roughness and fouling on propellers, either using different types of sand grain or rubber

protuberances to simulate barnacles (e.g. (Kan et al. 1958) or (Wan et al. 2002)). The exact effect of roughness on propeller performance is however difficult. Model tests suffer from scaling errors, while full scale experiments suffer from inaccuracies and uncertainties from measurement of ship performance in varying environmental conditions.

Apart from the severity of the blade roughness fouling, the location of fouling and roughness is also important. Approximately 70% of the energy of a propeller is absorbed at the outer edges ($r/R > 0.7$) of the propeller (Townsin et al. 1985). Fouling generally does not attach in these regions since the high blade speed at the tips and the high thrust force tears off any kind of bio-fouling. Roughness is therefore of primary importance to torque characteristics of a propeller. Thrust on the other hand is affected by fouling even near the boss of the propeller, resulting in a decrease of the propeller efficiency (Kan et al. 1958).

Figure 3.12 shows an example of open water propeller tests from Wan et al. for a propeller artificially roughened by sand grains (Wan et al. 2002). It shows that as the surface roughness of propeller blade (ks) increases, the propeller torque coefficient K_Q increases and thrust coefficient K_T and propeller efficiency η_P decreases.

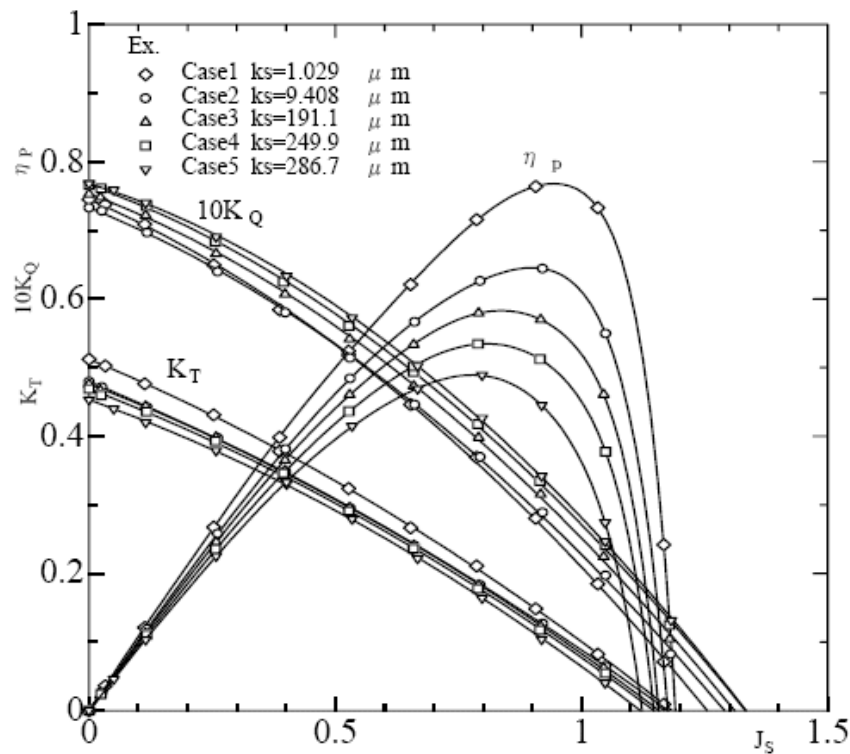


Figure 3.12: Propeller open water tests for with different propeller blade roughness ((Wan et al. 2002) fig. 3)

For large merchant vessels, it may be assumed that the propeller is well maintained and that the propeller is polished before macro fouling has appeared. Therefore, large-scale fouling (modelled by sand grains or rubber protuberances), which significantly changes both frictional and form drag and is difficult to model numerically, can be avoided. A development that has recently gained particular interest is propeller coating to protect against fouling. Foul-release coatings reduce the need for underwater cleanings and keep the propeller free from fouling, especially at the inner area of the propeller. In demonstrating the effect of foul release coating on the performance of a propeller, Atlar et al (Atlar et al. 2002b) assumed that foul-release coatings have approximately the similar roughness characteristics of the equivalent blade section drag of a new or well polished propeller. Based on this approach they demonstrated through calculation that the reduction in propeller efficiency through especially blade fouling can therefore be significantly reduced.

3.3.5.3 Drift

Drift causes transverse velocities that alter the effective wake field of a propeller, by changing the propeller behaviour. However, in extreme cases, drift may also affect the propeller characteristics. Calculations by Abramowski (Abramowski 1999) using lifting line methods with lifting surface corrections on a bulk carrier during a turning manoeuvre show that a significant loss of the propeller efficiency takes place during a turning manoeuvre, as an effect of drift. Decreases of thrust and torque of up to 8% and 15% were estimated respectively due to changes in inflow velocity. During normal operation, without abrupt course deviations and small drift angles, the effect of drift on propeller performance may be neglected.

3.3.5.4 Water density and viscosity

the density, viscosity, vapour pressure and dissolved gasses in sea water also all affect propeller performance in some way. Vapour pressure and concentration of dissolved gasses are mainly important for cavitation, which, under normal conditions, is assumed not to occur. The seawater viscosity is however important. The effect of the change in viscosity will manifest itself in the frictional resistance losses of the propeller, e.g. by the following relationship:

$$C_f = \frac{0.075}{[\log_{10}(\text{Re}) - 2]^2} \quad (\text{ITTC}'57 \text{ correlation line}) \quad (3.6)$$

The difference in frictional resistance coefficient C_f for a water temperature varying from 5°C to 30°C for a propeller Reynolds number (Re) of $106.96 \cdot 10^6$ is approximately 9% due to changes in viscosity. When the propeller losses are split into axial, rotational and frictional components, it can be shown that frictional losses contribute with about 10-16% of the efficiency loss of the propeller (depending on thrust loading) (Glover 1987). Axial losses dominate with 15-40% and rotational losses contribute to about 6-7%. Relatively speaking, a change in frictional losses of 9% due to the effect of temperature will influence the propeller performance with roughly 1% compared to the standard used

during the scaling of model test results (15°C , $\nu = 1.188 \text{ mm}^2/\text{s}$). It seems therefore not worth to make the correction.

3.3.5.5 Local conclusions regarding to propeller performance

Propeller performance forms backbone of performance analysis: the propeller acts as a torque absorber and is therefore directly related to ship performance. From the above review, the following set of requirements can be listed for the use of the propeller behaviour during service performance analysis:

- The propeller immersion depth should be outside the range $T_o / R < 1.5$
- Performance monitoring should be ceased when large torque fluctuations due to ship motions are present
- The propeller should not be fouled with macro fouling
- Performance monitoring should not be done during manoeuvres when drift angles are large
- The effect of changes in water density in salt water on propeller efficiency may be assumed negligible.

3.3.6 Draft, trim and Squat

As the draft increases, the underwater surface area increases and underwater hull shape usually becomes fuller, resulting in an increase in resistance. Apart from draft, trim has also a large effect on resistance, especially on vessels with a bulbous bow. Trim optimisation studies have shown differences in power in the order of 1-4% at constant displacement due to changes in trim alone (Kanerva and Salana 2004; Knaggs 2006; O'Mahony 2007). Due to the complex relationship between resistance and fore- and aft draft, there is no simple general applicable relationship to account for draft deviations. Simply interpolating a service draft from model tests results between laden and ballast draft may be incorrect. Figure 3.13 shows an example of the speed-power relationship for a 2400TEU container vessel. For this particular ship, there is a large difference between the scantling draft and the design draft, while there is a relatively small difference between design and ballast condition (with trim). The small difference with the ballast

condition may be explained by a large reduction in frictional resistance, but an increase in wave induced resistance due to the inefficient bulbous bow at this draft, making the combined reduction in resistance small. The large increase in resistance at scantling draft may be explained by (a), the resistance from the transom stern immersion and (b), the added wave resistance caused by the blunt bow shape at this draft. Apart from a vertical offset between the curves, there is also a difference in gradient visible, especially between the ballast and design draft.

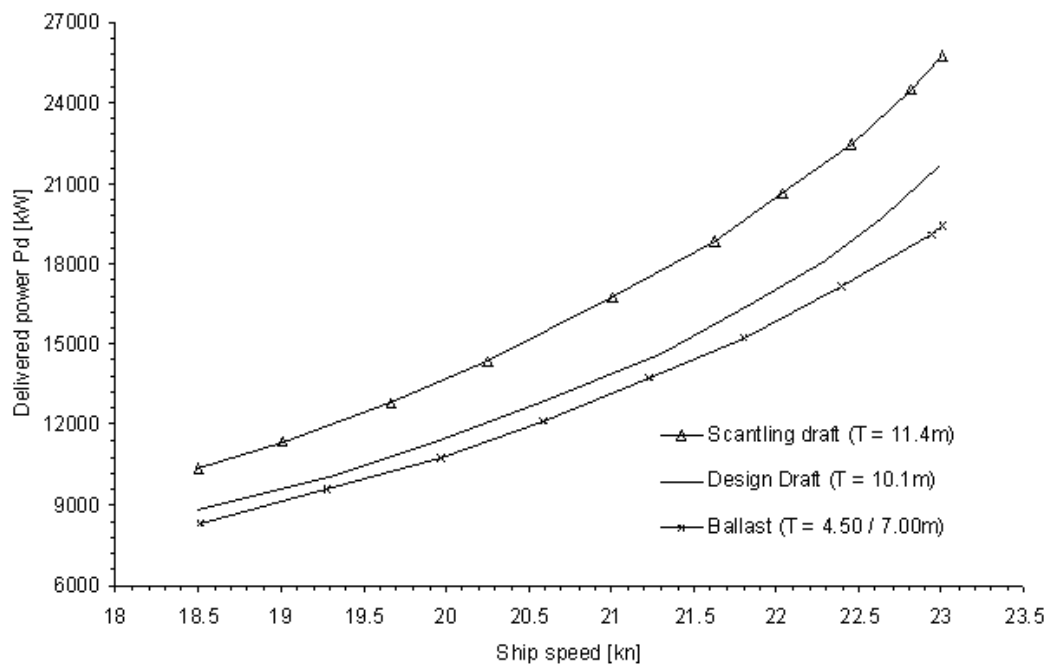


Figure 3.13: Speed-power curves for a 2400TEU container vessel for three loading conditions obtained from model tests (HSVA 1997)

This simple example shows the difficulty in simple interpolation between loaded and ballast conditions to predict the resistance at part-load.

Squat

During sailing, especially in shallow water areas, the displacement of a ship may increase. Pressure induced forces and pressure & friction induced trimming moments, caused by the forward speed of the ship, are counteracted by a sinkage and trim (referred to as ‘squat’) to maintain equilibrium. At low speeds there is a general bodily sinkage and

a slight trim by the bow as compared with the at-rest condition. As speed increases the movement of the bow is reversed and at $Fn = 0.30$ or thereabouts the bow begins to rise appreciably, the sterns sinks still further and the ship takes on a declined trim by the stern (SNAME 1989c). The additional sinkage and trim causes an increase in resistance. The trim by stern causes a higher resistance at low speeds, because the increase draft aft makes the stern virtually fuller, with a consequent increase in form and separation resistance. At high speeds, this is offset by the reduction in wave-making due to the finer entrance in the trimmed condition (SNAME 1989c). Sinkage is dependent on a number of factors, as listed in Table 3.1 (Ferguson 1984).

Table 3.1: Factors influencing sinkage and dynamic trim

Factors influencing sinkage and trim
<ul style="list-style-type: none">• Hull form• Propulsive device• Speed• Ratio water depth / draft at rest (h/T)• Hull roughness• Sea state• Density layers, thermoclines• Rapid transition from deep to shallow water• Manoeuvring• Initial trim• Distance to other vessels, fixed or floating

A number of attempts have been made to develop a general applicable algorithm to predict the resistance change as a function of dynamic trim, e.g. (Miller 1963; Moor and O'Connor 1964; Rocchi 1994; Tsugane and Kagoyashi 1987), but with limited success due to the complex interaction of the factors listed in Table 3.1.

The influence of hull roughness and sea state on sinkage is relatively small (Ferguson 1984). It is therefore assumed that the sinkage has a constant relationship to ship speed when the vessel sails in moderate sea state and deep water over the service life of the vessel. When the water becomes shallow, or the ship sails in a restricted canal, sinkage

becomes significant and introduces drag and changes in propulsive coefficients. Its effects can then not be ignored.

3.3.7 Shallow water effects

When a ship sails in shallow water, the ship's forward motion in combination of the proximity of the bottom causes potential flow. As a result, the water passing under the hull must speed up, with a consequent greater reduction in pressure and increased sinkage, trim and resistance. Additionally, there will be a change in wave pattern. As the depth decreases, the speed of a wave of given length decreases.

The maximum speed of a wave in shallow water with depth h , known as the critical speed, is given by \sqrt{gh} , where g is the acceleration due to gravity. As the ship speed approaches the critical speed where the depth dependent Froude number given by $Fn = \frac{V}{\sqrt{gh}}$ approaches to 1.0, the wave pattern changes and the wave resistance

increases. At ship speeds below but close to the critical (valid for nearly all merchant displacement ships), the resistance in shallow water is greater than that in deep water.

The appearance of shallow water effects depends on hull characteristics, ship speed and bottom typology. For example, following speed penalty predictions by Lackenby (Lackenby 1961), shallow water effects for a 318m, 270,000dwt VLCC sailing at 16 knots appear at depths about 100m, with a predicted speed loss of 0.7% (2% power loss). In a water depth of 40m, the speed loss is approx. 7.7%, which corresponds to a power loss of almost 18%. Contrary to the VLCC predictions, a 231m, 2400TEU container vessel, sailing at 22kn is subject to an estimated speed reduction of 1.9% (8.5% power loss) in waters of 40m deep, whilst no shallow water effects appear at 100m deep water.

Shallow water effects influence the calm water resistance, seakeeping characteristics, wake fraction and propeller efficiency. The prediction of shallow water effects is therefore complex to deal with accurately. For the analysis of ship performance, periods of sailing in shallow waters should therefore be avoided if possible.

3.3.8 Seakeeping characteristics

The external forces acting on a vessel due to incoming waves result from the phase relationship between the ship motions and waves, as initially described by Havelock (Havelock 1942). The work that must be done to keep the ship motions in a constant phase relationship with the exciting waves is the energy lost. The energy loss, or added resistance, consists of waves generated by the ship motions and diffraction of waves mainly at the bow of the vessel. In short wave lengths (wave length / ship length ≤ 1), the wave diffraction is the dominant component; in long wave lengths the resistance due to motion becomes dominant. The way the ship responds to waves, in terms of ship motion and resistance, is, apart from the design of the hull form and characteristics of the propulsion plant, dependent on a number of factors that may change during the operation of a ship:

- Draft and trim: Seakeeping characteristics are a function of hull shape, and are therefore directly influenced by draft and trim
- Ship speed: Added resistance due to waves is primarily caused by the combined heave and pitch motion in addition to the effect of wave diffraction. Especially heave is affected by ship speed
- Load distribution: A ship with larger longitudinal moments of inertia (ie. weights concentrated away from the midship section) suffers more speed loss than the one with the concentrated weights at amidships. The differences are particularly apparent in conditions where ship motion is significant ($BF > 4$). For example, Swaan showed for a 150m bulk carrier with a longitudinal radius of gyration of $0.26L$, a speed loss due to wave resistance from 18 to 14.6 knots in $BF7$, while for a radius of gyration of $0.22L$ radius of gyration, a speed loss of 2 knots was measured (at constant power in head seas) ((Swaan and Rijken 1964) in (Bhattacharyya 1978)). The effect of change in the longitudinal moment of inertia is more pronounced for smaller vessels than for larger ones (Bhattacharyya 1978).
- Water depth: as described in the previous section, the decrease in pressure under the hull causes squat, which will alter seakeeping characteristics.

Motion induced wave resistance, generated mainly by heave and pitch motions, is approximately proportional to the square of the wave height (Lloyd 1998). Furthermore,

wave direction, sea spectrum, directional spreading and swell all affect the behaviour of the vessel in the sea. They must therefore be accurately known.

Seakeeping affects not only the added wave resistance, the wake fraction, thrust deduction and propeller characteristics are also influenced. Because seakeeping is a function of many different parameters, prediction of seakeeping characteristics requires detailed modelling of hull shape, loading conditions and sea characteristics. They can be determined by means of model tests, computer models or CFD simulations. The increase in torque and thrust of a ship in waves has been reported and discussed continually by the Seakeeping and Performance Committees of the International Towing Tank Conferences (ITTC 1978; ITTC 1981). However, the difficulty in predicting ship motion and the added wave resistance caused by wave diffraction and reflection, which is nonlinear in nature, makes the predictions highly inaccurate (Kwon 2008). Yet, together with wind resistance, added resistance due to waves is one of the most important external loads on ships. A rough indication of the speed loss due to wave, as a function of the Beaufort Number can be obtained from (Kwon 2008); for a 318m, 273,000dwt VLCC sailing at 15 knots in BF4 (significant wave height of 4m), the speed loss is approx. 2.7%, or 6% power loss. For a 231m, 2400TEU container vessel, sailing at 22 knots, the speed loss is at these conditions is approximately 3.1%, or 13% power loss. Higher sea states rapidly increase the speed and power losses. Being proportional to the square of vertical motion, added resistance can become of the order of calm water resistance for smaller ships in severe sea conditions.

3.3.9 Windage, yawing and rudder resistance

The wind load on the hull and superstructure of a vessel causes a direct increase in propeller load and a decrease in speed. Wind load depends on the above water hull geometry, wind speed and air density, and generally reaches a maximum when the apparent wind blows approx. 30° from the bow where the windage area of the hull is at its maximum. Wind resistance contributes for a significant part to performance deviations of ships. For example, as analysed by the Author, the power loss for a laden 273,000dwt VLCC sailing at 15 knots, with a true wind speed of 20kn (approx. BF4) is approx. 12%.

For a laden 2400TEU container ship, sailing at 22kn, the same wind causes a power loss of approx. 18%.

When the ship sails in quartering to beam winds, the wind load introduces a transverse force. then the wind force can be compensated for by a combined heading to windward and shift of rudder. The shift of rudder induces a longitudinal force component that may be regarded as added resistance. It is, apart from the rudder angle, a function of rudder type, aspect ratio, distance to the propeller, propeller slipstream, ship motion, sway velocity etc. Practical methods to predict the added resistance are therefore simplified, and have large uncertainties (SNAME 1989b). However, investigation of 4 months of performance data collected by the Author of a tanker sailing worldwide at 16 knots indicated that most of the time wind direction relative to the bow is within $\pm 50^\circ$. It is therefore expected that the yawing amplitude and the drift angle during normal operation are small. For rudder angles up to 4 degrees, rudder resistance is generally less than 1% of the total resistance of a ship. It is therefore questionable whether corrections for rudder resistance give any improvement in performance analysis.

3.3.10 Engine performance

The performance of marine diesel engines is subject to constant change. Air temperature, humidity, cooling water temperature, fuel quality and the aging of valves all affect the performance. To what extent these parameters affect the engine performance in terms of fuel efficiency is difficult to predict. Warkman (Warkman 1983) compared nine 25,000dwt sister ships, all fitted with the same make and type of engines but built at several different yards, and showed that regardless the fact that hull forms, engines, ballast conditions were supposed to be identical and within normal manufacturing tolerances, engine performance (expressed in specific fuel consumption) differed considerably. This could be explained by the variations in ambient conditions from one ship/sea trial to the next, variation in the fuel on the trials, maladjustments of engine valve timings and fuel system components and inaccurate measurements. From the analysis of performance data, it showed that sulphur content and specific gravity of the fuel and engine room and scavenge air temperature have significant effects on fuel

efficiency, while water content in fuel after treatment, ash content or ambient pressure in the engine room have comparatively little effect. These variations are application dependent, and make therefore the comparison of engines on sister ships difficult. Hence, to be able to compare engine performance changes between different engines or ships, a complete performance check of the initial engine condition must be made so that corrective measures can be taken (e.g. correction for ambient temperature). This includes the logging of combustion conditions, engine balance, load, and outside influences.

The effect of aging of diesel engines was investigated by McGillivray (McGillivray 1997) who tested for a number of diesel engine combustion components the change in overall engine efficiency (in terms of specific fuel consumption and NO_x/g/kWh) via accelerated ageing in laboratory experiments. The worn parts were either received from operating engines or were modified according to experimental and field service information of known wear patterns for each component. The tests only examined single component or element performance downgrade. Therefore, the overall cumulative effect could not be gauged accurately. However, the tests give an indication of the magnitude of performance downgrade that may be expected without proper and regular maintenance. The following figures for change in specific fuel consumption were obtained from tests on a Wärtsilä 6L46 and 4L20 engine:

- Turbine fouling: negligible changes
- Wear of radial turbine nozzle ring (typical wear for 12,000 running hours): increase in SFC of 0.5-1% at loads over 75%
- Wear of turbine shroud ring (typical wear for 20,000 – 25,000 running hours): increase in SFC of 0.5-1.5%
- Fouling of exhaust gas system comprising all the components located after the turbo charger through which the exhaust gasses pass, e.g spark arrester, silencer etc up to 40mbar back pressure (which is the maximum allowed): negligible changes
- Fouling of charge air cooler: negligible changes
- Wear of fuel injection pumps (typical wear for 15 000h): increase in SFC of 1-1.5%
- Wear of fuel injection nozzles: negligible changes

- Decrease of the fuel injection nozzle opening pressure (due to changes of the setting screw adjustments or a decrease of the spring load by fatigue): negligible change

At loads above 75% one could conclude that the total effect on the specific fuel consumption on the tested combustion parts would be an increase of up to 6% (McGillivray 1997).

The relatively small changes due to component wear also indicate that the specific fuel consumption can only be used as indicator for fuel efficiency when both the fuel flow meter and torque sensor have high long term accuracy.

Apart from the engine conditions, fuel characteristics also cause changes in the fuel efficiency. Vessels receive different types of fuel during bunkering in different countries and ports. Fuel characteristics, in terms of energy content, may therefore differ between fuel tanks. Furthermore, in certain areas, a switch to cleaner fuel must be made because of environmental regulations. During these periods, engine efficiency changes. In order to correct for these changes in energy content, the 'LCV' value, or Lower Calorific Value, of the fuel must be known. The Lower Calorific Value is the amount of heat (Joule) that is released during combustion of 1kg of fuel. As the LCV increases, less fuel is required to obtain the same power output. For example, if the bunkered fuel is of type IFO-380 with an LCV of 39.332 MJ/kg and if for some reason a switch is made to fuel with a better quality, e.g. IFO-40 with a LCV of 40.073 MJ/kg, a 1.85% reduction in fuel consumption can be expected. The exact LCV must therefore be known so that corrections can be made to the measured fuel flow for deviations from a standard.

It may be concluded that in order to evaluate engine performance in service, in addition to fuel consumption and power, a large number of other parameters must be monitored. Engine timing characteristics, fuel characteristics and engine room temperature are the most important parameters to be logged. Unless special monitoring campaigns are in place, comparison of engine performance between vessels is subject to large uncertainties and should be avoided.

3.3.11 Local conclusions regarding data acquisition requirements

In the previous sections the environmental and ship's characteristic factors that affect the ship performance were reviewed. Based on this review, the requirements with respect to data logging can be defined. One of the conclusions is that, in the periods of transit, due to acceleration, deceleration, course deviation, drift, excessive motions, and shallow water, the propulsive efficiency and hull resistance change significantly. The complex interrelationships between wake fraction, thrust deduction, propeller characteristics and engine efficiency make it impossible to account for each individual change. During these conditions, ship performance should therefore not be used for performance analysis purposes. The above mentioned transit periods can be identified by continuously monitoring of the following parameters at 1Hz (standard sampling frequency onboard for most equipment):

- Shaft torque
- Ship speed through water
- Engine speed
- Ship speed over ground
- Course over ground
- Heading
- Rudder angle
- Water depth
- Wind speed and direction
- Water depth
- Ship motion

Performance deviations due to wind, wave, shallow water, draft deviations, propeller roughness and engine performance can be predicted by measuring environmental and loading conditions. The following parameters must therefore be logged:

- To monitor wind resistance: wind speed, direction, air density, ship speed over ground
- To monitor the added wave resistance: wave and swell height, period, direction and spectrum
- To monitor shallow water resistance: water depth
- To monitor hull resistance: ship speed through water, draft, trim, water viscosity
- To monitor propeller efficiency: propeller roughness, torque, thrust, propeller speed

- To monitor engine efficiency: fuel consumption, fuel density, calorific value, inlet air temperature in combination with a large number of engine characteristics such as timing constants, temperatures, pressures etc.

Most parameters require continuous monitoring to be able to notice rapid and/or small changes. For certain parameters this is however not necessary, as described below:

- Air density and water viscosity do not change very rapidly and can be logged less frequently
- Sea characteristics: hourly, depending on location (at open seas, sea characteristics are likely to change even less frequently)
- Fuel characteristics only change when a change is made to fuel from a different source
- Draft and trim change during a voyage from the use of consumables. The requirements for logging are depending on type and size of the ship, and may vary from daily to weekly
- Propeller roughness can only be determined by diver inspections, and is therefore limited to 2-3 times per year, depending on the likelihood of fouling and likelihood of fouling.

In the following section, the way the required ship parameters are measured and which physical factors that affect their accuracy are described.

3.4 Sensors and measurement characteristics

The main objective of this section is to identify the sensitivities and uncertainties in logging ship performance data and environmental characteristics, and to describe signal processing methods to improve the quality of data collection for performance monitoring purposes, used later in this thesis.

3.4.1 Ship speed

Ship speed can be described in a number of ways, such as speed made good, speed through water, speed over ground, propeller ship speed etc. Figure 3.14 shows the speed vectors of a ship under the influence of current and wind. For performance monitoring, the forward ship speed through water, identified by V_{xw} in Figure 3.14, is of main importance. Furthermore, athwart speed through water (V_{yw}) and speed over ground V_g are important for the identification of drift and the calculation of air resistance respectively.

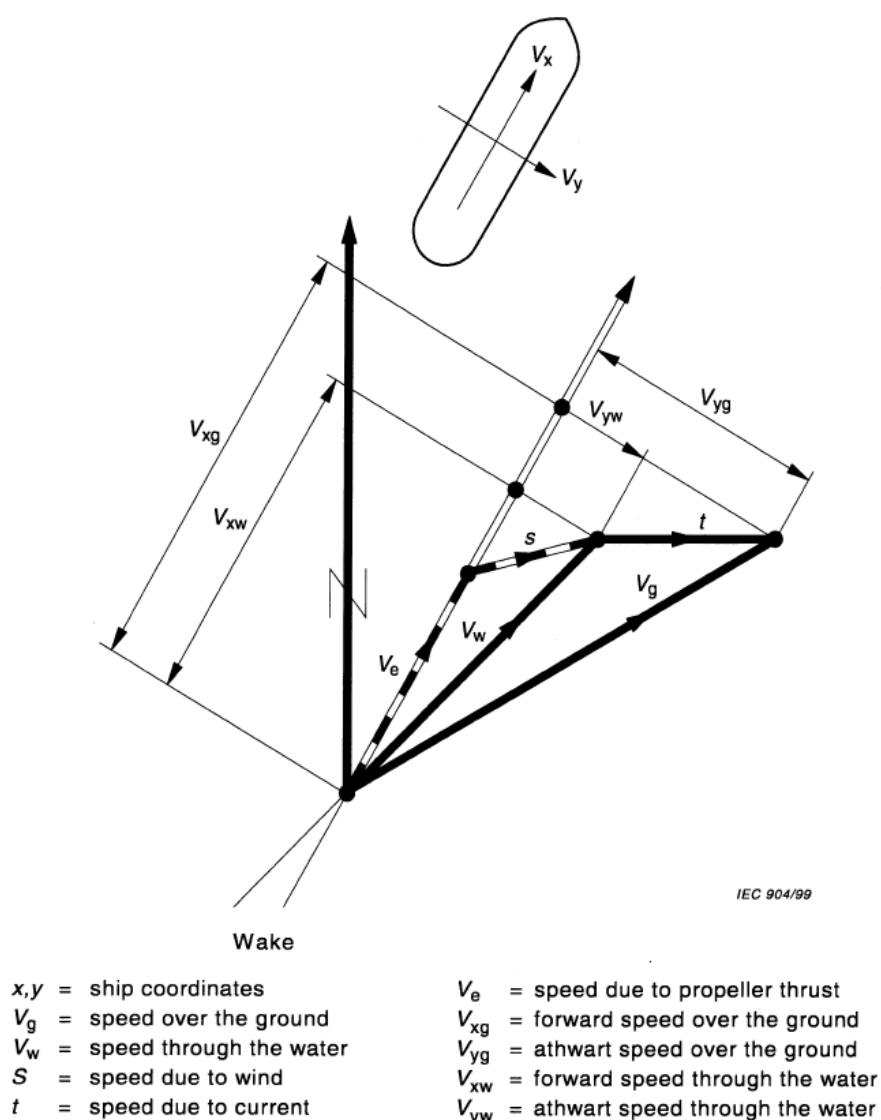


Figure 3.14: Ship speed velocity vectors
((BSi 2000) fig 1)

Ship speed is traditionally measured as speed over ground using a sextant or a Global Positioning System (GPS) and can be determined with high accuracy. Ship speed over ground is however affected by current, which makes it unusable for performance monitoring. In order to use the Speed Over Ground (SOG) for the estimation of the Speed Through Water (STW), the current must be deduced. Current is however difficult to measure and should be known whether the current is homogeneous over the whole depth of the ship's hull, so that the whole hull is affected. As discussed in section 3.2.2, this is often not the case due to waves, wind and temperature gradients.

Wind and waves create a drift relative to the water (s in Figure 3.14). The athward speed resulting from this drift is referred to as ‘leeway’ (V_{yw}). Leeway causes errors in the measurement of ship speed through water, and should therefore be known so that corrective measures can be taken. The measurement of leeway and the differentiation between leeway and drift is however not easy. In normal circumstances, surface currents are much larger than leeway, and difficult to distinguish from local wind-driven currents. Furthermore, leeway is not a linear function of wind velocity, and wind fluctuations affect leeway significantly. Predictions of leeway based on wind speed, for example as proposed by Berlekom (Berlekom 1981) or Richardson (Richardson 1997) are therefore based on statistical methods and relatively inaccurate. Furthermore, large ocean waves induce significant time-dependent lateral forces and yawing moments that require rudder action to counter. A down-wind and down-wave leeway may therefore be underestimated by the measurement of wind speed alone (Richardson 1997). Leeway is especially important at low speeds and ships with a large above-water surface area, where the effect of beam winds and waves is most apparent and the leeway relative to the ship speed large. Leeway magnitudes up to the order of 2 knots have been found (Scott 1971). In most cases however, leeway is small, in the order of 0.1 knot (Richardson 1997), and for the definition of ship speed through water may be ignored.

In the following sections the sensitivities and uncertainties in the measurement of the speed through water and over ground are discussed.

3.4.1.1 Speed over ground

SOG is a non critical parameter for performance monitoring, as it is not related to the actual performance of the ship. It can be used for the validation of the speed through water measurement and the identification of currents. Speed over ground and ship position can be determined by means of a Global Positioning System (GPS). A GPS receiver calculates its position by receiving signals from a number of satellites and calculating the time a signal takes to reach the unit from each satellite in range. The Differential Global Positioning System (DGPS) is an enhancement to the GPS and uses geostationary satellites (e.g. the Wide Area Augmentation System WAAS) who broadcast

information about the difference between the positions indicated by the satellite system and the known fixed positions (Bowditch 2002).

SOG can be calculated either by a combination of movement per unit time and computing the Doppler shift in the pseudo range signals from the satellites or from the movement per unit time only. The absolute speed accuracy of a GPS is difficult to define, since the data quality varies with receiving conditions, number of available satellites, speed and speed changes. Smoothing is therefore necessary. Only with a steady ship speed over a number of minutes the measured speed over ground will settle and indicate an accurate figure. The ITTC estimate for a 1 mile run at 15 knots a 95% confidence interval of the speed of $15.0 \pm 0.023 \text{kn}$, while at 25kn the confidence interval is $25.0 \pm 0.038 \text{kn}$ (ITTC 2002c). This is with the assumption of DGPS coverage of 95% and a positional uncertainty of 2 meters.

3.4.1.2 Speed through water

STW is the most important parameter of performance analysis. The high order of the speed-power curve (at design speed typically in the order of 3.5 - 4.5) results in a high sensitivity to ship speed. The requirements for accuracy and precision are therefore extremely high. Following IMO regulation A.824 (BSi 2007), speed logs are required to have an accuracy of less than 2% of the speed of the ship, or 0.2kn, whichever is greater. The accuracy is to be met when the ship operates free from shallow water effects and from the effects of wind, sea bottom type, current and time. In normal service conditions, this accuracy can however seldom be met. In this section, the likely causes of error and the principle of operation of speed logs is discussed.

STW can be measured by the following techniques on ships:

- Using a pitot tube
- Using a paddle wheel or impeller based devices
- Using the acoustic Doppler principle
- Using the Electromagnetic (EM) principle
- Using the Acoustic Correlation (AC) principle

Due to their vulnerability, the first two systems are not used in merchant ships. Doppler logs are most frequently found onboard such ships and operate by emitting 4 beams of high power acoustic energy ‘pings’ into the water, which echoes are received back. The Doppler shift in the returned echo is then related to the speed of the water flow passing the sensor. The layer of water that is measured ranges between 2-7m below the sensor surface, depending on water depth. The recommended location of Doppler logs is midship’s at the centre line of the ship or $1/3^{\text{rd}}$ of the ship’s length from the forward end (Skipper 2009) in order to reduce the effect turbulence and aeration of the water, which may cause inconsistent readings.

Electromagnetic (EM) logs are based on Kirchoffs right hand rule which states that a conductor (sea water) moving through a magnetic field (generated in sensor) will produce a current orthogonal to both field and movement. Movement of the vessel through sea water with at least 5ppt salinity will produce a current across two pins of the sensor orthogonal to the ships motion. This minute current is measured and converted to a speed. By principle, the sensor measures the water flow directly on the sensor surface. EM logs are therefore preferably installed as close to the bulb or bow as possible where the boundary layer is thinnest (Skipper 2009).

Acoustic Correlation logs are based on the correlation of reflected sound-energy pulses in the water at a fixed distance (13cm) from the sensor. By measuring the time delay between two similar sound-energy echoes, the ship speed through water can be calculated. In order to receive the echoes from the pulses from the water, a certain amount of particles in the water is necessary (Consilium 2009). As with EM logs, AC logs should be installed as far forward as possible, to reduce the effects of boundary layer changes as much as possible.

Due to the difference in operation, the three types of logs behave differently to aeration, particulate matter, salinity etc. In Table 3.2 the properties of these types of systems are listed for relative comparison.

Table 3.2: Speed log characteristics

Parameter	EM Logs	AC Logs	Doppler logs
Sensitive to aeration of water (e.g. due to wake from other ships, waves, propulsion system)	Negligible	Yes	Yes
Sensitive to seawater salinity	No	No	Yes
Sensitive to seawater temperature	No	No	Little
Sensitive to Particulate matter in water	No	Yes	Yes
Sensitive to boundary layer	Yes	Yes	No
Sensitive to rolling & pitching	No	No	Yes
Distance of flow measurement from hull	On sensor surface	13cm below hull	2-8m below hull
Ability to measure bottom track	No	Yes	Yes
Price	\$	\$\$	\$\$\$

As can be seen from Table 3.2, EM and AC logs are more robust to seawater characteristics than Doppler logs. However, the fact that they measure close to the hull surface, often inside the boundary layer of the ship, means they are influenced by hull roughness, fouling, draft, trim, water depth, vertical ship motions and the ship's speed. Calibration procedures to account for varying conditions are often not done because they are time consuming, expensive and there is little motivation (the accuracy searched for performance monitoring is not required for normal operation of the ship) and awareness.

Yet, even Doppler logs do often not meet the required accuracy;

- Surface winds and waves give rise to irregular sea currents and water movements at the proximity of the sea surface, which affects Doppler readings (as discussed in section 3.2.2). Furthermore, roll and pitch motions generate false movements of the vessel relative to the water which tends to give over-readings, especially with rolling and pitching motions of more than $\pm 10^\circ$ (Babbedge 1976)
- Improper location of sensor may cause systematic errors, for example when the sensor is positioned too close to the propeller, thrusters, drain tubes or the echo sounder transducer

- Disturbances in the propagation of sound waves in water occur when aerated water is present under the transducers. When a ship is sailing in ballast, its draft is at its minimum, and the probability of disturbances caused by induced air is greatest. The depth to which air has penetrated the water in a sea state is approximately equal to the wave height in meters (SAM 1998). Other causes of disturbances are when the vessel is sailing behind another ship, when the vessel sails in the aerated wake generated by the propeller action of the ship ahead. During such disturbances, the speed is generally underestimated, depending on frequency and severity of the air bubbles
- Depth under the keel might be too little for the Doppler log to differentiate between flow of seawater or bottom.
- Doppler logs rely on an accurate definition of the speed of sound through water. The speed of sound is dependent on water temperature and salinity. The salinity is often not measured, and should be entered manually. If the incorrect salinity is entered, errors in the order of 0.3% are possible. Temperature is much more important but often measured by the sensor on the surface.
- Incorrect Calibration. Experience shows that speed logs are often only calibrated at one speed or following wrong calibration procedures. Especially for EM and AC logs, which measure within the boundary layer, calibration is however crucial for correct operation (Steier 2009).

As a result of the above factors, it is often experienced that speed logs have an uncertainty in the order of knots rather than fractions of a knot (Munk 2006a).

The ability of Doppler logs to measure bottom track in water depths up to 400m, allows them to switch to bottom track if the measured STW is of insufficient quality or the water depth becomes low. Figure 3.15 shows an example of a sailing of the *Overseas Tanabe* through the Java Sea where Doppler log first measures STW, and later automatically switches to bottom track and follows the GPS speed over ground. Around timestamp 9000 the log switches back to water track. When collecting performance data, the internal conditioning of sensors should therefore be well known, to avoid these errors which affect performance monitoring accuracy. Often this setting can be adjusted in the controlling electronics of the speed log.

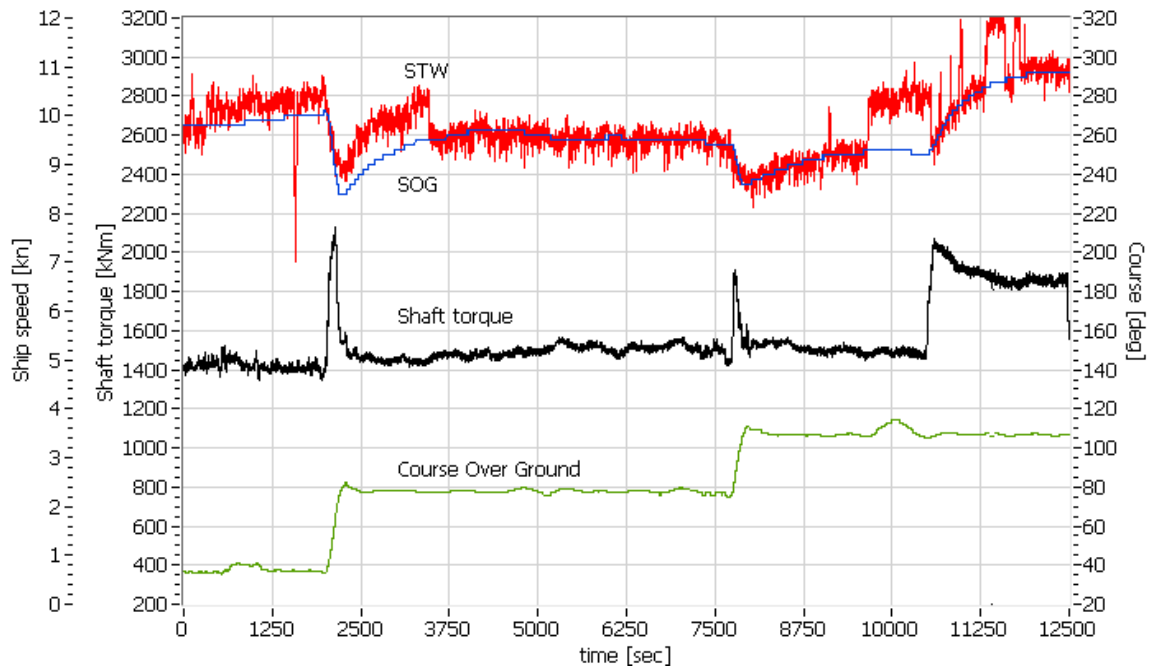


Figure 3.15: Doppler log switching from water track to bottom track from the *Overseas Tanabe*

3.4.1.3 Validation of STW measurements

Validation of STW measurements requires a complete picture of the forces acting on the vessel, in combination with engine data. Validation is done by comparing the performance of the ship (speed and absorbed propeller power) with the environmental conditions. If the environmental forces do not change, it is expected that both speed and power remain constant. Moreover, if the ship speed changes, e.g. due to windage, this will always affect the propeller absorbed torque, and can therefore be seen in deviations in shaft power. If the shaft power does not vary, speed deviations are not actually experienced by the ship (or propeller). Figure 3.16 shows a time series of shaft power, STW, SOG, course and calculated wind resistance collected by the Author on the *Overseas Tanabe* while sailing in deep water along the Namibian Coast. The plot represents 24h of data, whereby all displayed parameters are filtered for outliers using a median filter and averaged using a simple running average over 60s. The sea state was reported force BF5 from head direction. Course deviations were small.

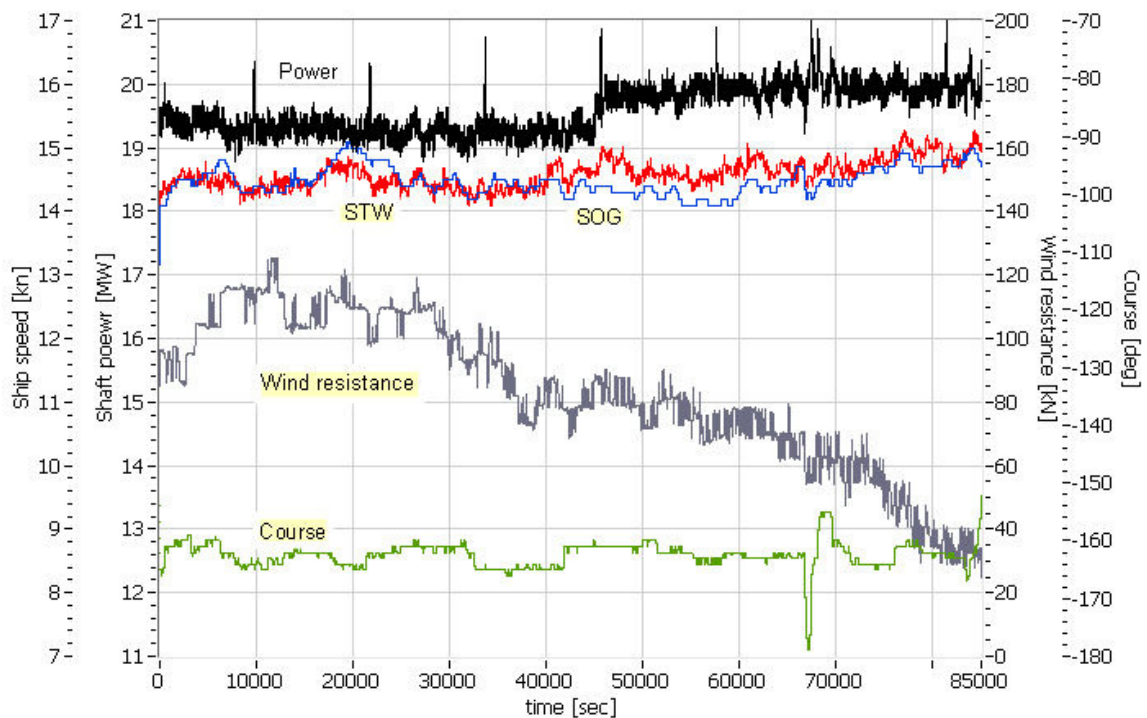


Figure 3.16: 24h Performance log of the Overseas Tanabe in deep water

The two largest forces acting on the vessel are from the waves and wind. Wave resistance has been reported as constant over time, while wind resistance varied as indicated in the graph. The variations in speed through water can in some instances be explained by course variations and changes in wind resistance, yet often there is no relation. There is however a weak relationship between SOG and STW, e.g. between timestamp 10,000 – 35,000. This indicates that either Doppler log readings are somewhat affected by current, or there are slow varying forces (here with a period between 1-1.5h) that are not measured. If it may be assumed that in open ocean wave conditions are relatively constant and related to wind speed and direction, it follows that Doppler logs are in some extent effected by current.

Figure 3.17 shows another example of typical errors that can be contributed to speed log errors. The time series represents a sailing in the South China Sea in deep water and calm weather BF3.

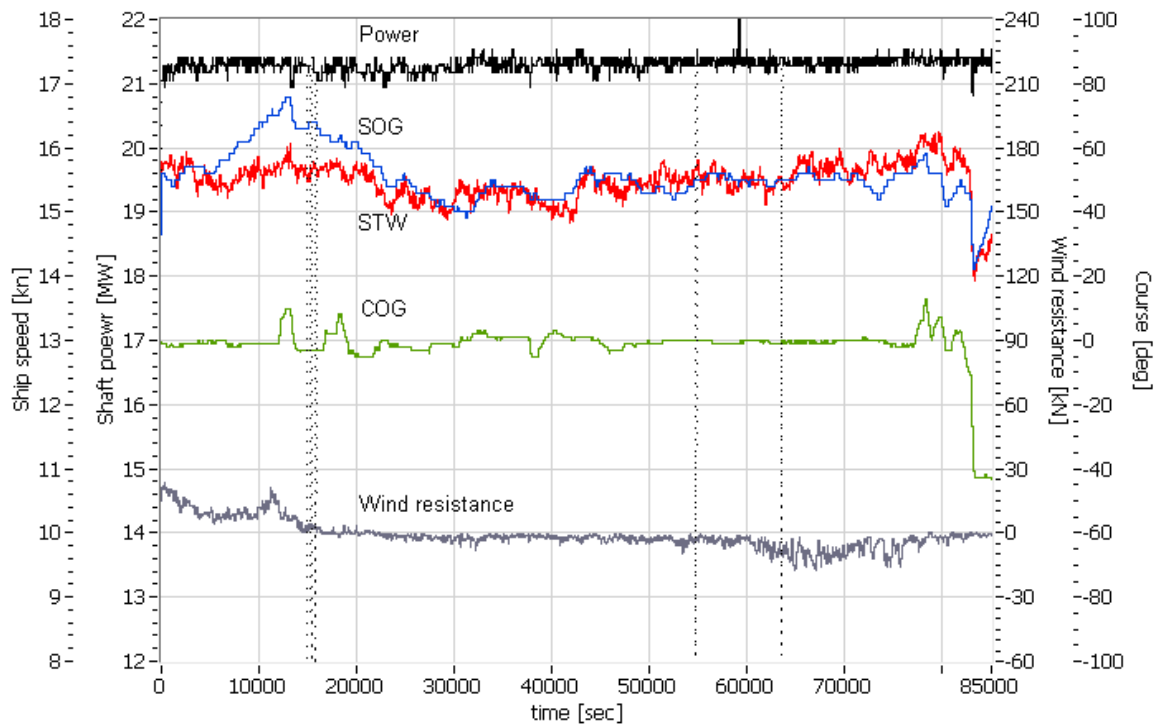


Figure 3.17: 24h Performance log of the Overseas Tanabe in deep water

The ship sails with constant power with beam winds (wind resistance negligible). The ship speed varies however between 15 and 16 kn without direct relationship with either course deviations or changes in wind and wave resistance. This indicates again that either the Doppler log is affected by currents or other disturbances in the water layer under the ship, or forces other than wind and wave affect the ship performance. Since the speed deviations cannot be related to shaft power (a reduction in ship speed should go hand-in-hand with a change in absorbed propeller power), this gives problems when analysing ship performance.

To be able to use the speed log for performance monitoring, special filtering is required to improve reliability. Under certain conditions, the Doppler log is known to be erroneous;

- In shallow water, where the water under the hull is accelerated
- During course deviation, where the flow under the hull is not parallel to the x-axis of the ship
- In rough weather and large ship motions

- When the transverse speed through water is significant ($>0.5\text{kn}$), indicating that the ship drifts. If no measure of the transverse speed through water is available, the wind and wave direction can be monitored. In beam wind and waves, the ship is most likely to have a transverse speed through water
- When STW fluctuates violently in the order of $>2\text{kn}$, indicating measurement errors from e.g. disturbances in the propagation of sound waves

The abovementioned factors can be identified automatically by a performance monitoring system. Other characteristics that can be used to identify the quality of the speed log signal are the relationship with shaft power, periods of constant speed etc. In section 5.3.5 a filter is described to evaluate the quality of the speed sensor for a VLCC. In order to have a continuous measure of STW on the bridge for real-time performance monitoring, the inflow speed of the propeller may be related to STW. In the following section this is further discussed.

3.4.1.4 Propeller as speed indicator

For real-time performance monitoring, a continuous measure of ship speed through water is required. Yet, in order to be able to rely on the speed log, a large number of conditions should be met (as listed in the previous paragraph). As a result, no continuous, reliable measurement of speed through water is available. Instead, the Generalised Power Diagram (further indicated as ‘GPD speed’) as discussed in section 2.3.3 can be used. The use of the propeller as a dynamometer always represents the speed obtained by the energy transmitted through the propeller by the engine, as long as the wake fraction and propeller characteristics remain constant. It accounts for slowly developing deviations in torque due to wind, waves etc. In principle, the GPD speed matches therefore the speed – power relationship better than if the Doppler log is used. The GPD speed is calculated using the measured shaft torque, shaft speed and propeller as following:

- The torque coefficient is calculated using the measured shaft torque and propeller revolutions, deduced by the shaft losses:

$$K_Q = \frac{Q - Q_{loss}}{\rho n^2 D^5} \quad (3.7)$$

- If the propeller open water torque coefficient can be approximated by a second order polynomial, the advance coefficient can be calculated using:

$$J = c_1 K_Q^2 + c_2 K_Q + c_3 \quad (3.8)$$

- GPD speed V_{GPD} is calculated using a measure of the wake fraction, as following:

$$V_{GPD} = \frac{JnD}{1-w} \quad (3.9)$$

Where:

K_Q = Torque coefficient

Q = Measured shaft torque [Nm]

Q_{loss} = Estimated transmission losses in shaft seal and bearings [Nm]

n = Propeller speed [rps]

D = Propeller diameter [m]

J = Propeller advance coefficient [-]

c_1, c_2, c_3 = Polynomial regression coefficients [-]

w = Taylor wake fraction [-]

The GPD speed is based a constant wake fraction and constant propeller characteristics. During transient periods, or periods where the wake fraction changes (drift, excessive ship motion, shallow water etc), the calculated GPD speed is unreliable. Moreover, in long waves, the orbital velocity motions of waves result in changes in wake velocities, affecting the GPD speed. Speed variations caused by windage and small, short waves however do not affect the GPD speed, as accelerations and rate of turn resulting from these forces are low. The GPD speed works best with fixed pitch propellers, as for controllable pitch propellers the propeller characteristics are difficult to determine. The

pitch angle must be very accurately measured and model tests should be done for all pitch angles and a wide range of loading conditions, which is often not available.

Data validation for GPD speed

As stated earlier, prior to estimating the GPD speed, the open water diagram and wake fraction must be validated for the true full-scale behind conditions. Because the effective wake fraction is calculated with the propeller open water diagram in sea trials, the validation of the latter is difficult (both are unknown). An open water diagram is often obtained from model tests and using corrections scaled to the full scale (Grigson 1990). If no model tests are available, propeller characteristics can be estimated using suitable standard propeller series or numerically estimated using basic blade geometry figures. Here, the first uncertainties are introduced.

The effective wake fraction can be determined using model tests or computer calculations. If speed trials are done to determine the effective wake fraction, the measured and predicted wake should match closely if the ship speed is determined correctly. Deviations may be due to uncertainties in the measurement of torque, ship speed and RPM, or errors in the prediction of the open water diagram. To assess which parameter has the largest uncertainty, the combined characteristics of the wake fraction and GPD speed can be used.

Figure 3.18 shows an example of the problems that could be faced when speed trial data is analysed using the propeller open water diagram. The dataset is taken from dedicated speed trials on the *Bernicia*, performed and collected by the Author. The torque, RPM and ship speed from the speed trials are converted to the torque coefficient K_Q and advance coefficient J using a predicted wake fraction of $w = 0.1$ from semi-empirical methods (Holtrop 1984).

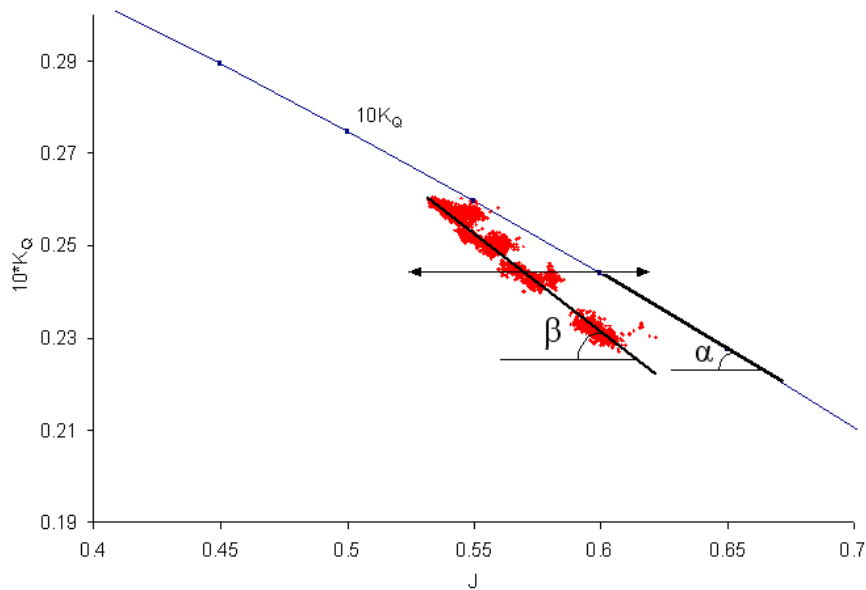


Figure 3.18: Open water diagram with sea trial performance data from the *Bernicia* indicating uncertainties in the estimation of wake fraction

If a linear regression curve is drawn through the data points, two differences may be noticed: the gradients α and β differ and there is a horizontal offset between the propeller K_Q -curve and the measured data points. The horizontal offset between the K_Q -curve and the data points is directly related to the wake fraction. If the measured data points lay left of the K_Q -curve, the selected wake fraction is too large. If the points are right of the K_Q -curve, the used wake fraction is too small. The wake fraction may be calculated by equation (3.12). The differences in gradient between the data points (β) and the open water diagram (α) may be caused by the following factors:

- Wake fraction is not constant but a function of ship speed or propeller load. The larger the difference in gradient, the more the wake fraction is affected by ship speed. When $\alpha \leq \beta$, it would seem that the wake fraction increases with speed, while $\alpha \geq \beta$ indicates a decreasing relationship. Investigations on model tests by Harvald (Harvald 1950) show that for ships with small propellers, which are more affected by wake, w falls at rising speed, while ships with relatively large propellers (tugs, pilot boats etc.) have a very small increase in w at increasing speed.
- Errors in the open water diagram. Assuming the wake is constant throughout the trials, the difference in gradient indicates possible errors in the derivation of the

full-scale behind conditions (e.g.(Grigson 1990)). For the calculation of the GPD speed, the gradient of the K_Q -curve (α) determines the extent to which the speed changes with a change in torque and RPM. A sheer gradient causes a large change in GPD speed to a unit change in torque or RPM, while a gentle gradient makes the GPD speed relatively insensitive. By comparing the calculated GPD with accurate ship speed measurements over a range of ship speeds, an assessment can be made about the accuracy of the gradient of the K_Q -curve.

- The speed sensor is in error. The analysis of up- and downstream speed trails or periods in which current is negligible allows the speed sensor to be validated with the GPS speed over ground. The average speed between two short runs in opposite direction should be equal to the average speed through water. In this way, the accuracy can be determined with high accuracy.
- Systematic error in the torque sensor. Torque sensors are sensitive instruments susceptible to sensor drift and rely on the availability of shaft characteristics (elasticity modulus). Incorrect estimation of these characteristics or infrequent calibration of the sensors to account for drift may cause systematic errors in the estimation of the GPD speed.

In Section 5.2 the above methodology is used to validate the open water diagram for the *Bernicia*. It is important to have an accurate set of propeller characteristics in order to get and accurate measure of ship speed and analysis of ship performance data.

Effect of hull & propeller fouling on GPD speed

The propeller and wake characteristics are both affected by fouling and roughness. The calculated GPD speed is therefore expected to be affected as well. Periodical corrections/calibrations are therefore necessary. The development of hull fouling causes two performance parameters to change:

- The propeller load increases (higher torque absorption at same RPM) due to higher frictional hull resistance, resulting in a lower advance coefficient J
- The wake fraction increases due to a thicker boundary layer around the hull.

Furthermore, for an uncoated propeller, the roughening of the propeller blades causes an additional change:

- Decrease in open water efficiency due to a higher torque coefficient and slightly lower thrust coefficient (as discussed in section 3.3.5).

The accuracy of the GPD speed is not affected by propeller loading, and is therefore not affected by the higher frictional resistance due to hull fouling. The increase in wake fraction and decrease in propeller efficiency however have a direct influence on GPD accuracy. Propeller efficiency can only be measured with a simultaneous measure of torque and thrust. Propeller thrust is however very difficult to measure onboard ships (see section 3.4.14), and empirical methods, based on the measurement of blade roughness (section 3.4.15), have to be used instead. Since blade roughness measurements do not account for fouling, and are based on the extrapolation of model tests and computer simulations (section 3.3.5) they have a certain level of uncertainty. The implications of this uncertainty on the accuracy of GPD speed calculations are discussed in the following section. Three cases are examined; clean propeller with a fouled hull, fouled propeller with a clean hull and a fouled propeller and hull.

Hull resistance itself does not affect wake. In the following analysis into the effects of changes in wake and propeller efficiency on GPD speed, the ship speed is therefore considered constant. Changes in advance coefficient J (equation 3.12) may therefore be used directly to indicate changes in wake fraction.

Clean propeller, fouled hull

A fouled hull results in an increase in wake fraction, which can be measured using propeller characteristics and a measure of speed through water from a speed log, shaft torque and speed of rotation. The calculation method is similar as the calculation of the GPD speed, and follows as:

$$K_Q = \frac{Q}{\rho n^2 D^5} \longrightarrow J = c_1 K_Q^2 + c_2 K_Q + c_3 \longrightarrow w = 1 - \frac{JnD}{V_S} \quad (3.10)$$

Figure 3.19 shows a propeller open water K_Q -curve. In clean hull and clean propeller conditions, the propeller operates at (J, K_Q) . An increase in boundary layer of the hull results in a decrease in water speed into the propeller plane (referred to as ‘advance speed’). If during sea trials the propeller is used to determine the wake fraction, the decrease in advance speed will result in a higher absorbed torque at constant RPM, and a higher observed effective wake fraction (see (J_1, K_{Q1}) in Figure 3.19). The new ‘measured’ higher wake fraction corresponds to the actual change in effective wake fraction of the ship. In later analysis, it will be seen that the ‘measured’ wake fraction not always represents the true wake fraction.

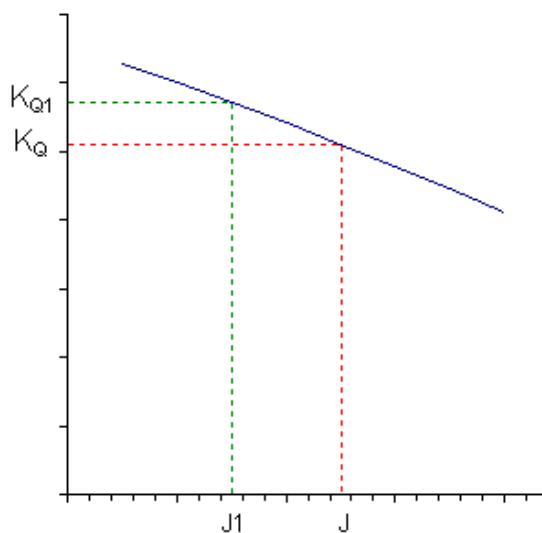


Figure 3.19: Definition of wake fraction using open water diagram

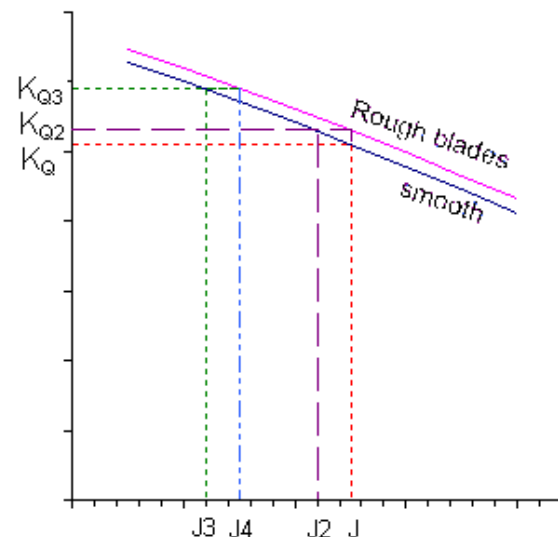


Figure 3.20: Effect of propeller roughness on the definition of wake fraction

The GPD speed is defined by $V_{GPD} = \frac{JnD}{1-w}$. As long as the wake fraction is correctly

calibrated, the changing hull resistance and changing boundary layer around the ship will not affect the GPD speed. If, however, the wake fraction is not calibrated regularly, the GPD speed will become systematically too low. The ‘calibration’ of the wake fraction, or re-definition, can be done using dedicated up-and-down stream speed trials or in areas where the ship speed can be determined accurately (e.g. automatically by a PM&A system, as discussed later in the thesis in Section 4.5).

Fouled propeller, clean hull

In Figure 3.20, the K_Q -curve for a roughened propeller is included in addition to the clean propeller K_Q -curve. As a result of the lower propeller efficiency, a roughened propeller absorbs more torque at any shaft revolutions compared to a clean propeller. With a fouled propeller but clean hull, the absorbed torque for the same RPM and ship speed will therefore be increased from (J, K_Q) to (J, K_{Q2}) .

If the increase of K_Q -curve of the fouled propeller is not taken into account (e.g. because the propeller blade roughness is not measured), the higher propeller loading (K_{Q2}) results in a lower advance coefficient with constant ship speed and RPM ($J2$). During wake calibration runs, it would seem that the wake fraction has increased from $J \rightarrow J2$ while this isn’t actually the case. Yet, by using the newly measured wake fraction, the GPD speed will be calibrated and will represent the correct ship speed. It is hereby assumed that the change in K_Q -curve may be represented as a vertical offset (no change in gradient). If both the K_Q -curve hasn’t been corrected and the wake fraction is not calibrated, the GPD speed will be systematically too low.

If the change in propeller characteristics are corrected accordingly, the increase in torque ($K_Q \rightarrow K_{Q2}$) has no effect on the advance coefficient (J). As a result, the GPD speed will remain unaffected and remain correct.

Propeller and hull fouled

When both propeller and hull are fouled, the wake fraction is increased and propeller efficiency reduced. The implications of not correcting the propeller open water diagram on the accuracy of the GPD speed can be described as following: If the propeller characteristics have not been corrected, the increase in absorbed torque from the propeller fouling results in a decrease in advance coefficient ($J \rightarrow J2$). Furthermore, the increase in boundary layer results in an increase in absorbed torque ($K_{Q2} \rightarrow K_{Q3}$). During wake calibration runs, it would seem that the wake fraction has increased more ($J \rightarrow J3$) than is actually the case ($J \rightarrow J2$). However, with the new obtained wake fraction, the GPD speed remains calibrated.

If the propeller characteristics have been corrected for propeller roughness, the increase in torque due to propeller roughness would be accounted for ($K_Q \rightarrow K_{Q2}$) and the increase in propeller load due to the larger boundary layer of the hull is measured by the decrease in advance coefficient ($J \rightarrow J4$), which is equal to ($J \rightarrow J1$). With the new obtained wake fraction, the GPD speed remains unaffected.

It may be concluded that neither hull fouling nor propeller fouling affects the GPD speed, as long as the wake fraction is regularly calibrated. Furthermore, if the wake fraction is measured using the propeller during sea trials, it is affected by both propeller and hull fouling.

Example wake fraction inaccuracy

To demonstrate the contribution of the inaccuracy of the wake fraction obtained with a fouled propeller, a numerical calculation has been made for a tanker with a propeller diameter of 9.5m, absorbing 2391kNm at 62.8rpm to reach a ship speed of 14.82kn (based on trial results described in (ISO15016 2002)). For the prediction of the increase of wake fraction and propeller fouling the following assumptions have been made:

- The wake fraction ($w = 0.17$) increases with 30% to $w = 0.221$ as a result of hull fouling. The ship speed and propeller speed of rotation are hereby assumed to remain constant

- The propeller torque coefficient K_Q increases with 3% due to propeller fouling scale *Rubert D-E* (based on findings of (Townsin et al. 1985)). The propeller roughness only affects propeller absorbed torque; ship speed and propeller speed of rotation remain constant.

The higher wake fraction (30% increase) results in a torque increase from 2391 to 2520kNm (5.4% increase). The propeller fouling results in an additional increase of 3%. If the wake fraction is determined in service using the uncorrected propeller open water diagram (K_Q curve), the wake fraction becomes $w = 0.238$, an over prediction of 33% (40% increase in wake instead of 30%).

Numerical calculations on a container ship with a propeller diameter of 6.15m, absorbing 1271kNm at 120.6rpm to reach a ship speed of 20.24kn (based on speed trials described in (Journée 2003)) with similar increases in wake fraction and torque coefficient, show similar results (wake over prediction of 30% as a result of the use of an uncorrected K_Q curve).

From the above example it shows that the wake fraction cannot be used directly as an indicator for hull fouling alone. It is necessary to correct the propeller open water diagram for propeller roughness to avoid over prediction.

3.4.2 Shaft torque

Torque absorbed by the propeller can either be determined indirectly using pre-defined relationships between measured fuel consumption or fuel rack and output power, by means of the measured mean indicated pressure of each cylinder, or directly by means of a torque sensor on the propeller shaft. Indirect ways are most common and form part of normal engine monitoring practices. The drawback is that changes in engine conditions or fuel characteristics affect the conversion factors to obtain output power. Moreover, indirect measurements such as mean indicated cylinder pressure measurements can often not provide a continuous measure of power. Direct methods to measure shaft torque rely on the measurement of strain. Strain measurement consists of the measurement of the elastic deformation of the material under load and relating them to torque by special

calibration or calculation from the known mechanical properties of the material, the geometrical dimensions of the shaft, and the electrical characteristics of the strain measurement sensor. The following sensing techniques can be named:

- Strain gauges
- Vibrating string sensors
- Magnetic field sensors
- Linear Variable Differential Transformers
- Angular deflection sensors.

A functional description of the latter systems can be found in (Fleming 1982; Hundley and Tsai 1992). From the torque measurement techniques listed above, strain gauges are most widely applied. They benefit from their simplicity, low cost and accuracy. A strain gauge consists of a flexible, insulating foil which supports a metallic foil pattern. The gauge is glued to the shaft and stretches as the shaft strains. The result is an increase in resistance in the foil. For shaft torque, four strain gauges are configured in a Wheatstone bridge to amplify the signal from the gauges. This increases reliability, signal-to-noise ratio and reduces sensor drift from temperature fluctuations in the shaft.

The signals from strain gauges are in the order of milli-volts and must be amplified using a differential operational amplifier to increase the signal-to-noise ratio. To further enhance the signal to noise ratio, signal conditioning is done as close to the strain gauge as possible, on the propeller shaft. The signal is then transmitted to a static receiver either by means of slip rings or a wireless telemetry system. Figure 3.21 shows the principle components of a torque sensor with telemetry system. It consists of a strain gauge glued to the shaft, a data-conditioning unit and a power source (here in the form of a 9V block battery). The data conditioning system consists of a stabilised power supply for the strain gauge, a data conditioning unit (amplifier, filter, and digitiser), telemetry system and antenna.

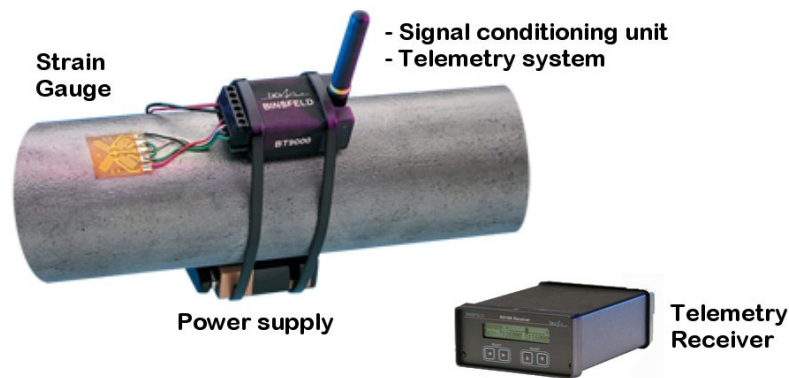


Figure 3.21: Principal components of a shaft torque sensor
(Binsfeld 2008)

There are a number of factors that affect the accuracy of a torque sensor based on a strain gauge. The main factors are:

- Installation: It is crucial to maintain the proper angle between the axis of symmetry of the gauge and the shaft. A misalignment error of $\pm 3^\circ$ results in a standard uncertainty in the measured strain of approx. 0.32% (ITTC 2002c). Furthermore, errors from improper adhesion (e.g. air bubbles) or incorrectly connected cables would result in additional errors, but should be visible for an experienced measurement operator. The quality of the protective layer applied to protect the gauge against oil and dirt is furthermore critical for the lifetime of the sensor
- Type of gauge that has been used (uncertainty in gauge factor and gauge resistance), which results in a typical 95% confidence level uncertainty of $\pm 0.46\%$ (ITTC 2002c)
- Accuracy to which the shear modulus of the shaft is defined. This data is either defined from shop tests carried out on the shaft lines, obtained from statistics or from information provided by the shaft manufacturers. The recognised bias error is $\pm 2\%$
- Location: Strain gauges installed in the vicinity of bearings cause sinusoidal readings as the shaft rotates due to misalignments in the shaft line. The effect can be reduced by installing two half bridge configurations on opposite sides of the shaft, but in practice readings will be effected regardless installation and configuration (Heijde 2008). Aliasing issues should therefore be addressed
- Type and quality of signal conditioning and processing.

Due to the many practical uncertainties, the accuracy of a strain gauge is difficult to estimate. It is often found that two identical systems installed on the same shaft show significant differences (Cooper 1995). The ITTC predict a combined uncertainty (installation, instrumentation, transmission) of a typical torque sensor installed by experts of 2.7% (ITTC 2002c).

Calibration of torque sensors

The quality of the bonding of a strain gauge is difficult to assess. Degradation of the bonding causes hysteresis and creeping and experience learns that torque sensors based on strain gauges need to be re-calibrated 2-3 times each year to guarantee stability. The most frequently applied method of calibration is calibration of the no-load condition. The no-load condition can be found by turning the propeller shaft clockwise and anticlockwise using the turning gear of the main engine. The mean of the measured values should be zero. The following conditions should be considered:

- The shaft should be turned a number of times (5-10) to generate enough lubrication between shaft and bearing (ITTC 2002a). Setting the zero in this manner means that the torque measured with the ship underway includes the torque required to overcome any bearing friction.
- The conditions where the torque sensor can be calculated should be chosen carefully. Current in port areas puts a static load on the propeller shaft, which is counter balanced by mechanical friction in the main engine and gearbox. The load of the current can be observed by turning the shaft clockwise and anticlockwise: the torque read should be of equal but opposite sign due to the friction in the propeller shaft. If this is not the case, the propeller is under the influence of current and cannot be calibrated. Another indication of current while the vessel is docked may be obtained from the speed log. Calibration should therefore be done manually.

Other means to determine the no-load condition, e.g. using the drag shaft run procedure (ITTC 2002a) are less frequently used and not discussed here.

Another method of torque calibration is validation of the sensor readings with duplicate systems, such as mean indicated pressure measurements. Pressure measurements can be used to confirm the correct selection of the modulus of rigidity, as they do not rely on the material of the propeller shaft. However, the uncertainties in the measurement of pressure and the estimation of the mechanical efficiency are likely to be higher than the errors in the estimation of the modulus of elasticity.

In short, shaft torque is one of the most important parameters for performance monitoring but is prone to errors. Yet, in order to measure the micro strain in the propeller shaft, highly sensitive instrumentation is required. Uncertainties from installation, calibration and ageing of the system should always be considered critically and actions taken where necessary to improve reliability.

3.4.3 Fuel consumption and LCV

Measuring fuel consumption on shipboard installations requires care if used for performance monitoring. Not only are there many stages in a fuel supply system, also the fuel quality may vary. Most merchant vessels run on heavy diesel oil. The requirements with respect to calorific value, water and sludge content for this type of fuel are relatively flexible. As a result, engine efficiency in terms of consumed tons of bunkered fuel versus output power changes. Furthermore, at sea, fuel is pumped from the storage tanks to the settling tank, where water and sludge is drained off. The fuel is then fed into the service tank via the purification system where further amounts of water and impurities are removed. It is therefore important to measure fuel flow as close to the engine as possible, after the fuel purification system.

Fuel flow can be measured using flow meters inline with the engine's fuel system, or by means of tank soundings. Chief engineers often have their own procedures to account for fuel consumption deviations that seem inexplicable, such as hidden reserves, using rule of thumbs to average out fluctuations or by calculating daily averages from the total fuel consumed during a voyage. Electronic measurements and data storage is therefore of primary importance. With automatic flow measurement, care must however be taken not

to measure the total fuel in circulation; this can indicate up to three times more fuel than actually used. It should exclude fuel used for purposes other than propulsion (auxiliary pumps, boilers, generators etc.) and fuel leaks from fuel pumps and injectors should be measured and deduced.

The quality of the fuel that is used must be known. The use of fuel with a lower LCV will cause an increase of flow for the same engine output, while the actual engine efficiency does not degrade

- In marine diesel engines using heavy fuel oil, the oil is heated to temperatures in the range of 125-140°C to get the required viscosity for proper combustion. Differences in supply and return fuel temperature of up to 20°C are possible, which causes inconsistencies in the measured fuel flow if not corrected to a standard temperature (KRAL 2005)
- In some modern engine condition monitoring systems the (specific) fuel consumption can be read-off directly from a computer. However, these systems may indicate calculated values by means of the characteristics of the injection pumps of fuel rack, instead of true fuel flow. Unless they are regularly calibrated and accounted for leakage due to wear or different fuel quality, their reliability and accuracy must be considered
- For fuel meters, an additional complication arises for the direct measurement of fuel flow. The pistons of the injection pumps cause fluid pulsation in the low pressure fuel lines. This pulsation may cause pressure surges on the system components, the flow rate of the fuel varying at high frequency and in rare cases brief reversals of the fuel direction of the fuel (KRAL 2005). The accuracy of most conventional flow meters relies on a constant flow. The pulsations in the fuel lines may therefore cause inaccuracies in fuel measurement if standard flow meters are used for fuel measurement. To dampen the fluctuations in flow, special fuel buffers can be installed the position of the meter can be chosen such that the fluctuations are damped by other components of the fuel system. Alternatively, special flow meters may be installed that are insensitive to pressure fluctuations (KRAL 2005).

Fuel Lower Caloric Value

Vessels receive different types of fuel during bunkering in different countries and ports. As a result, the fuel characteristics, in terms of energy content, may differ between fuel tanks. The switchover to a fuel with different characteristics should therefore be identified. Fuel injecting temperature can be used to identify this change over. After the separation of water and oil, heat is used to adjust the kinematic viscosity ν_f to a suitable level for fuel injection and atomising ($\nu_f \leq 15$ cSt) (Stapersma 2005). The required temperature is dependent on the fuel characteristics. A sudden change in fuel injection temperature would therefore indicate the change-over to a new type of fuel.

The Lower Calorific Value (LCV) can be obtained from fuel bunkering reports or calculated using the following equation (BSi 1996):

$$LCV = \left(46.704 - \frac{8.802\rho_{15}^2}{10^6} + \frac{3.167\rho_{15}}{10^3} \right) \left[1 - 0.01(x_{H_2O} + x_{Ash} + x_S) \right] + 0.01(9.420x_S - 2.449x_{H_2O}) \quad (3.11)$$

Where:

ρ_{15} = fuel density at 15°C in kg/m³

x_S = sulphur content in % Mass

x_{H_2O} = water content in % Mass

x_{Ash} = Ash content in % Mass

The following equation can be used to correct the measured fuel flow for changes in fuel calorific value (Hitachi-Zosen 2002):

$$\dot{Q} = q\rho_{corr} \frac{LCV}{LCV_{std}} \quad (3.12)$$

Where

\dot{Q} = Corrected fuel flow in kg/h

q = Measured fuel flow in litre/h

LCV = LCV value of the fuel currently used in MJ/kg

LCV_{std} = LCV value to which the fuel is corrected to (e.g. 42.27 MJ/kg)

ρ_{corr} = Corrected density for temperature in kg/m^3 , as defined by (Stapersma 2003):

$$\rho_f^\theta = \rho_f^{15} - 0.68(\theta - 15) \quad (3.13)$$

with θ the fuel temperature in $^\circ\text{C}$.

3.4.4 Shaft revolutions

The engine speed is a vital parameter for engine controlling and may be measured on the flywheel by means of a proximity sensor giving a pulse signal for each tooth on the flywheel. The resolution and accuracy of this sensor depends on the number of teeth on the fly wheel or propeller shaft, the averaging time and the clock speed of the pulse counter. The higher the number of pulses used to calculate the speed of revolution, the higher the accuracy. The clock speed of the pulse counter and the averaging time are generally high enough for an accuracy of up to 0.01% (ITTC 2002a). Proximity sensors are not subject to sensor drift and do not require calibration. If properly maintained, engine speed measurement is therefore considered the most accurate measurement on a ship for performance analysis.

3.4.5 Course & Heading

The heading of the ship is used in performance monitoring to identify course alterations (using the heading as function of the time (Rate of Turn), to determine the drift angle (difference between heading and course over ground) and to calculate the added wave and wind resistance. To accurately determine the rate of turn, a continuous measure of the heading is required, which can be obtained from the Gyro compass or GPS. Heading can be related to different references; based on the true meridian, magnetic meridian, compass or gyro compass. In certain areas, differences in the order of 0-10° exist between these references, caused by the magnetic variation of the earth. It is therefore important to use the same basis when collecting data.

3.4.6 Draft and trim

The ship's draft can be obtained from a loading computer, draft gauges or from the draft markings on the hull when the vessel is in rest. Hull markings give the most reliable way of measurements. During a voyage, the draft of the ship changes due to the use of consumables and change in water density, or due to a voluntary ballasting. In order to account for these changes, it is desirable to have a continuous measure of the vessel's true draft so that the crew is not required to interact with the performance monitoring system so frequently. Draft gauges can only be used when the ship is sailing slowly or in port, as the dynamic pressure during sailing causes incorrect readings.

The loading computer should not be used; it is a calculated value based on manually entered data or data from tank soundings. It is not a physically measured value of the draft, and large differences have been found between actual draft and indicated draft from the loading computer. It can therefore not be used for performance monitoring. A better alternative are draft gauges.

3.4.7 Wind speed and direction

The estimation of the wind speed can be done by visual estimations, forecast information or direct measurement using an anemometer. For performance monitoring, a continuous reading of the apparent wind speed and direction is required. Visual observations are therefore not suitable. Anemometers are installed on most merchant ships. Their location on the ship is important;

- The presence of the ship distorts the flow of air, resulting in measured wind speeds which are accelerated or decelerated compared to the free stream, or undisturbed flow, as shown in Figure 3.22.

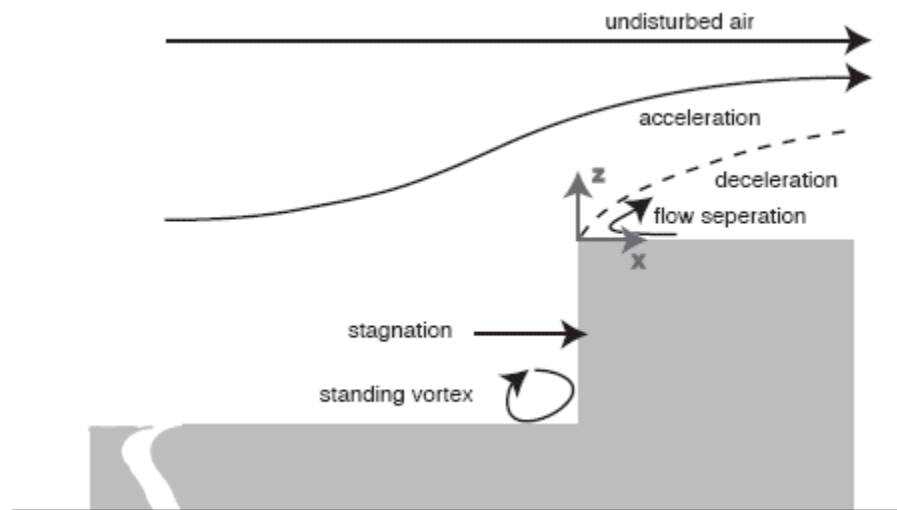


Figure 3.22: The general flow pattern above the bridge of a generic tanker/bulk carrier.

The dashed line indicates the 'line of equality' where the wind speed is equal to the free stream wind speed (Moat et al. 2005).

Using computational fluid dynamics (CFD) to analyze the air flow over container vessel and tanker shapes, Yelland et al. (Moat et al. 2005; Yelland et al. 1998) showed that there is a plume of accelerated air above the wheelhouse top (Figure 3.23). The shape of this plume depends on the geometry of the ship's accommodation block. An anemometer mounted above the wheelhouse may be below, in, or above the plume maximum depending on how high and how far aft it is mounted and cause over-readings over 10 % or under readings by 100% of the true free wind speed, depending on the anemometer location (Moat et al. 2005) .

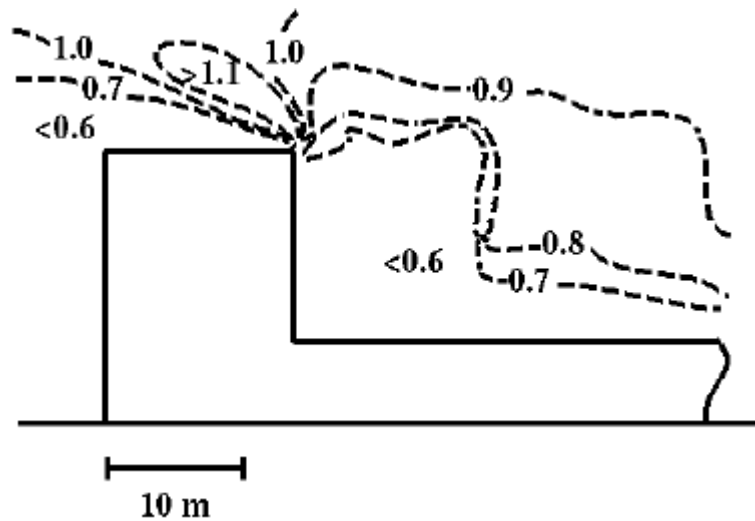


Figure 3.23: Airflow distortion over the stern of a typical tanker determined by CFD modelling (Yelland et al. 1998)

A method to predict the wind speed bias for known anemometer locations on tankers/bulk carriers is still to be developed. The following recommendations can be made with respect to anemometer locations (Moat et al. 2005): ‘...A mast in the bow of the ship, well upwind of any obstruction, is the ideal location. If this is practically not possible and anemometers can only be placed above the bridge, they should be placed as far forwards as possible and as high as possible; ideally on a slim mast located at the forward edge of the bridge. If an anemometer cannot be located at the front edge of the bridge it should be located above a height of the order of $z/H=0.3$ (where z is distance from front of bridge to anemometer and H bridge to deck height) in order to measure wind speeds outside the decelerated region (see Figure 3.22). An anemometer should not be placed close to the line of equality (normalised wind speed of 1.0), as high velocity gradients are present in this region.’

- At present there are no absolute calibration methods for marine winds. Wind speed estimates obtained using hand-held anemometers are different in character to those from fixed instruments (Taylor et al. 1994) and the best data sources that could be used for calibration would be anemometer measurements from ocean weather ships, research ships, or meteorological buoys. However, there are biases in each of these data types. Estimates of the wind stress using the inertial

dissipation method could be used to calibrate marine winds, but the costs of these instrumentation systems are significant (Taylor and Kent 1999).

- In use, the anemometer is exposed to a turbulent flow, which fluctuates as the ship rolls and pitches. Anemometer errors due to ships roll may be because of (i) ‘anemometer pumping’, (ii) the tilt of the anemometer, and (iii) the variation of height in the near surface wind gradient. For large merchant vessels, whereby the roll period is high (order of 10-20 sec), anemometer height is between 30-45 meter above sea level and roll angle is low (5°), errors remain small and negligible compared to probable air-flow disturbance effects. Only the errors from anemometer pumping has the potential to contribute an error significantly above 1% (Taylor et al. 1994)

Because of all the uncertainties, the accuracy of an anemometer is difficult to determine. Carefully positioning the anemometer on the wheel house, using CFD to determine the most suitable location, is the best way forward.

3.4.8 Air density

Air density may be calculated using a measurement of pressure, temperature and humidity. For the calculation of air density, humidity is of minor importance and may be neglected. A simple measure of barometer pressure and temperature is therefore sufficient to determine density, which may be calculated as following:

$$\rho_{Dry-air} = \frac{p}{287.05T} \quad (3.14)$$

Where

p = Barometric pressure in Pascal

T = Dry-air temperature in Kelvin

The accuracy of the estimation of the air density is determined by the frequency of observation. Air density is strongly temperature dependent, while temperature may vary

between morning and afternoon by as much as 20°C, especially in coastal areas. Continuous, electronic measurement is therefore recommended.

3.4.9 Wave characteristics

The state of the ocean surface can be characterised by means of its energy spectrum. Unless the sea spectrum is measured directly, use has to be made of standard sea spectrum models that are adjusted to the current sea conditions by a number of sea parameters. The parameters; significant height, mean period and direction for both wind generated waves and swell can be obtained from weather forecasts, direct measurement, from the Voluntary Observing Ship scheme (NOAA 2008b) or from visual observation. Visual observation, backed with information from a weather fax, is the most frequently used method. It is however also the least accurate.

For the visual observation of wind driven wave height, two scales are in use: the Beaufort and Douglas scale. The Beaufort scale was originally derived for wind estimations at sea, but has been related to wave height by different researchers (e.g. (ITTC 1972) or Pierson-Moskowitz (Bhattacharyya 1978)). The relationships are derived considering a fully developed sea, defined as wind having blown steadily for a long time (roughly ten-thousand wave periods) over a large area (roughly five-thousand wave lengths on a side) so that the waves are in equilibrium with the wind. The differences between the different scales relating wind speed to wave height are large. Figure 3.24 shows the differences between the ITTC (ITTC 1972) recommended scale and Pierson-Moskowitz scale (Bhattacharyya 1978).

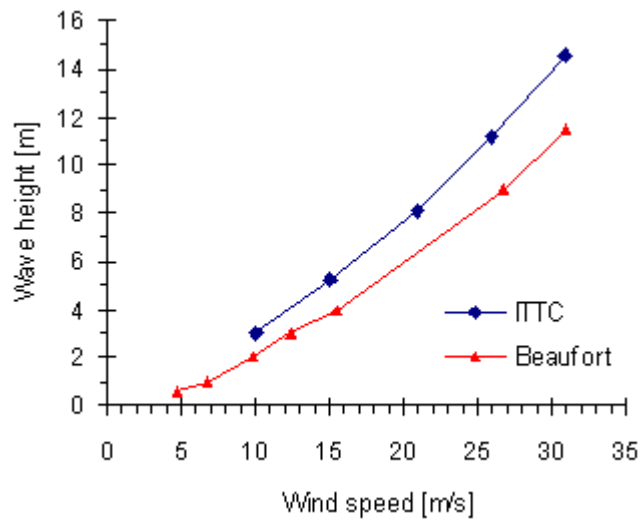


Figure 3.24: Wind speed and significant wave height relationship derived by Pierson-Moskowitz and ITTC for fully developed seas

The difference between the two scales can be contributed to the sea spectrum that has been used to derive each scale. Other inaccuracies are introduced in the regression analysis between wind and wave height measurements. Due to the large scatter, the statistical significance of regression analysis is difficult and therefore sensitive to the used statistical methods (Kent and Taylor 1997). Moreover, Gulev and Hasse (Gulev and Hasse 1998) showed that most of the wind generated waves are not fully developed. The relationships are therefore not valid anymore.

The Douglas Sea scale (Bowditch 2002) is more consistent. It relates directly to significant wave height and allows a separate observation for wind generated waves and swell. The scale is displayed in Table 3.3 and Table 3.4. The description in Table 3.4 is a shortened version. A more elaborate wording can be found in seamanship's books, e.g. (Bowditch 2002).

Table 3.3: Douglas Sea scale

Code	Description	Height [m]*
0	<i>calm-glassy</i>	0
1	<i>calm-rippled</i>	0 - 0.1
2	<i>smooth wavelets</i>	0.1 - 0.5
3	<i>slight</i>	0.5 - 1.25
4	<i>moderate</i>	1.25 - 2.5
5	<i>rough</i>	2.5 - 4
6	<i>very rough</i>	4 - 6
7	<i>high</i>	6 - 9
8	<i>very high</i>	9 - 14
9	<i>phenomenal</i>	Over 14

Table 3.4: Douglas Swell scale

Character of the sea swell		
	0	None
Low ¹	1	Short or Average ²
	2	Long
Moderate	3	Short
	4	Average
	5	Long
Heavy	6	Short
	7	Average
	8	Long
	9	Confused

**The average wave height as obtained from the large well-formed waves of the wave system being observed (Bowditch 2002). ¹A short wave has a length between 0 - 100m, Average wave = 100 - 200m, Long wave = over 200m. ²A Low height is characterised by a significant wave height of 0 - 2m, Moderate = 2 - 4m and Heavy = over 4m.*

Making wave observations

The Douglas scale requires the separation of wind-driven waves from swell, which is particularly difficult when sea and swell propagate in close directions (within the same 60° directional sector). The eye tends to concentrate on the nearer and steeper short-period waves, thereby ignoring the longer-period and more gently sloping waves (swell), even though the latter may be of greater height and energy (Ewing and Carter 1998). Figure 3.25 shows a typical record drawn by a wave recorder and is representative of waves observed in the sea. Waves invariably travel in irregular groups of perhaps five to 20 waves with relatively calm areas in between groups. It is essential that the observer should note the height and period of the higher waves in the centre of each group; the flat and badly formed waves (marked with arrows) in the area between the groups must be entirely omitted.

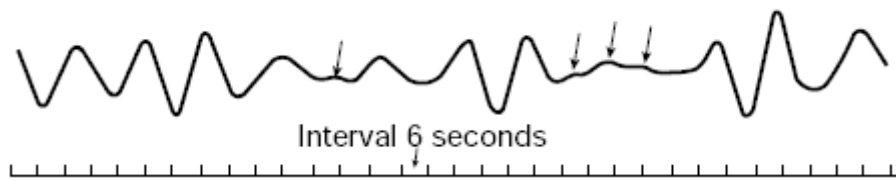


Figure 3.25: Example of a wave record
In wave observations the waves marked with arrows are to be ignored
((Ewing and Carter 1998) p. 90)

Visual observations are mostly influenced by the distance between the observer from the sea surface and the size of the ship. Waves observed from a large ship seem smaller than those same waves observed from a small ship, and especially waves with relatively short lengths with respect to the length of the ship require the observer to be as close to the surface as possible. In general, observed data tends to overestimate low waves and underestimate high waves (Cotton et al. 2000). To help the observer make accurate estimation about wind generated seas, use can be made of a set of standardised photographs, such as those derived for the Beaufort scale (see e.g. (Bowditch 2002)). The availability of photographs allows a more objective observation to be made, compared to the purely descriptive scales of the Douglas scale.

Wave period is often difficult to derive even by experienced observers. Global wave statistics, such as (BMT-Fluid-Mechanics 2008), can be used to relate wave height to mean wave period. Wave probability plots can only be used in relatively mild seas. For severe seas, there is often not sufficient statistical information available to make a reliable relationship between wave height and period. Other sources for wave period are weather forecasts or direct measurements.

Sea spectrum cannot be observed visually. It has to be chosen from a database of sea spectra based on the current location or wave characteristics. In coastal areas, where the sea is affected by currents and not fully developed, the standard spectra are too inaccurate. The use of measured spectra from wave buoys or wave radars is here required.

Automatic wave observation

To reduce the errors of visual estimations and to enhance the accuracy of the sea spectrum, wave radars can be used. Wave radars can be divided in Satellite synthetic Aperture Radars (SAR), radar altimeters, microwave radiometry radars, ground-wave and sky-wave HF radars. The most popular wave observation systems rely on Plan Position Indicator (PPI) radar or microwave radars. The PPI radar, based on the X-band radar, uses the backscattering of electromagnetic waves from the sea-surface around the vessel (Figure 3.26) to calculate a full 3D wave spectrum. Furthermore, using the backscatter and ship speed, the magnitude and direction of near surface currents can be calculated. From the wave spectrum all important sea state parameters can be derived (Borge et al. 1999). Because there is no direct relation between wave-height and radar backscatter modulation amplitude, the X-band radar is an indirect wave sensor. The calculated wave spectrum is unscaled with respect to wave height and must be calibrated to relate the measured data to true wave height. Several empirical calibration methods exist which work well under most conditions but may occasionally fail completely. It is therefore impossible to quote reliable wave height performance figures valid for all conditions (Grønlie 2004).

The microwave radar works on a similar principle of transforming backscatter into a usable wave spectrum. A downward looking emitter and transmitter use radar pulses to measure the distance to the sea surface from the sensor. It provides a more precise measure of wave height, but gives little information about direction, wave spectrum or currents. Furthermore, it is by definition influenced by ship motion and corrective measures must be taken to reduce these effects. For performance monitoring the PPI radar, with its ability to measure sea spectrum, is therefore most suitable as it allows the measurement of the sea spectrum.

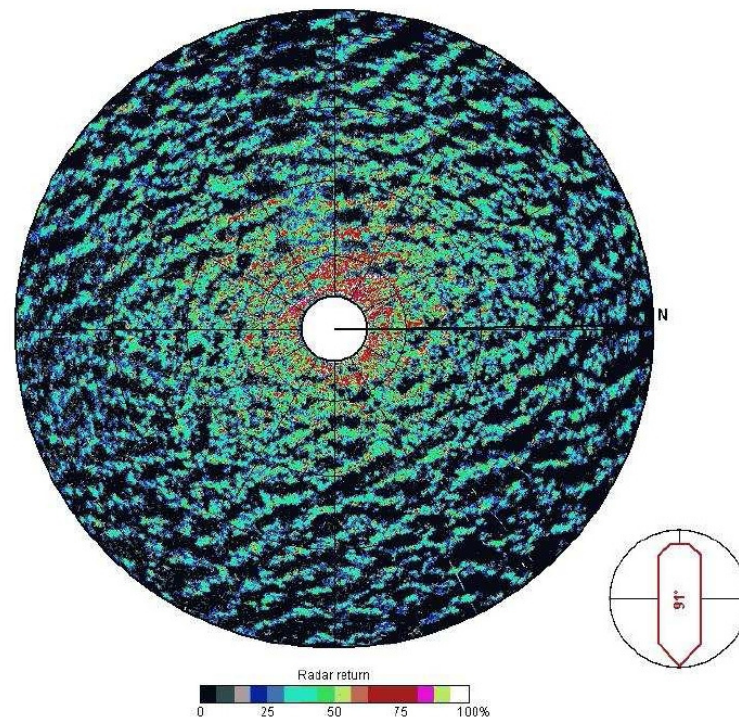


Figure 3.26: Nautical radar image, showing back scatter from surface waves which can be seen as lines, from an X-band radar. The colour coding corresponds to the radar back scatter strength where black indicates no return and white maximum return ((OceanWaveS 2004) fig. 4)

3.4.10 Water depth

Water depth is normally measured using an echo sounder based on the Doppler principle. Ship motions and bottom typology (mud, stones, sand etc.) influence the measurement. For performance monitoring, the requirements with respect to accuracy and sampling frequency are low and within the accuracy range formulated by ISO (ISO-9875 2001). Accuracy in the order of $\pm 1\text{m}$ and sampling every e.g. 30sec in is sufficient. The echo sounder, directly connected to the data acquisition system is therefore suitable for performance monitoring.

3.4.11 Water density and viscosity

Changes in water viscosity have significant effect on the viscous friction of ships. The most common method to determine viscosity and density is to measure salinity and, temperature. Seawater temperature observations can be taken from direct measurements from the engine water intakes. Depending on flow rate and the location of supply- and return openings of heat exchangers, care must be taken to make sure the measuring point is not affected by return cooling water from the engine. Salinity can be measured onboard using simple instrumentation or based on salinity charts. Figure 3.4 in Chapter 3.2.4 may be used to determine seawater density from a measure of temperature and salinity. Viscosity can be determined using equation (3.5).

3.4.12 Ship motion

Considering ship motions generated by external waves, long, regular waves such as swell have the most influence on motions. For performance monitoring, heave and pitch are especially important, as they are the major contributors to the added wave resistance and changes in propulsive characteristics (wake, propeller characteristics). The measured motion spectra over a set time span can be used to compare with the predicted motion spectra from hydrodynamic calculations and information of the sea state. Using this, an indication of the quality of the added (motion induced) wave resistance can be obtained. Moreover, a real-time measure of ship motion can be used to define when ship performance is affected too much by wave conditions and monitoring should be ceased. Heave and pitch motions may be measured using simple accelerometers and gyro sensors.

3.4.13 Rudder angle

The rudder angle can be measured with high accuracy using a potential meter connected to the rudderstock. The rudder is continuously in action, and a time average must be taken to take the slow response of the vessel to rudder actions into account.

3.4.14 Thrust

By measuring thrust and torque a separation in performance can be made between hull, propeller and engine, by separately defining the propeller efficiency. The measurement of shaft thrust can be classified into four categories:

1. Direct force measurement on ship's trust block, if fitted (in many cases the thrust bearing is integrated in the gearbox or main engine)
2. Measurement using a special transducer build into an intermediate propeller shaft
3. Measurement by monitoring the compression of the intermediate propeller shaft
4. Measurement by monitoring the compressive strains on the intermediate propeller shaft by means of strain gauges

Formerly, mechanical thrust meters (1) and (2) had been favoured and several successful designs emerged. However, they were never easy to install, operate, manage and evaluate and required unique skills from specialists (ITTC 1999a; Suzuki et al. 1992). With the constantly improving strain gauge technology and its instrumentation, the emphasis in recent years has been towards stress measurement using strain gauges. There are however a number of problems involved with thrust measurements using strain gauges directly on the propeller shaft:

- The propeller shaft diameter is designed to accommodate the torque it transmits. As a result, the strain from thrust is very low, about 15 times smaller than torque (Hylarides 1974). It is therefore difficult to measure. Furthermore, classification societies require over-dimensioning of the propeller shaft for safety reasons and to keep resonant vibrations far removed from the working frequencies, which makes deflection due to strain even smaller
- Even if the strain gauges are fitted in a laboratory, the thrust signal from a strain gauge contains a torque contribution of about 35% of the pure thrust contribution due to cross-talking of the torque and thrust and misalignment of the gauges (Caprino and Della Loggia 1993; Hylarides 1974). The cross-talk can be reduced by installing hollow intermediate shafts where the thrust signals are noticeably higher than equivalent solid shafts. However, in principle systematic errors due to cross-talk can only be accounted for by calibration. Because calibration in service is not possible, special instrumented and laboratory calibrated intermediate shafts

can be used (Schmiechen 1991b). The replacement of intermediate shafts is often practically difficult

- The temperature of the shaft is not uniform. The engine and bearings are sources of heat, and the propeller acts as a heat sink. This results in thermal strains that influence the thrust strain readings of the sensor. Propeller shafts are made by forging. As a result, their structure is anisotropic. It is therefore necessary to find out whether their expansion coefficients are the same in all directions. Temperature differences of only 3°C can account for as much as the maximum recorded thrust strain itself (Suzuki et al. 1992). Thermal inertia effects on the thermal strains caused by rapidly changing load conditions magnify the uncertainties in temperature distribution even further. Figure 3.27 shows two different strain gauge configurations for thrust.

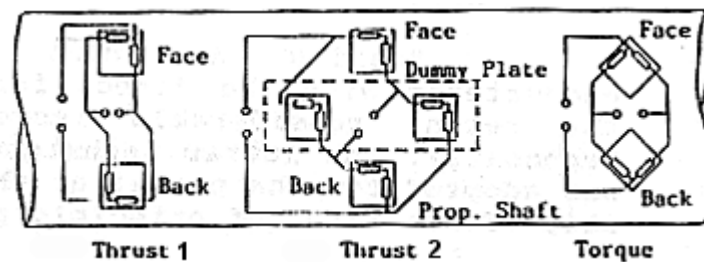


Figure 3.27: Full Wheatstone bridges for thrust and torque measurement (Suzuki et al. 1992)

The full Wheatstone bridge configurations on the left and right hand side for thrust and torque respectively are most well known. The middle is the ‘Hylarides’ strain gauge Wheatstone bridge configuration. In this configuration, the Wheatstone bridge consists of four pairs of rectangular crossing strain gauges, two of which are passive on a dummy plate and subject to no strain deformations. They are included to further reduce the thermal strain effects (Hylarides 1974)

- Misalignment of the gauges and thermal strains can be accounted for by careful calibration. For propeller shafts, calibration is however practically not possible.

Because of the abovementioned problems, axial thrust measurement has generally only been done for specific measurement exercises under carefully controlled circumstances. When this measurement has been attempted on a continuous service basis the long-term

stability of the measurement has frequently been a problem. The measurement of propeller thrust on ships with a controllable pitch propeller, which have a hollow propeller shaft, gives the highest reliability, on the condition that the effective propeller pitch can be measured accurately.

3.4.15 Propeller roughness

The surface roughness of propeller blades directly affects the frictional losses of the propeller, and hence efficiency. As with hull roughness, roughness indication for propeller blades by height scales alone is insufficient. The physical characteristics of the surface degradation and the hydrodynamic importance of the surface of propeller blades requires a texture parameter in addition to height scales. Musker (Musker 1977) proposed the characteristic roughness measure h' to characterise a surface by a single parameter, taking both the amplitude and texture of the roughness into account. The measurement may be done by using a portable stylus instrument or by taking a replica of the surface and measuring it under laboratory equipment such as optical measurement systems (Atlas et al. 2003). For practical applications, this is not viable. However, research has shown that the human finger is a very valuable and sensitive metrology instrument. By using the finger tips, trained observers can compare the propeller blade roughness with the roughness of a number of reference test patches. This type of tactile and visual comparison can be made using the Rubert propeller comparator, as shown in Figure 3.28.

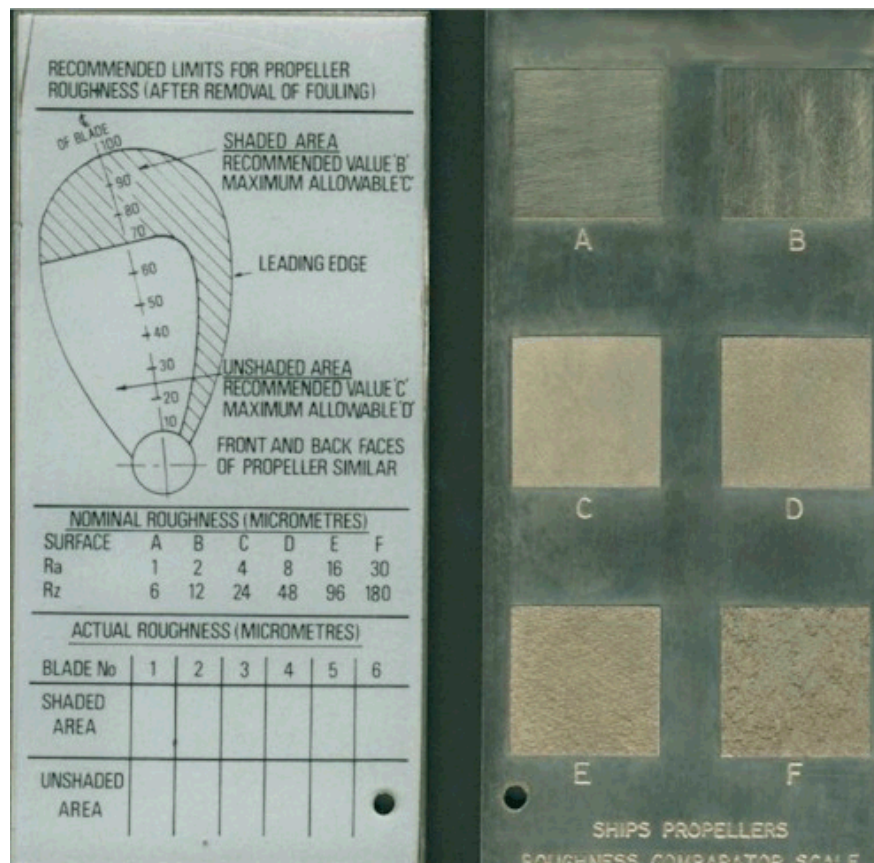


Figure 3.28: Rubert Propeller Roughness Comparator Scale

The Rubert comparator gauge consists of 6 specimens *A*, *B*, *C*, *D*, *E* and *F* of replicas of surface finish of propeller blades. *Rubert A* represents a degree of smoothness unlikely to be achieved in practice. *Rubert B* is representative of a new or well-polished propeller and *Rubert D* to *E* would be equivalent to the roughness of the blade after 1 to 2 years in service. *Rubert F* represents very poor and normally unacceptable roughness. For each test patch, the characteristic roughness measure h' can be defined. In this way, the blade roughness may be estimated (Mosaad 1986).

The gauge is relatively cheap and can be used underwater by trained divers. However, comparators have their limitations on accuracy especially at the higher roughness where the change in successive steps becomes large. Because there are no ways to quantify fouling, no corrections can be made for marine fouling.

The assessment of the Average Propeller Roughness (APR) is described by (Mosaad 1986) as following: ‘*Propeller roughness measurements by divers should be done after fouling removed from areas randomly selected for measurement. This may be done by scrubbing or light scraping but not by abrasive or metallic implements. Prior to roughness measurements of the propeller surface, an inspection should be made to ensure that each of the blades has the same roughness character. The roughness may then be estimated based on one propeller blade (face and back). Three roughness measurements shall be taken (widely and evenly spaced in the direction of a streamline) within each grid outlined in Figure 3.29. Care should be taken to avoid measurements of cavitation-eroded areas*’.

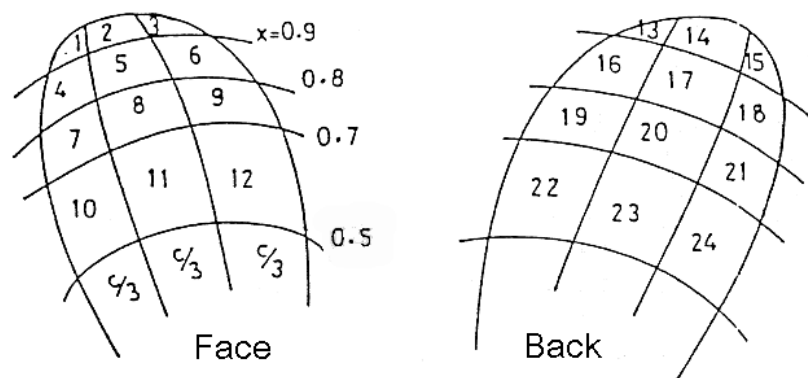


Figure 3.29: Propeller roughness measurement locations (Mosaad 1986)

The measurements using the Rubert scale can be converted to Musker’s h' parameter following Table 3.5 (Mosaad 1986). To obtain the average propeller roughness of the whole propeller, the measurements of the face and back are averaged using the appropriate weights (Table 3.6).

Table 3.5: Musker's characteristic roughness measure of Rubert Gauge surface

Rubert Scale	h'
<i>A</i>	1.3
<i>B</i>	3.4
<i>C</i>	14.8
<i>D</i>	49.2
<i>E</i>	160
<i>F</i>	252

Table 3.6: Weights for calculating Average Propeller Roughness APR

Region [r/R]	Weight [-]
0.2-0.5	0.07
0.5-0.7	0.22
0.7-0.8	0.21
0.8-0.9	0.27
0.9-tip	0.23

The calculation procedure for the APR is as following:

1. The Rubert measurements are converted to Musker's h' roughness parameter using Table 3.5
2. For each region, the average h' is calculated
3. Each average h' is multiplied with its corresponding weight (Table 3.6)
4. The sum of the average h' multiplied with the weight is calculated, represents the APR of the face of the propeller
5. Steps 1-4 are repeated for the back of the propeller. The APR $(h')^{1/3}$ of the propeller is obtained from the mean of the APR_{FACE} and APR_{BACK} .

Because propeller roughness cannot be measured or identified while the vessel is in service, it is important that measurements are done periodically, e.g. every 6 months depending on voyage profile. Coated propellers may require less frequent inspections, since the propeller is not affected by fouling as much as uncoated propellers. However, coated propellers may still need periodical inspection and roughness measurement for areas damaged by cavitation or floating objects in the water as well as the unavoidable effect of slimes.

3.5 Data conditioning

The main reason for data conditioning is to improve data accuracy and reliability. An often found mistake is that performance indicators instead of input data are filtered. Although this makes regression analysis easier, it does not improve the reliability of the performance data in any way, resulting in ill-defined trends in ship performance. In this section, data conditioning is described in terms of removal of outliers, identification of periods where ship performance is inconsistent and data smoothing. In the following sections, the latter steps are described. Section 3.5.4 concludes with a description of the requirements of a dedicated data conditioning system for performance monitoring which will be implemented in this thesis.

3.5.1 Identification of outliers

Practically all signals from sensors onboard ships contain outliers and must be filtered before it is further processed. Outliers occur due to electrical noise, errors in data transmission and incorrect readings from sensors. They can be identified using the statistical techniques such as the Chauvenet's Criterion, Peirce's Criterion or median filter or by means of cross validation with other parameters. For small ships, where physical parameters can change rapidly, e.g. due to acceleration or course deviation, it is important that the filter does not result in a time delay and that sharp changes in performance are preserved. The Chauvenet's and Peirce's criterion (Ross 2003), which both base the rejection of outliers on a statistical probability, are found not satisfactory in transient conditions. The median filter however is more suitable and its principle function is easily to understand. Filtering is performed by using a window consisting of an odd number of samples. The values in the window are sorted into numerical order and the sample in the centre of the window is selected as the output. The oldest sample is discarded, a new sample acquired, and the calculation repeats.

3.5.2 Transients filter

In section 3.3.11, it was concluded that during periods of transit, ship performance should not be logged for performance monitoring. In order to identify these periods, a number of parameters must be continuously monitored:

- To identify course deviations: course, shaft torque
- To identify acceleration: torque, STW and engine speed
- To identify drift: heading and course over ground, transverse STW or apparent wind speed and direction and rudder angle,
- To identify excessive ship motion: apparent wind speed and direction in addition to wave height and direction, or direct by means of a heave and pitch motion sensor
- To identify shallow water: water depth under keel

Transient periods can be identified simplest and transparently by continuously calculating the rate of change of the course, torque, STW and engine speed using linear regression over a fixed period of time (e.g. 5 minutes). When the gradient of the regression curve exceeds a certain pre-set threshold, a conditional filter is triggered. The threshold values depend on the time span over which the regression is performed, the ship's characteristics (mainly ship size), and the required sensitivity. The time span should be long enough to dampen natural fluctuations to but short enough to avoid time delays in the identification of transient periods. The correct time span and threshold values can be found by iteration during the initial tuning of the filter. Figure 3.30 shows a simplified transients filter designed for the *Bernicia*. The course, engine speed, ship speed and shaft torque are here monitored simultaneously. The red data points indicate the data that is used to determine the rate of change. The blue line represents the regression curve calculated with these points.

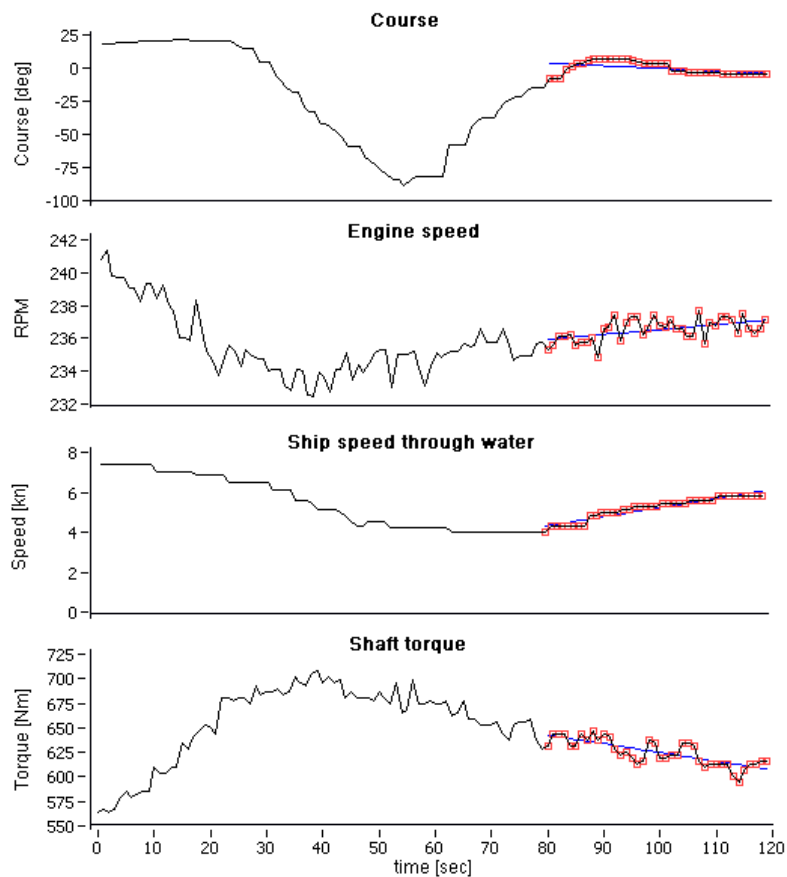


Figure 3.30: Example of simplified transients filter on Bernicia for acceleration and rate of turn

The use of linear regression, instead of e.g. the standard deviation for the identification of changes, gives a more reliable and intuitive way to identify inertia effects during acceleration and course deviation. Moreover, by looking at the sign of the regression coefficients an additional check can be made whether the performance is steady.

The identification of the start of transient periods is easier than the identification when steady state conditions have returned. Especially for large vessels, it can take a considerable time before steady state conditions have returned after deceleration or changes in course. The gradients obtained from the regression become then too small to be separated from the natural fluctuations in torque, rpm and speed from wind and waves. A time delay (e.g. 30 minutes) can then be used after a transient period has started to make sure the steady-state condition has been reached before normal performance monitoring is continued.

The selected time period in the calculation of the regression curves is a compromise between response time and accuracy in the identification of transient periods. Especially in heavy weather the torque and speed variations are large, marking a large time frame necessary to avoid incorrect triggering of the transients filter. To allow a large time frame without compromising on response time in the identification of transients, an additional condition can be used, based on the standard deviation over the time frame. Figure 3.31 shows a transient situation on the *Bernicia* where the slope of the regression curve for both shaft speed and torque are small and therefore the filter not triggered. The ship is however in transient, shown by the sharp rise in RPM and torque at the last data point. By using a threshold on the standard deviation, this situation can be identified.

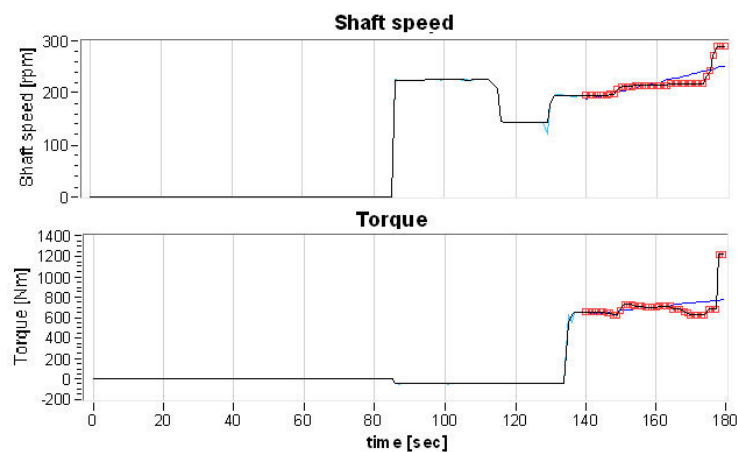


Figure 3.31: Identification of transients using RPM and torque

3.5.3 Smoothing

Smoothing is used to capture important patterns in the data, while leaving out noise. One of the most common algorithms for the smoothing of time series is the ‘simple moving average’. A simple moving average is calculated by the mean over a set number of most recent data points. It gives equal weight to all data points. By averaging data after the transients filter, the time delay that is caused by using simple moving average smoothing has no adverse effects, as the data after the transients filter represents almost steady-state conditions.

The sampling duration or averaging time of each parameter should be chosen short enough to capture environmental loading changes that result in changes in ship performance (e.g. changes in wind speed), but long enough to smoothen natural fluctuations (e.g. torque fluctuations in heavy seas). The size (mass) of the vessel dictates the time constants of the different parameters. For example, a small fishing vessel responds to wind gusts as short as 5 seconds, while a loaded super tanker acts as a low-pass filter and will respond only to gusts in the order of minutes.

The random uncertainty of a measured parameter can be reduced by averaging. If the random uncertainty of each measured value can be described by a standard deviation σ , and N readings are taken, the standard deviation over the N data points is reduced by (Coleman and Steele 1998):

$$\sigma_{\bar{x}} = \frac{\sigma}{\sqrt{N}} \tag{3.15}$$

Hence, to reduce the standard deviation around the mean by a factor of two, four times longer measurement of a (constant remaining) parameter is required. 100 Times as many readings must be taken to reduce the standard deviation by a factor 10. A high sampling frequency is therefore useful to obtain a higher precision without sacrificing response time.

3.5.4 Data conditioning system design

The data conditioning steps described for ship performance monitoring, aimed at increasing the validity and accuracy of ship performance data are shown in a flow diagram in Figure 3.32. Parameters required for the transients filter are logged at 1Hz and filtered for outliers. The transients filter acts as a valve. If steady-state performance is identified, the filtered data is passed through for further data validation (mainly ship speed and torque) and averaging. Environmental conditions that are not affected by the ship's behaviour and can be measured periodically, do not require filtering and can be used directly, after a simple data validation (range check). The filtered and conditioned data forms the basis for further performance analysis.

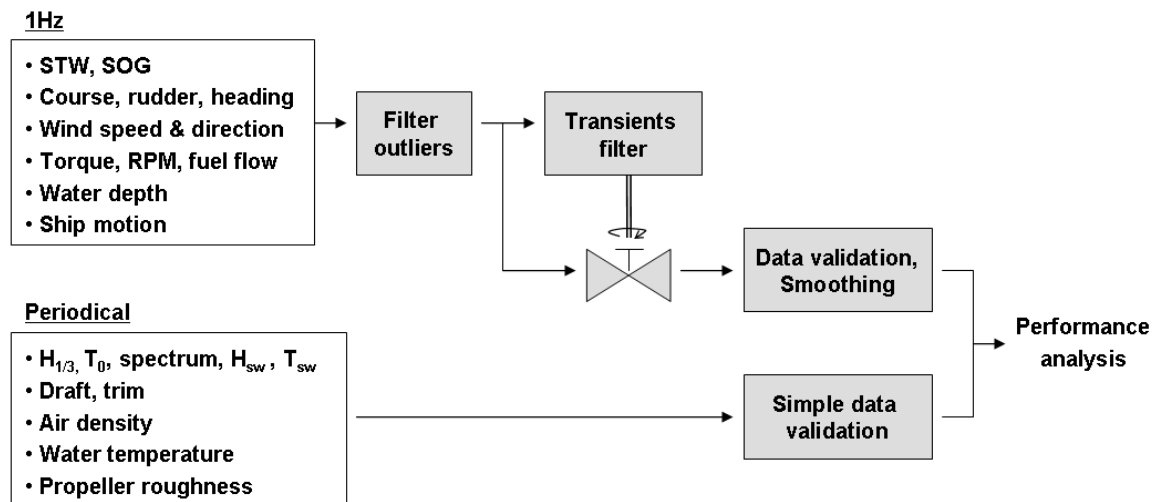


Figure 3.32: Data acquisition system for ship performance monitoring

Figure 3.33 shows the effect of the three steps of data conditioning (filter outliers, transients & smoothing) on the torque and RPM for a set of sea trails conducted by the Author on the *Bernicia*. The data represents trials in strong winds (up to 30 knots) from both head and stern directions. The significant reduction in fluctuations and errors from the three data conditioning steps shows the improvements that can be made with the availability of an automatic, continuous data logging system onboard.

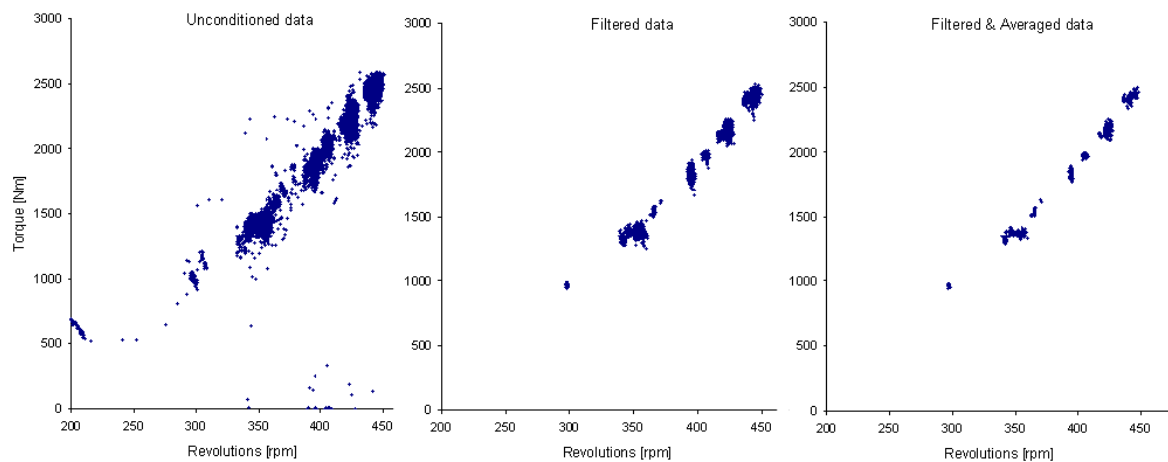


Figure 3.33: Effect of transients filter and smoothing for sea trials on the Bernicia

The described way of data conditioning is based on rational time series based conditioning. It filters performance data based on hydrodynamic characteristics and performance of the vessel. This stands in strong contrast with data analysis based on statistics only, where no reference is made to time dependent changes in performance. Especially for performance analysis of small vessels that manoeuvre frequently, this is important. The reduction in scatter in Figure 3.33 can also be obtained with strong statistical smoothing. Yet, this will not improve data validity and reliability. Periods where ship performance changes, e.g. due to weather or differences in loading, will incorrectly be treated as outliers, and smoothed resulting in ill-defined KPIs. Assessing the effect of data conditioning on standard deviation alone is therefore incorrect. One should look at the physical meaning of the data, and condition the data based on this.

3.6 Conclusions

In this chapter, the factors that affect ship performance, sensor readings and their output signals were reviewed in order to identify the parameters that must be logged for rational, reliable and accurate performance monitoring, and the practical issues related to measuring them. Based on this review and some analysis using the data collected with test vessels used in this study, the following main conclusions are obtained :

- The main factors affecting ship performance are speed, displacement, wind, waves, fouling and shallow water. To be able to account for these factors, a large number of parameters must be logged. A list is given in Table 3.7 including their uncertainties in measurements. Special attention should be paid to the speed log, long term stability of the torque sensor, definition of the sea spectrum, position of the anemometer and measurement of propeller roughness. A detailed sensitivity analysis of the individual parameters is included in Chapter 5 of this thesis.
- During periods of transit; acceleration, deceleration, course deviation, leeway and sailing in extreme shallow water, ship performance becomes unsteadily and cannot be used for performance analysis. By continuously monitoring a number of parameters with a real-time data acquisition system with high sampling data rate (e.g. 1Hz), these periods can be identified using a rate of change filter. A high sampling of data acquisition is furthermore required to allow filtering of outliers and averaging to reduce random uncertainty
- The most important but difficult to measure parameter for the performance monitoring of a ship is the ship speed through water. Using propeller characteristics and a real time measure of torque and shaft RPM, the speed through water may be approximated (hereafter referred to as ‘GPD’ speed) to give a more reliable figure compared to a speed log measurement. The GPD speed relies on accurate propeller open water diagram and wake fraction estimations. The wake fraction is affected by hull fouling, and should therefore be calibrated periodically to avoid underestimation of the ship speed as the hull fouls. Propeller roughness also results in underestimation of the GPD speed and hence must be taken into account

- Currently there are no established and reliable methodologies to quantify hull and propeller fouling using simple, practical tools. Fouling can therefore only be measured indirectly by looking at the effects on the overall performance of a ship and filtering out of the above mentioned periods and through appropriate analysis
- Onboard, real-time automatic data logging in combination with filtering and averaging is the way ahead to obtain ship performance data with sufficient accuracy for performance analysis.

Table 3.7: Parameters required for ship performance monitoring

Parameter	Measurement considerations & uncertainties	Impact of uncertainty
Speed through water	Heavily influenced by ocean currents and ship motion. Should be measured using dual axis Doppler log	• • •
Speed over ground	Measured using DGPS with sufficiently high accuracy	•
Torque	Dedicated torque sensor on propeller shaft required. Sensitive instrumentation, susceptible drift which is difficult to identify. Frequent calibration is therefore required	• • •
Engine speed	High accuracy easy to obtain by pulse measurement on flywheel and high spec counter electronics. Sensor does not drift	•
Fuel consumption	Influenced by fuel quality, pressure fluctuations in flow, leakages and fuel return. The position of fuel flow meter is therefore important. Should be corrected to ISO standard conditions using density and LCV	•
Fuel characteristics	LCV and density from fuel sample reports. Change of characteristics may be noticed by change in injection temperature.	•
Wind speed & direction	Anemometer reading affected by wind distortion: location of sensor important. Visual observations not suitable for performance monitoring due to low reliability and wind gustiness	• •
Wave parameters	Visual estimation of wave and swell height, period and direction required. Large errors due to subjective character of observations. Period may be obtained from sea statistics. Wave spectrum should be obtained from database depending on location. Wave radar highly recommended in coastal areas or for short-sea shipping	• •
Draft and trim	Can only be obtained in port. Loading computer not suitable; only calibrated (!) draft sensors provide required accuracy	• •
Water depth	Only important in shallow water, approx. <100m deep. Echo sounder provides sufficient accuracy	•
Air density	Deviations due to temperature & Pressure. Continuous logging necessary	•
Water temperature	Used to calculate changes in sea water viscosity. If measured in engine room; affected by heat from machinery	•
Rudder angle	Only used for transients filter; accuracy not of major importance	•
Rate of turn	May be obtained by integrating the ship's course (from GPS) over time	•
Ship motion	May be measured by means of simple electronic inclinometer. Only used for transients filter; accuracy not of major importance	•
Propeller roughness	Fouling cannot be quantified. Comparator roughness scale as good as we can get in practice to assess condition. Measurement periodically by diver inspections.	• •

• = low, •• = medium, ••• = high impact of uncertainty to ship performance analysis

4

MODELLING OF PERFORMANCE ANALYSIS SYSTEM

4.1 Introduction

Ship performance analysis is the process of converting or correcting ship performance data (speed & power), which is obtained through performance monitoring, to a pre-defined state so that it can be compared with a baseline (or reference) condition which is well defined in priory in terms of speed, power and other conditions that affect performance (e.g. trial conditions). This can be done real-time (direct feedback on operation), semi real time so that the energy lost to overcome environmental conditions can be evaluated, or over a longer time frame to indicate the performance deviation due to changes in hull and propeller. The quality of the performance analysis depends on the quality of the input data during monitoring (e.g. in terms of accuracy, availability etc.), the accuracy and sensitivity of the correction (or conversion) method to errors in the input parameters, and the sensitivity of the key performance indicators to changes in performance.

In Chapters 1 and 2 of the thesis, the design requirements for a performance monitoring and performance analysis system were discussed. It was concluded that to be able to make optimal the use of a performance monitoring system, performance analysis should be done in real time onboard the ship. This requires a system to be transparent in operation, easy to interpret and stand-alone, without need of user intervention. In terms of analysis, it should be able to make a differentiation between engine, propeller and hull efficiency and should produce clear, easy to interpret KPIs that can be plotted on a time basis to identify long-term trends in ship performance. From Chapter 3, it was shown that availability of performance data, accuracy of ship speed through water and uncertainties in the estimation of the wake fraction are important aspects that must be addressed. A

further consideration in the design of an analysis methodology is the inaccuracy of the measurement of sea state characteristics and wind speed.

Based on the above background, the main objective of this chapter is to propose a correction methodology that meets the performance analysis requirements and is theoretically sound. Furthermore, it can be validated onboard by experts and uses minimal statistical regression techniques to keep the system as transparent as possible. The methodology, in combination with the data acquisition and condition system described in Chapter 3, forms the back-bone of the proposed PM&A system. The PM&A system has been programmed using LabVIEW (NI 2004) and implemented by the Author on the two test vessels; the RV *Bernicia* and the MT *Overseas Tanabe*. The evaluation and discussion of the results of the analysis of performance data from these vessels is described in Chapter 5. Chapter 4 describes therefore the mathematical correction model in Section 4.2 and proposes ways to visualise performance data in a usable and meaningful manner in Section 4.3. By means of a sensitivity analysis on different types of vessels, conclusions are made with respect to the impact of errors on important input parameters (such as speed and torque) in section 4.4. Finally, the system architecture, or back-bone of the proposed PM&A system is described in section 4.5.

4.2 Correction methodology

The correction of ship performance to standard conditions requires the calculation of the added resistance from wind, incoming waves, changes in draft and trim, shallow water and water viscosity, and mathematically deducing the effects of these factors from the measured performance in service. Added resistance however also results in a change in propeller efficiency and change in calm-water hull resistance. When correcting the service performance to the standard performance, these changes should be taken into account. In this section, the correction method and added resistance calculation methods are described. The correction is based on fixed pitch propellers. For controllable pitch propellers, the pitch angle should be measured continuously. The propeller characteristics and propeller operating point should then be calculated using a database of propeller characteristics for each pitch angle.

4.2.1 Mathematical model for correction to standard conditions

The interaction of wind and incoming waves on a ship mainly causes an increase in hull resistance. As a result of this, the ship speed decreases and consequently, compared to a ship sailing in no-wind and no-wave conditions:

- 1) the ship resistance increases due to external forces and
- 2) the drop in ship speed resulting from (1) causes a reduction of (calm water) hull resistance.

Most correction methodologies are based on constant RPM and do not take the reduction of hull resistance (2) into account. This effect can however be of the same magnitude as the increase in resistance, and should not be neglected (Taniguchi and Tamura 1966). By calculating ship performance to a basis of constant ship speed, the effects of (2) are automatically taken into account. The proposed methodology in this thesis for the analysis of ship performance is therefore based on the correction using constant ship speed, as outlined by (Taniguchi and Tamura 1966). Figure 4.1 shows the flowchart of the correction model.

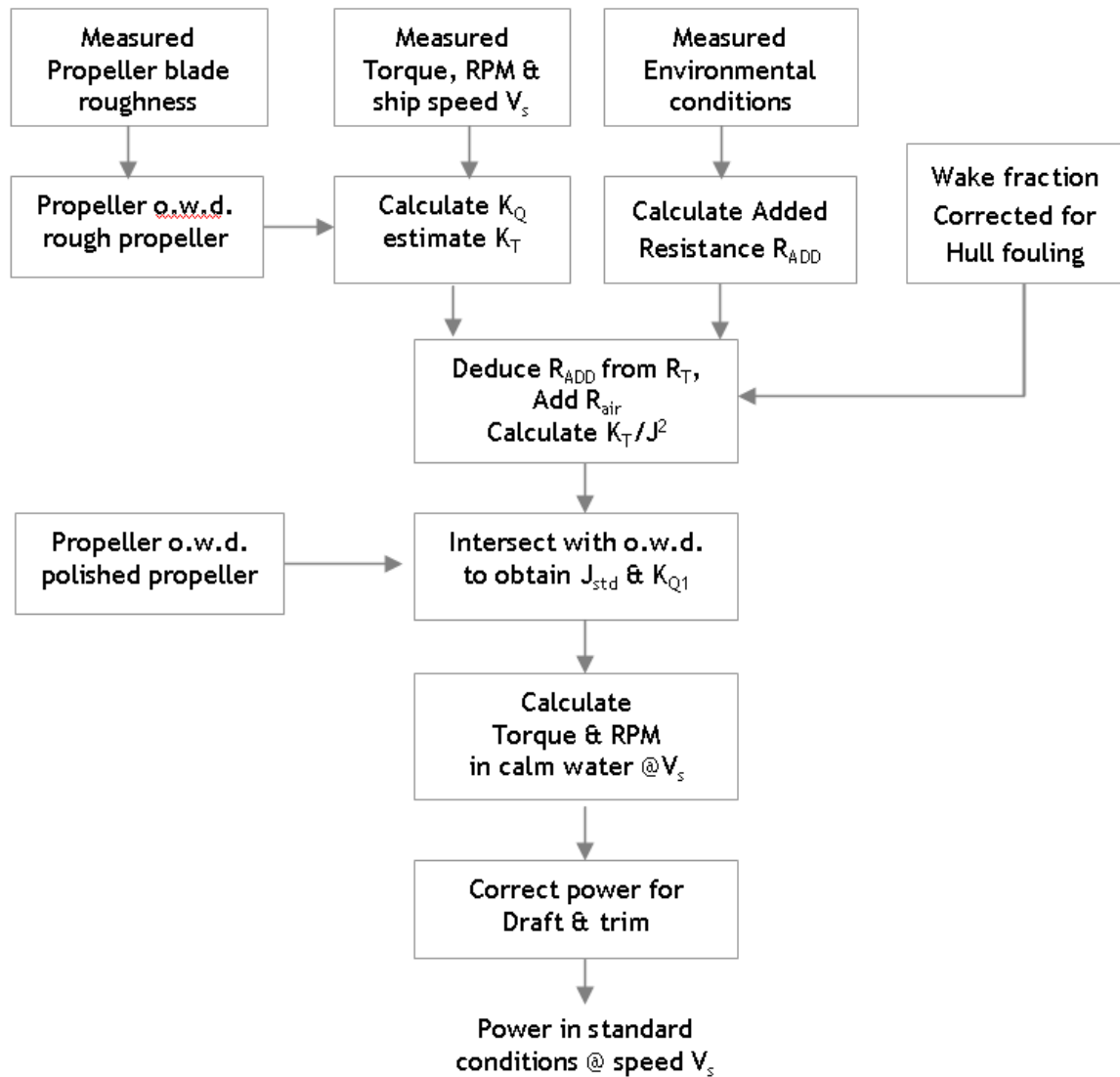


Figure 4.1: Flow diagram of proposed ship performance correction methodology

The flow chart can be described by the following steps:

1. The propeller open water diagram is corrected for surface roughness using the roughness parameter corresponding to a freshly measured or the latest value of measured propeller data from inspections
2. Using measured environmental data and appropriate methods, the added resistance R_{ADD} due to wind, wave, viscosity and shallow water is calculated

3. The absorbed torque of the propeller is calculated by deducting the transmission losses from the measured shaft torque. The transmission losses may be approximated by a constant torque loss (KleinWoud and Stapersma 2002). The torque loss is based on the design condition. If P_{ref} and n_{ref} represent the design power and RPM respectively for which the shaft efficiency η_{shaft} is known, the constant torque loss can be calculated by;

$$Q_{loss} = \frac{(1 - \eta_{shaft})P_{ref}}{2\pi n_{ref}} \quad (4.1)$$

4. In fair to moderate weather conditions, where the wake fraction and propeller characteristics can be considered steady, the torque coefficient K_Q is determined using the measured shaft torque Q and propeller revolutions n deducted with the shaft losses Q_{loss} :

$$K_Q = \frac{Q - Q_{loss}}{\rho n^2 D^5} \quad (4.2)$$

5. The propeller open water torque coefficient, available from tests and corrected for blade roughness, can be approximated by a second order polynomial. The advance coefficient J can then be calculated by:

$$J = c_1 K_Q^2 + c_2 K_Q + c_3 \quad (4.3)$$

6. The thrust coefficient can be evaluated by using J and the open water thrust coefficient curve, which is also available similar to the torque curve, as below:

$$K_T = aJ^2 + bJ + c \quad (4.4)$$

7. Using K_T and the thrust deduction fraction t available from the tests or from a suitable database, the resistance overcome by the propeller can be calculated as:

$$R = (1-t)K_T \rho n^2 D^4 \quad (4.5)$$

8. By deducting the added resistance R_{ADD} due to the external conditions from the resistance overcome by the propeller, the performance in standard (base line) conditions can be calculated. As for the calculation of wind drag the measured apparent wind speed is used, the still air drag R_{air} (caused by the forward motion of the ship through air) must be added. If not, the performance of the ship sailing in vacuum (no air resistance) would be calculated.

$$R_{std} = R - R_{ADD} + R_{air} \quad (4.6)$$

9. To convert the resistance in step 8 back to power, steps 4-8 can be reversed. However, in the new standard condition, shaft speed is an unknown. This can be resolved by dividing the thrust coefficient K_T' by the squared advance coefficient J so that the unknown propeller speed n_1 is eliminated from the equation. The ship speed through water is measured using the speed log of the ship, and the wake fraction follows from periodical wake calibration runs, to account for hull fouling (discussed further in Section 4.2.3).

$$\tau = \frac{K_T'}{J^2} = \frac{\frac{T}{\rho n_1^2 D^4}}{\left(\frac{V_a}{n_1 D}\right)^2} = \frac{R_{std}}{\rho(1-t)[V_s(1-w)]^2 D^2} \quad (4.7)$$

10. Based on the assumption that for moderate surface roughness, an increase in propeller roughness only expresses as an increase in absorbed torque (decrease in thrust can be assumed negligible), the loading coefficient τ can be considered the same for a fouled or smooth propeller. This characteristic is used to convert ship performance to standard conditions with a smooth propeller. Using the standard, uncorrected propeller open water diagram, the intersection of τ with the propeller K_T' curve can be calculated using;

$$\begin{aligned}\frac{K_{T'}}{J^2} &= \frac{aJ^2 + bJ + c}{J^2} \\ \tau &= \frac{K_{T'}}{J^2} \\ \tau J^2 &= aJ^2 + bJ + c \\ 0 &= (a - \tau)J^2 + bJ + c\end{aligned}\tag{4.8}$$

Which can be solved using the standard quadratic formula:

$$J_1 = \frac{-b \pm \sqrt{b^2 - 4(a - \tau)c}}{2(a - \tau)}\tag{4.9}$$

11. With the new advance coefficient, the engine speed in standard conditions n_1 , but with fouled hull (if applicable), can be calculated:

$$n_1 = \frac{V_s(1-w)}{J_1 D}\tag{4.10}$$

The assumption of equal wake fraction between service and the benchmark (calm) weather condition requires that ship motions are small, the ship is not manoeuvring and leeway is negligible.

12. The advance coefficient J_1 is used to get K_{Q1} from the standard (uncorrected) open water diagram.

$$Q_1 = K_{Q1} \rho n_1^2 D^5\tag{4.11}$$

13. With the torque, the power in no-wind, no-wave, standard water viscosity, deep water and smooth propeller can be calculated:

$$P_1 = 2\pi n_1 Q_1\tag{4.12}$$

14. The draft and trim affects both wake and thrust deduction fraction as well as hull resistance. The correction for changes in draft and trim from the reference condition can therefore best be estimated from model test results, expressed as percentage change in power per unit change in draft for the ship speed in consideration. In this way, possible errors from changes in wake and thrust deduction fraction can be avoided. The standard power in no wind, no wave, standard water viscosity, deep water, smooth propeller and standard draft and trim, but with fouled hull (if applicable), $P_{D,corr}$ follows from:

$$P_{D,corr} = P_1 \frac{P_{D-std}(Vs)}{P_{D-T\&trim}(Vs)} \quad (4.13)$$

Where $P_{D-T\&trim}(Vs)$ is the predicted delivered power in calm water obtained from model tests for the draft and trim and ship speed corresponding to the measured (service) performance data. $P_{D-std}(Vs)$ is the predicted delivered power in calm water at reference (standard) loading condition, at the same ship speed, also obtained from model tests.

The following sections describe the calculation of the added resistance components, wake fraction calibration and the correction of the propeller open water diagram for in-service blade roughness, in more detail.

4.2.2 Effect of propeller roughness

The best way to account for changes in propeller open water efficiency is by measuring thrust and torque directly, so that step 2-7, which are most sensitive to errors in the open water diagram, may be omitted. However, because thrust is extremely difficult to measure with the accuracy and long-term stability required for the identification of propeller roughness, indirect methods have to be used to determine the changes in propeller characteristics. Indirect methods are based on the measurement of blade roughness that is converted using empirical relationships into a blade section drag. The blade section drag for the roughened propeller is subsequently used in propeller design

and analysis procedures (e.g. using Lerbs' equivalent profile method (Townsin et al. 1985), (Mosaad 1986), (UPCA91 2005)) to predict the propeller open water characteristics.

Mosaad (Mosaad 1986) showed that the increase in total drag coefficient for moderately roughened propellers can be calculated by:

$$\Delta C_D = 2 \left(1 + \frac{t}{c} \right) \Delta C_F \quad (4.14)$$

Where t is the maximum thickness of the blade section, c the section chord length and ΔC_F the change in the friction coefficient, defined by:

$$1000 \Delta C_F = 8.1 Re^{0.093} \left[\left(\frac{h'}{c} \right)^{1/3} - 4.5 Re^{-1/3} \right] \quad (4.15)$$

with Re the blade section Reynolds number and h' the Musker's roughness parameter, derived from roughness measurements with the Rubert comparator gauge (see section 3.4.15). The increase in C_D due to roughness must be calculated as the difference between the values of ΔC_D corresponding to the Rubert surface in service and that for a new or well-polished propeller if the propeller is coated using a foul release type coating (often equivalent to Rubert B (Atlar et al. 2003)).

4.2.3 Wake calibration for hull fouling

The wake fraction is dependent on hull roughness, as discussed in Section 3.3.3. In order to account for this variation, the wake fraction must be calibrated periodically. The wake can be determined during dedicated speed trials or carefully conditioned service performance data, collected during periods where the speed log can be considered most accurate. The wake can be calculated as following:

$$K_Q = \frac{Q}{\rho n^2 D^5} \longrightarrow J = c_1 K_Q^2 + c_2 K_Q + c_3 \longrightarrow w = 1 - \frac{JnD}{V_S} \quad (4.16)$$

By developing a database with periodically estimated wake fraction value, regression analysis techniques can be used to reduce variations from measurement errors. Different databases should be made for laden and ballast conditions, as wake is affected by draft.

4.2.4 Wind resistance

Major wind loading acting on a ship in lateral plane can be split in longitudinal and transverse force components, a yawing moment about the vertical axis and a rolling moment about the longitudinal axis in the vertical plane. The transverse force is counteracted by the rudder and hydrodynamic hull drift force and in addition may result in leeway. For the propulsion point of view, the resistance forces acting in the longitudinal direction are of the main interest. The wind force in longitudinal direction can be calculated by:

$$R_{wind} = 0.5 \rho_{Air} C_X(\epsilon) A_F U^2 \quad (4.17)$$

Where:

$C_X(\epsilon)$ = non-dimensional longitudinal wind loading coefficient as function of wind direction relative to the bow

A_F = frontal projected area of the ship above the waterline

U = apparent (or relative) wind speed

ρ_{air} = air density

4.2.4.1 Air resistance

The wind resistance, as calculated with the apparent or relative wind speed accounts for all air and wind generated forces. For performance monitoring, only the wind resistance must be deduced. The air resistance, generated by the forward motion of the ship, must be

added to the wind resistance. The air resistance is calculated in a similar way as wind resistance:

$$R_{air} = 0.5\rho_{Air} C_x(180^\circ) A_F V_{GPS}^2 \quad (4.18)$$

Where:

$C_x(180^\circ)$ = Longitudinal wind loading coefficient for head wind

V_{GPS} = Ship speed over ground

4.2.4.2 Definition of the apparent wind velocity (U)

For the calculation of wind resistance, only longitudinal, high energy wind turbulences with a relatively long time period and dimension that affect the whole ship are important. To filter out wind gusts of short duration, the wind speed must therefore be averaged over a 10-minute period (see section 3.2.3). Furthermore, the dynamic head of the wind on the ship, $0.5\rho_{Air}U^2$, acts on the ship's mean height, which can be calculated by (Blendermann 1996):

$$z = \frac{A_L}{L_{OA}} \quad (4.19)$$

Where A_L is the lateral-plane area of the above-water hull and L_{OA} the ship's length-over-all.

Due to the wind gradient over the sea surface, the wind speed at this height is different from the wind observed by the anemometer on the wheelhouse. To convert the wind speed to the reference mean ship's height, the following equation can be used (Blendermann 1996):

$$\bar{u}(z) = \bar{u}_{10,h} \left(\frac{z}{h} \right)^{\frac{1}{n}} \quad (4.20)$$

Where

$\bar{u}_{10,h}$ = 10-minute running average of the wind speed at anemometer height h above sea level

n = wind gradient. For winds $\bar{u}_{10,h} > 6$ m/s, $n = 10$. For light winds or winds over open harbour areas, $n = 6$ may be used (as described in section 3.2.3)

z = mean ship's height above water surface

h = height of anemometer above water surface

4.2.4.3 Definition of the frontal projected area (A_F)

The majority of present day investigators use the projected area above-water for the definition of A_F for all wind directions. To account for differences in frontal area for vessels with varying deck load, such as container ships, a range of wind tunnel tests are required in order to include the effects of gaps between e.g. container bays when the wind approaches bow-quarterming directions. Generally, the frontal projected area is calculated as following:

$$A_F = A_{superstr.} + B(D - T) \quad (4.21)$$

Where:

$A_{superstr.}$ = Frontal area of superstructure and deck load

B = Hull width at shoulders

D = Distance of keel to deck

T = Draft

4.2.4.4 Definition of the wind resistance coefficient (C_x)

The longitudinal wind resistance coefficient C_x can be obtained by means of Computational Fluid Dynamics (CFD) simulations, dedicated wind tunnel tests or from

published wind tunnel tests of similar ships. It is important that a good comparison is found between the geosimilar vessel and the actual ship. The effect of changes in the vessels load/ballast condition expresses mostly in changes in the yaw moment and lateral force coefficients but less in the longitudinal force coefficients (OCIMF 1977). Since most published with tunnel results are for one or two loading conditions only, simple linear interpolation may be used if the ship's displacement of interest lies between the full load and ballast conditions. The coefficients should be interpolated according to the percentage change in the midship's freeboard.

For many published wind tunnel tests, only the longitudinal profile of the test vessel is available. Without information on bow shape or transverse profile, it is difficult to make a reliable estimate of the similarity of hull and superstructure shape. Influences of deckhouse configuration of tankers such as rounding of deckhouse corners etc. are small, in general less than 10 percent (Berlekom 1981). Variations in aerodynamic properties of the bow or superstructure may however be much larger, and cannot be described by ship length, frontal or transverse projected area. Figure 4.2 shows the wind resistance coefficients for two tankers in ballast with different bow shapes. Large differences between the U and V-shaped bow can be seen, caused by large suction forces around the more rounded cylindrical, U-shape bow (OCIMF 1977).

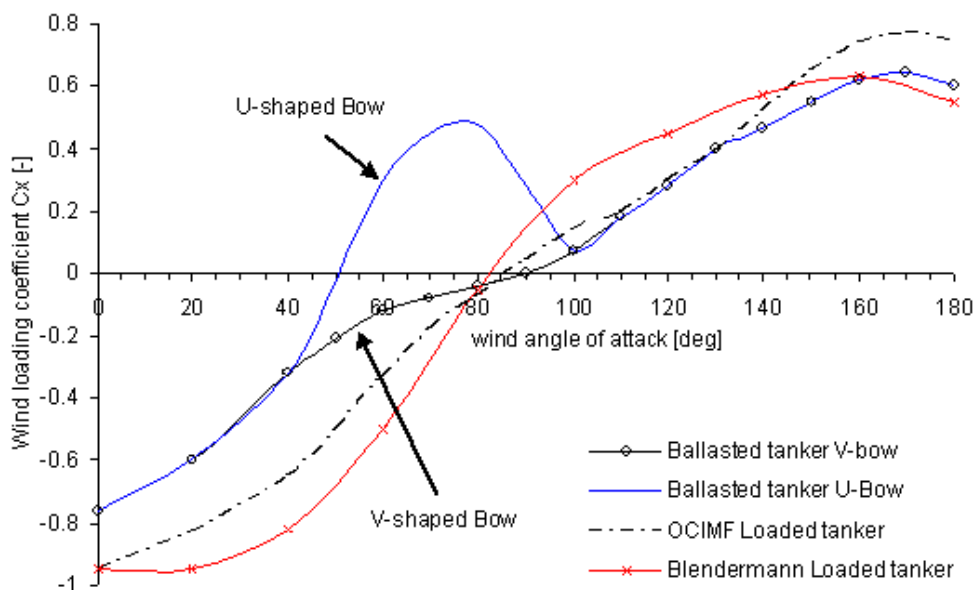


Figure 4.2: Longitudinal wind force coefficient for tankers in fully loaded and ballast condition for ships with different

bow shapes ((Blendermann 1996) and (OCIMF 1977)).

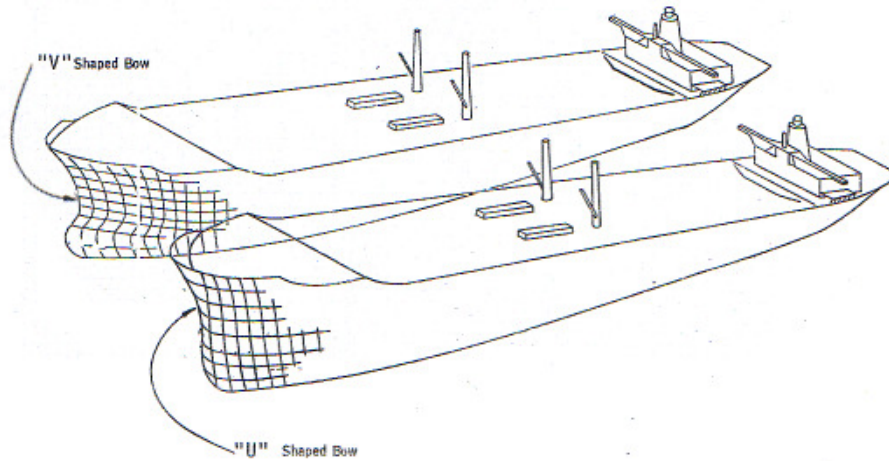


Figure 4.3: Variation in bow configuration (OCIMF 1977)

Figure 4.2 also shows an example of the uncertainty in wind loading coefficients. The C_x coefficients for two loaded, almost geosimilar VLCCs are plotted from different sources ((Blendermann 1996) and (OCIMF 1977)). Difference between the two curves is large, between ± 25 -40%. Causes of error may be contributed to:

- Differences in hull shape
- Experimental errors; ability to accurately measure the low wind loads associated with the scaled down models and other uncertainties during measurement (Kwon 1981; OCIMF 1977)
- Scaling errors; applicability of using model scale vessel in turbulent boundary layer around model to represent full scale ship (OCIMF 1977)
- Variations in the physical/geometrical characteristics of the tested range of ships of the same type, or the limitations of the describing parameters to correlate results to a particular vessel (e.g. using the frontal or transverse projected area or ship length squared)
- The use of different wind gradients to simulate the sea surface roughness

The lower the wind load, the higher the uncertainty from scaling errors. For tankers, the ballasted conditions are therefore much more accurately to define than laden conditions (OCIMF 1977).

In short, after the estimation of wind speed, the uncertainty of the wind resistance is dominated by the accuracy of the wind resistance coefficient C_x . The selection of a geosimilar vessel from a large database of model test results, paying specific attention to hull shape and deck loading, and interpolation of resistance coefficients for different loading conditions (if applicable) is therefore important.

4.2.5 Added wave resistance

Added wave resistance can be described as the combination of the ship motion generated waves and wave diffraction (mainly at the ship's bow). Added wave resistance can be estimated by model tests or using numerical methods such as more practical strip theory based methods. The strip theory is based on the assumption of a slender ship body, and can therefore not accurately predict the wave diffraction effects of large bodied ships. They are therefore often complemented with added wave diffraction resistance methods, such as (Nakamura and Fujii 1977), (Faltinsen et al. 1980) or (Kwon 1981). Large discrepancies between theory and experiments however still exist in the short wave length region (ITTC 1999b). Because of the complexities of the free-surface effects and the simplifying assumptions of the strip theory to estimate the diffraction in waves, many kinds of modified theories to predict added resistance have been developed in the past. Despite the number of different methods, none is able to predict accurately the added resistance over a wide range of ship forms and speeds (ITTC 1999b). Flikkema (Flikkema 2008) showed by comparison of a number of frequently used added wave resistance calculation methods with model tests for a cruise vessel and ferry, that the added wave resistance predictions are often too inaccurate to be used for performance analysis (with errors up to 100%). The use of an added wave resistance method for a hull form that hasn't explicitly been validated results therefore in a large uncertainty with respect to accuracy. The uncertainty of added wave resistance calculations becomes especially apparent at severe sea states where the ship pitches and heaves significantly. It is therefore recommended to restrict performance monitoring to moderate weather conditions, Beaufort < 6.

4.2.6 Shallow water resistance

Lackenby (Lackenby 1961) presented a method to calculate the speed loss due to shallow water effects from trials on measured miles around the British Isles. The method is still widely used and recommended by the ISO15016 committee (ISO15016 2002) for performance analysis. The method is based on the calculation of speed loss as a percentage of the speed in calm deep water:

$$\frac{\Delta V_s}{V_s} = 0.1242 \left(\frac{A_M}{h^2} - 0.05 \right) + 1 - \sqrt{\tanh \left(\frac{gh}{V_s^2} \right)} \quad \text{for } \frac{A_M}{h^2} \geq 0.05 \quad (4.22)$$

Where:

- A_M = Midship section area under water in m^2
- g = Acceleration due to gravity in m/s^2
- h = Water depth in meters
- V_s = Ship speed in m/s

Using the resistance-power curve, either from model tests or from speed trials, this may be converted into power loss at constant speed.

4.2.7 Frictional resistance due to viscosity variations

The frictional resistance of a ship is a function of the kinematic viscosity. It can be calculated using the ITTC-57 frictional resistance coefficient:

$$C_F = \frac{0.075}{[\log(Rn) - 2]^2} \quad (4.23)$$

Where:

- Rn = Reynolds number

$$Rn = \frac{V_S L}{\nu} \quad (4.24)$$

- V_S = Ship speed through water
 L = Ship length at water length
 ν = Kinematic viscosity of seawater

Furthermore, the resistance is a function of density. However, because the difference in density globally varies by less than 0.5%, the errors in calculation are likely to be larger than the actual corrections and are not worth the transformation.

To calculate the change in resistance due to changes viscosity R_v , the difference in frictional resistance compared to a reference viscosity can be calculated (ISO15016 2002) as follows:

$$R_v = R_F \left(1 - \frac{C_{F0}}{C_F} \right) \quad (4.25)$$

Where:

- R_F = Frictional resistance calculated using prevailing density & viscosity using

$$R_F = 0.5 C_F \rho S V_S^2 \quad (4.26)$$

- C_F = Frictional resistance coefficient, calculated using equation 4.25
 S = Wetted surface area
 C_{F0} = Frictional resistance in reference conditions, calculated using equation 4.25

4.2.8 Changes in draft and trim

Draft and trim affects both wake and thrust deduction fraction as well as hull resistance. Empirical resistance prediction methods such as (Holtrop 1984) may be used to determine the changes in power from draft and trim deviations. However, most accurate and reliable methods to account for fractional draft and trim is by extrapolation of self-propulsion model tests or CFD analysis for a systematic range of loading conditions. By expressing the results of self-propulsion tests as a percentage change in power per unit

change in draft and trim, the effects of changes hull resistance, wake and thrust deduction can be taken into account simultaneously.

For small changes in displacement (within 2% of the displacement defined in the standard condition), empirical corrections may be used to calculate the added resistance directly. The ISO15016 Committee (ISO15016 2002) recommends the following correction:

$$R_{DIS} = 0.65R_T \left(\frac{\Delta_{ref}}{\Delta} - 1 \right) \quad (4.27)$$

Where:

R_T = Total resistance obtained from the measured propeller thrust coefficient and thrust deduction fraction (step 7 in section 4.2.1). Alternatively, it may be defined from model towing tests

Δ_{ref} = Reference displacement, determined from the hydrostatics of the vessel.

Δ = Ship's displacement, obtained from draft and trim readings and the hydrostatics booklet of the vessel

4.3 Performance indicators

The advantage of an online, onboard PM&A system is, apart from the increase in data quality, that it enables the operator to receive feedback on the current condition and operation of the vessel. However, only when data is analysed and converted into a format that is useable, easy to understand and unambiguous, it will result in an increase in knowledge on the vessel performance and will aid in the optimisation of the vessel operation. A display of real-time fuel flow, for example, is difficult to understand as it is affected by many factors. The selection of the right performance indicator is therefore important.

There are three levels of performance indication:

1. Real-time, for feedback on actions or changes in environmental conditions of short duration, e.g. acceleration or steering. Because of the short duration, most of the data interpretation can be done by the operator
2. Semi real-time, where the conditions are too complex or long to be interpreted by the operator; for example the effect on ship performance from wind, waves, trim variations, shallow water etc.
3. Long-term, for monitoring of the physical condition of the vessel, such as hull & propeller fouling or engine wear. This requires logging and analysis of large amounts of data over a considerable period of time, which cannot be done by the operator himself. Moreover, indicators of the condition of the hull and propeller have far-reaching consequences on maintenance and design procedures. The requirements for accuracy and clarity on interpretation are therefore high.

The three stages of performance indicators are discussed separately in the following.

4.3.1 Real-time performance indicators

During acceleration, deceleration and course deviations, the vessel behaviour is complex and affected by the vessel's inertia and unsteady flow conditions. Data conditioning and performance analysis is therefore difficult. However, because of the typically short duration, performance information may be interpreted by the operator directly, hereby providing feedback on ship operation. Effects of abrupt steering or rapid acceleration for example can be clearly seen on a torque and fuel consumption chart. The availability of a real-time time history chart of e.g. 20 minutes (depending on ship type) of ship speed, torque, RPM and fuel consumption can therefore provide useful feedback of such short, transient conditions.

Signal conditioning (averaging, validation etc.) often results in a time lag in the signal, especially if the averaging period is large. The data displayed on screen should therefore only be filtered for outliers (measurement errors) so that real-time ship performance is displayed.

Figure 4.4 shows an example of how a real-time performance indicator could look like. The diagram is a screen dump from the real-time performance indicator screen, developed and installed by the Author on the *Bernicia* during a course deviation and deceleration manoeuvre. The power, speed through water and fuel efficiency in litre/mile travelled distance through water is indicated. The reduction in efficiency due to rapid course deviation and the improvement in fuel efficiency due to speed reduction can clearly be seen. The data represents non-averaged data, filtered only for outliers.

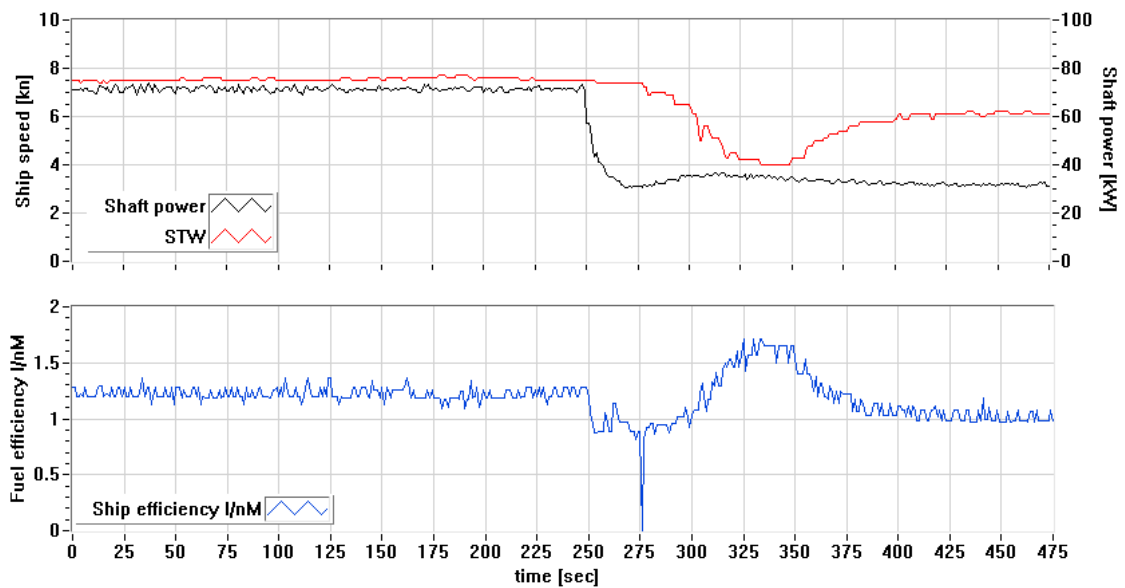


Figure 4.4: Real-time performance indicator for direct feedback on ship operation on Bernicia during course deviation and deceleration manoeuvre

4.3.2 Semi real-time performance indicator

The response of a ship to conditions with a longer duration, such as wind, waves or changes in water depth, is more difficult to identify from real-time performance indicators. They require monitoring of a large number of parameters over a longer time frame which may be difficult to interpret due to their complex interaction with ship performance. To be able to assist the operator in route optimisation and vessel operation, some analysis over a meaningful timeframe is necessary to display how the ship performs in the present environmental conditions. This can be done by comparing the present ship performance with a baseline, standard performance. In calm water conditions and design draft and trim, the difference will be small. However, when the vessel encounters a weather front or changes its draft or enters in a shallow water area, the difference represents the energy loss. The relative energy loss forms an intuitive and easy to understand indicator that can be used directly.

The reference condition can be expressed by different relationships, e.g. torque-RPM, speed-power, speed-RPM etc. Each relationship responds differently to changes in resistance and may be interpreted differently. Hull, wind, wave and shallow water added

resistance are all a function of the ship's speed, and speed should therefore be included in the derivation of a suitable performance indicator for changes in the ship's resistance. Engine speed on the other hand is not related to hull resistance, as the main engine of most merchant ships is RPM controlled and therefore constant regardless the ship's resistance. Shaft torque is directly related to the ship's resistance, but is an uncommon unit for the crew onboard and therefore difficult to interpret. Shaft power is more common. The relationship speed-power as indicator for hull resistance is therefore superior to the torque-RPM or speed-RPM relationship. The relative power loss may be calculated as:

$$\Delta P_D = \frac{P_{meas}(V_S) - P_{D,REF}(V_S)}{P_{D,REF}(V_S)} \quad (4.28)$$

Where $P_{meas}(V_S)$ is the measured shaft power at ship speed V_S and $P_{D,REF}(V_S)$ the reference power at this ship speed. If the reference speed-power curve is corrected for fouling and draft and trim, the indicator ΔP_D represents only temporary changes in ship performance.

Of particular interest is how much power is lost to individual resistance components (wind, wave, shallow water, trim or water viscosity). By correcting the measured speed and power ($P_{meas}(V_S)$) to standard conditions, $\Delta P_{D,corr}$ (as described in section 4.2.1) becomes (theoretically) zero. This characteristic can be used to identify the contribution of the individual resistance component to the total power lost. By dividing each resistance component by the total added resistance, the percentage power loss from each component may be calculated. For wind resistance the power loss would be calculated as:

$$P_{wind-loss} = \frac{R_{WIND}}{R_{ADD}} \Delta P_D \quad (4.29)$$

Where R_{WIND} is the wind resistance and R_{ADD} the combined added resistance from wind, wave, shallow water and changes in water viscosity. A separate correction can be made for fouling and changes in draft & trim. Figure 4.5 shows an example of the breakdown of power losses.

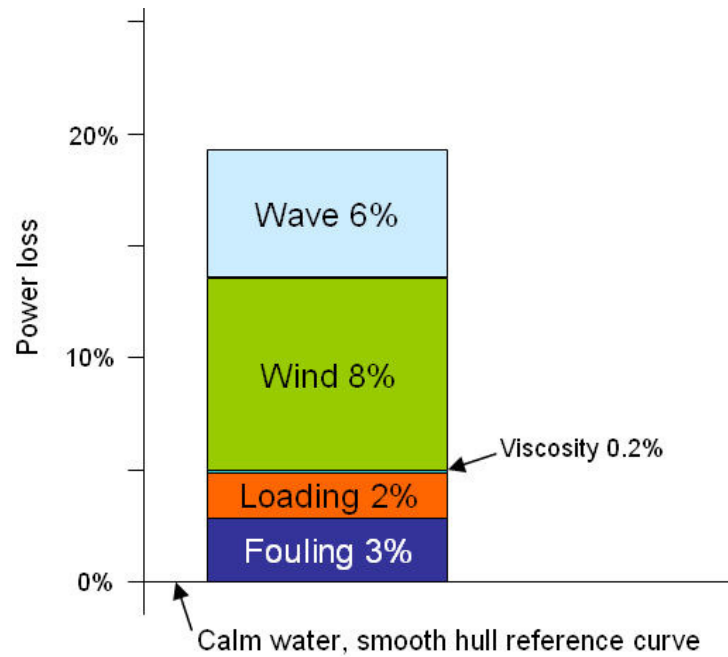


Figure 4.5: Example of a Semi-realtime performance indicator showing the breakdown of different performance loss components

To indicate power loss in different conditions, Figure 4.5 can be plotted on a time basis so that performance can be compared.

4.3.3 Long-term condition monitoring indicators

4.3.3.1 Hull condition

The selection of a suitable KPI to assess the effect of roughness and fouling on ship performance depends on the characteristics of frictional resistance. Resistance is a function of ship speed and can be represented by a number of associated coefficients, e.g. as recommended by the ITTC'78 procedure (ITTC 1978) in the following:

$$C_T = C_F (1+k) + C_R + \Delta C_F + C_{AA} \quad (4.30)$$

Where:

- C_T = Total ship resistance coefficient
- C_F = Equivalent flat plate frictional resistance coefficient
- k = Form factor from model tests
- C_R = Residuary resistance coefficient (wave and eddy resistance)
- ΔC_F = Correlation allowance mainly attributed to hull roughness
- C_{AA} = Still air drag coefficient.

If it may be assumed that only ΔC_F is a function of hull roughness and fouling, the relationship $\frac{C_{T-fouled}}{C_{T-clean}}$ may be considered constant. The effects of fouling and roughness may therefore be expressed as a percentage power increase over the smooth condition at constant ship speed (using the KPI ΔP_D , as described in the previous section). When the KPI $\Delta P_{D,corr}$ is plotted over time, it will slowly increase over time, representing the power loss due to hull fouling.

The correction methodology described in section 4.2.1 calculates the standard performance with clean propeller, and deviations in the standard performance can therefore be contributed to changes in hull performance. It is independent of the condition of the engine or fuel quality, since the propeller acts as a torque absorber and is not affected by engine behaviour.

The increase in $\Delta P_{D,corr}$ gives no characterisation of the hull surface; it only indicates the effect on performance. Figure 4.6 shows an example of the relationship between hull roughness and power loss as derived by (Schultz 2007) for a frigate sailing at 15kn for a range of roughness values, representative for different stages of fouling. It shows that the initial roughness of the hull causes the largest change in required power, and that increase in $\Delta P_{D,corr}$ cannot be linearly related to a hull roughness value, e.g. R_T50 .

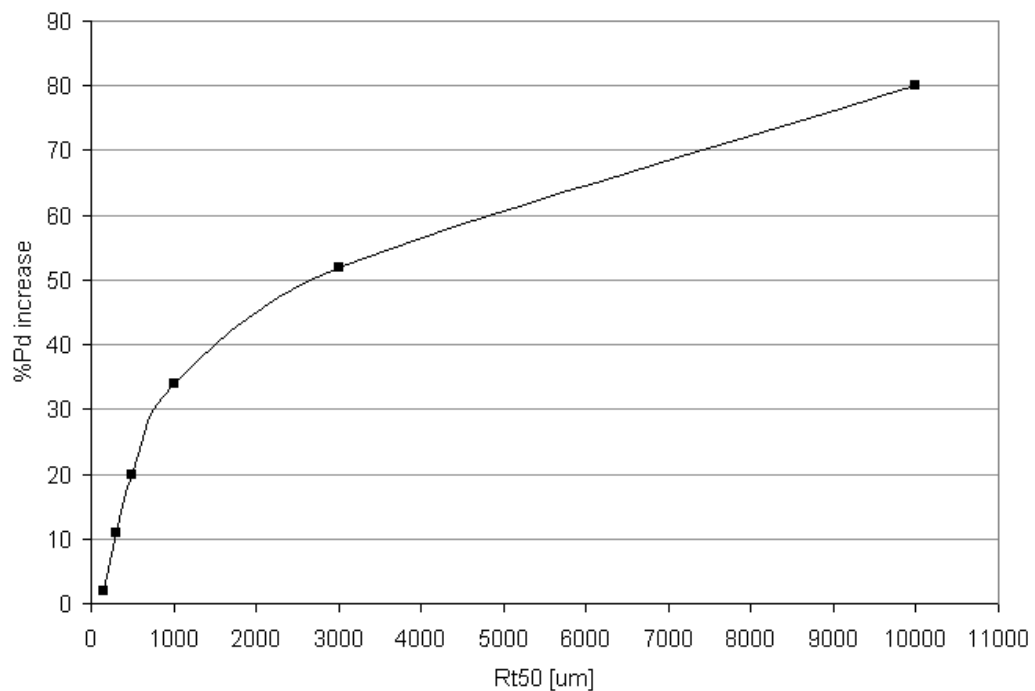


Figure 4.6: Hull Roughness versus power loss for different types of roughness comparable with hull fouling from slime(left) to heavy calcareous fouling(right) on a 124m, 9780dwt frigate at 15kn. (Schultz 2007)

In chapter 5, the ability of the suggested KPI to identify the effect on individual resistance components (such as fouling) is demonstrated. Furthermore, examples are given from analysed data from the *Bernicia* and the *Overseas Tanabe*.

4.3.3.2 Propeller Condition

The correction methodology described in section 4.2.1 calculates the standard performance with a clean propeller. It represents therefore only the condition of the hull. To get a rough estimate of the power loss at constant ship speed due to propeller roughness, a simplified method may be used described by Townsin et al. (Townsin et al. 1985) as shown below. The method is based on the propeller operating point in standard performance, as calculated by the correction methodology. The percentage power loss due to propeller blade roughness can be defined as:

$$\left(\frac{\Delta P}{P}\right)_{prop} = \left[\frac{2.2}{P/D} - 1.1 + \frac{3.3P/D - 2J}{2.2P/D - J} (0.45P/D) + 1.1 \right] \left(\frac{\Delta C_D}{C_L} \right)_{0.7} \quad (4.31)$$

With the blade lift coefficient C_L defined as:

$$C_L = \frac{2.37 \cdot 10^5 SHP \sqrt{1 + 0.207 \left(\frac{P}{D}\right)^2}}{zN^3 D^5 c/D (1 + 0.207J^2) P/D} \quad (4.32)$$

Where:

SHP = Delivered shaft horse power in standard, smooth propeller conditions in horse power

N = Engine speed in standard conditions in revolutions per second

c = Section cord length at 0.7 of the propeller radius in meters

D = Propeller diameter in meters

P/D = Pitch to diameter ratio

z = Number of propeller blades

J = Advance coefficient

4.4 Sensitivity analysis

The robustness of a correction methodology to errors in input parameters is highly important for ship performance analysis as performance data from ships is by nature scattered and subject to sometimes large measurement errors. A highly sensitive performance correction/analysis system is therefore as bad as errors in input parameters. In order to evaluate the proposed correction methodology, it has been compared with an existing method based on constant revolutions frequently found in publications (described in chapter 2.3.3). Additionally, the changes of sensitivity when using GPD speed instead of the speed log have been investigated. The sensitivity analysis gives information which input parameter is most important for performance analysis, the required accuracy for each measured or calculated parameter, and the accuracy of the KPIs that can be expected.

The used sensitivity analysis is sampling based, by repeatedly executing the correction model for small variations in any of 7 input parameters: torque, water density, shaft revolutions, wake fraction, thrust deduction coefficient, ship speed and calculated added resistance. The output from a unit change of a particular input parameter indicates the sensitivity of the method to that particular input parameter.

Because the correction methodology is a function of speed, power, wake fraction and propeller characteristics, the sensitivity of the methodology to input parameters is dependent on vessel characteristics. For the sensitivity analysis, the service speed has been used as a starting point, and three different type of vessels have been evaluated: the 16m research vessel *Bernicia*, a 318m, 274,000dwt VLCC (described in (ISO15016 2002)) and a 204m, 23,400dwt container vessel (described in (Journée 2003)). For all these vessels, trial data as well as propeller characteristics were known.

Trial data from the *Bernicia* has been used to evaluate the proposed methodology (based on constant ship speed, hereafter indicated with **Method 2**) with an existing method based on constant revolutions described in chapter 2.3.3, **Method 1**. The following graphs illustrate the sampling-based sensitivity analysis for shaft torque for the RV *Bernicia* when sailing at a service speed of 7.2kn. Figure 4.7 shows the reference speed-

power curve and the calculated standard performance for the two correction methods for changes in torque readings. The variations in power represent the error that result from a $\pm 2\%$ variation in torque, e.g. due to sensor bias or measurement error. Method 1 follows a constant revolutions line, Method 2 constant ship speed. Figure 4.7 shows that the deviation of Method 1 from the reference curve is larger than for method 2, indicating its higher sensitivity to the errors in torque.

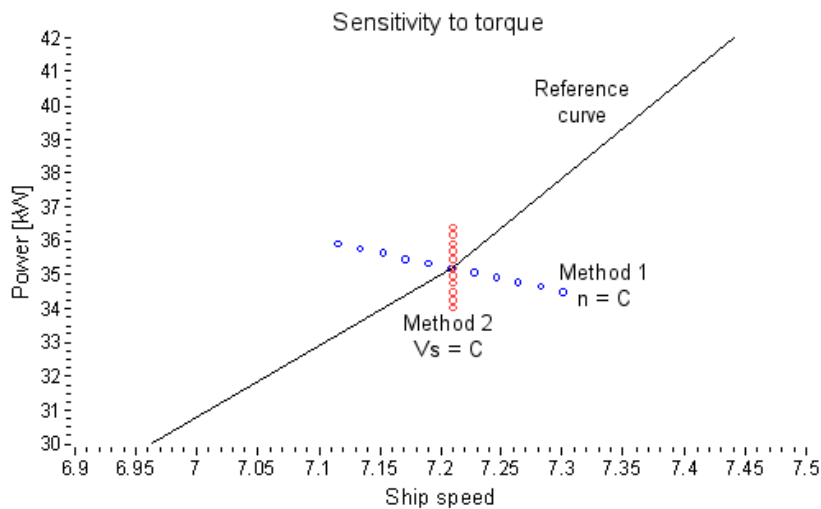


Figure 4.7: Effects of a $\pm 2\%$ measurement error in shaft torque for two correction methods for the Bernicia

Figure 4.8 shows the relative difference in power from the reference curve at constant ship speed ($\Delta P_{D,corr}$) from the same $\pm 2\%$ change in torque. The gradient of each curve indicates the sensitivity of the correction method to changes in torque. The minimum and maximum deviation from the reference curve represents the uncertainty of $\Delta P_{D,corr}$.

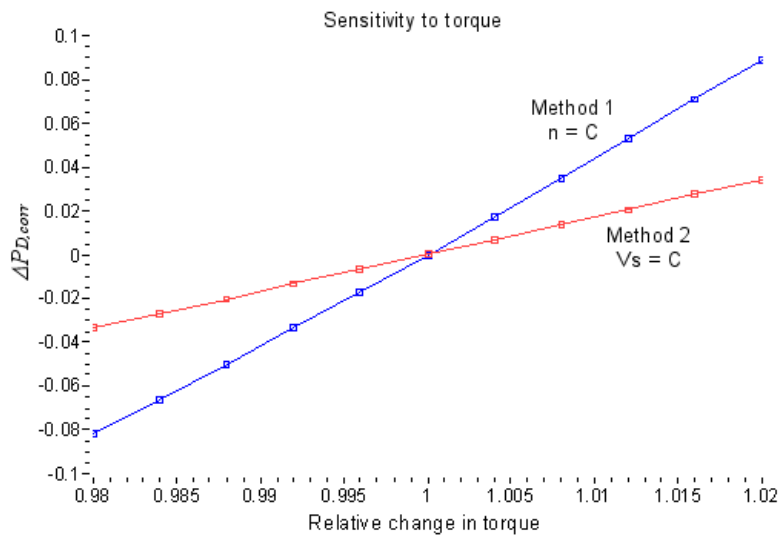


Figure 4.8: Effects of a $\pm 2\%$ measurement error in shaft torque on $\Delta P_{D,corr}$ for two correction methods

The gradient of Method 1 is larger than Method 2, indicating a higher sensitivity to torque. A measurement error of $\pm 2\%$ results in a $2 \times 4.28 = \pm 8.6\%$ deviation of $\Delta P_{D,corr}$ for Method 1 and a $2 \times 1.69 = \pm 3.4\%$ deviation for Method 2. In Table 4.1 the uncertainties from the remaining parameters are listed for the *Bernicia*.

The uncertainty of the input parameters can be divided in random errors and errors with a systematic nature. Systematic errors are mainly important for long-term performance analysis, where accuracy is important. Random errors may be accounted for by statistical smoothing when sufficient performance data is available. For instantaneous performance analysis, precision is important as smoothing is not possible, while accuracy is less crucial. Input parameters of the model with errors of a systematic nature are:

- Torque: sensor drift over time. The random error of torque sensors is considered to be less than 0.1% and not separately used in the analysis as random error.
- Wake fraction: increases slowly over time due to roughness and fouling. The wake is also dependent on ship's draft, and may therefore be different for each sailing passage, which may last for more than a month depending on route. Although this can be considered a random uncertainty, the duration can be relatively long depending on operating profile

- Water density, if this is not measured periodically to account for changes in water density in which the ship sails. Yet, water density varies only marginally and the errors are therefore small
- Propeller open water diagram (O.W.D): due to fouling the K_Q curve will increase, while the K_T curve remains approximately constant. If this is not calibrated periodically, the shift in propeller characteristics can be considered a systematic error.

The engine speed, ship speed, thrust deduction fraction and added resistance are considered random. Doppler logs have large errors due to current, ship motion etc, but are practically unaffected by sensor drift. The uncertainty can be considered to be independent of ship speed, as the errors are caused by the environment and not by the sensor itself.

Table 4.1 shows the sensitivity of the different input parameters for Method 1 and Method 2. The tested uncertainty range for each parameter (for torque, density and wake fraction the uncertainty represents a systematic error) is based on typical uncertainty levels discussed in (ITTC 1999c), (ITTC 2002a) and the Author's experience from ship performance data analysis. They are merely examples to show typical uncertainties resulting from systematic and random errors in the performance indicator. The mean level of the parameters represents a typical service condition of the *Bernicia*.

Table 4.1: Sensitivity and uncertainty analysis for the *Bernicia*

Parameter	Mean	Uncertainty Test range	Gradient	Uncertainty	Gradient	Uncertainty
			Method 1	$\Delta P_{D,corr}$	Method 2	$\Delta P_{D,corr}$
Systematic errors:						
<i>Torque</i>	1053 Nm	± 2%	4.28	± 8.6%	1.69	± 3.4%
ρ_{sea}	1025kg/m ³	±3 kg/m ³ (0.3%)	-3.28	± 1.0%	-0.69	± 0.2%
<i>w</i>	0.086	±60% (0.05)	-0.48	± 28.8%	-0.10	± 6.1%
<i>O.W.D</i>	$P_D = 35kW$	$K_Q + 3\%$		+2.8%		+2.8%
Random errors:						
<i>RPM</i>	319.2PM	± 0.05%	-10.63	± 0.5%	-1.45	± 0.07%
<i>t</i>	0.237	± 20%	-0.06	± 1.2%	-0.03	± 0.6%
<i>Vs</i>	7.21 kn	± 11% (0.8 kn)	-	-	-4.11	± 45.7%
<i>R_{ADD}</i>	0 N	± 5% of R_T	-2.45	± 12.2%	-0.96	± 4.8%

The absolute magnitude of the sensitivity and uncertainty in $\Delta P_{D,corr}$ should be interpreted with care. The uncertainty range depends on sensor characteristics and the accuracy of the hydrodynamic characteristics for the vessel used in the calculation (*w*, *t*, added resistance coefficients etc). The tested uncertainty range for the *Bernicia* is only a rough estimate to calculate the gradients (= measure of sensitivity) and to indicate which parameter is most important in performance analysis.

Furthermore, the following aspects should be considered:

- The sensitivity of the thrust deduction can only be determined when there is an added resistance. Therefore, an added resistance of 10% of the calm water resistance R_T has been used, which is a typical value when sailing in calm weather at service speed for the *Bernicia*
- The correction model does not predict ship behaviour. The results can therefore not be used to e.g. evaluate the increase of $\Delta P_{D,corr}$ with a 1.0kn increase in speed. The results merely indicate measurement errors or uncertainties

- The operating condition (speed, power) used in the analysis has a direct effect on sensitivity and uncertainty. Yet, the order of the sensitivities of the different parameters remains constant for different operating conditions.

From looking at the gradients in Table 4.1, it can be concluded that Method 1, based on constant RPM, is more sensitive to uncertainties in torque, RPM and wake, since it calculates ship speed using these parameters. Method 2 uses the ship speed from the speed log, and has therefore a high level of random uncertainty, but significantly lower sensitivity of the remaining parameters. The same differences in uncertainty between Method 1 and 2 hold therefore for other vessels and operating conditions.

By using the GPD speed instead of the speed log, the large random uncertainty caused by the speed log may be avoided. The GPD speed provides theoretically an accurate representation of ship speed, as long as the wake fraction is calibrated for the loading and hull condition and propeller roughness. However, this has implications on the sensitivity of the torque, RPM and wake. In Table 4.2, the GPD speed is used in Method 2 and compared with Method 1.

Table 4.2: Sensitivity analysis for the *Bernicia* for Method 1 and Method 2^{GPD}

Parameter	Mean	Uncertainty Test range	Gradient Method 1	Uncertainty $\Delta P_{D,corr}$	Gradient Method 2 ^{GPD}	Uncertainty $\Delta P_{D,corr}$
Systematic errors:						
<i>Torque</i>	1053 Nm	±2%	4.28	± 8.6%	4.28	± 8.6%
ρ_{sea}	1025kg/m ³	±3 kg/m ³ (0.3%)	-3.28	± 1.0%	-3.28	± 1.0%
<i>w</i>	0.086	±60% (0.05)	-0.48	± 28.8%	-0.48	± 28.8%
<i>O.W.D</i>	$P_D = 35\text{kW}$	$K_Q + 3\%$		+2.8%		+2.8%
Random errors:						
<i>RPM</i>	319.2RPM	±0.05%	-10.63	± 0.5%	-10.63	± 0.5%
<i>t</i>	0.237	±20%	-0.06	± 1.2%	-0.03	± 0.6%
<i>GPD</i>	7.21 kn	-	-	-	-	-
R_{ADD}	0 N	±5% of R_T	-2.45	± 12.2%	-0.97	± 4.8%

From Table 4.2 follows that the methodologies become comparable in terms of sensitivity from systematic errors. In terms of robustness, there is therefore no direct advantage of Method 1 over the proposed methodology (Method 2) using the GPD speed. The inability of Method 1 to account for changes in hull resistance due to changes in ship speed, as discussed in chapter 2.3.3, makes Method 1 however inferior to the proposed methodology, Method 2.

The use of the GPD speed instead of the speed log has however consequences on the long-term accuracy of Method 2. Table 4.3 and Table 4.4 show the differences in sensitivity for a typical container ship and VLCC respectively.

Table 4.3: Sensitivity and uncertainty analysis for a container vessel at 21.6kn

Parameter	Mean	Uncertainty Test range	Gradient Method 2 ^{GPD}	Uncertainty $\Delta P_{D,corr}$	Gradient Method 2	Uncertainty $\Delta P_{D,corr}$
Systematic errors:						
<i>Torque</i>	1175 kNm	±2%	2.42	±4.8%	1.48	±2.9%
ρ_{sea}	1025 kg/m ³	±3 kg/m ³ (0.3%)	-1.44	±0.4%	-0.50	±0.2%
<i>w</i>	0.261	±30%	-0.72	±21.6%	-0.25	±7.5%
Random errors:						
<i>RPM</i>	119.56 rpm	±0.1%	-3.95	±0.4%	-0.73	±0.7%
<i>t</i>	0.189	±10%	-0.03	±0.5%	-0.03	±0.5%
<i>V_S</i>	21.6 kn	±3.7% (0.8kn)	-	-	1.33	±4.9%
<i>R_{ADD}</i>	0 N	±5% of <i>R_T</i>	-1.11	±5.5%	-1.11	±5.5%

Table 4.4: Sensitivity and uncertainty analysis for a laden VLCC at 15.7kn

Parameter	Mean	Uncertainty Test range	Gradient Method 2^{GPD}	Uncertainty $\Delta P_{D,corr}$	Gradient Method 2	Uncertainty $\Delta P_{D,corr}$
Systematic errors:						
<i>Torque</i>	2614 kNm	$\pm 2\%$	3.53	$\pm 7.1\%$	1.64	$\pm 3.3\%$
ρ_{sea}	1025 kg/m ³	± 3 kg/m ³ (0.3%)	-2.52	$\pm 0.8\%$	-0.65	$\pm 0.2\%$
<i>w</i>	0.1856	$\pm 30\%$	-0.61	$\pm 18.3\%$	-0.16	$\pm 4.8\%$
Random errors:						
<i>RPM</i>	65.59 rpm	$\pm 0.1\%$	-6.71	$\pm 0.7\%$	-1.01	$\pm 0.1\%$
<i>t</i>	0.13	$\pm 10\%$	-0.02	$\pm 0.3\%$	-0.02	$\pm 0.3\%$
<i>V_S</i>	15.7 kn	$\pm 5\%$ (0.8kn)	-	-	1.96	$\pm 10.0\%$
<i>R_{ADD}</i>	0 N	$\pm 5\%$ of <i>R_T</i>	-1.13	$\pm 5.7\%$	-1.13	$\pm 5.7\%$

The higher ship speed and different propeller characteristics of the container ship and tanker compared to the *Bernicia* result in a lower the random uncertainty resulting from the speed log. However, the increase in sensitivity in torque and wake fraction when using the GPD speed remains large. These systematic errors may incorrectly be interpreted as a performance reduction. The use of the GPD speed is therefore inappropriate for long-term performance analysis. For direct performance indication, it gives a more precise measurement as it is unaffected by the large fluctuations in Doppler speed. A ship-based performance monitoring system would therefore ideally incorporate both a system for short-term performance analysis, with stable and precise KPIs, and a long-term analysis part with high accuracy so that trends can be made based on reliable data. In section 4.5, the system structure for this is described.

4.5 Performance monitoring system structure

In the previous section, using a sensitivity analysis it was shown that the proposed analysis methodology provides a robust platform to correct service performance if a Doppler speed log is used to indicate ship speed through water. It results in accurate KPI's, but lacks precision due to typical large fluctuations of Doppler logs. Statistical regression techniques are therefore necessary to account for this random uncertainty. For direct performance indication to the user on the bridge, the GPD speed gives a more precise KPI, on the condition that the wake fraction is calibrated frequently. The proposed PM&A system consists therefore of a short-term and long-term data analysis routine, running parallel to each other.

The long-term performance analysis is used to indicate slowly developing changes in performance, e.g. from hull fouling, or effects of a new energy saving device, propeller cleaning etc. Real-time performance monitoring on the other hand is based on the display of energy loss to different temporary conditions such as such as wind, waves, shallow water, trim variations and water viscosity over a period of e.g. 12 hours, so that the operator can compare ship operation in different conditions. Because the comparison is made over a relatively short period, bias errors from e.g. wrong calibrations in shaft torque or wake fraction will not affect the interpretation of KPIs. Precision is however important, as averaging over time to reduce random errors is limited if analysis is done over a short time frame.

In this section, the system architecture of a complete PM&A system, that satisfies the data monitoring, conditioning and analysis methods described in the previous chapters, is described.

A PM&A system consists of data collection, signal processing, analysis (short term / long term) and data presentation. In order to combine these sub-components to a complete performance monitoring and analysis system, the following aspects should be considered:

- It is not always possible to obtain real-time information about the sea state (unless a dedicated wave radar is installed)
- The wake fraction is difficult to determine and varies depending on displacement and hull roughness. Frequent (automatic) calibration of the wake fraction is

therefore necessary so errors in wake estimation can be reduced using regression analysis

- Random errors of the speed log result in relatively large variations in calculated KPI's. However, because Doppler logs do not drift, statistical smoothing techniques may be used to derive accurate trends in long-term KPIs
- The ship speed through water measurement has long periods where the reliability cannot be guaranteed. In order to make any judgement of the reliability possible, the ship performance should be monitored continuously. When the ship sails in steady-state conditions for a long period of time, and the measured ship speed varies little over this period, it may be assumed that the speed log measures the speed of the vessel through the water accurately. For maximum reliability, only these periods should be used for performance analysis. This reduces the availability of data for performance analysis significantly. For real-time performance indication on the bridge, the GPD speed should therefore be used.
- To guarantee the accuracy of the GPD speed for long term performance monitoring, the wake fraction must be periodically recalibrated to account for the development of hull roughness, fouling, draft and trim.

In other to take the abovementioned factors into account, the proposed performance monitoring and analysis system consists of two streams, indicated in Figure 4.9.

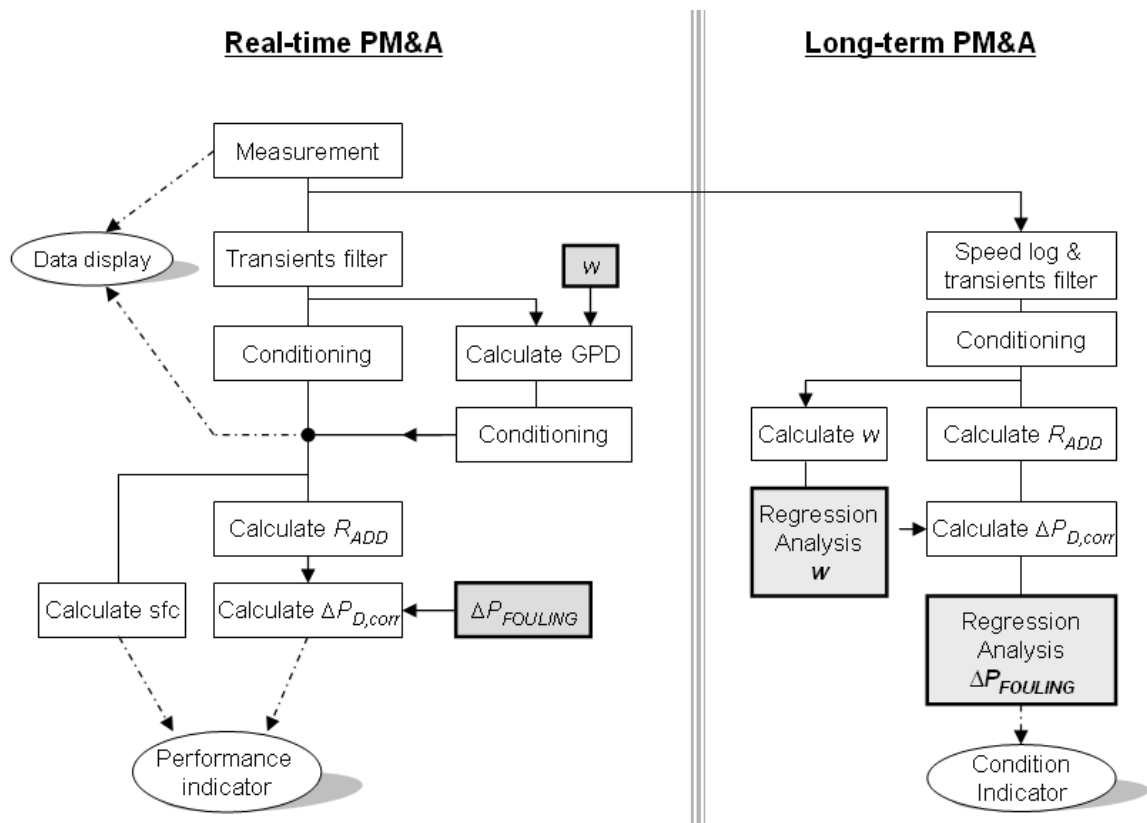


Figure 4.9: System architecture of the proposed PM&A system.

The system can be described in the following steps:

Real-time PM&A

- The principle benefit of continuous data logging and monitoring is the ability to improve the quality of data collection. Continuous data monitoring allows data validation and conditioning. The ‘Transients filter’ (see Section 3.5.2) forms the first step in data improvement process; performance data is continuously monitored and assessed for suitability to be used for performance analysis. The validated data is then averaged and checked for consistency in the ‘Conditioning’ subroutine (Chapter 3.5).
- The GPD relies on the accuracy of the torque sensor and the wake fraction. The wake fraction is defined in the long-term condition monitoring part of the PM&A system where it is determined periodically and using statistical techniques smoothed and validated for consistency (Section 4.2.3). The calibration of the

torque sensor requires manual intervention and cannot be done automatically (see Section 3.4.2).

- In transient periods, ship performance data cannot be conditioned and displayed (as discussed in Section 4.3.1). In order to provide feedback to the operator in transient periods, un-conditioned data is displayed in conjunction with conditioned data (GPD speed).
- With information about sea state, wind, water depth, water temperature and draft and trim, the added resistance compared to a reference condition can be calculated (as discussed in Section 4.2). By dividing the added resistance by the total resistance of the ship, the percentage power that is lost due to individual added resistance components can be displayed. Furthermore, with information from the long-term performance monitoring system, the power lost to overcome hull fouling can be indicated. This can be used directly as operational feedback to the officers on the bridge (see Section 4.3.2).
- In addition to feedback related to hull performance, it is also useful to indicate engine efficiency (specific fuel consumption) in relation to ship operation.

Long-term PM&A

- Long term condition monitoring is based on the identification of periods where the speed log is least affected by the environment. The subroutine responsible for the identification of these periods is similar as the ‘Transients’ filter, but monitors over a longer time frame in order to identify a longer period of steady-state performance. An example the filter subroutine and filtering constants for a VLCC, as developed by the Author, is described in Section 5.3.5.
- The periods identified by the Speed log & transients filter represent periods of constant performance and environmental conditions. The performance data and environmental conditions may therefore be conditioned and averaged over this complete period, resulting in a single value
- The filtered and conditioned data is used to calculate the added resistance components and $\Delta P_{D,corr}$

- The wake fraction is determined using the filtered and conditioned data. Small variations in wake relative to previous measurements will occur due to unavoidable errors in ship speed measurement and effects of draft and trim. Using regression analysis, fluctuations can be reduced by relating the measured wake to draft using a database of previous wake fractions, complemented with model test results. Small variations in speed can be reduced by statistical smoothing techniques such as trend analysis.
- The new and validated ‘calibrated’ wake fraction is used for the calculation of $\Delta P_{D,corr}$ and the GPD speed in the real-time performance monitoring system.
- A combination of errors in the prediction of R_{ADD} and an increase in resistance from hull roughness and fouling causes a deviation of $\Delta P_{D,corr}$ from the previous obtained $\Delta P_{D,corr}$. The errors in the prediction of R_{ADD} have a random character (assuming wind, wave and displacement vary randomly) and may be reduced by statistical smoothing. Using regression analysis, the general trend in $\Delta P_{D,corr}$ may be obtained, representing the power loss due to hull fouling, $\Delta P_{FOULING}$. The $\Delta P_{FOULING}$ is used in the real-time performance monitoring system for the separation of the R_{ADD} components.

For small ships which manoeuvre and alter speed frequently, the identification of periods where the measured ship speed can be considered accurate is difficult. In this case, the GPD speed can be used. To account for fouling, up and downstream speed trials are then required to provide the corrections for changes in wake due to hull fouling. When insufficient data is available for strict filtering of performance data, such as done in the ‘speed log & transients filter’, often the case for smaller vessels, the quality of the measured ship performance should be evaluated by different means. One way is to evaluate the performance over a single voyage or e.g. 6h sailing period and using statistics to determine the quality of the corrections.

Figure 4.10 shows the measured and corrected ship performance from a set of trials on the *Bernicia*. Each data point represents a 10 second average of the uncorrected (filtered for transient conditions) and corrected performance.

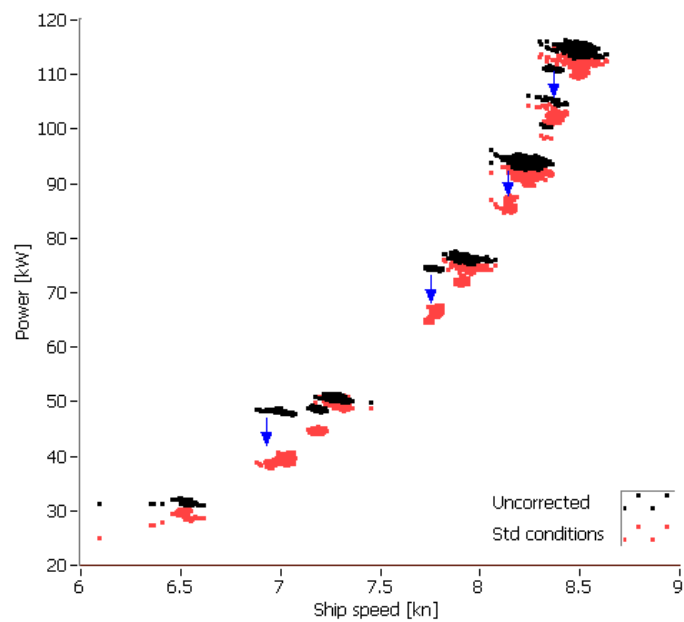


Figure 4.10: Correction of ship performance to standard conditions

In order to evaluate the quality of the performance data, the quality of the corrections can be determined. If the analysis methodology is able to correct ship performance accurately to standard conditions, it may be assumed that the measured performance data is of good quality. The quality of corrections is however difficult to evaluate from Figure 4.10. When the performance is plotted as ΔP_D versus time (Figure 4.11), this is possible.

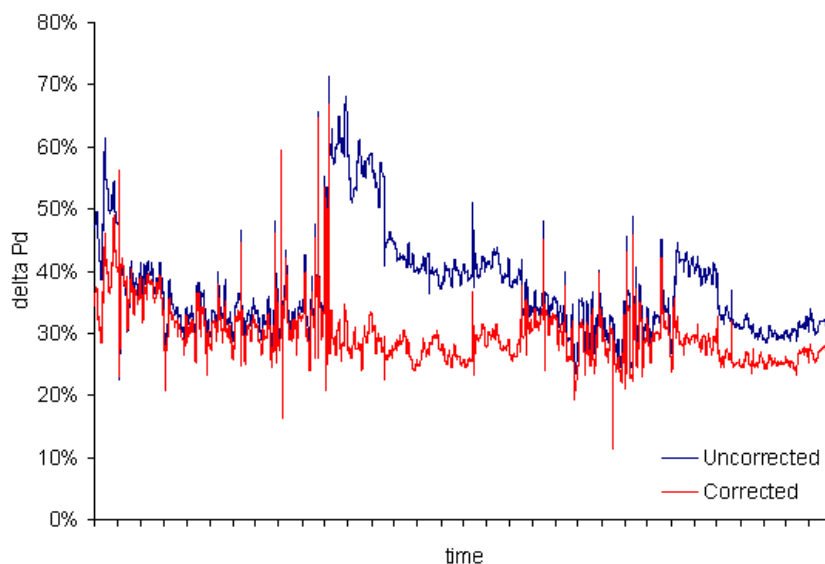


Figure 4.11: Effect of corrections to standard conditions

The quality of the performance corrections to standard conditions can be assessed by deviations from a horizontal line on the ΔP_D versus time plot. The offset of this mean line from 0% (approx. 30% in Figure 4.11) represents the difference in hull condition between the ship as it is and the reference, ‘standard’ condition. By setting a limit to the standard deviation of a dataset, the quality can be assessed. The statistical ‘mode’ can be used to determine the average performance after correction, indicating the change in hull fouling.

To visualise the effects of correction on the standard deviation, the histogram of the dataset of Figure 4.11 is plotted in Figure 4.12. The effect of the corrections expresses in a slender and single peaked histogram, in comparison to a wide and multi-peaked histogram of the uncorrected performance.

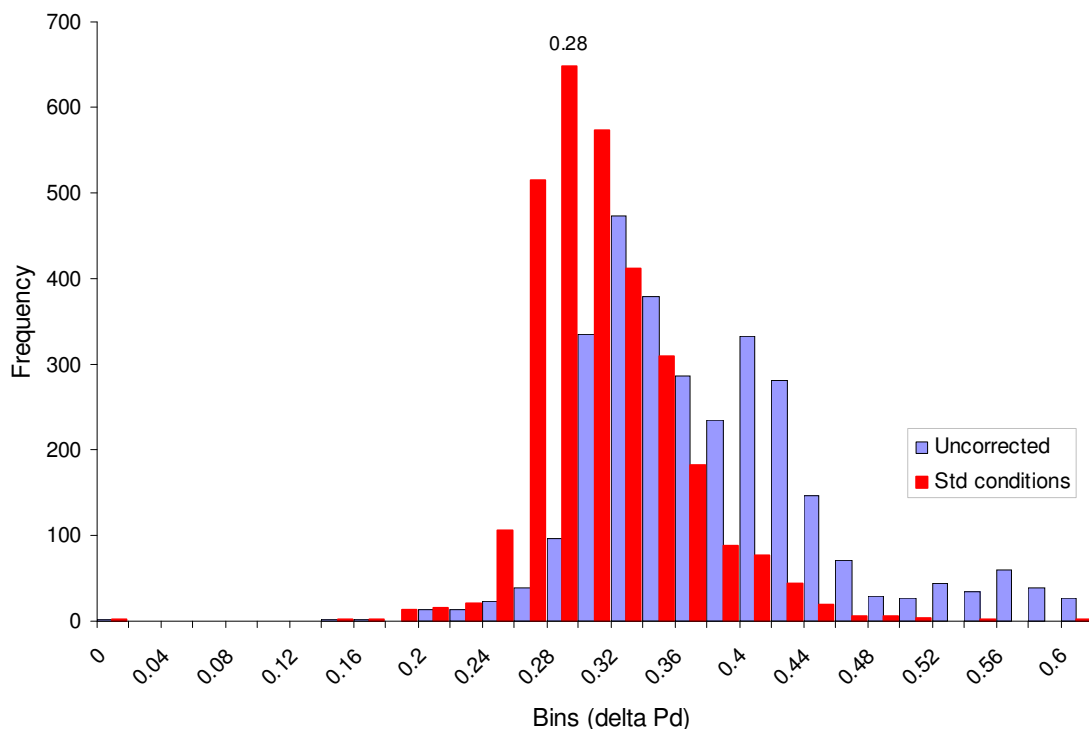


Figure 4.12: Histogram of the corrected and uncorrected ΔP_D for a sea trial on the Bernicia

A prototype of the PM&A system using both the system architecture described in Figure 4.9 and using the standard deviation has been developed by the Author and tested on two vessels. Chapter 5 and Appendix B give details of this development.

4.6 Conclusions

Performance analysis is the correction of ship performance (speed, power) to a pre-defined standard condition so that it can be compared with the reference (standard) performance. In this chapter, a methodology to convert ship performance to standard conditions has been described. The proposed correction methodology is based on the calculation of the new operating point on the propeller open water diagram for the performance in standard conditions, with the same ship speed as in the measured condition. Corrections are made for environmental conditions (wind, waves, shallow water and water viscosity), loading conditions (draft and trim) and propeller efficiency (roughness and variations due to propeller load changes). It is assumed that when all environmental and loading conditions are accounted for accurately, the remaining difference between the corrected power and the power in standard conditions can be contributed to changes in hull condition.

By using the above proposed methodology;

- The condition of the hull and propeller can be expressed as a percentage power loss at constant speed. By dividing the corrected power by the power at the same ship speed from the reference speed-power curve, a one-dimensional parameter is obtained that describes the added power required to overcome resistance from hull roughness and fouling. By plotting this parameter on a time basis, the slow increase in resistance due to roughness and fouling, which is difficult to estimate using empirical or physical methods, may be monitored.
- The proposed analysis methodology is highly sensitive to ship speed, which often has a large error margin. This results in a large uncertainty in the calculated standard performance. For real-time analysis, the GPD speed can be used instead, giving a precise measure of ship speed. The GPD speed relies however on the frequent calibration of the wake fraction and torque sensor and it increases the sensitivity of the correction method to errors in these parameters. For long-term performance analysis where long-term stability of sensors and wake fraction is important, a Doppler speed log should be used as it is not affected by sensor drift or fouling.

- To reduce the random errors from Doppler logs, periods should be identified where the speed log can be considered reliable. Only these periods should be used for the evaluation of ship performance. It is expected that irregular currents influence speed through water measurements most. Monitoring the difference between SOG and STW, drift speed in combination with the filtering for transient conditions allows those periods to be identified where currents are expected to be least and the speed log most accurate
- By calculating and real-time displaying the power loss due to wind, waves, displacement, viscosity, shallow water and hull fouling, direct feedback can be given to the operator. With this information, the crew can quickly get an understanding of ship behaviour and the accuracy of the correction methodology, so that ship operation can be optimised.
- A calibrated Doppler log and a high quality, easy to calibrate torque sensor are the most important parameters for long term condition monitoring. The separation of the effects of hull fouling on performance and the effects of sensor drift or errors in the calculation of the added resistance components (wind, wave, draft etc) which not necessarily behave as random error, is difficult. Frequent calibration is therefore of primary importance
- Among the component of resistance that are superimposed on the calm water resistance, the calculation of the mean added resistance in waves is likely to have the largest uncertainty. Added resistance calculations using strip theory model are valid for a limited range of vessel types only and the calculations suffer from inaccurate wave observations. Vessel specific model tests are therefore important, together with wave radar measurements if the vessel sails in coastal areas.

5

SYSTEM EVALUATION

5.1 Introduction

In Chapter 3 and 4 various aspects of an online PM&A system were discussed and associated algorithms proposed. Based upon the knowledge gained in these chapters, the main objective of Chapter 5 is to develop appropriate hardware and software to implement the associated algorithm onboard the two target test vessels and to evaluate their performance

Therefore, following this introduction, the knowledge and experience was obtained of software development, sensors and electrical installation, data acquisition and ship behaviour onboard the research vessel *Bernicia*, owned by Newcastle University. After the evaluation of the proposed PM&A system on this vessel, a similar system was developed, implemented and evaluated on the *Overseas Tanabe*, a 330m, 300.000dwt VLCC owned by OSG Shipping Management in Section 5.3. In both sections the installation of the hard and software is described and the proposed data acquisition, conditioning, data validation and analysis methodologies evaluated. Examples of the software are included to illustrate the principles of system design (transparency, ease of interpretation etc.) described. Finally a set of conclusions from the chapter is presented in Section 5.4.

5.2 PM&A system implementation onboard RV Bernicia

5.2.1 Vessel characteristics

The *RV Bernicia* is a 1970's purpose-build research vessel owned by the School of Marine Science and Technology, Newcastle University, and is based in Blyth, Northumberland. Her mission is mainly dictated by marine science and biology related research activities; trawling, bottom surveying, water sampling, coastal mapping, etc. Furthermore, she offers test platform for anti-fouling research on her hull and propeller. The vessel makes short trips to sea, and is therefore most of the time stationary in port – almost a half of a year- with brackish water. Marine fouling therefore develops rapidly. Each year around May, the vessel is dry-docked, blasted and recoated with a range of novel anti-fouling coatings for research purposes. The main particulars and general arrangement are shown in Table 5.1 and Figure 5.1.

Table 5.1: Main particulars RV Bernicia

Parameter	value
Overall Length	16.2m
Length LPP	13.86m
Beam Mld	4.72m
Normal service draft	1.91m
Normal service trim	0.89m by stern
Gross tonnage	46.25t
Service speed	8.0kn
Number of crew	3 persons
Engine: Gardner 8LXB	125kW, 1500RPM
Propeller	Ø1.117m, 4 bladed

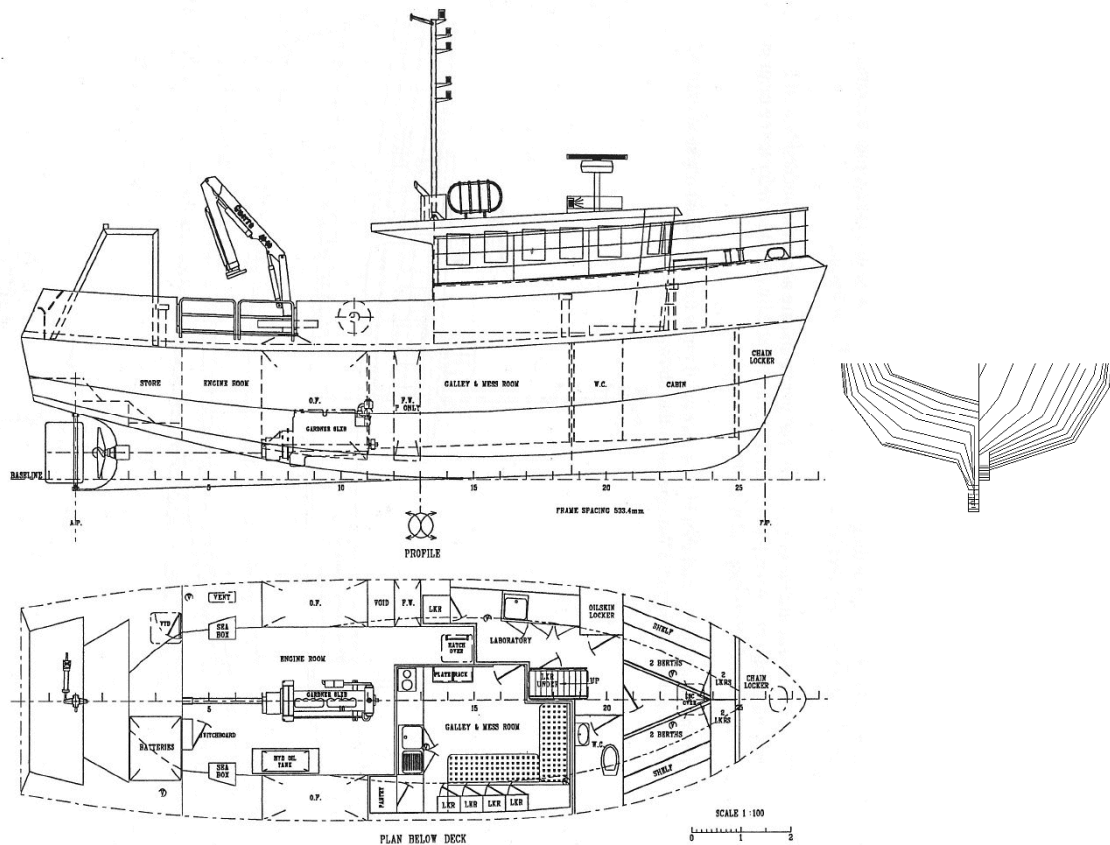


Figure 5.1: General Arrangement and body plan of the RV Bernicia

The main advantages of selecting the RV *Bernicia* as one of the test vessels were manifolds. Firstly the vessel was accessible anytime by the Author; Secondly the technical data including tailor-made model test results were available; Thirdly the vessel represented a typical small craft class which provided an interesting spectrum of vessel as opposed to a large commercial vessel class.

The availability of the RV *Bernicia* allowed performance in a wide range of conditions to be tested in a short time frame. The effects of shallow water, rudder action, ship motion, wind resistance and towing on ship performance could be tested in a period of weeks. This allowed a quick familiarisation of ship behaviour and insight into sensor characteristics and reliability.

5.2.2 Installation of sensors & data acquisition system

Most required parameters for PM&A mentioned in section 3.6 are standard equipment available on ships. Onboard the *Bernicia*, a number of sensors were missing. In order to collect accurate and reliable data of ship performance and environment, a range of sensors were therefore purchased, installed, calibrated and interconnected to a centralised data acquisition system by the Author himself. Others were already available and were linked to the centralised data acquisition system. The following sensors installed by the Author:

- Shaft torque sensor, by means of a set of *TSM* strain gauges installed on the propeller shaft, just after the stern gland. A *Mantracourt Electronics TLC1* and *TIO* telemetry system, powered by a high capacity battery pack (*Tadiran SL-790*) was used to transfer the signals wireless from the strain gauges data acquisition system
- Engine speed indicator, by means of a photologic reflective object sensor type *OPB715* on the engine alternator shaft
- Draft gauges, by means of four ‘*Cerabar T PMC 131 A4 5 F1 D12*’ pressure gauges installed in the bow and stern, on port and starboard side, approximately 0.5m under the water line
- Fuel flow sensor, by means of a *Metra-flow OGI* oval gear flow meter located between the fuel lift pump and fuel injectors
- Rudder angle sensor by means of a potentiometer connected directly on the rudder stock and a differential amplifier type *UA741CP*

Additionally, the following sensors were linked to the data acquisition system:

- A *Walker 4020* Electro Magnetic speed log, installed amidships parallel to the keel
- A *Furuno DS-50* DGPS receiver, providing ship speed over ground, position, transverse speed, course, rate of turn and time
- A *JMC V-122* Echo sounder, measuring water depth under the keel
- Cup anemometer (manufacturer unknown), installed 1.5m above the wheelhouse in the mast for apparent wind speed and direction

Figure 5.2 to Figure 5.10 show the sensors on the *Bernicia*.



Figure 5.2: Anemometer and wind vane of the *Bernicia*



Figure 5.3: DGPS receiver of the *Bernicia*



Figure 5.4: EM Speed log of the *Bernicia*



Figure 5.5: Fuel flow sensor of the *Bernicia*

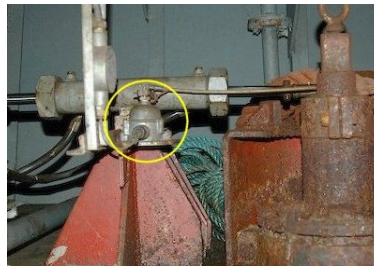


Figure 5.6: Rudder angle sensor of the *Bernicia*

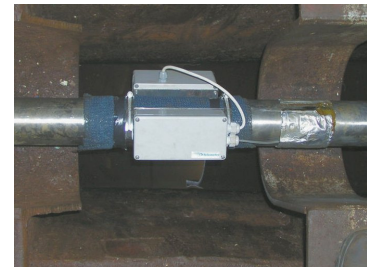


Figure 5.7: Torque sensor of the *Bernicia*



Figure 5.8: Draft (pressure) sensor of the *Bernicia*



Figure 5.9: Echo sounder of the *Bernicia*

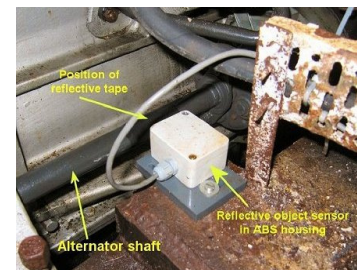


Figure 5.10: RPM sensor of the *Bernicia*

The data acquisition system was purpose build by the Author to accommodate all types of signals (analogue, digital and NMEA0183) from the sensors on the *Bernicia*. The data acquisition system consists of a multifunctional data acquisition card with analogue and digital inputs and outputs, a digital to analogue frequency converter, a serial RS232 multiplexer, a USB hub and a number of relays to switch communication lines to the data acquisition computer on and off. The data is stored on a ruggedized laptop which is connected to the data acquisition system shown in Figure 5.11. The signal

interfacing of all sensors and electronics is controlled using LabVIEW 7.1 (NI 2004). Analogue and digital channels are sampled at 50Hz to avoid aliasing. NMEA0183 data is received at sampling rates between 0.1 – 1Hz, depending on instrumentation. The control of the torque sensor (calibration, battery check, remote starting & stopping of telemetry system and sampling) is done at a frequency of 2Hz. A full report on the characteristics, installation, calibration and interconnection of the sensors onboard the *Bernicia* can be found in (Hasselaar 2008).

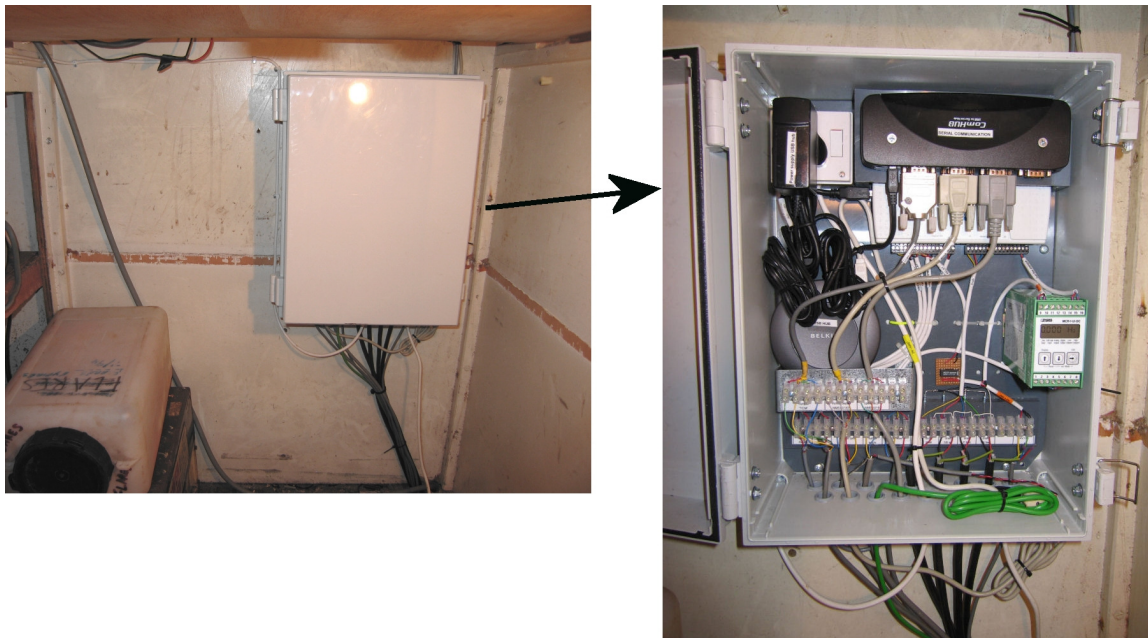


Figure 5.11: Centralised, tailor-made data acquisition system installed on the Bernicia

Apart from a number of technical difficulties with interconnecting sensors from different manufacturers and different output formats, the following more general applicable problems were experienced:

- The fuel flow in the fuel line of a reciprocating engine pulsates with high frequency, due to the characteristics of the lift pump and backflow of injector pumps. A flow meter installed directly in the fuel line is heavily influenced by these pulsations. Careful selection of the location of the flow meter is therefore important. To avoid pressure pulses from the diaphragm lift pump and the fuel

injectors on the *Bernicia*, two flow dampers and a non-return valve were installed in series with the fuel flow meter. The flow dampers consist of a closed cylinder filled half with fuel and half with air. The compressibility of the air trapped in the cylinder acts as a damper and reduces the fluctuations of the fuel that flows through the dampers. The high frequency of the injector pumps could be damped with a small damper of approx. 50 cm³, while the low frequency pulse fluctuations from the lift pump were damped with a large damper with a volume of approx. 1000 cm³

- No material characteristics of the propeller shaft were available. To estimate the validity of the assumed elasticity modulus, the torque sensor was therefore calibrated. Physical calibration of strain gauges on propeller shafts is practically impossible for most ships. However, because of the frequent dry-docking periods and the relatively small engine power of the *Bernicia*, physical calibration was possible by applying a number of known loads on the propeller shaft (by means of a leverage system and calibrated weights). Hysteresis due to static friction from the water lubricated shaft bearings affected the accuracy of the calibration procedure. However, good agreement (within 2%) was found between measured and applied load. Details of the calibration can be found in (Hasselaar 2008)
- The Electro Magnetic (EM) speed log has been calibrated in service by the Author using a VECTRINO 3D Doppler log (Nortek 2007) over a range of ship speeds. Instrumentation errors, which could not be solved within the time frame of the PhD project, made the calibration however soon ineffective
- Sensors with analogue output are heavily influenced by electrical noise and floating grounds caused by induced currents in the ship's hull. The effects could be reduced by using differential amplifiers, galvanic isolation (opto-couplers) and digital signal transmission. However, cross-interference between outputs remains a sensitive aspect of analogue transmission.
- Post-processing indicated that the software routine for automatic torque calibration (setting the zero-point before departure in port) did not function properly, which caused an offset in the measured torque.

5.2.3 PM&A software and User Interface

In the design of the data acquisition system software, special attention has been paid to system transparency. One of the causes of confusion and misunderstanding of data collection onboard ships is that the origin of displayed parameters is often unknown. Whether data originates directly from a sensor, is averaged over a day or is calculated for example, are important aspects for the trustworthiness of a system. The architecture of the user interface of the PM&A system has therefore been divided in 4 steps, as shown in Figure 5.12.

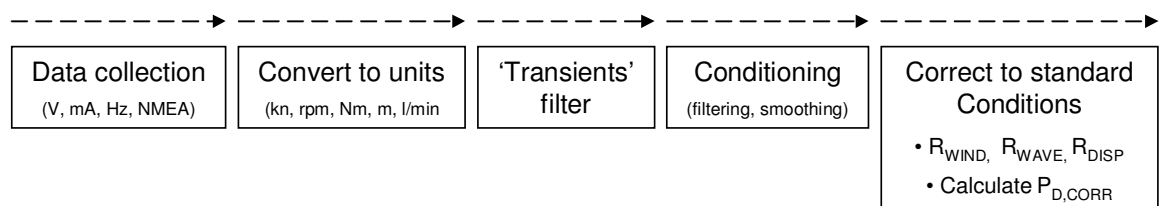


Figure 5.12: Software architecture of the PM&A system

For each parameter the steps in Figure 5.12 can be displayed real-time on screen. Hence, each parameter that is used in the correction of ship performance to standard conditions can be tracked back to the source. Photographs are included where appropriate to indicate which sensor is used and where it is positioned on the ship. The main screen of the PM&A system shows time series of filtered data of the ship speed, power, fuel consumption and wind speed for real-time operational feedback on ship performance. Due to the character of the operational profile of the *Bernicia*, no user interface has been implemented for long-term KPIs (as discussed further in section 5.2.6.3).

Figure 5.13 shows the main screen of the user interface of the PM&A system on the *Bernicia*. In the menu bar, individual screens can be opened to get real-time information how data is collected, converted to units, conditioned or used in performance analysis. On the left hand side of the screen, the most important parameters for performance monitoring are shown real-time. Three buttons on the main screen remind the user to (1) start a calibration procedure ‘CALIBRATE TORQUE’ of the torque sensor before commencing a sea trail, (2), enter sea state characteristics ‘ENTER SEA STATE’, and (3), make a record of the draft ‘CAPTURE DRAFT’ (when the ship is about to leave

port). Visual and audible reminders are included to remind the user when each action requires attention.

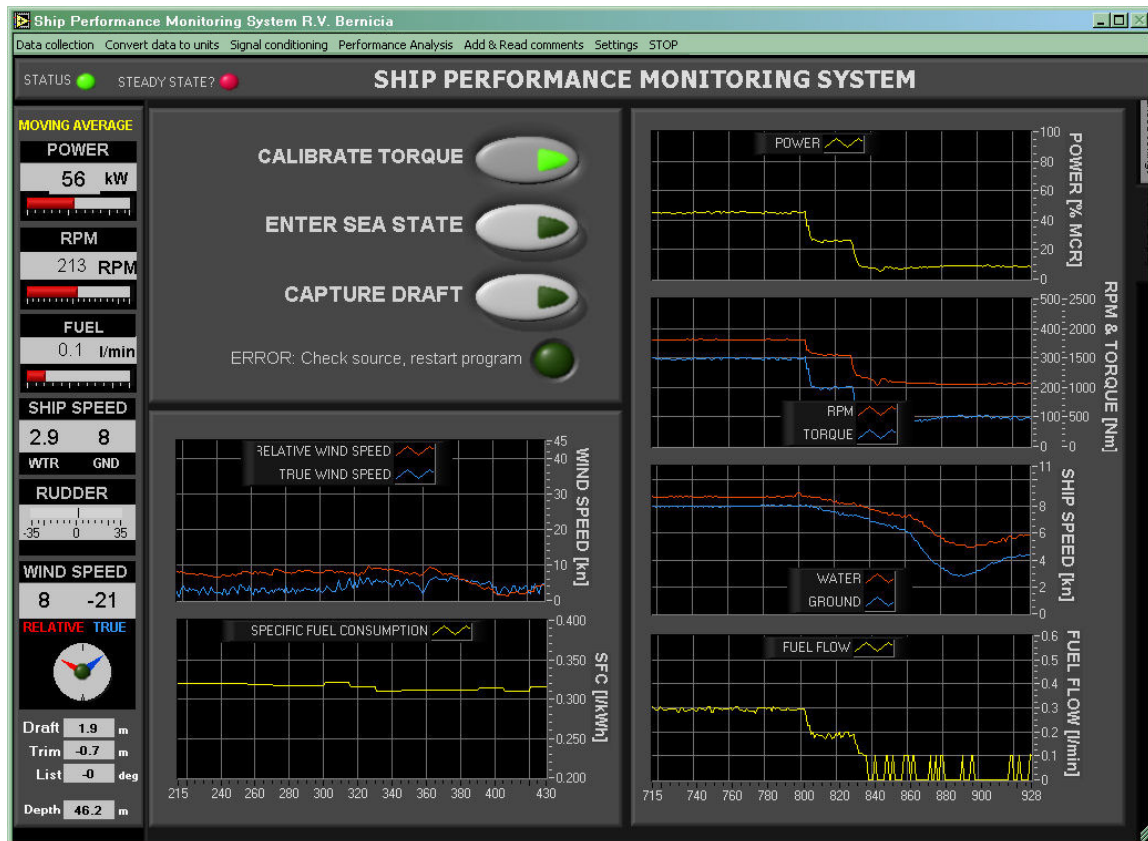


Figure 5.13: Main user interface of the PM&A system on the Bernicia

In the menu 'Data collection', the user can choose to see how serial data is collected, analogue data or how the wire-less communication with the torque sensor takes place. An example of the 'Data collection' interface page for the serial NMEA0183 data is shown in Figure 5.14

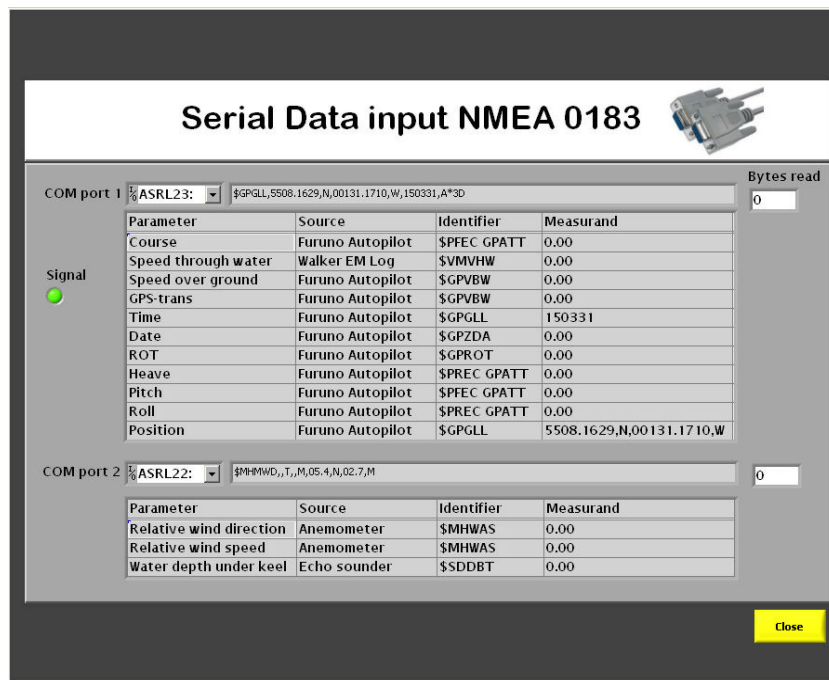


Figure 5.14: 'Serial data input' interface

In this interface the real-time the NMEA0183 sentences are visible that are received by the system. In this case, the relevant data from the sentences is filtered and displayed. The source and identifying NMEA0183 sentences characters are shown. This way of presentation avoids confusion and gives maximum clarity into data collection.

Using the menu 'Convert data to units', the user can choose to see how the analogue and digital data is converted in units (Draft, trim, list, rpm, torque, fuel flow and rudder). The NMEA0183 is received in usable units and therefore not included in the list. In Figure 5.15 the interface screen of the data conversion to units for the Fuel flow is shown. In three steps, the conversion from Volts to Litre/min is shown using the calibration characteristics of the frequency converter (volts to Hz) and flow meter characteristics (Hz to Litre/min). A time series plot shows a history of the last 100 seconds of the raw signal.

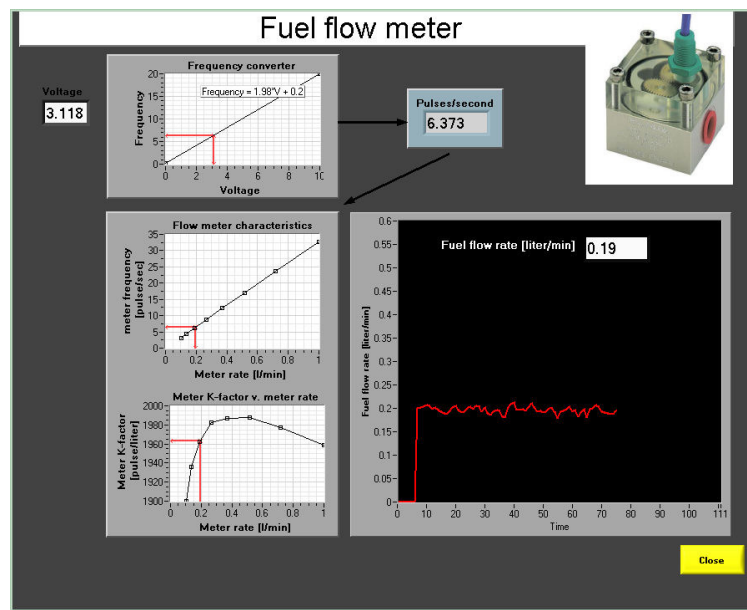


Figure 5.15: ‘Conversion to units’ interface for fuel flow

In the menu ‘signal conditioning’, the user can obtain real-time information how data is conditioned. The following screens can be selected; static ship characteristics, transients filter, speed log, speed over ground, draft, trim, rpm, torque, fuel consumption, wind, depth and rudder angle. Figure 5.16 shows the ‘Signal Conditioning’ interface screen for the Wind speed and direction. In two time series, the unfiltered, filtered and averaged data is shown. The used filtering and averaging characteristics are shown. Additionally, the calculation method for true wind speed and direction is shown. All figures are updated real-time for clarity.

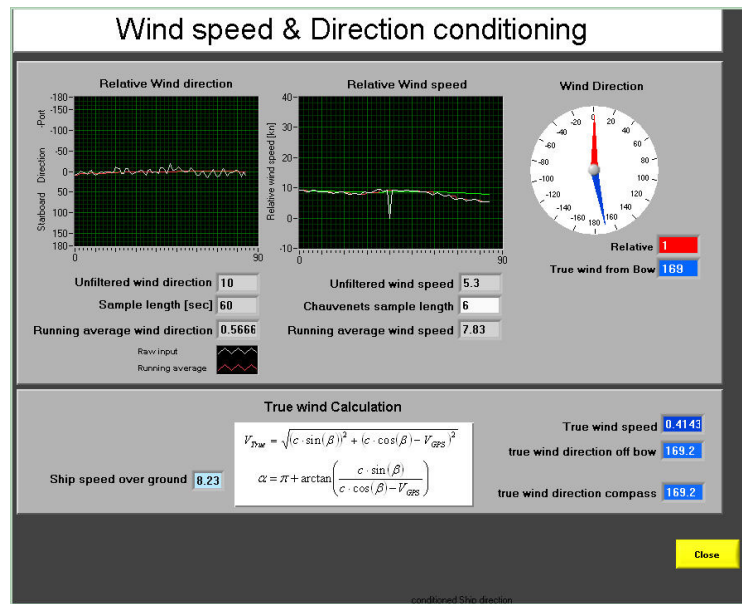


Figure 5.16: ‘Signal conditioning’ interface of apparent Wind

The interface for each parameter is different, but follows similar principles regarding transparency in data conditioning as in Figure 5.16. A screen dump of each interface is shown in Appendix B.

Using the menu ‘data analysis’, the user can see real-time how the conditioned data is used to calculate wind, wave, shallow water resistance, and how these figures are used to correct ship performance to standard conditions. Figure 5.17 shows the user interface of the correction of ship performance to standard conditions. Real-time, conditioned data is shown and the calculation is displayed in steps, where intermediate answers are calculated real-time. This provides optimal transparency and reliability of the system.

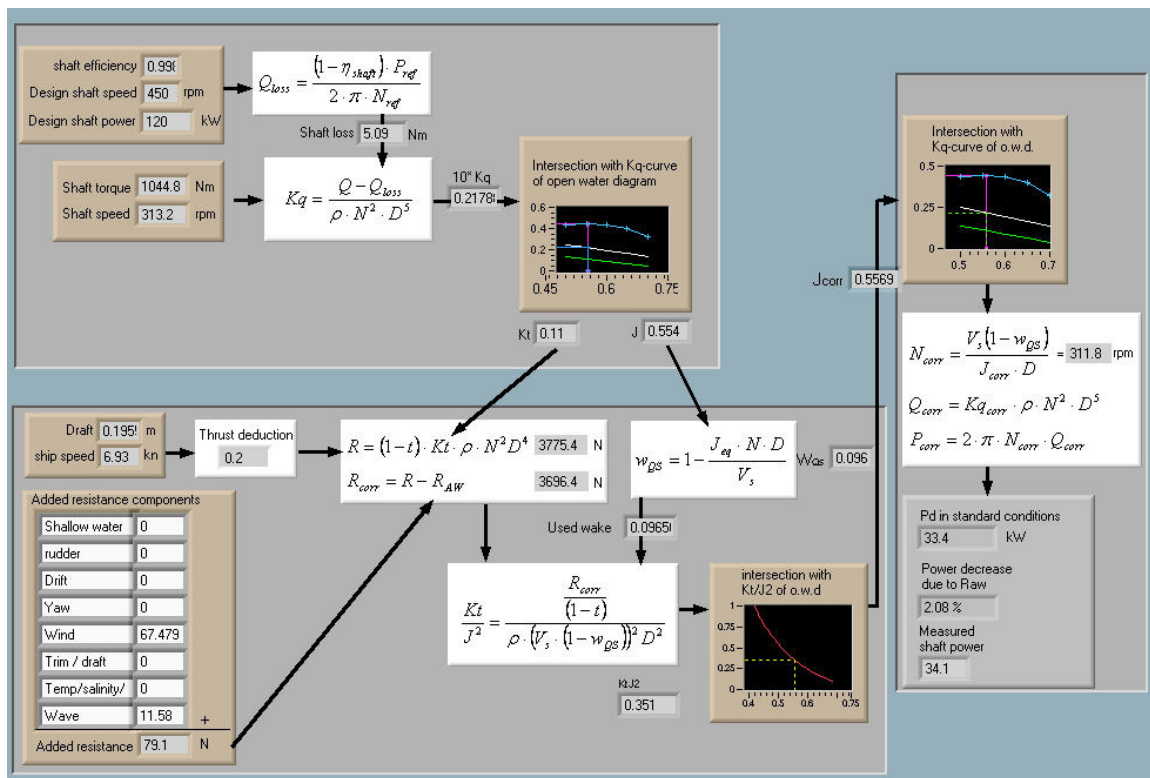


Figure 5.17: 'Correction to standard conditions' interface

The developed software is a working prototype example of how an ideal PM&A system should work and look like. Further details are included in Appendix B.

5.2.4 Data collection

Because of the unfavourable operating profile of the *Bernicia* (mainly short trips with much manoeuvring), not enough useful information for the evaluation of the PM&A system could be obtained from performance logging during normal operation. Therefore, 14 dedicated sea trials were made in the period between October 2006 and May 2007 along the coast between Blyth and Amble. A typical sailed track from speed trials is shown in Figure 5.18. During the measurements, the draft, trim and list remained practically constant (within 3%). Furthermore, the seawater temperature over the period varied only little, between 7-10°C. Assuming salinity remained constant, the changes in resistance due to variations in water density and viscosity may be ignored (<0.7% of total resistance at 7.5kn).

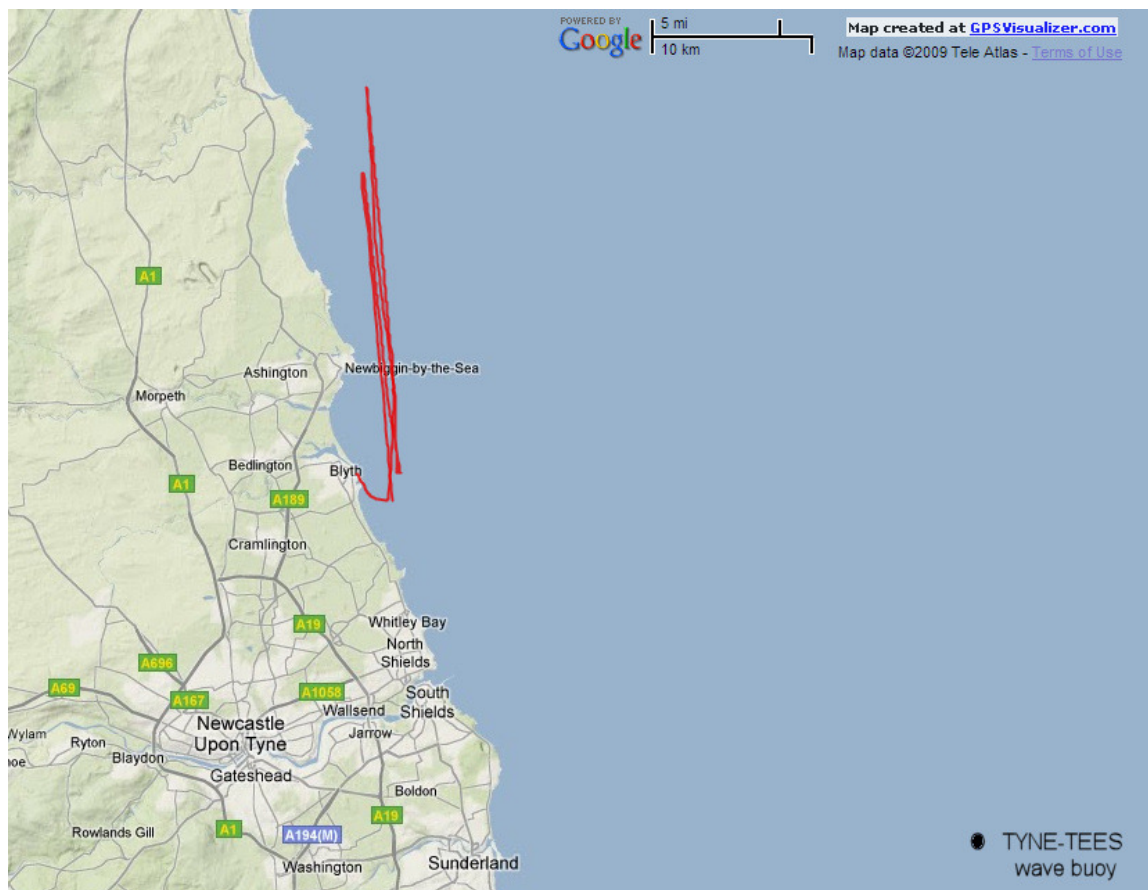


Figure 5.18: Typical track of sea trials on the *Bernicia*

Wave characteristics were determined visually by the Author and the skipper, and included in the electronic data files. The definition of the sea energy spectrum was however more difficult to determine. Shallow water effects, strong currents and shore winds affect the sea state locally and as a result, the sea may be assumed not fully developed, which makes the estimation of the sea spectra and wave conditions difficult. In December 2006, a Datawell WaveRider buoy was deployed by CEFAS (Cefas 2008), approx. 30 miles South East of the area where most experiments were done (as indicated in Figure 5.18). This gave information about sea temperature, wave period, significant wave height, wave direction and sea spectrum with an update frequency of 30 minutes.

Data about the ship's performance, the environment and loading conditions were logged with an update frequency of 1Hz and stored in ASCII format. In Appendix B1, a description is given of contents of the data files. Through post data analysis a number of problems with the speed log and anemometer was identified, as discussed in the following sections.

STW measurements

The *Bernicia* has an Electro Magnetic speed log. Due to unknown reasons the speed log drifts when turned on. This 'warming up' period is variable, and may last between 1-4h. It was therefore not possible to rely on the speed log. Figure 5.19 shows the speed through the water from the EM speed log, the speed over ground (from DGPS) and the GPD speed for a set of up- and downstream speed trials in calm weather conditions. The data in the figure is conditioned using the transients filter. Periods of acceleration, deceleration and course deviations are therefore left out. For ease of understanding the gaps of transient performance have been left out from the time axis, so that the curves are more compact and easier to read (total period of trials was 4h 45min).

In the bottom graph of Figure 5.19 the difference between the speed log and the calculated GPD speed is displayed. The large initial difference between GPD and speed log indicates the large drift in the speed log. Over a period of approximately 4 hours the sensor drift changes from about 2.0kn to 0.5kn due to unknown reasons. The speed log is located on port side close to the keel line and protrudes the hull by about 5cm. The

boundary layer is here approximately 7cm thick when sailing at 7kn (Harvald 1983) and has therefore little effect on the flow over the log. Moreover, using calibration, the effect of the reduced speed or irregular flows in the boundary layer can be taken into account. Unless the boundary layer changes rapidly over a period of hours, the sensor drift can therefore not be contributed to boundary layer effects.

Figure 5.19 shows another characteristic of the speed log. The GPD speed indicates the speed that the ship experiences, while the speed log indicates the water speed relative to the sensor. When a ship is affected by different current layers, the current that the speed log experiences not necessarily represents the mean current the hull experiences. However, the fact that there is no difference in the measured speed between up-and-downstream trial runs indicates that currents do not affect the speed log. Hence, it may be concluded that the errors of the speed log may be considered to come from the sensor itself, and not from its environment.

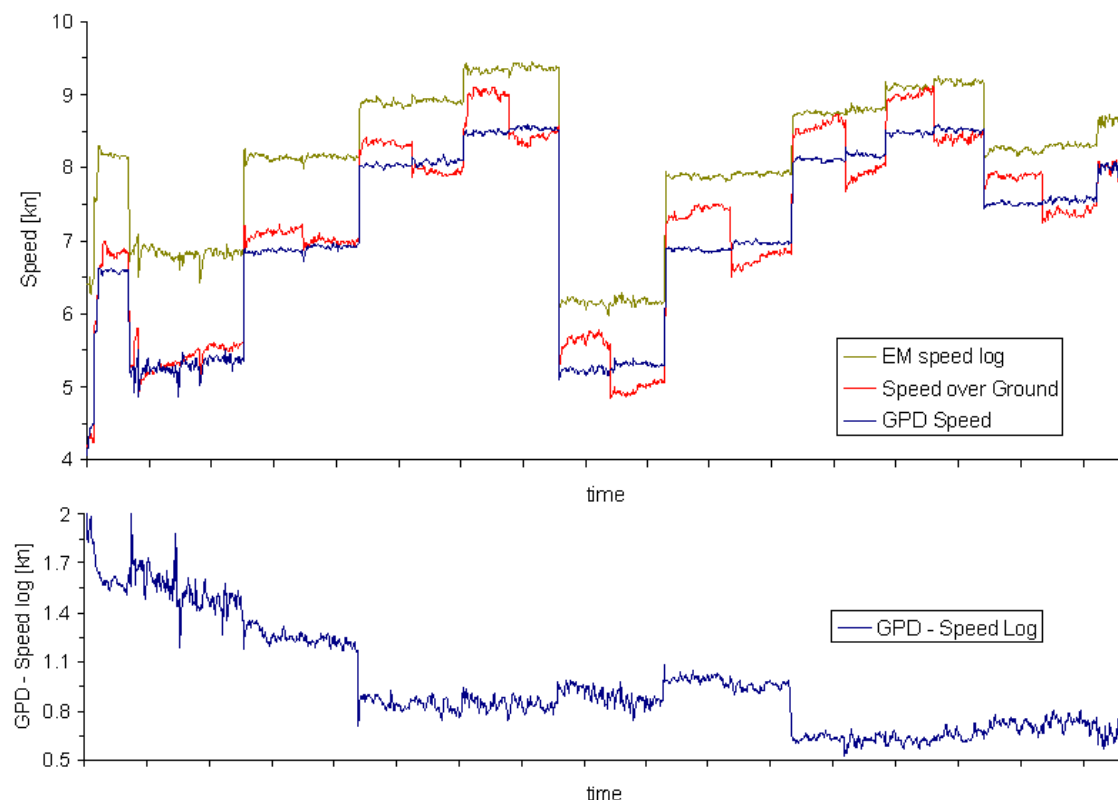


Figure 5.19: Conditioned dataset of ship speed during speed trials on Bernicia (conditioned for transient conditions) on the Bernicia. Bottom: Difference between the EM speed log and GPD speed, indicating the sensor drift from the EM speed log.

The sensor drift as indicated in the bottom graph in Figure 5.19 was experienced during most sea trials. The long, but variable time dependent sensor drift made calibration impossible. The GPD speed was therefore the only reliable speed indicator.

Wind speed measurements

By analysing speed trial results, uncertainties in wind speed measurements from wind distortion and instrumentation errors can be identified. Figure 5.20 shows the measured apparent and calculated true wind speed and direction for a set of 9 up-and-downstream speed runs (same as in Figure 5.19) in calm weather conditions (filtered for transient conditions). Using ship speed and course over ground from DGPS, the apparent wind speed is converted to true wind. The resulting calculated true wind speed and direction are expected to remain fairly constant throughout the day. However, the calculated true wind speed varies systematically with each speed run, indicating that the measured apparent wind speed is distorted or that the anemometer requires re-calibration.

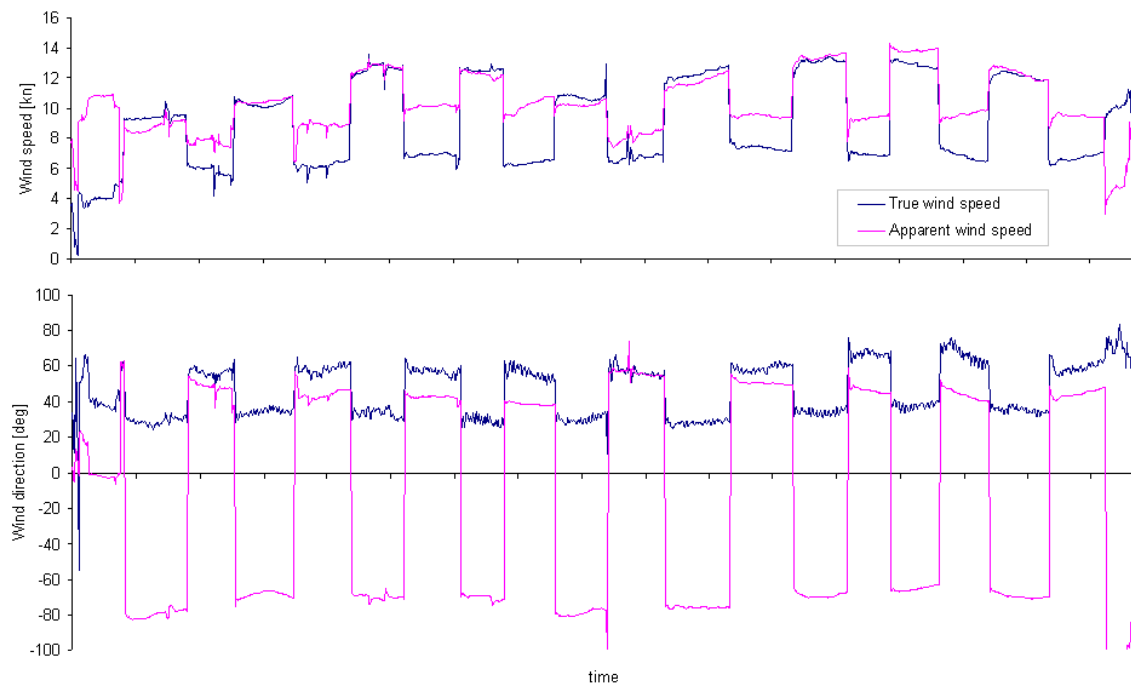


Figure 5.20: Apparent and true wind speed & direction during speed trials on the Bernicia.

The large errors in calculated true wind speed and direction are however also affected by the conversion from apparent to true wind, which is sensitive to measurement errors. Even small errors (e.g. due to wind distortion) result (at certain angles) in large errors in calculated true wind. For example, for a run with a course over ground of 141°, ship speed of 7kn and an apparent wind speed 10kn, a measurement error of 1.0kn results in an error in the calculated true wind direction of 5°.

The symptoms experienced on the trials on the *Bernicia* are frequently found on ships, and can be contributed to wind distortion. One way to account for errors from distortion is to convert the apparent wind speed to true, and calculate the mean speed and direction over the course of the day. These results can then be converted back into apparent wind and used in wind resistance calculations. For service performance analysis, up and downstream speed trials cannot be done and these conversions cannot be made. Errors are therefore inevitable. Based on Figure 5.20 and other analysed datasets, the uncertainty of the wind speed and direction measurements for the *Bernicia* has been estimated as $\pm 20\%$ (in Figure 5.20, the wind speed deviates 25% from a mean of 8kn, while wind direction deviates 20% around a mean of 50°). The location of anemometers on merchant ships should therefore be carefully selected to avoid distortion effects, e.g. using CFD analysis (see e.g. (Moat et al. 2005)).

5.2.5 Data conditioning

Data conditioning for performance monitoring consists of filtering for outliers, filtering for transient conditions and smoothing and averaging. The following section describes these individual parts of the PM&A system for the *Bernicia*.

5.2.5.1 Filtering for outliers

On the *Bernicia*, outliers are filtered using a median filter with a window of 30 seconds. This proved to provide sufficient filtering for outliers, without affecting the speed of response of the system.

5.2.5.2 Transients filter

For the *Bernicia*, which manoeuvres a large part of its time, the transients filter is one of the most important parts of the data conditioning. The designed transients filter for the *Bernicia* is based on the monitoring of the following parameters:

- Heading (*Dir*)
- Rudder angle
- Engine speed (*n*)
- Ship speed through water (*Vs*)
- Shaft torque (*Q*)
- Apparent wind speed & Direction

The small displacement and inertia of the *Bernicia* allowed steady state conditions after deceleration to be identified by STW and torque only. Because transients are easier to identify at high speeds than at low speeds, for speeds below 5 knots a 4x longer time frame is used for the definition regression curve. Using a longer time frame, natural fluctuations affect the regression analysis less and the gradient can be defined with higher accuracy. The limitation on the gradient can then be made stricter. The threshold values of the slope and gradients and time frames are determined by trial and error.

Figure 5.21 shows the developed user interface of the transients filter for the *Bernicia*. Four time series are displayed; heading (*Dir*), shaft speed (*n*), ship speed through water (*Vs*) and shaft torque (*Q*). The black curves show the data filtered for outliers using a median filter; the light blue curves the uncorrected, raw data. The data points used for the calculation of the regression (dark blue line) are indicated by red points. On the right hand side the real-time calculated regression coefficients and standard deviation are displayed, together with the set threshold values. Boolean indicators indicate whether the

values are within range or not. This way of presentation gives a clear, and easy to understand picture of one of the more important parts of a PM&A system.

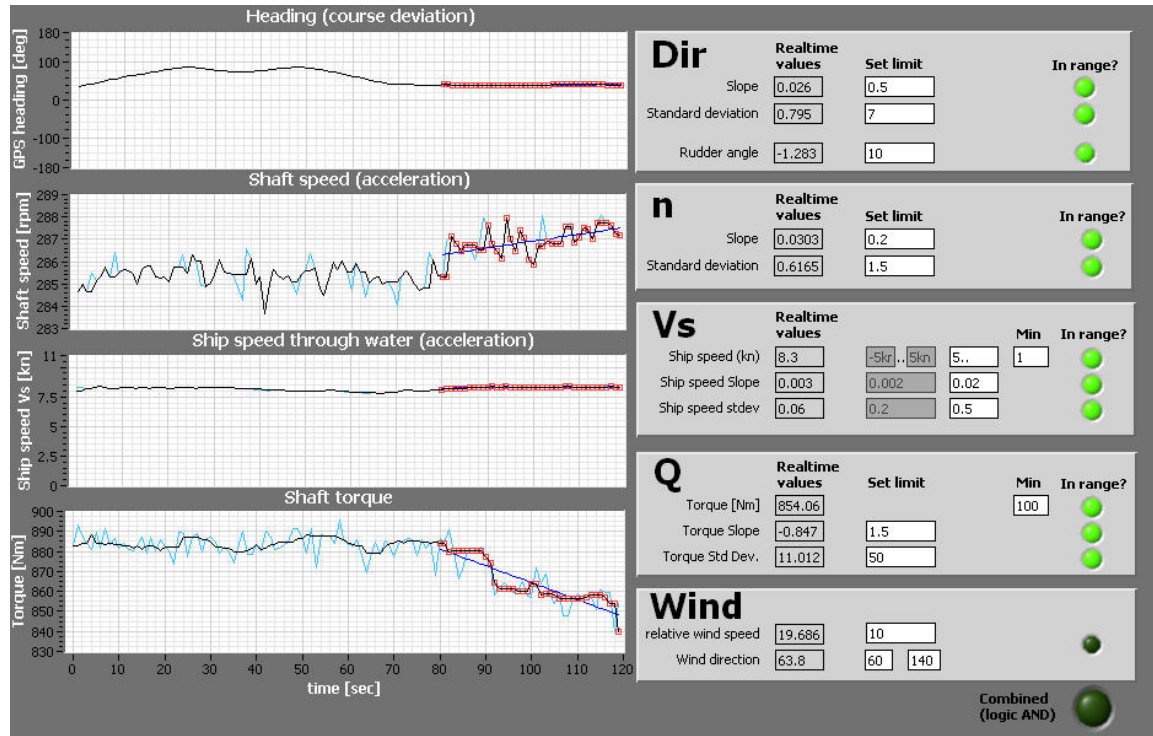


Figure 5.21: Transients filter user interface of PM&A system on Bernicia

5.2.5.3 Smoothing and averaging

After the filtering of the data for outliers and the transient conditions, the processed data is averaged using a running average to reduce random errors. The selection of time constants for smoothing depends on vessel characteristics, and the level of detail that should be captured. For the *Bernicia* the following constants have been selected based on trial and error:

- Torque and RPM: 30 seconds
- Speed through water: 30 seconds
- Speed over ground: 30 seconds
- Wind speed & direction: 30 seconds
- Water depth: 10 seconds
- Fuel consumption: 15 seconds
- Rudder angle: 5 seconds

The measured performance after the transients filter is practically reached to a steady state; only small accelerations remain due to the effects of wind, wave and shallow water. The time delay that results from using a running average is therefore not critical.

The slow deviations in torque and speed caused by environmental conditions and that pass the transients filter are important for the correction of the performance to standard conditions. The *Bernicia* responds rapidly to changes in environment and the averaging time frames have therefore been chosen relatively short. For larger ships, that respond slower to changes in environmental conditions, the periods may be increased to further reduce random errors.

5.2.5.4 Validation of open water diagram

Because technical problems with the EM speed log on the *Bernicia* made the speed log for performance analysis not suitable, the GPD speed was used instead. The accuracy of the open water diagram and wake fraction is hereby highly important. Because there was no original, test based propeller open water diagram or propeller offset data available for *Bernicia*, a propeller was designed based on the propeller geometry obtained by manual

drop-height measurements (Sampson 2004). The lifting surface computer program UPCA91 (Szantyr and Glover 1990) was then used to calculate the propeller open water diagram (Mutton 2003). The program is particularly sensitive to the blade geometry (pitch) at the tip regions. However, due to imprecise information in these regions, extrapolations had to be made for data in the regions $r/R = 0.95$ and $r/R = 0.975$. Furthermore, assumptions had to be made with regard to thickness distribution. Two different extrapolations of the propeller geometry were made by (Wang 2007). In Figure 5.22 both propeller characteristics are shown.

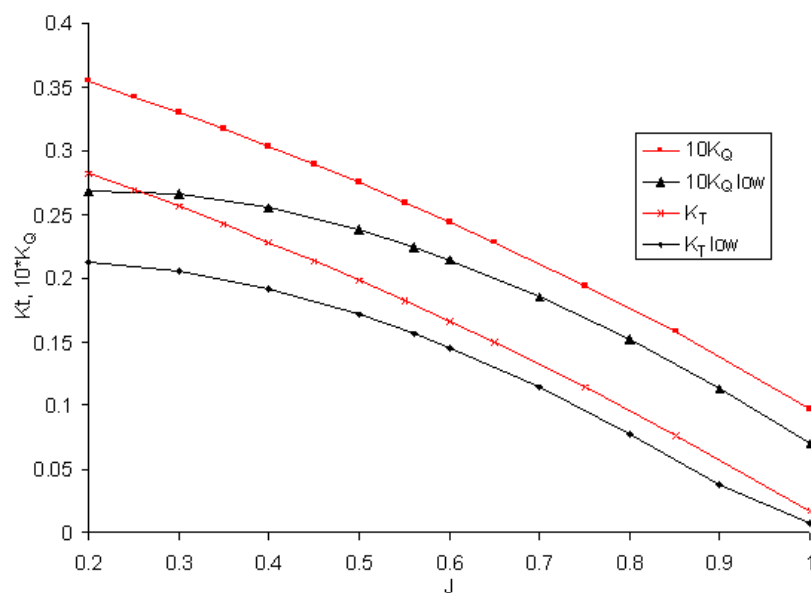


Figure 5.22: Propeller open water diagrams for Bernicia

With the propeller open water diagram in Figure 5.22 and an assumed wake fraction, the GPD speed can be calculated, using torque and RPM data from sea trials. For the *Bernicia*, a wake fraction between $w = 0.05 \dots 0.15$ is expected, based on the open shape of the stern section. Using dedicated speed trials, where the ship speed can be accurately determined from speed over ground measurements, the accuracy of the open water diagram and wake fraction has been assessed. Figure 5.23 shows the speed over ground and the GPD speed, calculated with the K_Q and K_{Q-low} curve in Figure 5.22, for a number of measured mile speed trials. Due to the short duration of each leg (6-10min), little wind and negligible wave height on the day of the trials, the ship STW during each trial can be determined from the measured SOG. When wind and wave resistance can assumed

negligible, the mean of the SOG during a consecutive up and downstream run represents the STW of each run, as the engine power during two runs does not change.

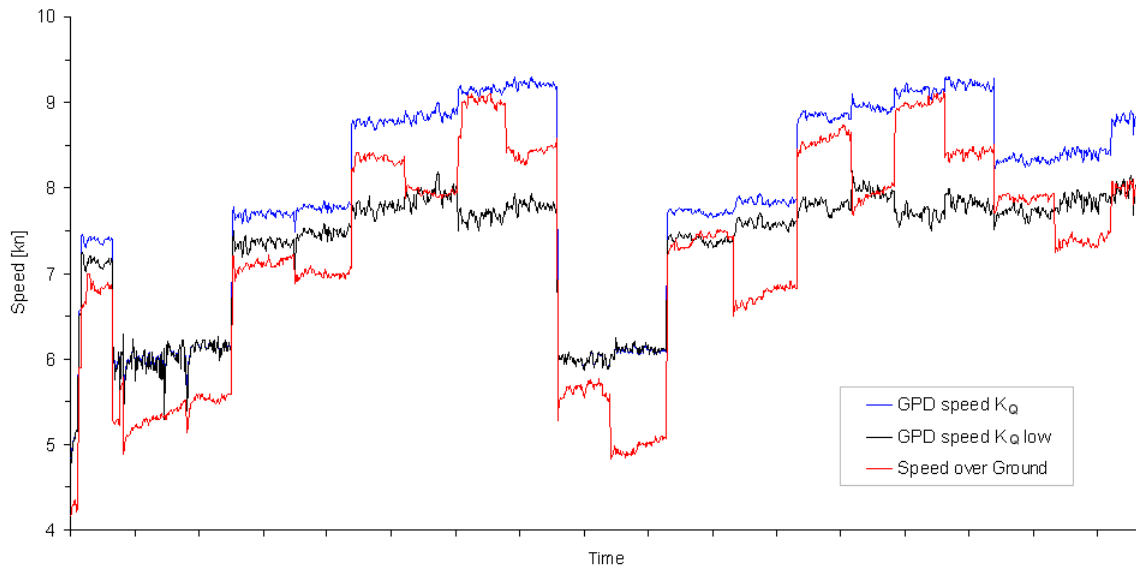


Figure 5.23: SOG and GPD speed calculated using different K_Q curves

The large differences between the K_Q and K_{Q-low} curves in Figure 5.22 result in different magnitudes of calculated GPD speed. To be able to minimize the differences between GPD and actual STW (calculated using SOG assuming negligible added wind and wave resistance), the wake fraction for GPD calculated with ' K_Q ', a wake fraction of $w = 0.0$ was used. For the calculation of the GPD speed with K_{Q-low} , a wake fraction of $w = 0.1$ was used.

From the figure, two aspects can be concluded. Firstly, even though an unrealistically low wake fraction of $w = 0.0$ is used, the GPD using the higher K_Q -curve still has a positive offset compared to the true ship speed. The wake fraction can not be reduced further to reduce the magnitude of the GPD speed, as a negative wake fraction of this type of vessel is unrealistic. The higher K_Q curve is therefore unrealistic. Secondly, the GPD speed calculated with the lower K_Q -curve does not follow the changes in speed accurately and is at certain speeds irregular. For example, where the SOG increases from 8 to 9 knots in Figure 5.23, the calculated GPD speed decreases instead of increases. It is therefore expected that the gradient of the K_Q -curve is too small.

The above aspects suggest that both K_Q curves are too inaccurate to be used. Instead, using the STW calculated from the SOG from the trials and the torque and rpm calculated from the mean of consecutive up and downstream speed runs, a new K_Q curve has been calculated. A wake fraction of $w = 0.1$ has hereby been assumed.

The data from speed trials in April and May 2007 has been used. The environmental conditions during these tests were calm; wind speed approx. 6-8kn, significant wave height: 30cm and (for the *Bernicia*) deep water (40m). Figure 5.24 shows the K_Q -curve based on measurements from the two speed trials.

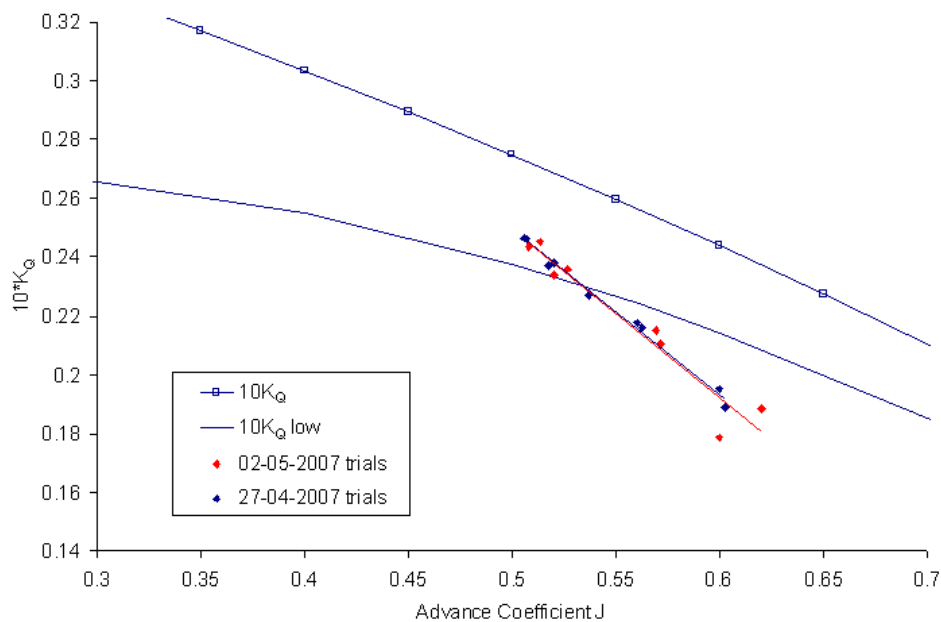


Figure 5.24: Measured torque coefficients of the Bernicia during calm water speed trials and predicted based lifting surface calculation methods

The close match of the data points between the two independent sea trials indicates an accurate data collection and gives confidence in the derived regression curve from the data points. The regression curve from the measured data can be considered a true representation of the propeller characteristics, and can be described by:

$$10K_Q = -0.5682 J + 0.5328 \tag{5.1}$$

Which is valid for the range $J = 0.50 \dots 0.63$ or $10K_Q = 0.17 \dots 0.25$

Kt curve

Because of the large inaccuracies of the K_Q curve, it is expected that the thrust coefficient is also incorrect. One way to validate the K_T -curve is to use the available calm water model test results for the *Bernicia* (Gursoy 2006). Figure 5.25 shows the resistance from a set of trials in calm weather, calculated using the K_T -low thrust coefficient from Figure 5.22 and the K_Q relationship of equation (5.1). A thrust deduction fraction of $t = 0.2$ has been assumed, based on published results from other tugboats and statistical regression methods (Holtrop 1984). The speed through water is calculated using the GPD speed calculated using eq (5.1).

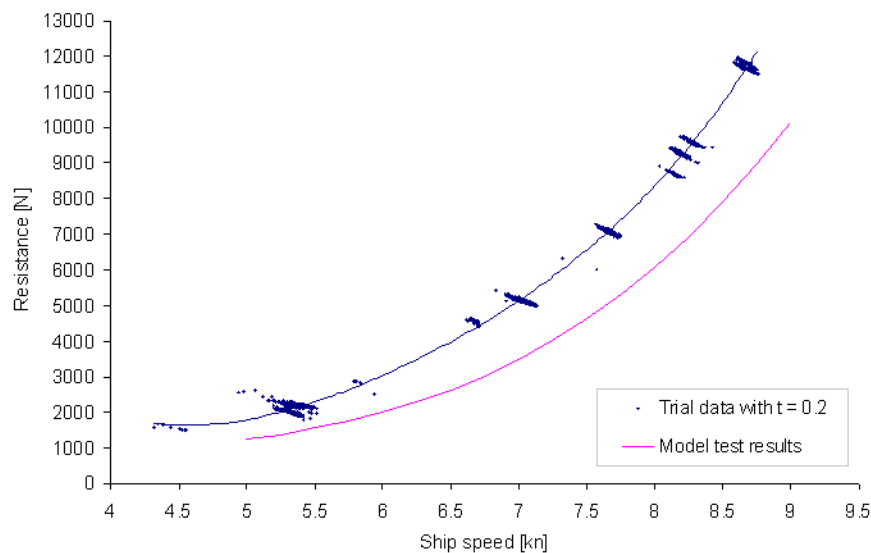


Figure 5.25: Resistance – speed curve from model tests and calculations based on the predicted open water diagram of the *Bernicia*

The difference between the measured resistance and model test results in Figure 5.25 can be explained by the following error sources:

- Errors in the estimation of the thrust deduction fraction: For the *Bernicia*, no self propulsion tests were available to determine the thrust deduction fraction. Reference had therefore to be made to empirical prediction models and data from other tugboats. If a thrust deduction is chosen so that both curves match, a thrust deduction of $t = 0.4$ results, which is for the type of vessel highly unlikely.

- Experimental errors from towing tests and scaling errors from model to full scale. However, the *Bernicia* has been repeatedly tested in the towing tank of Newcastle University by (Gursoy 2006) and (Gaganatsios 2007) with closely matching results. Scaling to full scale has been done using the ITTC recommended form factor and 3D extrapolation approach, is assumed correct
- Incorrect open water diagram

If the estimated thrust deduction fraction of $t = 0.2$ is assumed correct, the differences between the two curves in Figure 5.25 can be contributed to errors in the open water diagram.

To derive the propeller K_T -curve using model towing tests, the relationship $n - V_S$, measured during calm weather speed trials, has been related to the $R_T - V_S$ relationship from model tests. By using the averaged ship speed, shaft revolutions and torque between two consecutive runs (up and downstream, parallel to the wind direction) and the favourable environmental conditions, the added resistance from wind and waves can be considered to be averaged-out and negligible. The thrust coefficient at speed V_S can be calculated by:

$$K_T(V_S) = \frac{R_T(V_S)}{(1-t)\rho[n(V_S)]^2 D^4} \quad (5.2)$$

Where:

$R_T(V_S)$ = model resistance scaled to full scale at ship speed V_S

t = assumed thrust deduction fraction ($t = 0.2$)

$n(V_S)$ = propeller revolutions measured during speed trials in calm water conditions at ship speed V_S

Figure 5.26 shows the coordinates of the calculated (J, K_T) data points for two sets of sea trials in April and May 2007, together with the K_T -curves calculated using UPCA91.

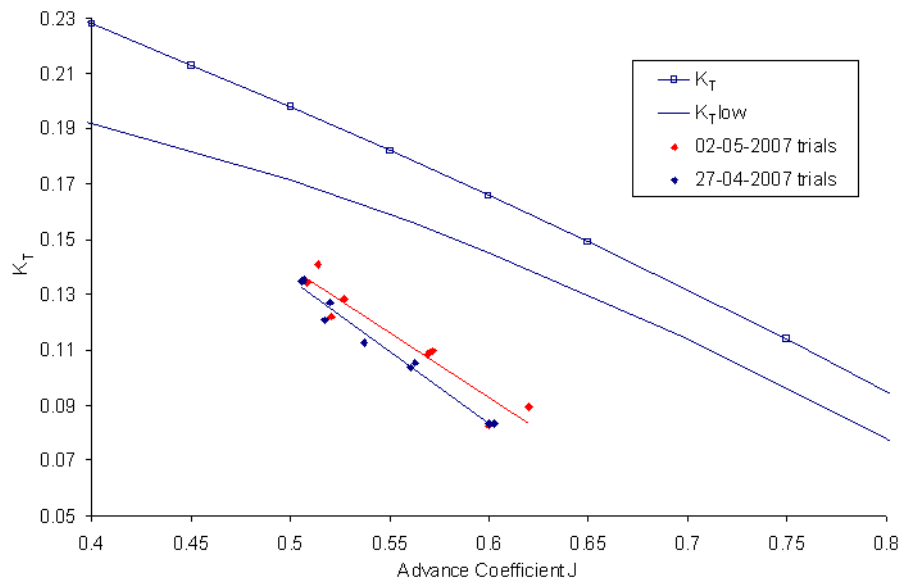


Figure 5.26: Measured and computer modelled K_T – curves for Bercia

The differences in thrust coefficient between the speed trials in April and May can be explained by small differences in wind speed and by differences in hull roughness; in May the wind speed was on average 3.0kn lower than in April and the hull (coated with a thick layer of slime) was just cleaned (pressure wash) in dry-dock, resulting in a slightly higher ship speed from a set engine speed.

The mean K_T -curve, calculated using both speed trials, can be approximated by a linear regression curve as following:

$$K_T = -0.4881J + 0.3806 \quad (5.3)$$

for the range $J = 0.51 \dots 0.62$ or $K_T = 0.08 \dots 0.15$

Using the calibrated open water diagram, the GPD speed can be calculated with high accuracy and the vessel's resistance can be determined more accurately.

5.2.6 Data analysis

With the calibrated propeller open water diagram and a precise estimation of ship speed, the ship performance data can be corrected to standard conditions. For the *Bernicia*, the main external loads on the hull are from the wind and waves. Existing added wave and wind calculation methods are however often developed for larger vessels, and not valid for small craft like the *Bernicia*. In the following sections, the used wind and added wave resistance calculation models and results of the correction to standard conditions are discussed bearing in mind this restriction

5.2.6.1 Wind resistance

As described in chapter 4.2.4, the wind resistance can be calculated by:

$$R_{wind} = 0.5\rho_{Air}C_x(\epsilon)A_FU^2 \quad (5.4)$$

The total estimated uncertainty can be defined as following (Coleman and Steele 1998):

$$\frac{U_R}{R} = \sqrt{\left(\frac{U_\rho}{\rho}\right)^2 + \left(\frac{U_{C_x}}{C_x}\right)^2 + \left(\frac{U_{A_F}}{A_F}\right)^2 + 2^2 \cdot \left(\frac{U_U}{U}\right)^2} \quad (5.5)$$

The 2^2 term for the uncertainty of the wind speed indicates that the uncertainty of the wind speed is the main contributor to the overall uncertainty of the calculated wind resistance. With an estimated uncertainty in wind speed of $\pm 20\%$ (see section 5.2.4), air density uncertainty of $U_\rho/\rho = 0.005$, wind resistance coefficient uncertainty of $U_{C_x}/C_x = 0.2$ and frontal windage area uncertainty $U_{A_F}/A_F = 0.02$, U_R/R becomes 45%. 89% of this is caused by the uncertainty in wind speed estimation alone.

Few methods have been published for wind resistance coefficients for small ships. The closest form for the above water profile in comparison with the *Bernicia* was the *Research Vessel RES0201BN*, found in (Blendermann 1996), as shown Figure 5.27.

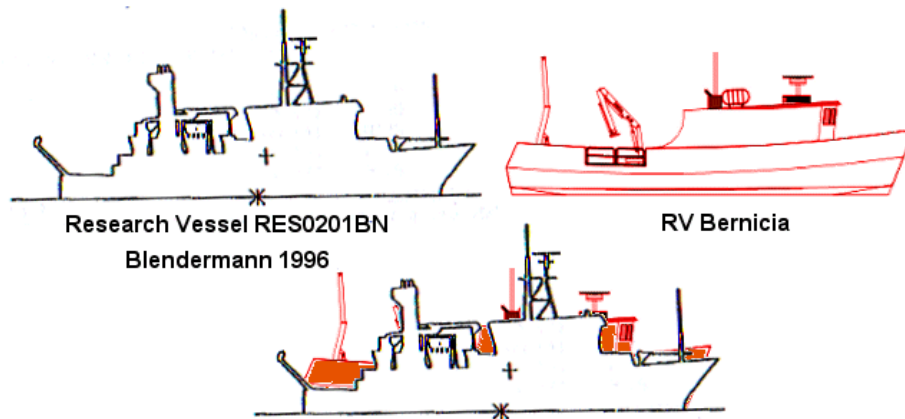


Figure 5.27: Above water profile of Bernicia and ship model RES0201BN

5.2.6.2 Added wave resistance

The added wave resistance coefficients have been calculated using *TRIBON Hydro* (AVEVA 2007). *Hydro* is a 6 degrees-of-freedom vessel motion prediction program using strip theory to calculate the coupled motion response of the vessel in deep water with arbitrary wave heading. Conformal mapping (standard Lewis form or Frank close fit) are used to calculate the sectional added mass and damping for the vessel. Strip theory is then used to calculate the global vessel added mass, damping and cross-coupling terms. For the calculation of the added wave resistance, *TRIBON* uses the Gerritsma and Beukelman (Gerritsma and Beukelman 1972) method, which only considers the vertical motions (heave and pitch). This method also includes the added resistance due to the effect of wave diffraction. In addition to the added wave resistance predictions, model tests have been done by (Gaganatsios 2007) for a number of wave encounter frequencies in order to validate the predictions. There was generally a good match between the results using strip theory and model tests, giving confidence in the results.

5.2.6.3 Correction to standard conditions

The correction to standard conditions is based on the described methodology in chapter 4.2. Because the speed log of the *Bernicia* can not be relied upon, the separation between long and short term performance analysis could not be evaluated. Instead, the analysis has been based on the short term analysis part; the GPD speed is used in combination with a constant wake fraction. The use of a constant wake fraction will result in a gradual underestimation of the ship speed over time due to hull fouling, as discussed in chapter 3.4.1.4.

The correction to standard conditions could be restricted to wind and wave only, as displacement, trim and water temperature remained practically constant over the duration of measurement. Moreover, the propeller of the *Bernicia* is coated, and it is therefore assumed that blade roughness remains constant. Figure 5.28 shows the $\Delta P_{D,corr}$ mode values for the tests on the *Bernicia* before and after dry-docking. Because of the limited amount of data logs available (12 days), for clarity purposes all tests have been included, regardless the large differences in quality of performance correction. The standard deviation of each KPI, indicating the width of the corrected histogram, is included. The smaller the standard deviation, the higher the precision and certainty is of the calculated performance indicator.

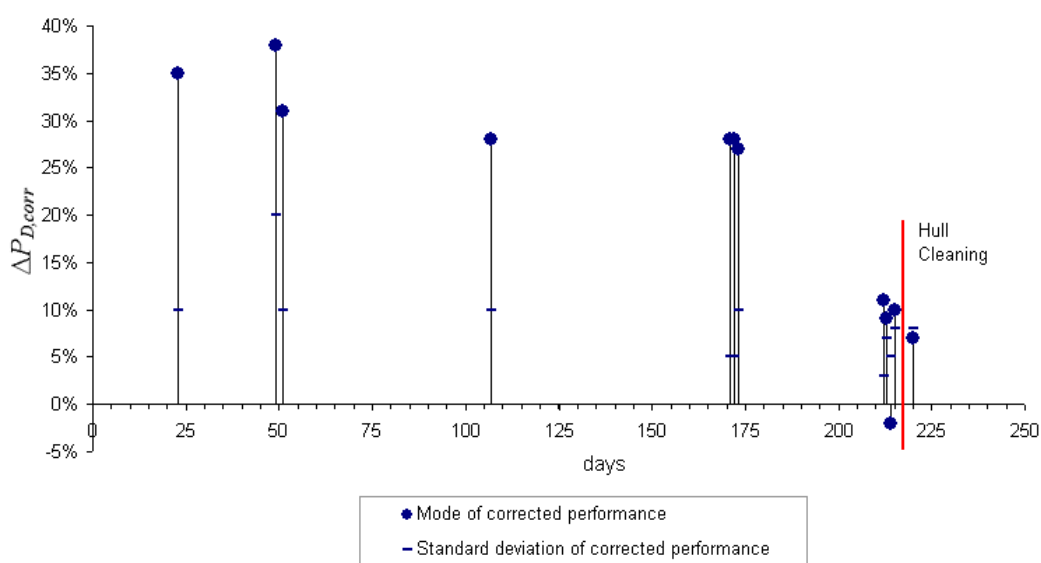


Figure 5.28: Corrected ship performance for 12 trials on the *Bernicia*

The large deviation in indicated performance after day 180 is most probably caused by errors in the torque measurement. Post-analysis showed that due to an error in the PM&A software, the automatic calibration routine of the torque sensor did not work satisfactory. Because of the use of GPD in the analysis system, the KPI $\Delta P_{D,corr}$ is highly sensitive to torque errors, which might be a cause of the performance deviation.

Regardless the drop in $\Delta P_{D,corr}$ due to sensor errors, it can be seen that the performance deviations remain within approximately $\pm 5\%$. Large deviations, such as on day 49 can be explained by external environmental conditions that could not be accounted for accurately, indicated by the high standard deviation. By setting limits on the standard deviation, as explained in Section 4.5, these outliers can be filtered accordingly.

The effect of hull cleaning is difficult to evaluate due to the few days measurements after drydocking. A small improvement in performance can be noticed (3%), but it can not reliably be said whether this deviation is the effect of hull cleaning or the result of errors in the correction for wind and wave etc. In the following section, the significance of the effect of drydocking is discussed in more detail.

5.2.6.4 Effect of hull cleaning

To assess the ability of the analysis method to identify the effects of hull cleaning from an 11-month service period, up-and-downstream speed trials over a length of 1 mile were done before and just after dry-docking on 27 April and 2 May 2007. During dry docking, it was found that no macro fouling in the form of weed or barnacles had developed and only a layer of slime with a thickness of approximately 0.5 – 2mm had developed, most apparent at the bow and side flanks (Figure 5.29 and Figure 5.30). Because the vessel is normally docked on port side, the fouling on starboard side was considerably more developed compared to port side, as this side receives more hours of light (Figure 5.30). The slime layer was not constant distributed over the hull, as the hull is coated with a large number of different coatings for research on foul-release coating purposes.



*Figure 5.29: Slime fouling on the Bernicia in April 2007.
The different coloured patches on the hull represent different anti-fouling
coatings that are being tested for research purposes*



Figure 5.30: Slime fouling on starboard side of Bernicia.

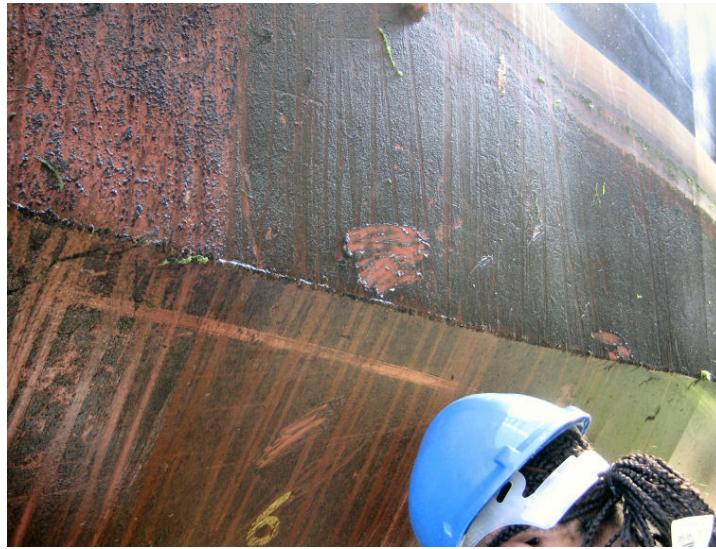


Figure 5.31: Slime on test patch no.6 starboard side developed over a period of 11 months

Four double runs were executed in the morning and repeated in the afternoon at different engine speeds. The trial conditions were done in very calm weather and sea conditions (true wind speed of approx. 9 and 6kn for before and after dry-docking respectively).

The performance for each double run was determined from the average of a consecutive up and downstream measured-mile run using the GPS speed and measured shaft power. Furthermore, the STW was determined using the GPD speed. For maximum accuracy, the performance was not corrected for wind and waves, as the weather conditions were calm and constant throughout the test period, and the trials were done parallel to the wind and wave direction, and can therefore be considered to average out. Figure 5.32 shows the uncorrected measured performance using the averaged speed over ground from two consecutive runs (left figure) and using GPD speed (right). The logarithm of the power is taken to indicate changes in performance more clearly.

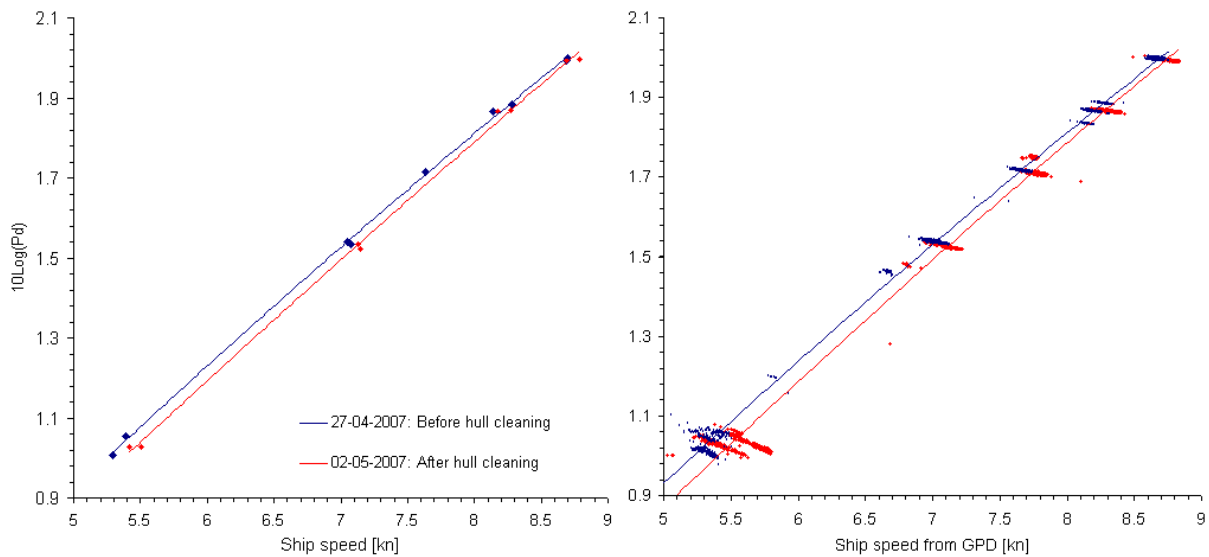


Figure 5.32: Speed trial results before and after hull cleaning calculated using SOG (left) and GPD (right)

The close correlation between the average power and speed between the trials in the morning and afternoon indicates a high accuracy executed trials. The difference in (uncorrected) power between before and after hull cleaning in the left plot of Figure 5.32 ranges from 9% at 6kn to 1.5% at 9kn.

Expressed in ship speed, the differences are much smaller and the significance of the difference is less clear. The difference expressed in ship speed is the range 0-0.15kn. This level of accuracy can only be obtained from dedicated speed trials and manual data analysis, so that the average speed between consecutive runs can be determined. For automatic, real time data analysis, the accuracy is more difficult to obtain since, for the *Bernicia*, the GPD speed must be used.

The right plot of Figure 5.32 shows the difference between the speed trials from automatic data analysis using the GPD speed, whereby the wake fraction between the two runs is assumed equal. The difference between the two curves ranges 11% at 6kn and 1% at 9kn. The slightly larger difference may be contributed to the use of the constant wake fraction. In reality, the wake fraction in clean hull condition is slightly lower, and the GPD speed is therefore slightly over estimated.

Correction to standard conditions results in significant changes in indicated performance. While the difference before correction is average 6%, after correction the difference is on

average 9%. The difference can be contributed to the high sensitivity of the correction methodology to wake fraction and the errors in wind resistance prediction.

The aim of the trials is to indicate the ability of the performance monitoring system to automatically detect changes in performance. It may be concluded that with the use of the GPD speed, even small changes in ship performance, e.g. due to fouling, can be identified. However, the GPD speed relies on the accurate definition of wake fraction, which in turn is affected by hull fouling. If the wake fraction is not corrected for fouling, the calculated GPD speed before hull cleaning will be underestimated, which results in an overestimation of the effects of fouling on ship performance. Vice versa, if the wake fraction is not corrected after hull cleaning, the GPD speed after cleaning will be overestimated, which results in an overestimation of the difference in performance before and after hull cleaning. In order to avoid confusion, a Doppler speed log, which is unaffected by hull fouling, should be used for long-term performance monitoring and the identification of fouling.

5.2.6.5 Identification of external loads

In order to demonstrate the ability of the correction methodology to identify external resistance sources (e.g. fouling), a number of trials were done on the *Bernicia* while dragging different loads through the water. The following loads were towed on a 15m line behind the vessel:

- Two car tyres bundled together
- A small sea anchor

Figure 5.33 shows the power-speed relationship for the trials, corrected to standard conditions. A reference performance curve is included to illustrate the quality of the corrections to standard condition. At constant engine speed, the tires correspond to a torque increase of approx. 7-20% (depending on towing speed), while the sea anchor corresponds to a torque increase of approximately 10-20%. At constant ship speed however, the difference between reference curve and measured power is much larger: between 30-60% for the tires and between 90-120% for the two towing conditions for the sea anchor

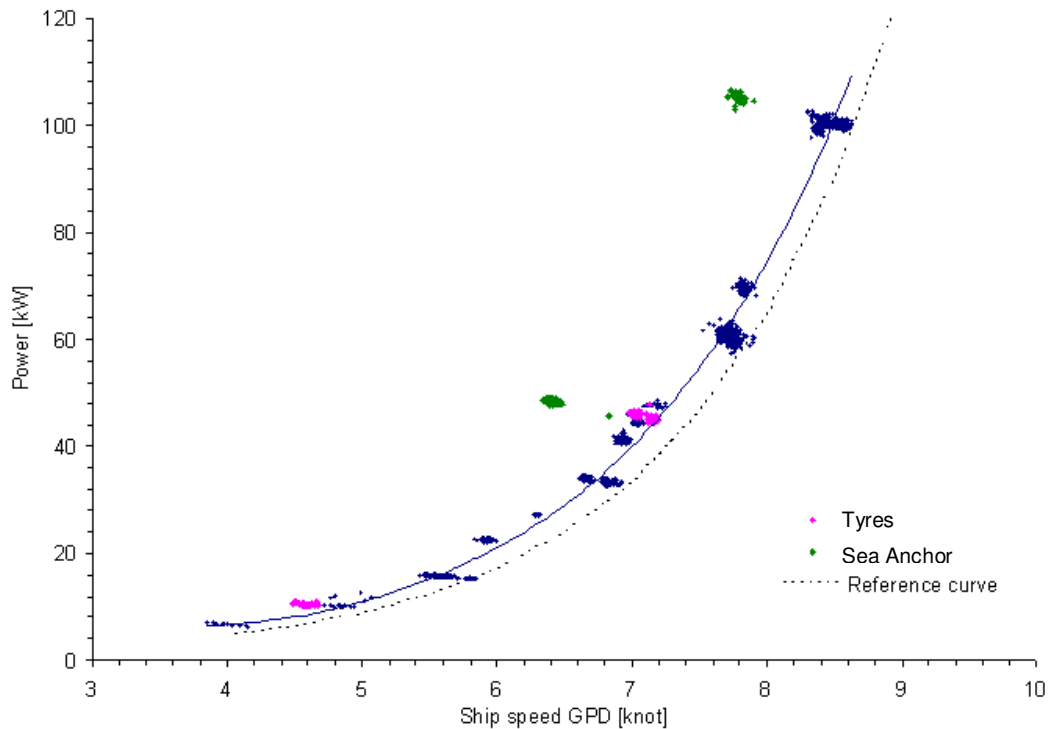


Figure 5.33: $GPD-P_D$ relationship during trials while dragging loads

Figure 5.34 shows the performance expressed in ΔP_D and $\Delta P_{D,corr}$ to a basis of time. The ship speed is calculated using GPD. Despite some small deviations, the corrected performance curve shows a constant power loss, indicating the corrections to standard condition are done with high quality. Three periods of significant power losses, which have not been corrected to standard conditions, can be noticed. They represent the added resistance from the tyres and sea anchor. The corrections for added resistance only account for wind, wave, shallow water, viscosity and displacement. They are not able to correct for the resistance from the tires and sea anchor, and these periods show therefore clearly in the $\Delta P_{D,corr}$ plot. The same principle is used for the identification of hull fouling. Because no corrections are applied for fouling, over time the mean deviation $\Delta P_{D,corr}$ from the reference curve will increase.

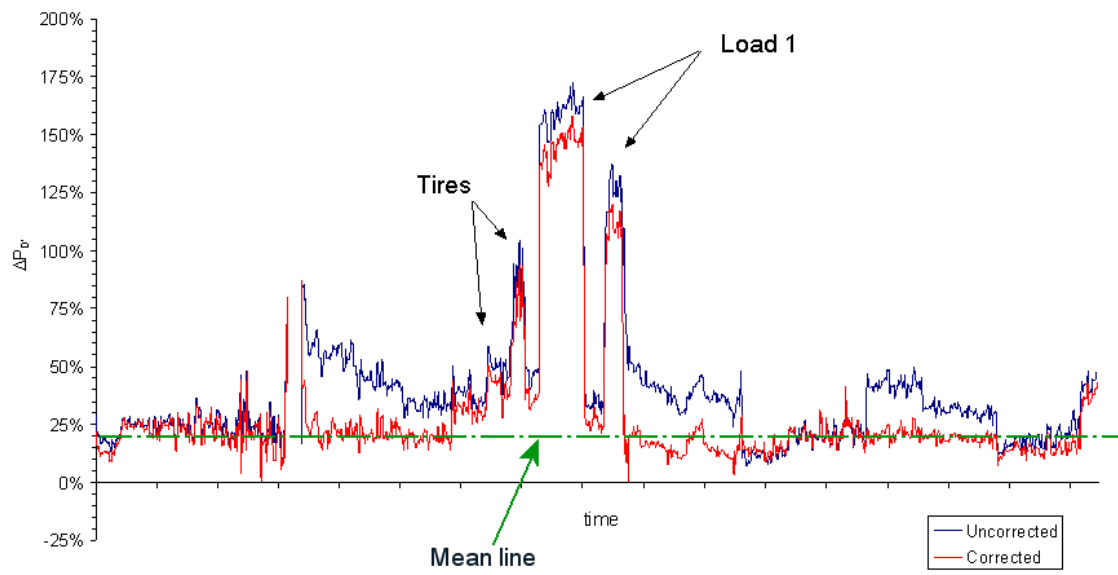


Figure 5.34: ΔP_D and $\Delta P_{D,corr}$ for trials while dragging loads
Indicating ability of correction methodology to identify external sources of resistance

5.2.7 Concluding remarks of PM&A on *Bernicia*

The *Bernicia* has been used as a test bed for the development of a ship performance monitoring and analysis system. The vessel has been equipped with a range of sensors and a dedicated data acquisition system, allowing signals from different instruments to be logged simultaneously. Because the installation of the instrumentation and the development of the data acquisition system have been done by the Author himself, conclusions could be made regarding the accuracy and reliability of the logged and analysed data:

- After installation and testing of all relevant systems, it was found that the EM speed log, regardless re-calibration, could not be relied upon. Instead, the ship performance was analysed using the GPD speed
- During dedicated sea trials, it could be shown that the available open water diagram of the propeller of the *Bernicia* was not accurate. Using towing tank tests and up-and downstream speed trials, the propeller characteristics could however successfully be derived. Using these characteristics, it was proven that the GPD speed can successfully be used to indicate STW accurately when the vessel is not in transient conditions or experiences drift
- Due the propeller characteristics and the use of GPD for performance analysis, the algorithm to correct service performance to standard conditions is highly sensitive to errors in the measurement of torque. Yet, using ship performance data logged during 12 trials along the Northumberland coast (UK), the proposed PM&A system and novel user interface could be evaluated successfully
- Due to the operational profile of the *Bernicia*, ship performance was calculated based on the average corrected performance for each day, filtered for transient conditions rather than using the proposed speed log filter. The quality of the correction was evaluated using the standard deviation of the corrected dataset
- It was shown that ship performance could be determined with a scatter in KPIs of only 8%, which includes errors due to wind speed distortion at the position of the anemometer, uncertainties in the calculation of the added wave resistance and uncertainties in the estimation of wave characteristics.

- Using dedicated trials, it was successfully proven that the system is able to identify fouling. The transparent user interface gives the user confidence in the collection and interpretation of data. More performance data is required to separate the scatter in KPIs from changes in performance due to hull fouling.

5.3 PM&A system implementation onboard MT Overseas Tanabe

The small size and the readily availability of the *Bernicia* have allowed the Author to conduct some fundamental investigation into ship behaviour related to ship performance and allowed in a short time a large number of tests to be done for the development of a PM&A system. However, because of the characteristics of the vessel, crew and environment, this investigation gave relatively little insight into the performance behaviour and monitoring requirements for large merchant ships sailing for prolonged periods of time at constant speed, in open seas and with a frequent changing crew. To investigate the latter aspects, a 300.000dwt VLCC, owned by OSG Ship management (UK) Ltd., has been equipped with a dedicated data collection system. This section describes the vessel characteristics, the installation of the performance monitoring system onboard, the PM&A system and results from performance analysis are discussed.

5.3.1 Vessel characteristics

The *MT Overseas Tanabe* is a 300.000dwt crude oil tanker operating worldwide. It operates with a mixed European and Asian crew, who normally sail onboard for a period of 4 months. The vessel has short turn-around times, with loading times often less than 48 hours. The main characteristics and general arrangement are shown in Table 5.2 and Figure 5.35 respectively.

Table 5.2: Main particulars MT Overseas Tanabe

Length over all L _{OA}	333m
Length L _{PP}	320m
Beam	60m
Depth	29.55m
Normal service draft	18.96m
Gross tonnage	298,561dwt
Service speed	16.6kn
Engine:	MAN B&W 7S80 MC
Continuous service:	23,259kW @ 76.3RPM

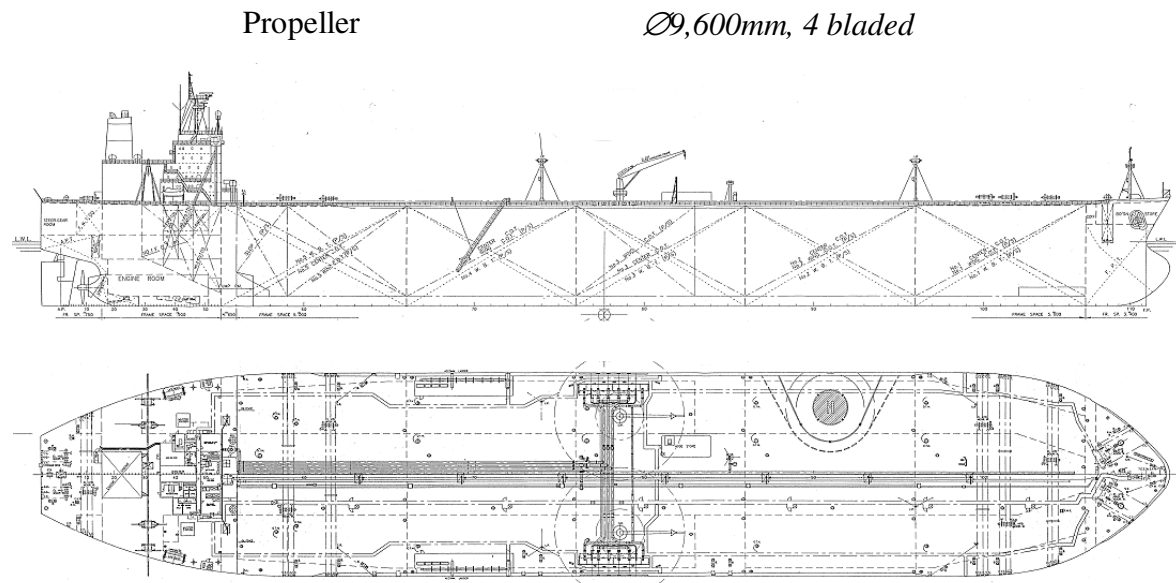


Figure 5.35: General arrangement MT Overseas Tanabe

The normal operating condition of its engine is ‘full navigational ahead’ at 76 RPM, where the engine is speed controlled by the governor. When the ship is operated at ‘economical speed’, the engine speed is reduced to 62 RPM. The vessel sails predominantly at two distinct loading conditions: ballast (mean draft 10m, trim 2-3m by stern) and laden (mean draft 17-19m, trim 0.5m). The trim in ballast conditions is used to avoid propeller racing and to increase controllability.

5.3.2 Installation of sensors & data acquisition system

After an assessment of the characteristics of the available sensors and instruments onboard in November 2006, the requirements for a performance monitoring system were determined. Most instrumentation required for performance monitoring was available onboard. However, not all sensors could be readily interconnected to the data acquisition system. The following list describes characteristics of the sensors:

- DGPS receiver (*JRC JLR 7700MK-II*): providing the true course over ground, speed over ground, time, date and position. NMEA0183 output through a new installed NMEA multiplexer

- Dual axis Doppler log (*Atlas DOLOG23*): providing speed through the water in longitudinal and transverse direction and bottom track speed. NMEA0183 output through a new installed NMEA multiplexer
- Power and rpm: A new *MetaPower* power measurement system was installed by *Metasystems AS*. The torque sensor is based on angular deflection measurement. Binary output using RS485 interface
- Anemometer (*NIPPON Electric Instrument*): relative wind speed and direction. NMEA0183 output through new installed signal converter (analogue to serial)
- Echo sounder (*JRC*): Water depth under keel. Due to technical difficulties in splitting the NMEA0183 outputs, and the fact that the echo sounder is only turned on by the crew in areas where it is necessary for safety in navigation (generally in water depths lower than 50m), the echo sounder was not connected to the performance monitoring system. Instead, a filter has been designed based on the recorded position and a database of known shallow water areas
- Fuel flow meter (*NITTO Seiko co*): fuel consumption. Digital TTL output giving one pulse (+12V) per 100 litre. By measuring the time between two consecutive pulses, the flow rate in liter/hour can be obtained
- Draft gauges (*NAKAKITA SEISAKUSHO CO*): *The ship is equipped with four pneumatically operated draft gauges. Because of the lack of electric output from the gauges and the costs involved in altering the system to obtain electrical outputs, it was decided to log the ship's draft manually through a user-friendly graphical user interface. The draft gauges are located in the cargo control room, and can therefore not be read directly by the officer on the bridge. Radio communication is therefore required to obtain the values*
- Rudder indicator: The rudder indicator has no output suitable for data acquisition. Because of the practical difficulties to install an additional indicator, and because the rudder indicator is not a critical part of the performance monitoring system, rudder angle is not logged.
- No wave radar was available onboard. Sea conditions had therefore to be logged manually.

Figure 5.36 to Figure 5.41 shows the sensors and indicators that have been interconnected to the data acquisition system.



Figure 5.36: (D)GPS receiver of Overseas Tanabe



Figure 5.37: Dual axis Doppler log indicator of Overseas Tanabe



Figure 5.38: Torque & RPM sensor on propeller shaft of Overseas Tanabe



Figure 5.39: Anemometer of Overseas Tanabe



Figure 5.40: Gear fuel flow sensor of Overseas Tanabe



Figure 5.41: Pneumatically operated draft indicators of Overseas Tanabe

The installation of the data acquisition system, cables and interconnection of all sensors was performed by the Author following ABS rules regarding the installation of electrical cables and instrumentation. The installation consisted of the installation of numerous NMEA splitters and signal converters, pulling cables from engine control room to the bridge, cabling from the anemometer, DGPS receiver and Doppler log on the bridge to the data acquisition system and the interconnection, design and installation of a dedicated data acquisition system on the bridge.

Central data acquisition system

For the connection to the different data interfaces from the sensors on the *Tanabe*, a dedicated modular data acquisition system was developed and installed by the Author on the bridge of the *Overseas Tanabe* in March 2007. The interface system consists of an NMEA multiplexer, an analogue input DAQ card, an RS485-USB converter, a USB hub and a power supply, installed in a waterproof casing. A computer program written in LabVIEW 7.1 (NI 2004) has been used to interface the different components and signal types into a single data format. Pictures showing the data acquisition system installed on the bridge of the *Overseas Tanabe* can be found in Appendix C. A manual of the software and the installed data acquisition interface on the *Overseas Tanabe* can be found in (Hasselaar 2007).

The collected data is stored and analysed on a commercial ruggedized laptop, protected against misuse by officers for activities unrelated to performance monitoring. The laptop has a DVD writer so that performance logs can be written on a DVD and send ashore for system development and back-up purposes. The PM&A system is installed on a easy to reach place on the bridge, so that the officers on watch can utilise the system for ship operation and get direct feedback on ship performance. In Appendix C, a picture is shown of the performance monitoring laptop installed on the bridge of the *Overseas Tanabe*.

5.3.3 PM&A software and User Interface

The performance monitoring system design is based on the same principles as the system on the *Bernicia*, and designed in close collaboration with the officers onboard. The initial aim of the installed PM&A system was to collect data in a transparent and unambiguous way to evaluate and test the developed analysis algorithm. The second stage of the implementation would consist of the inclusion of the analysis methodology and a user interface for long-term performance monitoring. Although the analysis methodology has been developed and tested for research purposes, the development and implementation of a suitable error-proof user interface could not be finished within the available time of the project. In this section, the user interface of data acquisition system installed (and running) is discussed.

Figure 5.42 shows the main interface of the PM&A system. The main parameters for performance monitoring are shown as 300sec running averages on the left hand side. Running averages are on a large vessel more reliable than real-time values with large fluctuations. In the middle graph, a 2-hour time series is shown from the speed through water, specific fuel consumption and wind speed. This can be used as real-time performance indicator, giving real-time feedback to manoeuvres and acceleration. On the right hand side, buttons are visible where the user (officer on watch) can enter wave characteristics, draft, fuel, voyage name and synchronize the computer time with the ship's time. Visual and audible alarms are given when the user is required to enter data. No alarms are given when the ship is sailing slow speed (<65rpm) or is manoeuvring, to avoid distraction from alarms during manoeuvring.

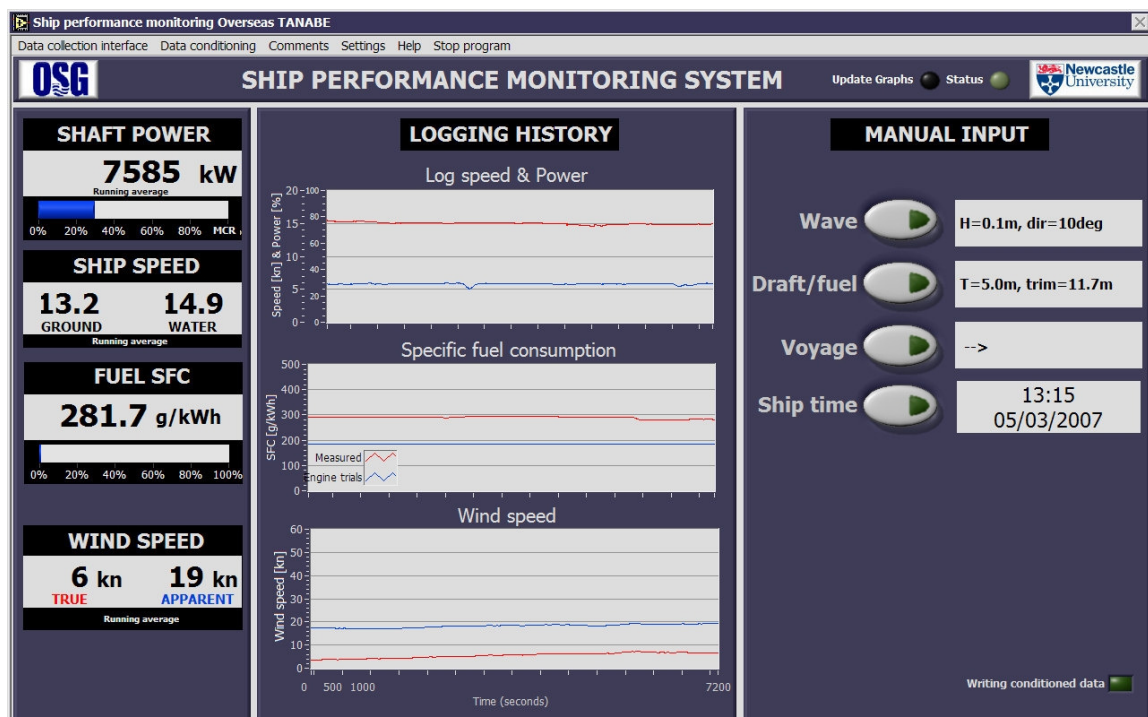


Figure 5.42: Main user interface of the PM&A system on the Overseas Tanabe

The menu structure is based on the same architecture as the system on the *Bernicia*. An example of an interface of each menu is shown in the following figures and in Appendix C. Furthermore, a manual and description of the system can be found in (Hasselaar

2007). Figure 5.43 shows the interface of the serial data received from the system. The NMEA strings are shown real-time and are split in the appropriate parameters. Photographs from the sensors shows from which sensor the data originates. In the bottom of the page, the raw data from the torque sensor is shown and displayed in a similar fashion. Using a help button, additional information about the interface and the displayed parameters can be obtained.

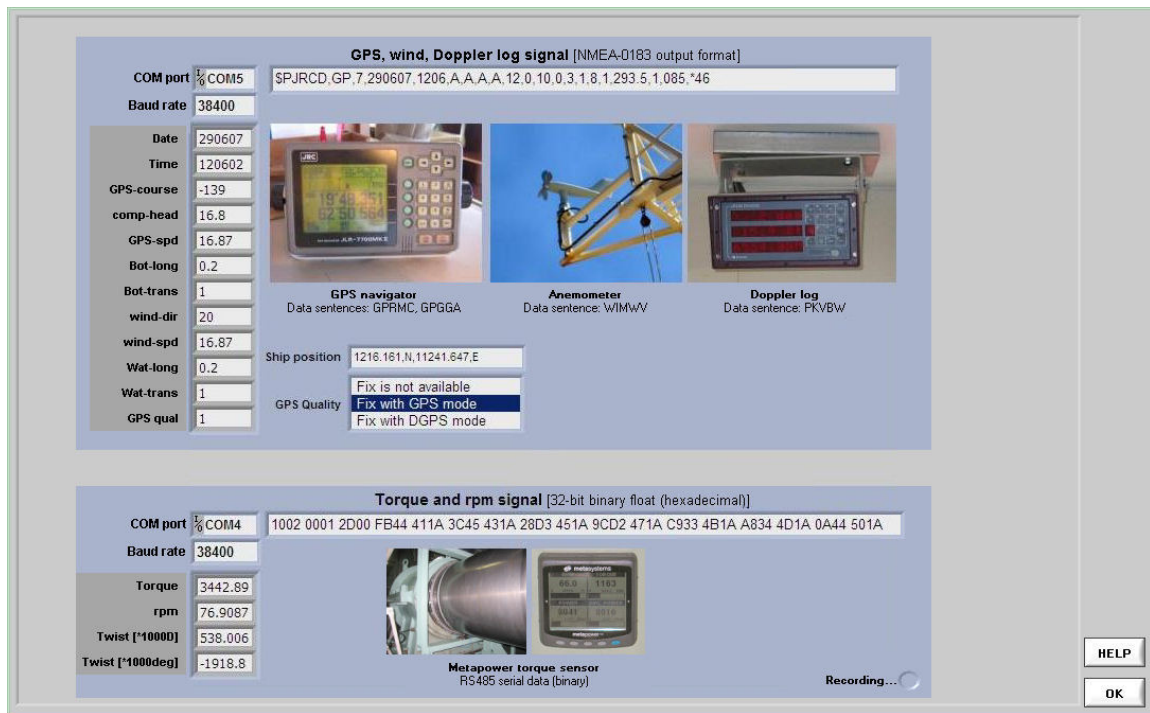


Figure 5.43: 'Serial data collection' interface

Figure 5.44 shows an example of a data conditioning interface. In a time series, the raw and averaged torque is shown. Each step in the conditioning is described and can be followed real-time. Using 'Help', additional information can be obtained.

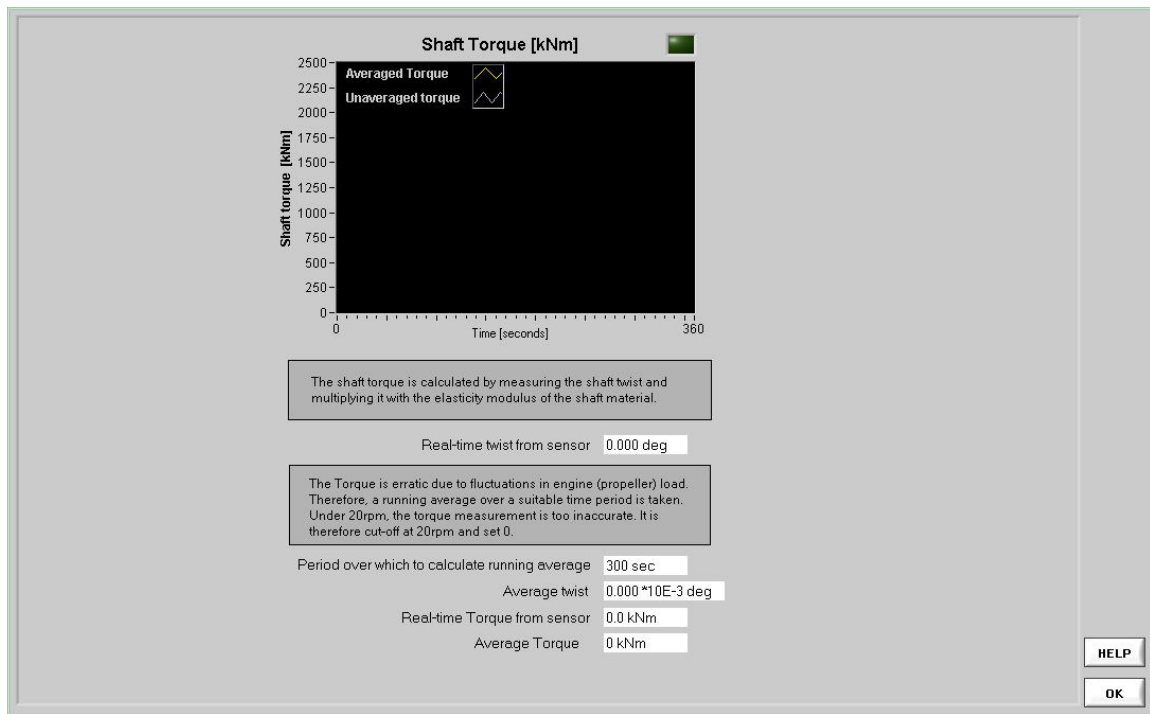


Figure 5.44: 'Torque data conditioning' interface

Manual input interfaces; Wave parameters

Figure 5.45 shows the input interface for wave conditions. For the calculation of the added wave resistance, a large number of parameters are required. However, because of the large height of the observer above the water surface, and the large size of the vessel, it is very difficult to define wave characteristics in detail. Marine officers are also not trained to determine wave characteristics with the accuracy and detail required for performance monitoring. To avoid confusion and unreliable estimations, a simplified wave observation system has been used. In coordination with the officers on watch, it was found that the level of detail in the input screen Figure 5.45 represents the information that can be observed with reasonable accuracy.

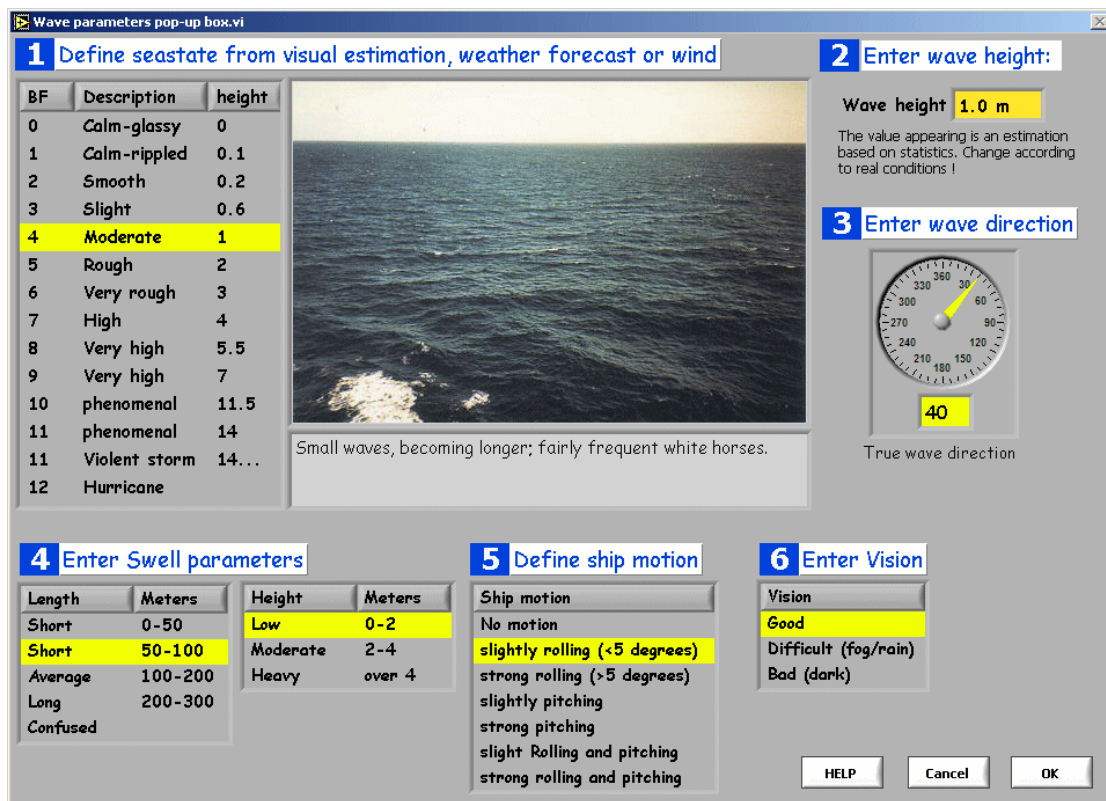


Figure 5.45: Manual input of wave parameters user interface

By clicking on any of the BF numbers on the left screen, a description and photograph (taken from (Bowditch 2002)) of the selected sea state are displayed. Using this easy to use look-up table, a more objective assessment of the sea state can be made than if the sea state is based on experience alone. Based on an ITTC Pierson Moskowitz sea spectrum, an estimation of the wave height is made. With information from weather forecasts and visual observations, the wave height can be defined more accurately in field no.2. Swell is described by means of the Douglas swell scale for length and height.

Fields 5 and 6 are included for validation purposes. For super tankers, ship motion is often negligible. If ship motion is clearly noticeable, it is likely that sea conditions are severe. The accuracy of added wave resistance calculations is then reduced. The field ‘Vision’ is added to validate the accuracy of the visual observations. In difficult or bad vision, the sea state observations should be discarded. To remind the operator to enter the wave characteristics, a visual and audible alarm is given ever four hours during daylight (between 06.30am and 18.30h ship’s local time).

Draft

Every start of a voyage the user is asked to enter the draft. The draft can be obtained from the loading computer or draft gauges. Furthermore, the draft readings at departure of each voyage are written down on a notice board on the bridge. Confusion which draft to use is therefore likely. The input interface is therefore designed to be as intuitive as possible. Figure 5.46 shows the actual draft gauges in the cargo control room, while Figure 5.47 shows the draft input data screen. Due to the familiar user interface and unambiguous data request, confusion is avoided.



Figure 5.46: Draft gauges on the Overseas Tanabe

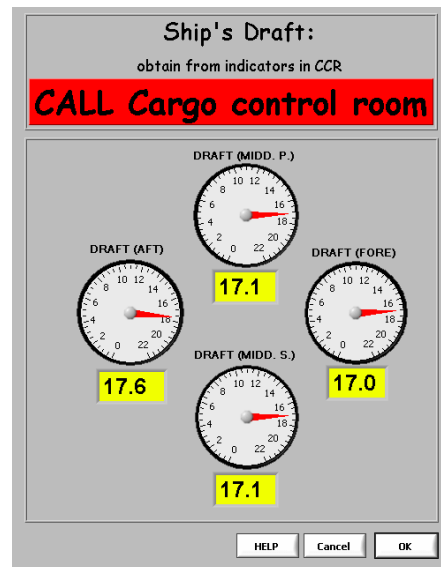


Figure 5.47: 'Ship's Draft' user interface

During the initial installation of the system, focus was put on accurate data collection so that the development of the analysis system could be made on shore. The interface for data conditioning and analysis and the visualisation of semi-real time and long-term performance indicators is therefore not included. A full description of the software is given in (Hasselaar 2007).

5.3.4 Data collection

The *Overseas Tanabe* operates world-wide. In order to design and evaluate the PM&A system in Newcastle, UK, data was written every month on DVD and send to the Author by mail. Data was received from March 2007 until July 2008. The data files are written in standard ASCII format and can be easily interpreted and opened using any spreadsheet program (see Appendix C.1: for details). The data is written with a frequency of 1Hz. A large part of the data could not be used for performance analysis due to problems with the anemometer and power sensor. The errors of the anemometer could be solved by a visit in May 2007 by the Author. The errors in the torque and RPM sensor were more difficult to identify and repair was not in the Author's hand. The problem solving by the manufacturer (more than 9 repairs were made) lasted longer than expected (>8 months). The torque and rpm sensor is the most important sensor for performance monitoring. IN order to still use the valuable data, other means to estimate torque had to be used. Because torque sensors are by nature sensitive instruments, the experience in error finding and calibration obtained on the *Overseas Tanabe* is described here.

5.3.4.1 Torque & RPM sensor

Because the *Overseas Tanabe* was not equipped with a continuous power measurement system, a new shaft torque measurement system was installed in February 2007. The selected torque sensor is based on angular deflection measurement using code wheels on the propeller shaft. Forks with optical sensors measure real time the relative deflection of the shaft (Figure 5.48). Torque measurement by means of angular deflection is technically more robust and reliable than conventional strain gauges, as there is no adhesive used (which ages over time, causing creep) and temperature fluctuations have no influence on the measurements. It has therefore in theory a higher long-term stability.

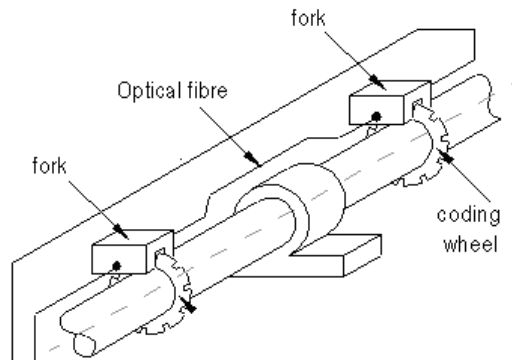


Figure 5.48: Torque measurement by means of angular deflection measurement

Requirement is that the forks are mounted on a rigid common frame; a small transverse movement of the two forks relative to each other (in the order of fractions of a millimetre) causes significant calibration errors. Figure 5.49 shows one of the coding wheels and fork with the optical sensors installed on the *Overseas Tanabe*.

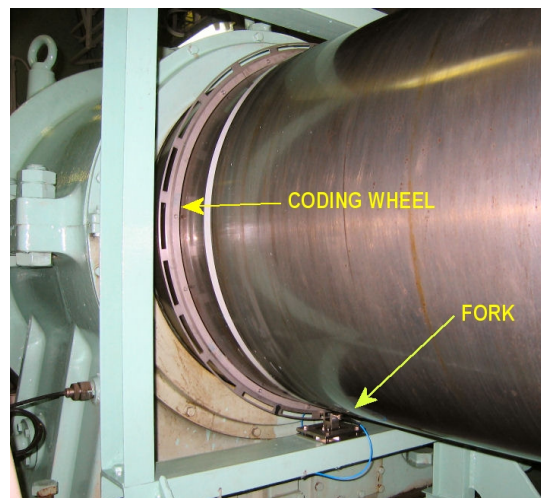


Figure 5.49: Torque sensor on the *Overseas Tanabe* showing one of the two coding wheels and fork with optical sensors.

The calibration of the system follows by rotating the propeller shaft using the main engine's turning gear five revolutions clockwise and five revolutions anti-clockwise. The five revolutions for calibration are required to build up a lubrication layer in the glands and bearings to reduce friction. By taking the mean of the clockwise and anti-clockwise

torque offsets, the torque loss due to friction in the bearings and glands is taken into account. Differences of up to 10% of the nominal torque have been found during calibration of the torque sensor on the *Overseas Tanabe*, indicating that calibration is of high importance.

5.3.4.2 Sensor errors

In March 2007, during a period of one month, measurements between an electronic Mean Indicated Pressure measurement system and the installed torque sensor indicated differences up to 35%. After inspection, one of the coding wheels of the torque sensor appeared to have become loose from the shaft, causing damage to one of the forks and optical sensors. Figure 5.50 shows the damage to one of the forks and the optical sensor.

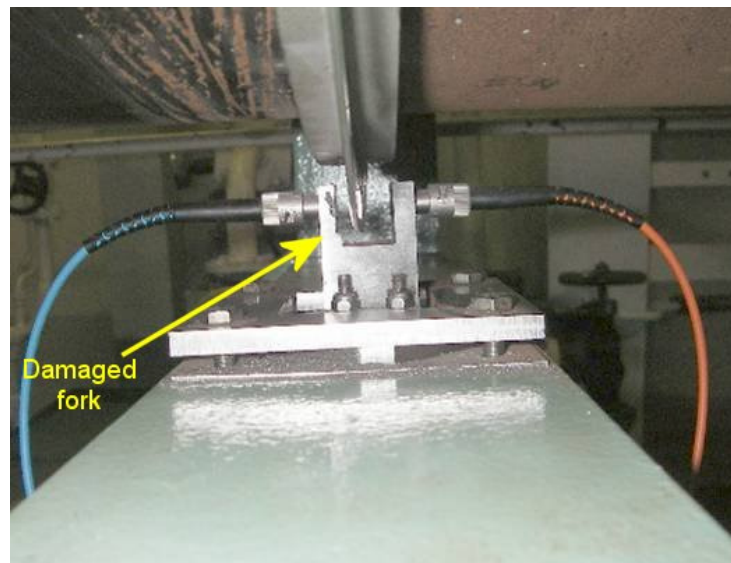


Figure 5.50: Damage on one of the forks of the torque sensor on the *Overseas Tanabe*

Even after the wheels had been reconnected to the propeller shaft, the forks, optical sensors and cables replaced, and the system recalibrated, the problems persisted. As a final measure, the code wheels were replaced with specially designed wheels of larger size. Yet, shortly after, the problem of sensor drift re-occurred.

The differentiation between drift from a torque sensor and changes in performance (e.g. due to fouling) or errors in readings from other sensors used to validate the torque sensor is difficult. In-depth investigation of the electronic Mean Indicated Pressure measurement system and power estimations from manual indicator diagrams and planimeters showed errors and uncertainties in both systems. Differences up to 15% between electronic and manual indicator diagrams were experienced, which could not be explained by the chief engineer onboard. The identification of sensor drift from the newly-installed torque sensor proved therefore difficult. To investigate whether a torque sensor remains within calibration, a number of checks were made:

- Relating the measured torque and RPM with the maximum operating profile of the engine
- Relating fuel flow to measured power
- Relating RPM with torque

Figure 5.51 shows 24 hour-averages of the torque and rpm filtered for transient conditions for the period May – July 2008. Also plotted in the figure are the engine trial curves, as supplied by the engine manufacturer when the ship was delivered. The upper curve represents the torque limit of the engine, while the lower curve represents the design engine load line given by the engine manufacturer.

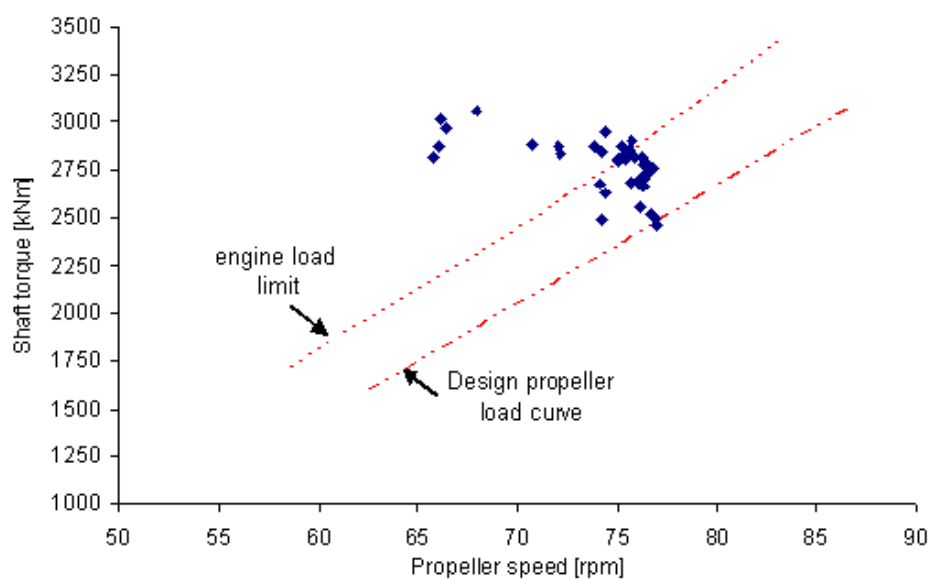


Figure 5.51: Torque and RPM recorded by the torque over the period May – July 2008

In order to visualise the development of the sensor drift over time, the same data is plotted as a percentage deviation from the design load curve in Figure 5.51.

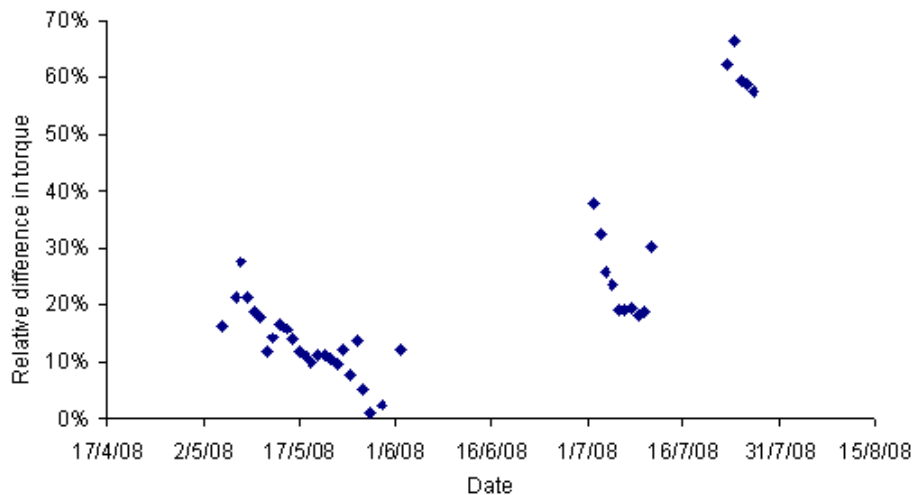


Figure 5.52: Relative torque deviation from propeller design load curve versus time

Figure 5.52 indicates that the torque sensor drifts, as the indicated torque lies outside the maximum operating point of the engine. Two trends can be identified: a decreasing trend over the voyage in May, and an increasing trend over the complete data set. The trend in May has no correlation with changing environmental conditions or loading condition, and can be related to sensor drift. The general trend over the complete dataset results in July in a 65% torque increase compared to the design propeller curve (35% compared to the ‘engine load limit line). This voyage was in ballast condition, where the propeller RPM was lower and the propeller expected to be lower loaded due to the shallow draft.

Another, more reliable way to identify sensor drift is to use engine characteristics to relate input power (fuel) to output power (shaft power). The specific fuel consumption curve of a marine diesel engine is dependent on the condition and timing settings of the engine, ambient air temperature, fuel quality, propeller and hull fouling etc. Yet, when it is known that engine overhauls are not made and fuel quality remains the same, the power-fuel relationship may be assumed to remain constant over a short period of time.

The fuel flow is measured on the *Overseas Tanabe* real-time using a gear flow meter. Flow sensors are relatively simple instruments, and not susceptible to drift. Moreover, the flow meter on the *Overseas Tanabe* only measures the fuel consumed by the main engine, and is not affected by fuel-return or fuel usage of the auxiliary systems. In the 3-month period in Figure 5.51, the fuel-power relationship of the engine is therefore assumed constant.

To indicate sensor drift, the measured power can be plotted against measured fuel flow. An approximately linear relationship is expected. If using the specific fuel consumption curves of the engine the fuel consumption is converted into output power, the measured power can be validated. Figure 5.53 shows this difference. The same deviations in torque can be seen as in Figure 5.52, yet, calculated in a completely different way. This indicates that the torque sensor is clearly out of calibration.

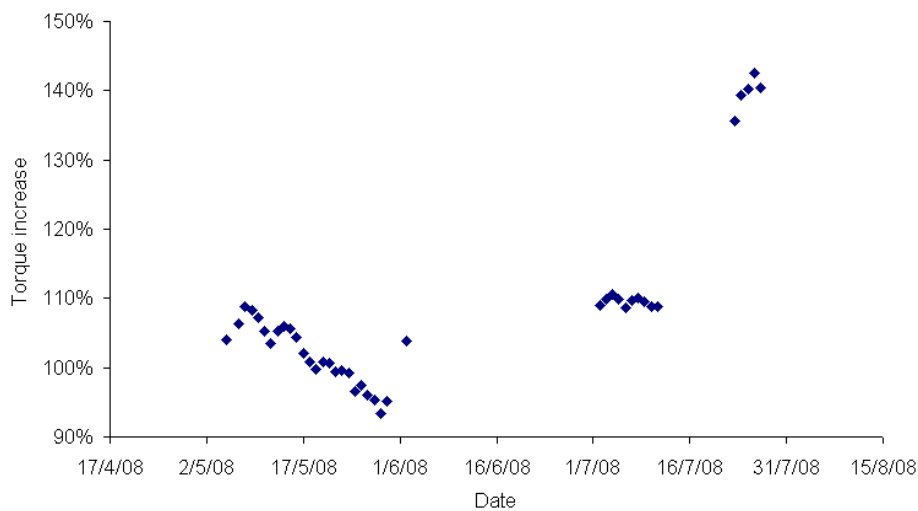


Figure 5.53: Deviation of measured torque from Power - Fuel consumption relationship

The problems are considered an exceptional case, but indicate the vulnerability of torque sensors to errors and the need for a real-time measure of fuel consumption for the identification of torque sensor errors, and frequent accuracy checks for the torque sensor.

5.3.4.3 Torque prediction

Without a measure of power, a reliable way of ship performance analysis is not possible. In order to still use the valuable collected performance data for the thesis and to be able to validate the performance analysis methodology, the real-time measured fuel consumption has been related to output power. As discussed in Section 3.3.10, relating power to fuel consumption introduces errors and uncertainties. However, for the objective of the thesis; to demonstrate the functionality and ability of the correction methodology to convert service performance data to standard conditions, it has been assumed that no engine timing adjustments are made and that the quality of the burned fuel remained practically constant. Furthermore, it is assumed that the relationship between power and fuel flow over the range 73-77rpm is linear. Based on these assumptions, the following relationship has been derived:

$$P_D = FC * 5.263 \quad (5.6)$$

P_D is the delivered power in kW and FC the Fuel Consumption in litre/hour. Figure 5.54 shows an example of the close match of the predicted torque based on fuel consumption and the actual measured shaft power, when the torque sensor was just repaired and calibrated by a service engineer onboard.

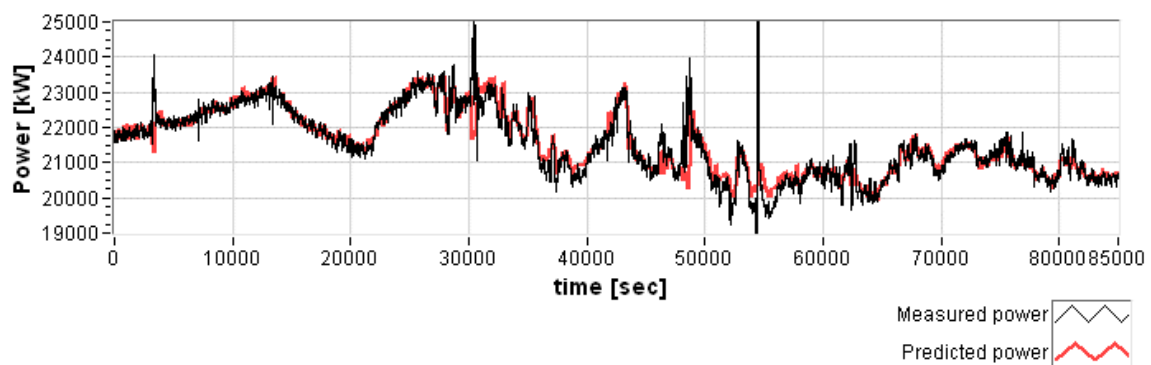


Figure 5.54: Measured power and predicted power based on fuel consumption on 13-06-2007

The close relationship indicates that it is possible to use instantaneous measured fuel flow for *real-time* performance monitoring purposes when it is known that the engine fuel

efficiency remains constant. It can not be used reliably for long-term performance monitoring. For the purpose of evaluation of the performance monitoring and analysis system proposed in this thesis, where the focus is on showing how the scatter in KPIs caused by environmental and loading conditions can be reduced, it can be used. Long-term trends following from these KPIs can not be related to changes in hull fouling, as it is likely that a slow drop in engine efficiency occurs due to engine wear.

5.3.5 Data conditioning

As identified in Chapters 3 and 4, ship speed through water is the most important parameter for performance monitoring. Data conditioning should therefore focus on the identification of periods where STW can be measured most reliably, i.e. in periods where ship performance is steady, the difference between SOG and STW is small and STW does not vary over a set period of time (discussed in Section 3.4.1.3). Figure 5.55 shows the designed transients and speed log filter for the *Overseas Tanabe* responsible for the identification of these periods.

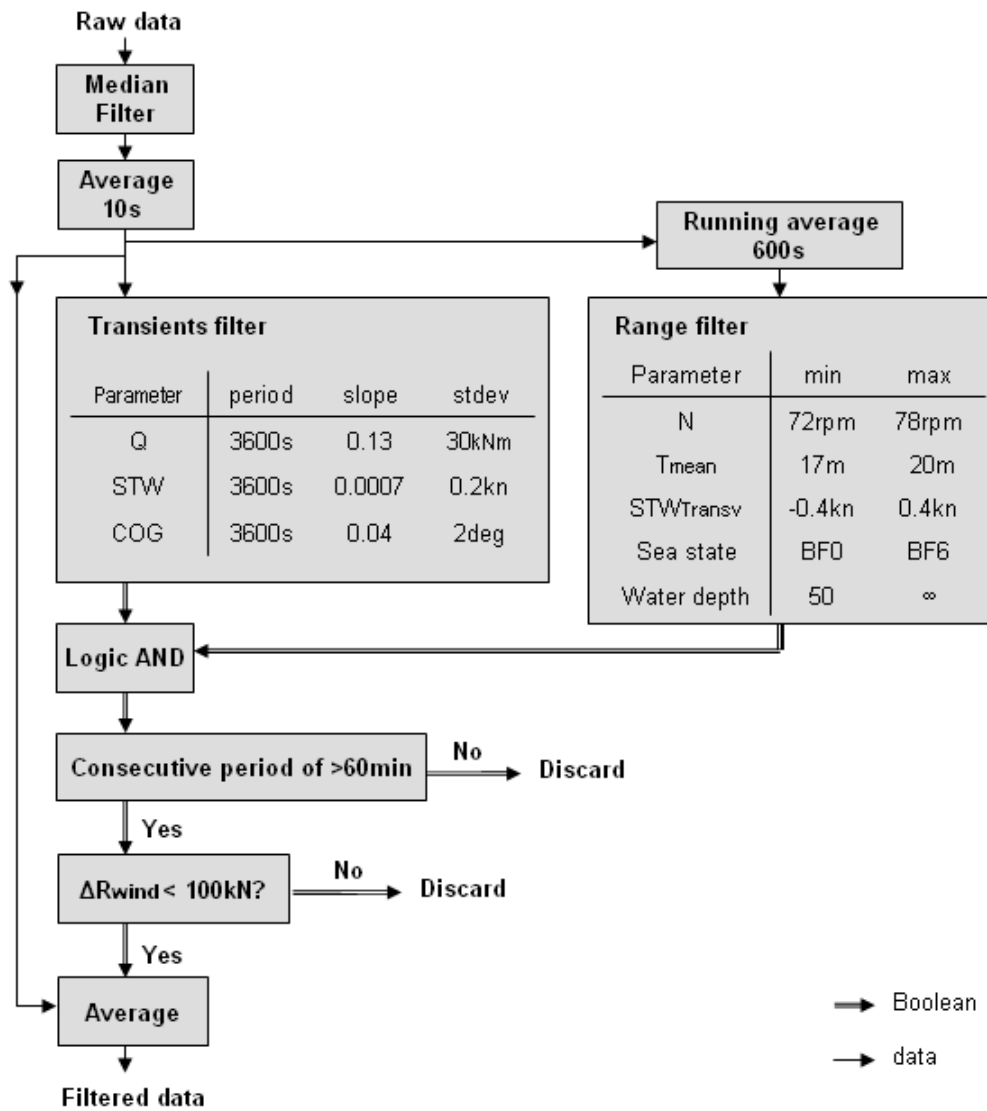


Figure 5.55: Data conditioning for Overseas Tanabe

The filter, which includes data conditioning, can be described by the following steps;

1. Data conditioning to remove outliers from signal noise, instrumentation errors etc. using a median filter
2. Smoothing and data reduction using simple average over 10 seconds to reduce random noise and computer processing time
3. Filter step 1: Transients filter using torque, ship speed through water and course over ground
4. Filter step 2: Range filter in order to reduce causes of erroneous STW readings. Data is first averaged using a running average to avoid fluctuations with a short

time constant to trigger the filter. The engine speed (N) and draft (T_{mean}) are included to avoid large changes in wake fraction

5. In case the data complies with the conditions in the transients and range filter, the periods are checked for duration. The performance should be constant for a meaningful period of time in order to get a reliable measure of STW. A period of 60 minutes has been chosen based on trial-and-error. The larger the period, the more reliable the STW can be defined, but the fewer periods will pass the filter
6. If the STW over the identified period is constant, the wind and wave resistance should have been constant as well (in theory). Using a filter, a check is made whether the wind resistance has not fluctuated more than a set threshold (here 100kN), which would suggest that the ship speed has incorrectly been identified as constant
7. If all conditions are satisfied, the performance and environmental conditions over the periods where ship speed and power are constant can be averaged. These points form reliable ship performance data, which can be used for further analysis (correction to standard conditions, identification of wake fraction etc.)

The filter coefficients have been based on trial and error. During this process, parameters should be found that result in steady state performance and signals, not only in shaft power and course, but most importantly in STW. For the speed log, it is most important that variations with a large period, which have a lot of ‘weight’ in further data conditioning, are identified. A time frame of 1 hour has therefore been selected. The limit on the standard deviation over this time frame is used to identify fluctuations with a smaller period. Figure 5.56 shows an example of the transients filter applied to the STW from the Doppler log of the vessel. The top curve shows the raw STW signal, averaged over 10 seconds and filtered for outliers using a median filter. The blue curve is the unfiltered data; the black sections represent the data that has passed the filter. The red filled curve in the middle of the graph shows the slope of the regression line that is calculated using a moving window of 3600sec. By limiting the maximum slope, periods of increase or decrease in STW (which not necessarily represent actual acceleration or deceleration of the ship) can be identified. The bottom curve represents the standard deviation calculated over the same moving time window. Because measurement errors in STW and actual acceleration of the ship are difficult to separate, an additional filter based

on shaft torque is included to identify acceleration and deceleration. Finally, the Course Over Ground (COG) is monitored to identify course deviations.

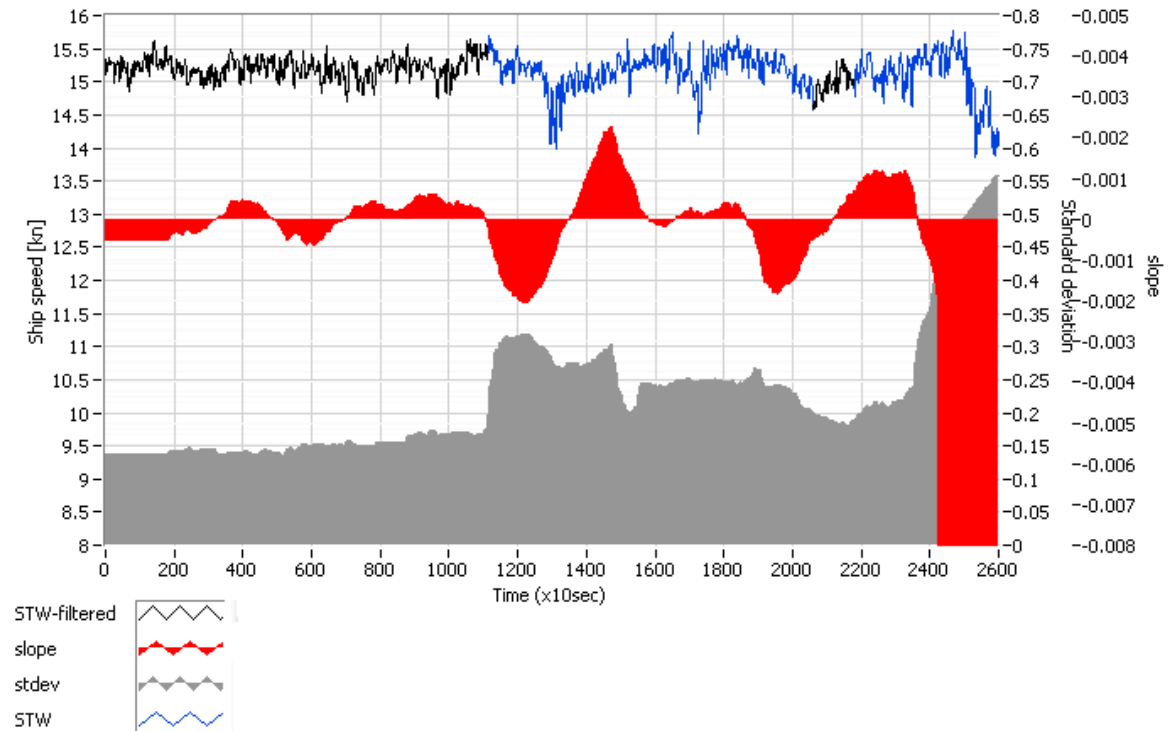


Figure 5.56: Example of STW filter on Overseas Tanabe performance data

The quality of the data that passes the data conditioning filter may be evaluated using the effective wake fraction, which is expected to be only affected by propeller loading as long as the draft does not vary and the weather conditions are mild, so that the effect of waves on the wake fraction may be neglected. The calculation of the effective wake fraction from service performance data is sensitive to the measurement of STW and torque. Fluctuations in the wake fraction can therefore in the first instance be contributed to errors in the measurement of the speed, the most difficult to measure parameter onboard. By plotting the wake fraction as a function of ship speed or the propeller torque coefficient K_Q , the load dependency of the wake can be separated from fluctuations caused by measurement errors.

Figure 5.57 shows the wake fraction versus ship speed calculated from 114 days where 107 periods passed the data conditioning filter. Due to the unavailability of an open water diagram or existing figure of wake for the *Overseas Tanabe*, the propeller characteristics

of a similar B-series propeller ($D = 9.600\text{m}$, $Z = 4$, $\text{BAR} = 0.4406$ and $P/D = 0.6835$ (Oosterveld and Oossanen 1975)) have been used for the calculation of the wake. The propeller characteristics can be represented by a second order polynomial in the form:

$$10K_Q = -0.1955J^2 - 0.1518J + 0.2725 \quad (5.7)$$

$$K_T = -0.1558J^2 - 0.2391J + 0.27755 \quad (5.8)$$

The torque has been calculated from the measured fuel consumption.

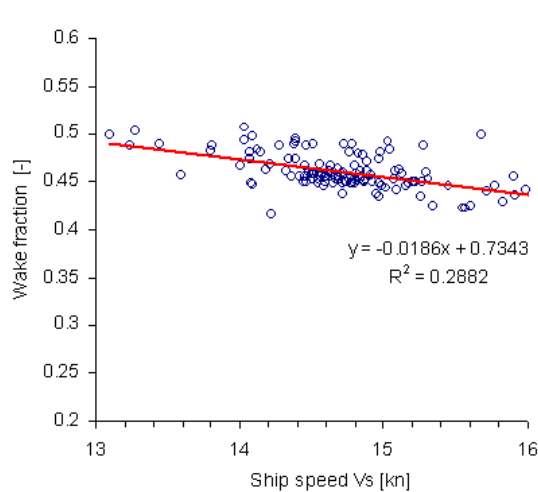


Figure 5.57: Wake fraction as function of ship speed

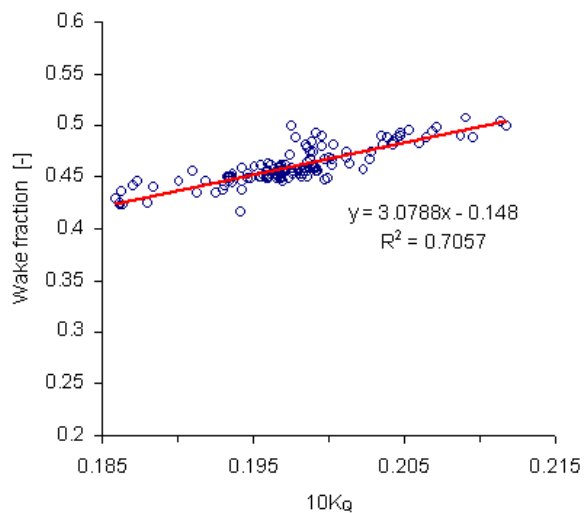


Figure 5.58: Wake fraction as function of torque coefficient K_Q

If regardless the large scatter in Figure 5.57 a regression curve is derived between wake and speed, it shows that for a speed increment from 13 to 16kn, the wake fraction changes from 0.493 to 0.437, a decrease of 11%. For this small speed increment, this decrease seems rather large. It is however known that the induced velocity in front of propeller has a strong effect on the effective wake due to a deformation of the boundary layer of the hull, especially for large ships with relatively small propeller that operate well within the boundary layer (Inukai and Ochi 2009).

Figure 5.58 shows the wake as function of the torque coefficient K_Q . It can be seen that there is a strong relationship between the torque coefficient K_Q (the propeller load) and effective wave. Yet, the large dependency may also be due to uncertainty in the propeller open water diagram (see Section 3.4.1.4). For simplicity and the relatively small errors, the open water diagram is considered correct. The relationship between K_Q and w as shown in Figure 5.58 is used to account for load fluctuations;

$$w = 3.0788 \cdot 10K_Q - 0.148 \quad (5.9)$$

In order to identify the errors in the dataset caused by inaccurate measurements, draft deviations or other unaccounted factors, formula (5.9) can be re-written;

$$w = c_1 10K_Q + c_2 \quad (5.10)$$

$$c_2 = w - c_1 10K_Q \quad (5.11)$$

Where c_1 represents the dependency of the wake fraction to propeller load and c_2 the part of the wake fraction that is independent of propeller load. Assuming c_1 is constant, variations in wake fraction due to fouling, draft deviations, ship motions etc. and errors in the measurement of Q , N or V_s express in changes in c_2 . In Figure 5.59, the deviation of the wake fraction uncorrected for propeller loading ($w - w_{mean}$) and corrected for propeller loading using equation (5.11) is shown ($c_2 - c_{2mean}$).

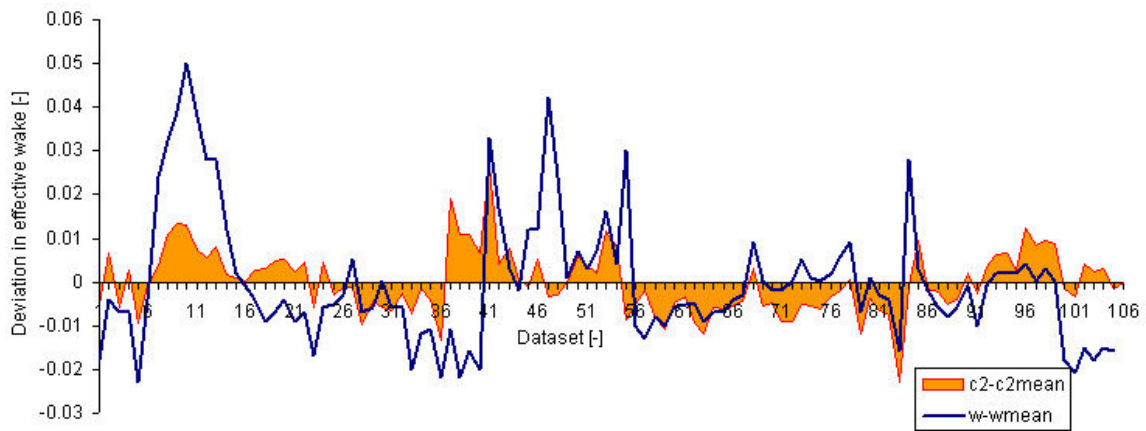


Figure 5.59: Deviation in wake fraction before and after correction for propeller loading

The correction for propeller load takes away most of the deviations in estimated wake. The remaining deviations can be contributed to measurement errors, hull fouling and unaccounted conditions. It follows that there is a 95% confidence interval that the deviation in wake remains within $w = 0.46 \pm 0.014$, or $0.46 \pm 3\%$. This is small considering the sensitivity of the calculation method for wake fraction to measurement errors in torque, ship speed and RPM. In Table 5.3 the sensitivity of the calculation of the wake fraction (following equation (4.16) in Section 4.2.3) using the selected B-series propeller is shown for a ship speed of 15.5kn. The tested uncertainty range has been chosen based on sensor characteristics (torque & rpm), the natural variation of water density, assuming it is not measured and accounted for (see Section 3.2.4) and an assumed worse-case accuracy of the speed log when used in periods identified by the speed-log filtering algorithm.

The uncertainty of the wake from the dataset falls well within the expected uncertainty in wake from the expected accuracy limits of the torque sensor and speed log. It can therefore be concluded that the filter algorithm performs well and results in reliable data.

Table 5.3: Sensitivity analysis wake fraction calculation for the Overseas Tanabe

Parameter	Mean	Uncertainty Test range	Sensitivity gradient	Relative	Absolute
				Uncertainty in wake	Uncertainty in wake
<i>Torque</i>	2617kNm	$\pm 1\%$	2.25	$\pm 10.8\%$	± 0.049
ρ_{sea}	1024 kg/m ³	± 3 kg/m ³ (0.3%)	-2.25	$\pm 1.5\%$	± 0.007
<i>RPM</i>	76.44 rpm	$\pm 0.5\%$	-5.72	$\pm 1.3\%$	± 0.006
V_s	15.46 kn	± 0.4 kn (3%)	1.23	$\pm 9.7\%$	± 0.044
<i>w</i>	0.452	-			

5.3.6 Data analysis

The performance of the *Overseas Tanabe* has been corrected for wind, waves and displacement variations. Because the water depth was not measured, areas with known

shallow water have been filtered out based on the position of the ship and a database with shallow water areas.

5.3.6.1 Draft and trim correction

The *Overseas Tanabe* sails predominantly in laden conditions. Only ship performance in this condition has therefore been analysed. To account for variations in displacement ranging between 17 and 20m, a correction has been applied. The correction is based on the empirical resistance prediction method described by Holtrop (Holtrop 1984). The relative difference in power between the benchmark performance ($T = 19.9\text{m}$) and number of loading conditions has been used as correction factor. For the conversion from resistance to power, a propulsive efficiency of $\eta_D = 0.693$ has been used (based on $\eta_O = 0.49$, $t = 0.22$, $w = 0.44$, $\eta_R = 1.025$ and $\eta_S = 0.99$). Using the same empirical prediction method, a correction for the wake fraction has been derived, as shown in Table 5.4.

Table 5.4: Draft correction factors

	16m	17m	18m	19m	20m
Power correction C_{DRAFT}	1.11	1.07	1.04	1	0.97
Wake fraction correction $C_{W-DRAFT}$	0.96	0.98	0.99	1	1.01

5.3.6.2 Wind correction

For the wind loading coefficients, the results from OCIMF (OCIMF 1994) have been used. Figure 5.60 shows the longitudinal wind resistance coefficients for both laden and ballast conditions.

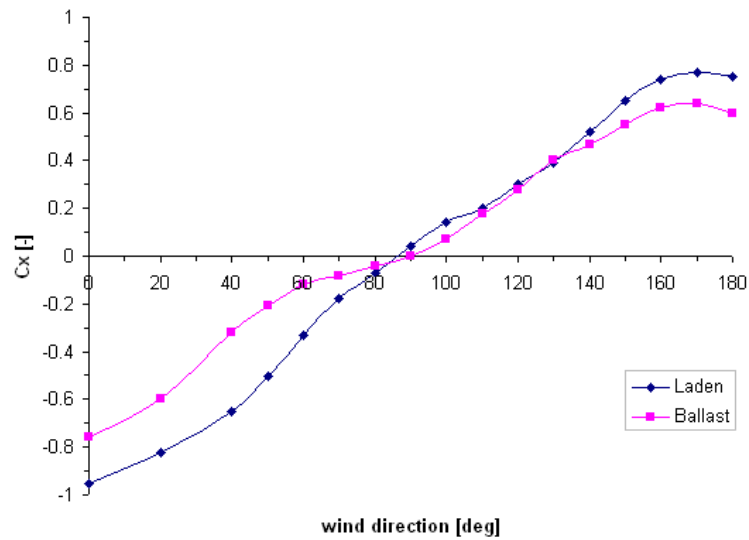


Figure 5.60: Longitudinal wind force coefficient for Overseas Tanabe (OCIMF, 1994)

The anemometer of the Tanabe is approx. 42m above sea level when the ship is in laden condition. To account for the gradient over the sea surface, the wind speed has been multiplied with 1.16 according to equation (3.4) (Section 3.2.3) with $n = 6$.

5.3.6.3 Wave correction

Due to the unavailability of a hull line plan, and due to time limitations of the project, it was not possible to calculate the response amplitude operator curves, necessary to calculate the wave resistance components accurately. Instead, a simplified added wave resistance method has been used based on (Kwon 2008). The required input to these calculations is restricted to C_B , Froude number, volume of displacement and a sea state description given by Beaufort number and direction relative to the bow. The output is in the form of a percentage speed loss. The method is limited to sea state BF6.

5.3.6.4 Correction to standard conditions

From March 2007 onwards, DVDs with logged performance were sent to the Author for analysis. A large part of this data could not be used for performance analysis due to errors

of the rpm sensor or due to discs not being sent to shore. From the data received between May 2007 and July 2008, 107 days of sailing were extracted. After filtering for slow speed steaming, sailing in shallow water areas, transient conditions, drift and rough weather, 106 periods of performance were identified by the transients and log filter. The periods represent data where the measured performance is constant and the reliability of the speed log is considered highest. The performance indicators ΔP_D and $\Delta P_{D,corr}$ are shown in Figure 5.61. In order to show the effect of the corrections most clearly, the results are plotted on a basis of order of analysis.

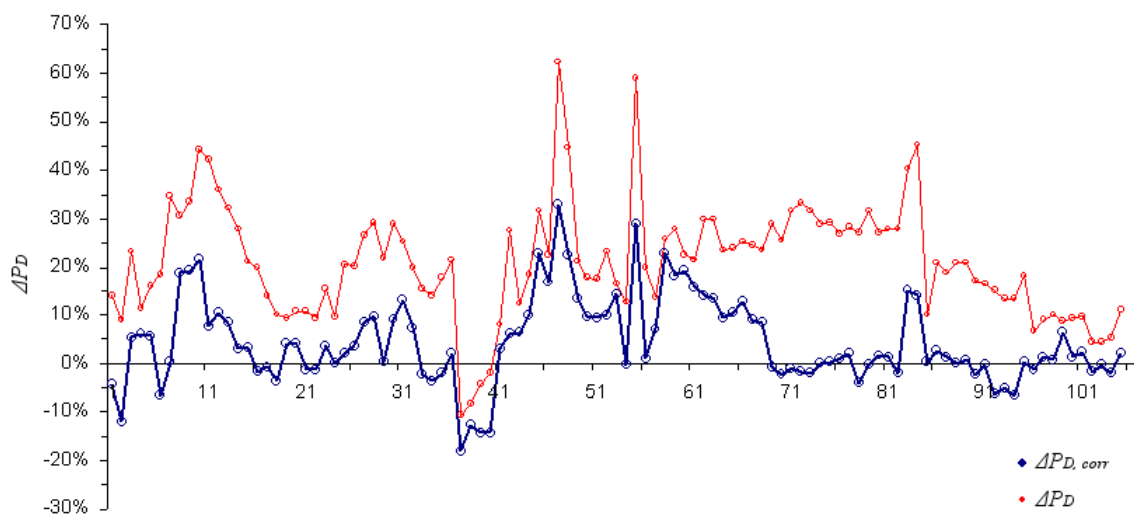


Figure 5.61: Corrected and uncorrected ship performance for 106 data points

As expected, the corrected performance in Figure 5.61 is much closer to the standard speed-power curve ($0\% \Delta P_D$ line) and the variations are smaller than the uncorrected data points. The fluctuations follow a mean around $\Delta P_D = 0\%$. However, there remain large deviations from the $0\% \Delta P_D$ line which can be contributed to environmental conditions that are not accounted for accurately. Also, in this particular case, the deviations can partly be explained by small changes in engine fuel efficiency, affecting the relationship between power and fuel consumption, and hence calculated torque.

The reduction in scatter could also be obtained with strong statistical smoothing. In contrast with the used deterministic, rational data filtering and analysis, this will not improve data validity and reliability. The results should therefore not be compared with

e.g. abstract logbook data, which reliability, accuracy and availability is not suitable for performance analysis.

Figure 5.62 shows the same results plotted against time, from April 2007 to July 2008. The large period where no (reliable) data was available is clearly visible. Because of the filtering, periods where weather conditions were calm and performance was particularly steady, more data points are shown. In regression analysis, these cluttered periods would get a higher ‘weight’ than more isolated points. However, for regression analysis, each day, week or month should weigh equally. It is therefore important to divide and average the data points in e.g. periods of a week. This is shown in Figure 5.63.

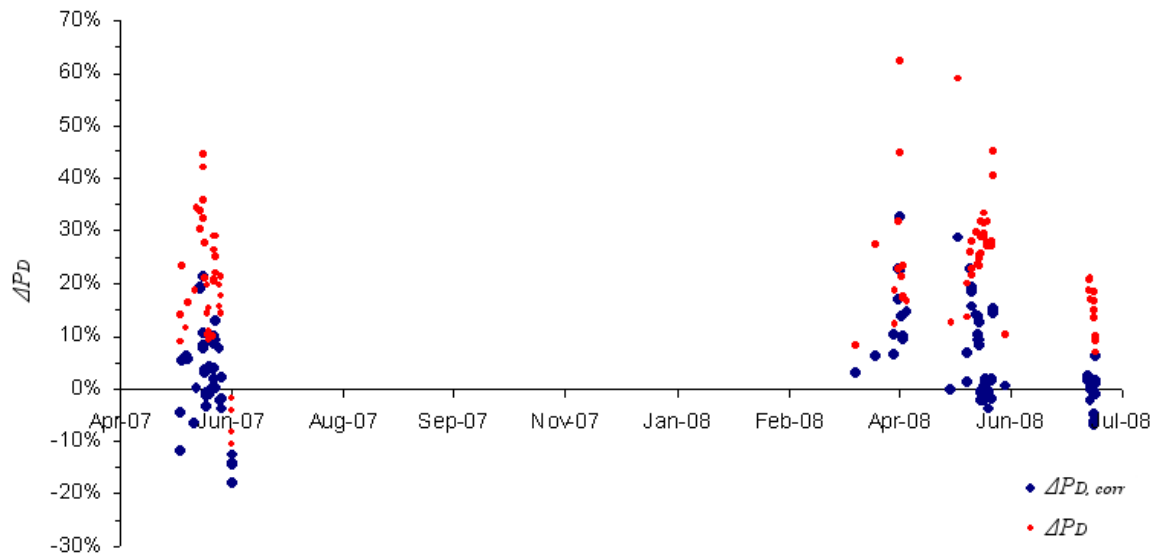


Figure 5.62: Corrected and uncorrected ship performance versus time

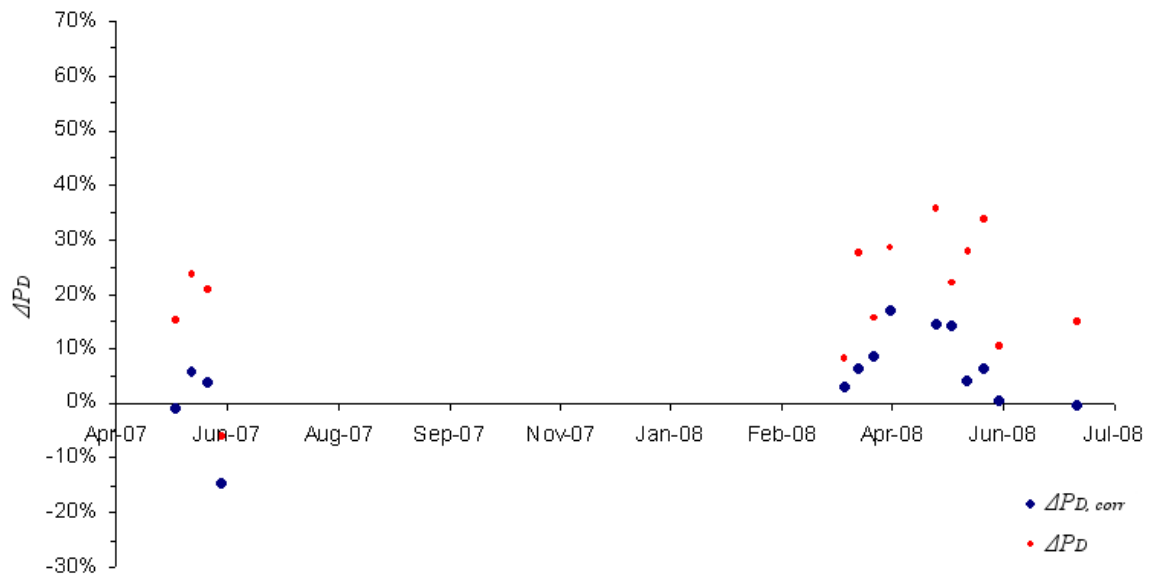


Figure 5.63: Corrected and uncorrected ship performance versus time averaged in weeks

While in Figure 5.62 the cluttered data points seem to indicate a decrease in $\Delta P_{D,corr}$ between March – June 2008, in Figure 5.63 this trend is less clear. This shows the importance of dividing and averaging data in fixed periods to avoid misinterpretation of results.

From Figure 5.63 no conclusions can be made regarding performance; the data is too sparsely distributed to draw any conclusions on fouling. This also advocates for an online PM&A system where no data has to be sent ashore which might get lost etc. It also shows the importance of having good quality sensors. Regardless the fact that long-term trends cannot be derived from this dataset, it does show the ability of the analysis methodology to reduce scatter in an objective, transparent and deterministic way. It also shows that there remain large performance deviations, which can be related to poor data regarding environmental conditions (mainly wave characteristics), as discussed in the following section.

5.3.6.5 Implication of inaccurate wave recordings

The deviations in $\Delta P_{D, corr}$ in Figure 5.61 can be contributed to measurement errors in ship speed, unaccounted environmental conditions and inaccurate corrections for added wave resistance. The following analysis shows the possible cause of the large performance deviations around data points 58-60 in Figure 5.61. The data points are filtered extracts of the ship performance while sailing along the African coast, as shown in Figure 5.64. The ship sails southwards to Cape Town, where it makes a short stop and continues in Easterly direction towards Indonesia. The water depth along the Namibian and South African coast at the position of the ship ranges between 100 and 200m (C-Map 2003). Shallow water effects are therefore not expected.

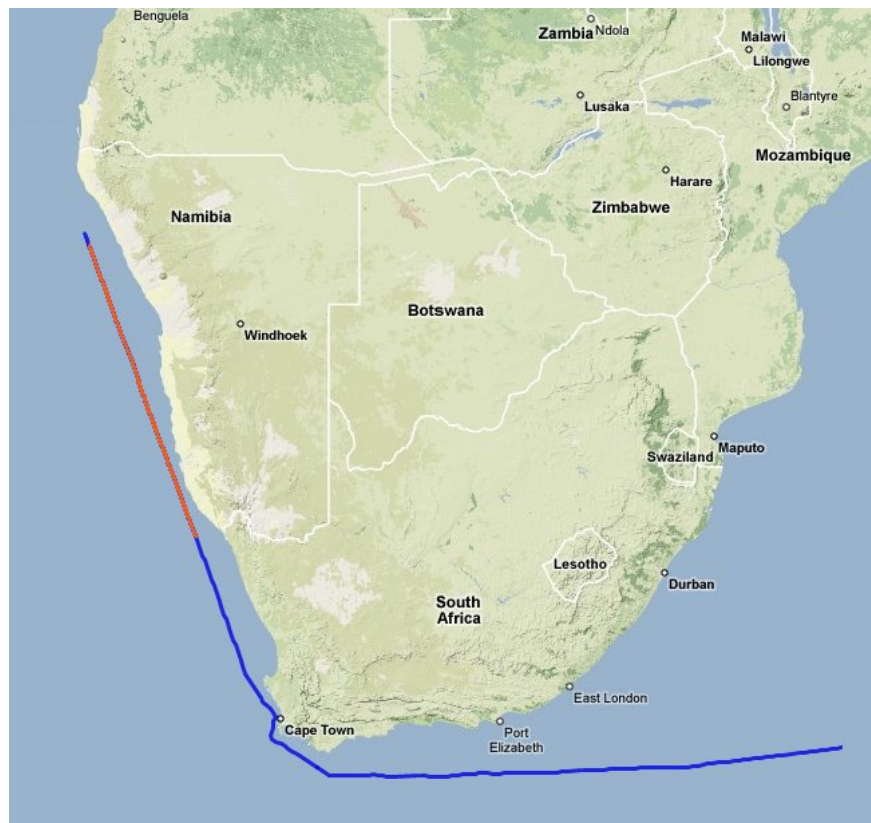


Figure 5.64: Sailing track Overseas Tanabe between 04-07 May 2008 (Google 2008), (NGDC 2008)

The ship performance and environmental conditions over the displayed route (4 days) is plotted in Figure 5.65. The ship sailed in laden conditions ($T_{mean} = 19.9\text{m}$). In the diagram, the torque, RPM, STW, SOG, wind speed, sea state, swell height, swell direction and relative wind direction are plotted versus time. The sea and swell

characteristics are entered manually in the data acquisition system (see Figure 5.45). They are obtained from manual observations from the officer on watch, and are therefore influenced by subjective judgements. Periods of nightfall or fog, where observations are less reliable are indicated.

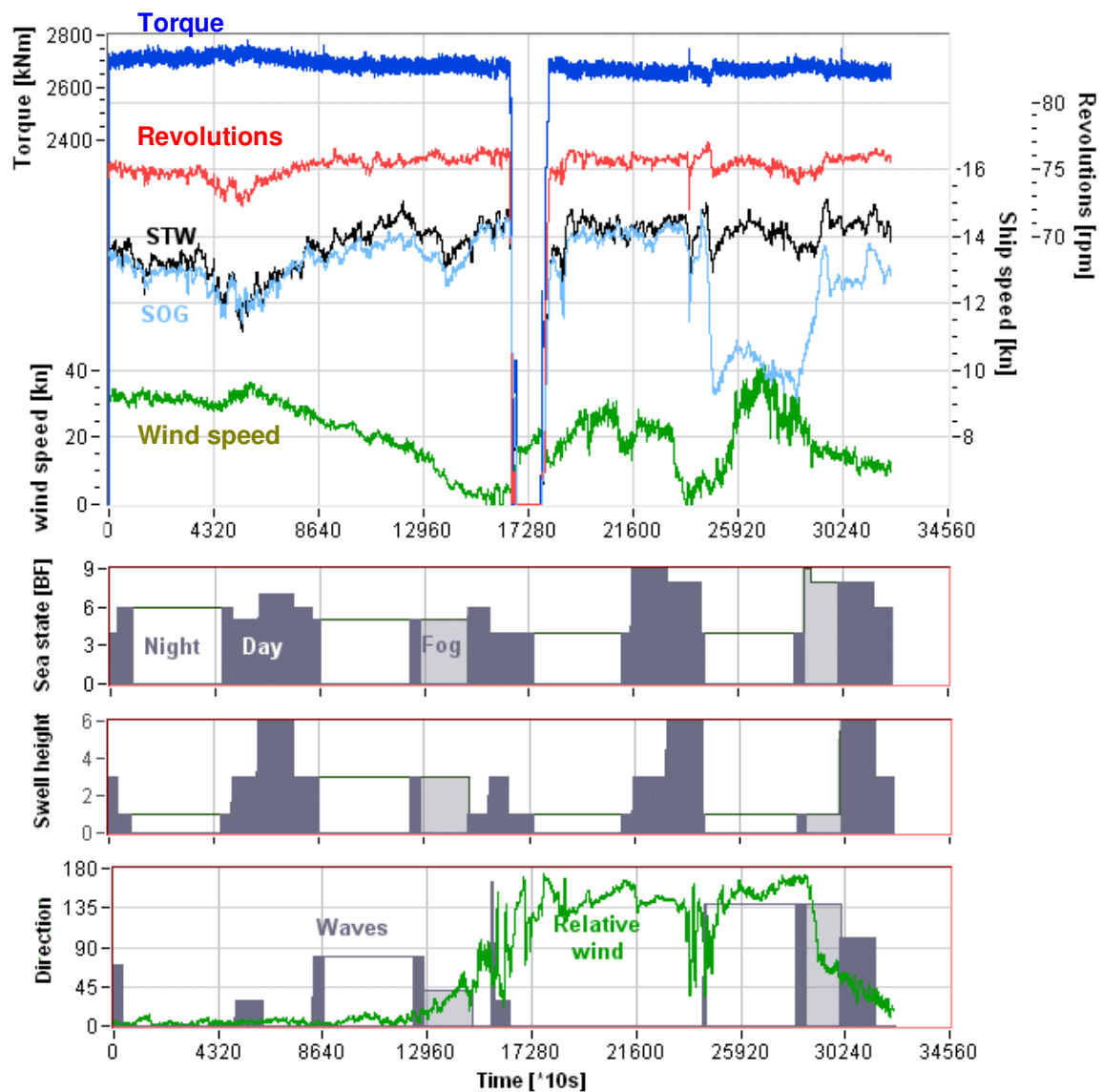


Figure 5.65: Ship performance Overseas Tanabe while sailing along African coast between 04-07 May 2008

From the figure, a number of aspects can be identified:

- The propeller speed varies very slowly over time, indicating that variations are not voluntarily by the user, but controlled by the engine control system. This

suggests that the engine is controlled based on constant fuel rack. The output power remains practically constant, while engine overload is controlled by reducing the engine speed.

- The STW and SOG match up closely during the first 2½ days. Together with constant power, deep water, negligible transverse speed through water, this suggests that the current speed was low and the STW measurements accurate. Moreover, power and RPM deviations correspond to the deviations in STW.
- During the first day, a speed reduction of up to 2kn can be noticed, which can partly be contributed to windage. As shown in Figure 5.65, there is a relative wind speed of 32kn from head direction, slowing down the ship. However, at time 4320, the ship speed decreases further with approximately 1kn, while the wind speed increases only 5 hours later to 36kn. This indicates that other forces affect the ship performance.

The increase in wind speed suggests that the sea conditions worsen. In the bottom graphs in Figure 5.65 the observed wave and swell conditions are shown. Sea observations can only be made during daylight and in clear weather (no fog/snow etc.). As a result, only approx. 40% of the time a description of the sea state is available, as shown in Figure 5.65. Between time 4400 and 8640, crew observations indicate that the wave and especially swell height increase. The observations are however approx. 4 hours lagging with the largest ship speed losses. This can be caused by the following factors:

- The sea state is observed every 4 hours. The observations are biased by the wave conditions over the past 4 hours which the crew experienced. They may therefore not necessarily represent the conditions at the time of logging. The observations in Figure 5.65 are extrapolated 4 hours ahead to the next observation. However, a better representation would be to extrapolate each measurement 2 hours back, and 2 hours ahead
- The increase in wind speed over the past 4 hours has developed the sea and resulted in a higher wave height, even though the wind speed has in the meantime decreased again.
- The wave observations are inaccurate, due to the difficulty of making accurate observations from a large distance to the sea surface. Errors in logging are also

shown by the recorded wave direction. The user is asked to enter the true wave direction. In the bottom graph in Figure 5.65, the wave direction as logged by the crew (as being the true wave direction) is plotted, together with the relative wind direction. Considering the wave direction is not directly opposite the wind direction (waves are here expected to have a negative impact on ship performance, while following waves cause very little resistance), the logged wave direction is likely to be the relative wave direction. Whether this error is made by all officers is questionable. At time 24000 either the wave direction suddenly changes direction with 140 degrees, while the wind direction remains unaltered (which is highly unlikely), or the wave direction is not entered and the default value (0°) is logged. This uncertainty makes the performance analysis difficult. Because of the expected errors it seems more reliable to use the calculated true wind direction as measure of wave direction.

The low reduction in ship speed in the last two days in heavy sea conditions (BF8-9) may be explained by the direction from which the wind and waves originate; the ship experiences almost following waves and wind, which do not contribute to a large resistance increase. Due to the errors in wave observations, the correction model is not able to correct the ship performance accurately to standard conditions, such as is the case for data points 68-70 in Figure 5.61. Other peaks in the figure can also be partly contributed to errors from the wave observations.

It can be concluded from Figure 5.65 that manual logs of sea surface characteristics can only provide useful information for ship performance monitoring if logged at high frequency (in the order of once every 30 minutes). Moreover, particular efforts should be put in unambiguous data input.

5.3.7 Concluding remarks on PM&A on Overseas Tanabe

A transparent, tailor-made data acquisition system was designed, developed and installed onboard the *Overseas Tanabe* in order to evaluate the PM&A system outlined in Chapters 3 and 4 for large, merchant ships. The system was successfully put in place by the Author in February 2007, and after a test and evaluation period, operational in May 2007.

Data analysis showed that the newly installed shaft torque and rpm sensor slowly lost calibration and finally stopped functioning properly in June 2007. Regardless numerous attempts to repair the torque sensor, the sensor could not be repaired successfully within the time frame of the PhD project. To still be able to use the data for evaluation purposes, a relationship was derived between the real-time measured fuel flow to the main engine and shaft power. Using this relationship the data conditioning and performance analysis methodology was evaluated. The relationship can however not be used to indicate long-term trends (e.g. fouling), as the long-term stability of the relationship could not be validated. It is solely useful to indicate the ability to reduce scatter in KPI's using the proposed analysis methodology. It is no substitute for a dedicated shaft power sensor for performance monitoring systems.

The availability of large amount of data allowed the transient and speed log filter to be evaluated using strict filter criteria in order to identify only the most reliable, constant periods where STW measurements are considered most accurate. Approximately 15% of the data satisfied the set criteria. Regardless the strict filtering, performance deviations from a benchmark performance of $\pm 12\%$ remained apparent after correcting for variations in displacement, wind and waves.

The uncertainties in ship speed measurement are believed to be one of the main causes of deviations in the KPI $\Delta P_{D,corr}$. With less strict filter settings, the deviations become larger. This indicates that more research is required to understand the errors of speed log measurements using a Doppler log further, so that data can be better filtered. Another cause of deviations in the KPIs is the uncertainty resulting from manual wave observations. Detailed analysis shows that 4-hourly manual entry of wave characteristics

does not provide the required reliability and detail for correcting ship performance for added wave resistance, even with an unambiguous, easy to interpret user interface. A wave radar or other way to automatically determine sea state characteristics proves therefore to be important for performance analysis.

The proposed and tested PM&A system is believed to be the way forward for performance assessment, due to its transparency, focus on data quality and accurate performance correction based on reliable data.

5.4 Conclusions

In this Chapter, the proposed PM&A system is implemented and evaluated based on two different size vessels; the 16m research vessel *Bernicia* and the 300.000dwt VLCC *Overseas Tanabe*. Through system evaluation on two types of vessels, the viability of the proposed algorithms and design principles for PM&A systems was illustrated and proved successfully.

Evaluation of the proposed PM&A system on the *Bernicia* showed that even for small vessels, service performance can successfully be filtered for transient conditions using time series analysis of the deviation and acceleration in horizontal and vertical direction over a fixed time frame. Furthermore, service performance can successfully be analysed using the proposed PM&A system. Care must be taken when using the GPD speed in the correction methodology avoid over estimation of the effects of fouling on ship performance.

Evaluation of the PM&A system on the *Overseas Tanabe* showed that the proposed data collection, filtering and analysis algorithm can successfully be implemented on large, merchant ships. Scatter in long-term KPIs is difficult to reduce to less than $\pm 12\%$ without statistical smoothing. Yet, with automatic logging of wave characteristics, this scatter can be reduced further. Furthermore, as no reliable torque sensor was available, the real-time measured fuel flow was used to predict power. It is likely that some scatter is also caused by this action.

A transparent data acquisition system and user interface was developed, displaying each step in the data collection and analysis process in real-time and intuitive way. With this important step, the quality and uncertainty in the data can be assessed and the causes of scatter in performance indicators can be traced back to their source. The software represents a working prototype of the proposed PM&A system and indicates the preferred transparency and interface of real-time PM&A systems installed onboard. A checklist for the development of a similar PM&A system is included in Appendix A.

The evaluation of the real-time transients and speed log filter proved effective and invaluable especially for small vessels that manoeuvre frequently. It results in significant reduction of scatter and improvement in data reliability. However, in spite of the use of carefully conditioned and reliable performance data, scatter in KPIs remain fairly large (approx. $\pm 12\%$) for accurate definition of long-term trends, e.g. for evaluation of the effects of fouling. It is therefore not possible to determine the effects of fouling from only a limited number of days. To be able to create statistically reliable trend lines, a large period of ship performance should be analysed, unless dedicated speed trials under stipulated conditions are done. The causes of scatter in the KPI $\Delta P_{D,corr}$ are as following;

- The validation of ship speed through water is difficult even with strict conditional filtering. Due to the high sensitivity of ship performance to ship speed, small errors result in large scatter. The use of the GPD speed may result in less scatter, but results in overestimation of the effects of fouling if not carefully calibrated for wake fraction and propeller characteristics in service
- Torque sensors are sensitive instruments and susceptible to drift. They require therefore frequent validation of their output through calibration or cross-validation with other parameters (fuel consumption or other power measurement systems). Without periodical calibration, the reliability of KPIs is questionable
- Manually logged parameters, used for the correction to standard conditions, lack reliability and accuracy even when used with intuitive and specially designed user interfaces. Data collection of critical parameters, such as draft and wave conditions should therefore be done automatic with high frequency. In order to reduce scatter from incorrect sea state observations, a wave radar or digital forecast system should therefore be installed.
- Added resistance calculation methods for small ships suffer accuracy and reliability, resulting in ill-defined corrections to environmental conditions and KPIs.

6

CONCLUSIONS & RECOMMENDATIONS

6.1 Introduction

This chapter presents an overall review of the thesis, main findings from the thesis and recommendations for future work. Reference is made to the main aim and objectives as described in Chapter 1, wherever is appropriate.

6.2 Review of thesis

Over the past years there has been a strong interest to improve ship performance. Fuel prices have risen sharply over the past 5 years, and fuel costs have gone up from 20% to 50% of the operational costs of a ship (Moller 2008). Every per cent saved in fuel consumption can therefore has a major impact on profitability for owners. The recent IMO ban on the use of TBT based anti fouling coatings has resulted in the appearance of numerous types of antifouling coatings in the market. As hull fouling can have a major effect on ship efficiency, ship owners are eager to select the most efficient coating, but are confused which type to select on a reliable basis. Furthermore, there is a strong environmental pressure on the shipping industry to reduce air pollution and Green House Gas emission through new MARPOL Annex VI amendments pressure towards energy efficiency measures by newly proposed Energy Efficiency Design and Operational Indices from IMO. Optimisation of ship operations starts with the measurement and monitoring of ship performance. Information about the performance of a ship in service and under stipulated conditions allows:

- Optimisation of ship operation (speed, trim, pitch) and voyage planning based on the actual capabilities of the ship
- Accurate estimation of the power margin for new vessels to be designed and built

- Improvement of hull, propeller and machinery maintenance strategies, such as accurate definition of the most optimal dry-docking intervals, effect of propeller cleaning etc.
- Improvement of new ship designs as well as the evaluation of novel ship design features, such as flow improving devices, new foul-release coatings, new propellers etc
- Accurate assessment of ship emissions, so that environmental class notations can be awarded easier and the ship rated more accurately in CO₂ indexing schemes
- More accurate definition of charter contracts concerning ship capabilities

Furthermore, the availability of real-time ship performance information on the bridge increases the understanding of the officers of ship behaviour in different conditions, so that ship operation can be optimised.

Most ship performance schemes are based on the collection of abstract logbook data. Statistical analysis methods are then used to derive performance indicators for the assessment of the effects of hull or propeller fouling on ship performance. The main problem faced with these performance analysis procedures is the poor quality of the abstract logbook data. Spot measurements are combined with averages over a day; parameters are misinterpreted or not entered due to insufficient or inadequate sensors. Data validation is not possible due to the low sampling rate of the collected data and incorrect or confusing data logging protocols results in incomplete and unreliable performance logs. As a result, performance analysis is often restricted to simple statistical trend analysis techniques.

Ship performance data should however be converted into a pre-defined ‘standard’ condition by using appropriate correction methods to be able to make reliable comparison and hence performance analysis possible. Existing methodologies for such corrections can be separated in (i) Trend analysis (with no correction for environmental conditions); (ii) Statistical analysis; (iii) Deterministic analysis based on the speed-power curve or propeller open water characteristics; and (iv) System identification techniques. All these four methods focus on the mathematical correction methodology, without paying much attention to the quality of the input data. Unless used with accurate and reliable data,

these analysis methods are not able to produce performance indicators with satisfactory accuracy.

The selection of the right Key Performance Indicator (KPI) introduces an additional uncertainty. Each KPI is affected by different factors such as engine condition, propeller loading, ship speed or propeller fouling. Separation of e.g. hull fouling from the other affecting parameters is therefore difficult. For a KPI to be meaningful, its exact characteristics and interpretation must therefore be well described.

To be able to shed light on the above described problems, this thesis aimed to investigate the feasibility of developing an advanced, on-line ship performance monitoring and analysis (PM&A) system for merchant ships that provides more accurate and reliable KPIs. In achieving this aim, the focus was put on the collection of accurate and reliable data, as well as developing an accurate correction methodology and meaningful KPIs. In order to collect reliable and accurate data for performance monitoring, a literature review has been given in Chapter 3 for all the possible parameters affecting the ship performance that vary during a ship in service, and the aspects involved when monitoring these parameters. Based on this review, it has been found that during acceleration, course deviation, drift, ship motion in waves, or sailing in shallow waters, the propeller characteristics, wake fraction as well as hull resistance change. Data should therefore be filtered for these transient conditions. Furthermore, variations in displacement affects ship performance in many ways and are difficult to account for. Performance should therefore be monitored in a narrow range of draft and trim variations. To account for changes in propeller absorbed torque due to propeller blade roughness, its roughness should be periodically measured by divers and corrections taken to account for the losses.

Apart from operational aspects, that affect performance monitoring, the measurement of physical characteristics should also be considered. Ship speed through water is the most important, but at the same time most difficult to measure parameter for performance monitoring. The measurement of ship speed is mainly affected by (wind driven) ocean currents and changes in the boundary layer of the hull. The measurements are therefore often too unreliable to be used for the performance analysis. Only by rational filtering, periods can be identified where the operation of the speed log can be considered

adequate. As an alternative for the speed log, the propeller characteristics in combination with the measured shaft torque and speed can be used to indicate the ship speed through water. The accuracy of the calculated ship speed, that has been indicated by GPD speed in this thesis, relies on the frequent calibration of the wake fraction, but is unaffected by hull or propeller fouling.

Shaft torque is the second most important parameter for performance monitoring. Shaft power is often related to fuel consumption, but as fuel flow is affected by many parameters and engine characteristics may vary due to wear, overhaul, timing adjustments and hull and propeller fouling, the long-term stability of this predicted figure of shaft power is questionable. A torque sensor on the propeller shaft is therefore the only way to separate engine from hull & propeller performance. Torque sensors are highly sensitive instruments and susceptible to drift. In order to monitor their reliability, they should be calibrated frequently.

Also the logging of the marine environment requires special care. Visual observations cannot provide the detail and accuracy required for the prediction of added wave and wind resistance. Improvements can be made by using wave statistics, forecast data, or wave radar installed on the ship to measure the wave characteristics underway. Wind speed measurement is best done using an anemometer, but is affected by wind distortion over the superstructure of the ship, which causes errors in wind load calculation. Other parameters that must be monitored to account for changes in performance include engine speed, ship speed over ground, air density, water depth, course over ground, heading and rudder angle. They can generally be measured with adequate accuracy. In order to obtain reliable data and allow data validation, filtering and conditioning, the data collection should be done automatically at a frequency of at least 1Hz.

Ship performance monitoring and analysis requires in-service speed-power data to be corrected to the standard (reference) conditions. There are various ways proposed in the open literature for this correction as discussed in detail in Chapter 2 of the thesis. Based on this discussion, it has been concluded that the most accurate way to correct ship performance to standard conditions is based on the correction of the delivered power on the basis of constant ship speed. A new analysis method has therefore been implemented

on the constant ship speed approach in order to calculate ship performance independent of engine or propeller performance. The propeller performance is isolated from the calculated performance by using periodical propeller surface roughness measurements and empirical calculation methods. One important assumption is hereby made that the change in thrust characteristics for moderate blade roughness may be neglected.

The correction of in-service performance to standard conditions is highly affected by the uncertainty in the measured ship speed. The replacement of the speed log by the GPD speed can therefore be a better choice for short-term performance monitoring. For long-term analysis however, the use of the GPD speed is not suitable, as it increases the sensitivity of the correction method to uncertainties in the measurement of torque, wake fraction and RPM and requires frequent calibration. The resulting large uncertainty in the KPIs makes it difficult to separate performance degradation from fouling and instrumentation errors.

The use of the GPD speed is particularly useful for direct performance indication to the operator on the bridge. Its accuracy relies on periodical calibration of the wake fraction, which can be measured during carefully selected periods where the speed log can be considered most accurate. By monitoring ship speed through water and over ground, transverse speed, torque, RPM, heading and wind direction simultaneously over a period of 2 hours, the periods where the speed log is likely to be least influenced by environmental conditions and currents may be identified. The same periods, in which the ship speed is assumed accurate, can be used for performance analysis for long-term condition monitoring.

The performance correction model based on the constant ship speed has been compared with a frequently used model based on the constant RPM. For long-term performance monitoring, the proposed model based on the constant ship speed provides a significant improvement in terms of robustness to errors in performance parameters and accounts for changes in added resistance more accurately. Performance deviations can best be expressed by percentage power loss at constant speed in relation to a pre-defined benchmark condition. Performance changes of the main engine are more difficult to identify. Deviations in specific fuel consumption cannot be related directly to deviations

in engine efficiency as SFC is affected by loading and environmental characteristics and affected by propeller and hull fouling.

Based on the investigations carried out in Chapter 3 and 4, the proposed data acquisition, conditioning and correction methodology has been developed into an algorithm for on-line PM&A system in Chapter 5. Based on this algorithm, the dedicated hard & software systems have been implemented in Chapter 5 on a 16m research vessel and a 300.000dwt VLCC and the implemented systems have been evaluated in the same chapter. Valuable insight has been gained into the installation, data collection, monitoring and analysis of the PM&A system on small and large vessels. The experiences with the research vessels have indicated that rational data filtering and signal validation is one of the most important aspects of performance monitoring.

The GPD speed can successfully be used for performance analysis but requires calibration of the wake fraction and propeller open water diagram using dedicated speed trials. While the implementation on small vessels is relatively easy, the calculation methods for the estimation of the added wind and wave resistance suffer accuracy. Automatic identification of the early development of fouling is therefore difficult due to large level of uncertainties involved.

The experiences with the VLCC indicated that the implementation of the PM&A system onboard large, merchant ships can be done within a short time frame. However, if new instrumentation is to be installed, e.g. shaft torque sensors, data validation is required to guarantee proper functioning. For a PM&A system to be accepted and relied upon by the crew, software layout and interfaces should be transparent and intuitive in use. Manual input, e.g. of wave characteristics, remains a weak aspect in data input even with highly intuitive user input interfaces. This uncertainty has direct consequences on the quality of the correction to added wave resistance. Using rational filtering, periods could be identified when the speed log is least affected by transient conditions, current or vessel drift. Fluctuations in KPIs of approx. $\pm 12\%$ could not be avoided due to the uncertainty in wave characteristics, ship speed and correction methods for loading, wind and waves.

6.3 Main conclusions

- This study has explored the viability of a real-time PM&A system focussing on data quality for the first time in the open literature by demonstrating its successful applications on two different size vessels
- The study indicated that the most important problem for inaccurate KPIs is the quality of input data. Only by real-time, automatic data acquisition and rational filtering can improve the accuracy and reliability of the input data
- The experiences with the PM&A systems implemented onboard the two vessels illustrated one important and common conclusion that a reliable torque sensor and Doppler log are the most important sensors for ship performance monitoring. The calibration of both sensors is also important to avoid misinterpretation of KPIs for performance assessment
- Practical difficulties associated with the measurement of ship speed through water suggest to use the propeller inflow speed. However, the GPD-based ship speed estimation requires regular calibration of the wake fraction in service and validation of the propeller characteristics using dedicated speed trials. Because of the uncertainty that is caused by this, the direct use of a Doppler speed log in carefully selected periods gives a more reliable estimate of ship speed for long-term performance monitoring
- Based on the experience with the data collection system of the both vessels it has been demonstrated that the automatic data acquisition and collection of the data during constant performance are the most accurate and the way ahead for an ideal PM&A system
- Controlling fouling growth and its effect on the ship performance for the dry-docking strategies is one of the main objectives of an accurate PM&A system, especially for ship anti-fouling manufacturers. Based upon the experience on both vessels and dedicated trails, it has been demonstrated that even with carefully conditioned and reliable performance data, scatter in KPIs remains fairly large (approx. $\pm 12\%$) for accurate definition of long-term trends, e.g. for evaluation of the effects of fouling. To be able to create statistically reliable trend lines, a large period of ship performance should be analysed, unless dedicated speed trials

under stipulated conditions are done. Reliability of the torque sensor and frequent calibration of the wake fraction is hereby important

- It has been demonstrated that the use of automatic collection of sea characteristics is crucial to further reduce the effects of performance indicators, but that the largest scatter in KPIs results from inaccuracies of speed logs
- It has been demonstrated that the design and implementation of a fully automatic, real-time, shipboard PM&A system is perfectly viable and can be installed on any ship with the use of reliable sensors

6.4 Recommendations for future work

As identified in the thesis, the most important aspects that cause scatter in performance indicators and that make it difficult to distillate the performance of anti-fouling coatings is the uncertainty of the ship speed through water and the uncertainty of the added wave resistance. In order to reduce scatter in KPIs even further so that it can be used to accurately determine the rate of growth due to fouling of the hull, further research should focus on the following aspects:

- Investigation into the exact causes of error of the speed log, so that methods can be developed to measure ship speed through water with higher reliability. Examples of improvement may be sensor location, sensor type (EM, AC or Doppler), multiple, interconnected sensors, calibration procedures etc.
- Improvement of added wave resistance prediction for the *Overseas Tanabe* by installing a wave radar or wave forecasting system and calculation of the added resistance response amplitude operators of the ship. It is expected that improved added wind resistance calculations reduce the scatter significantly. This can be achieved rather smartly by measuring the vessel motions on-line and combining the diffraction component through computations in a novel way.
- Long-term data collection and analysis on ships whereby all sensors are working correctly. The data collected on the *Overseas Tanabe* showed large gaps due to a broken power sensor. When more data is available, long-term trends can be derived more accurately and the accuracy of the proposed PM&A system to evaluate hull coatings can be evaluated.

Furthermore, the PM&A system can be expanded with additional features such as real-time performance optimisation feedback. Using the recorded ship performance data in different environmental and loading conditions together hydrodynamic relationships, an optimisation algorithm can be developed that provides operational decision support to the operator, specific for the actual capabilities of the vessel and conditions in which it sails. By giving forward predictions and feedback on actions taken, the reliability and accuracy of the system can be judged instantly by the user, which is important for acceptance onboard. Feedback can be given about optimal trim, optimal ship speed considering the

status of the hull (fouling), loading condition and environmental conditions and the consequences of changing course in terms of environmental loads.(Atlar et al. 2002a)

REFERENCES

- Abkowitz, M. A. (1980) "*Measurement of Hydrodynamic characteristics from ship maneuvering trials by system identification*" SNAME transactions, vol. 88 pp. 283-318
- Abkowitz, M. A. (1988) "*Measurement of ship resistance from simple trials during a regular voyage*" Report no. MA-RD-840-88019, Massachusetts institute of technology, Department of Ocean Engineering, Cambridge, Massachusetts
- Abkowitz, M. A. (1989) "*Use of system identification techniques to measure the ship resistance, powering and manoeuvring coefficients of the Exxon Philadelphia and a submarine from simple trials during a routine voyage*" 22nd American Towing Tank Conference 1989, p.363, St. John's, Canada
- Abramowski, T. (1999) "*Influence of the drift on ship's wake and propeller hydrodynamic characteristics*" HYDRONAV'99 - MANOEUVRING'99, pp. 151
- Aertssen, G., and Sluys, M. F. (1972) "*Service Performance and seakeeping trials on a large containership*" Trans Rina 1972, pp. 429
- Ambrogio, S. (2008) "*Ship CO2 emissions at 3.5 pct of global total: IMO*" uk.reuters.com. (accessed on 13-02-2008)
- Andersen, P., Borrod, A., and Blanchot, H. (2005) "*Evaluation of the service performance of ships*" Marine Technology, Vol. 42, No. 4. October 2005 pp. 177-183
- Ata, H., Hasselaar, T. W. F., and Atlar, M. (2006) "*Performance analysis on Qatar LNG vessels(confidential report)*" Newcastle University, Newcastle upon Tyne
- Atlar, M., Glover, E. J., and Candries, M. (2002a) "*Calculation of the effects of blade roughness on the performance of the propeller of M/T Guardian (Confidential)*" Report no. MT-2002-003, Newcastle University, Department of Marine Technology, Newcastle upon Tyne, UK
- Atlar, M., Glover, E. J., Candries, M., R.J., M., and Anderson, C. D. (2002b) "*The effect of a foul release coating on propeller performance*" ENSUS 2002: International Conference on Marine Science and technology for Environmental Sustainability, Newcastle upon Tyne, UK
- Atlar, M., Glover, E. J., Mutton, R. J., and Anderson, C. D. (2003) "*Calculation of the effects of new generation coatings on high speed propeller performance*" 2nd

- International Warship Cathodic Protection Symposium and Equipment Exhibition, Defence Academy of the United Kingdom, Shrivenham, UK
- Atlar, M., Hasselaar, T. W. F., and Wang, D. (2006) "*Comments on the performance analysis of the Yang Ming Transport Corp. Lines M-Class Containerships (confidential report)*" Marine Science and Technology department, Newcastle University UK, Newcastle Upon Tyne
- AVEVA (2007) "*TRIBON M2*" AVEVA Marine
- Baba, E., and Tokunga, K. (1980) "*Study of local roughness effect on ship resistance for effective cleaning and protection of hull surface*" Shipboard energy conservation symposium, p.315-330, New York, USA
- Babbedge, M. P. (1976) "*A statistical method of correcting log speeds*" Trans. RINA 1977, pp.121-124
- Barnes, J. (2008) "*Politicians to act on emissions if green initiatives stall*" Marine Engineers Review, April 2008 pp.40-42
- Bazari, Z. (2006) "*Ship energy performance benchmarking/rating: methodology and application*" World Maritime Technology Conference 2006, London, UK
- Berlekom, W. B. v. (1981) "*Wind forces on Modern ship forms - Effect on performance*" trans NECIES, vol 97 1980-1981 pp. 123
- Bhattacharyya, R. (1978) "*Dynamics of Marine Vehicles*" Wiley-interscience, ISBN 0471072060
- Binsfeld (2008) "*Binsfeld Engineering, Torque measurement on rotating shaft*" www.binsfeld.com (accessed 12-01-2009)
- Blendermann, W. (1996) "*Wind loading of ships - Collected data from wind tunnel tests in uniform flow*" Institut fur schiffbau der universitat Hamburg, Hamburg
- BMT-Fluid-Mechanics (2008) "*Global Wave Statistics Online*" www.globalwavestatisticsonline.com (accessed 20-03-2008)
- BMT-SeaTech (2004) "*SMARTpower monitors the effects of increasing hull fouling and hull roughness on current operational performance*" www.bmtseatech.co.uk (accessed 17-11-2004)
- BMT-SeaTech (2005) "*Hull Roughness*" www.bmtseatech.co.uk/bmt/html/products/hullroughness.html (accessed 1-2-2005)
- Bohlander, G. S. (1991) "*Biofilm effect on drag: measurement on ships*" Polymers in a Marine Environment; Marine Management (holdings), October 1991 (pp. 1-4),

-
- Borge, J. C. N., Reichert, K., and Dittmer, J. (1999) "*Use of nautical radar as a wave monitoring instrument*" Coastal Engineering, Vol. 37 (1999) pp. 331-342
- Bowditch, N. L. L. D. (2002) "*The American practical navigator*" National imagery and mapping agency, ISBN: 9780939837540
- Brix, J. (1990) "*Manoeuvring Technical Manual*" Schiff & Hafen / Kommandobrucke, Heft 4, 1990 pp. 47-48
- BSi (1996) "*Specification for petroleum fuels for marine oil engines and boilers*" B. S. Institute. British Standards Institute. BS MA 100:1996, ISO 8217:1996
- BSi (2000) "*Maritime navigation and radiocommunication equipment and systems - Marine speed and distance measuring equipment (SDME) - Performance requirements - Methods of testing and required test results*" B. S. Institute. British Standard. BS EN 61023:2000, IEC 61023:1999
- BSi (2007) "*Maritime navigation and radiocommunication equipment and systems - Marine speed and distance measuring equipment (SDME) - Performance requirements, methods of testing and required test results*" B. S. Institute. British Standards / European standard. EN 61023:2007
- C-Map (2003) "*C-Map World for windows*" CM Engine library version 3.02, C-Map Norway
- Candries, M., Atlar, M., and Anderson, C. D. (2001) "*Foul Release systems and drag. Consolidation of Technical Advances in the Protective and Marine Coatings Industry*" PCE 2001 Conference, pp.273-286, Antwerp, Belgium
- Candries, M. (2001) "*Drag, boundary-layer and roughness characteristics of marine surfaces coated with antifouling*" PhD thesis, Newcastle University,
- Candries, M., Atlar, M., and Anderson, C. D. (2003) "*Estimating the impact of new-generation antifouling on ship performance; the presence of slime*" Proceedings of IMAREST - Part A - Journal of Marine Engineering and Technology, Vol. 2003 No. 2 pp. 13-22
- Caprino, G., and Della Loggia, B. (1993) "*Recent developments on integrated ship performance monitoring systems*" 20th ITTC, pp.213-230,
- Carlton, J. S. (1994) "*Marine propellers and Propulsion*" Butterworth Heinemann, ISBN 075061143X

- Carlton, J. S., and Parsons, H. D. (1989) "*Ship service performance analysis - present capabilities and future trends*" IMAS 89 Applications of New Technology in Shipping, pp. 211, Athens
- Cefas (2008) "*Tyne/Tees WaveNet Site (WMO ID 62293), Deployment Id TYNETEESWN/001, Located at 54°55'.10N and 000°44'.85W in 65m of water*" www.cefas.co.uk/data/wavenet (accessed 19-06-2008)
- Coleman, H. W., and Steele, W. G. (1998) "*Experimentation and uncertainty analysis for engineers*" John Wiley & Sons inc., ISBN 0-471-12146-0
- Conn, J. F. C., Lackenby, H., and Walker, W. P. (1953) "*Resistance experiments on the Lucy Ashton*" Trans INA, vol. 93 (pp. 40-57),
- Consilium (2009) "*Manual SAL R1a Speed log*" Consilium AS, Stockholm, Sweden
- Cooper, D. (1995) "*NSMB-CRS Full scale monitoring working group*" report no. 2920410.1, BMT SeaTech Ltd, Southampton
- Cotton, P. D., Lindgren, G., Rychlik, I., M., O., P., P., Nerzic, R., C., L., P., B., and G., P. (2000) "*COMKISS (Conveying Metocean Knowledge Improvements onto Shipping Safety- Supported by CEO of the European Commission)*" report no. ENV4-CT98-0751, Satobsys,
- DNV (2009) "*Clean notation*" www.dnv.com/industry/maritime/servicesolutions/classification/notations/additional/clean.asp (accessed 24-11-2009)
- Ewing, J., and Carter, D. (1998) "*Wave data: observed, measured and hindcast*" Guide to wave analysis and forecasting, W. M. O. G. Switzerland, ed. WMO
- Faltinsen, O. M., and Minsaas, K. J. (1984) "*Added Resistance in waves*" NECIES Centenary conference on marine propulsion NEC100, Newcastle upon Tyne, UK
- Faltinsen, O. M., Minsaas, K. J., Liapis, N., and S.O., S. (1980) "*Prediction of resistance and propulsion of a ship in a seaway*" 13th Symposium on Naval Hydrodynamics, pp.505, Tokyo
- Ferguson, A. M. (1984) "*An extrapolation method for ship resistance based on the variation of sinkage and trim with Froude Number*" Trans RINA, Vol. 126 pp.17-32
- Ferreira, O. C. (1998) "*Efficiency of internal combustion engines*" Journal of Economy & Energy, Year II No 7 Mar/Apr 1998

-
- Fleming, W. J. (1982) "*Automotive torque measurement: a summary of seven different methods*" IEEE transactions on vehicular technology, vol. VT-31, No 3, August 1982 p.117-124
- Flikkema, M. (2008) "*Conference presentation: Service Performance Analysis*" Condition Monitoring Conference, London
- Force-Technology (2008) "*Seatrend - Performance monitoring of ships in service*" www.simflex.dk/cms/site.aspx?p=6034 (accessed 05-08-2008)
- Gaganatsios, D. (2007) "*Resistance Envelope of RV Bernicia*" MSc Thesis, Newcastle University, Newcastle upon Tyne, UK
- Gangadharan, S. N., Schultz, M. P., Collino, B., Clark, A., and Wimberly, C. (2001) "*Experimental investigation of enteromorpha clathra biofouling on lifting surfaces on marine vehicles*" Marine Technology, Vol. 38 January 2001 (No.1), pp.31-50
- Garg, B. R. (1972) "*The service performance of ships with special reference to tankers*" MSc. Thesis, University of Newcastle upon Tyne, Newcastle upon Tyne
- Gerritsma, J., and Beukelman, W. (1972) "*Analysis of the resistance increase in waves of a fast cargo ship*" International Shipbuilding Progress, Vol. 19, No. 217 september pp. 285-293
- GL (2007) "*Germanischer Lloyd: Guidelines for the Environmental Service System Section 2: Environmental Passport*" VI - part 12 Section 2 B Environmental passport GL 2007,
- Glover, E. J. (1987) "*Propulsive devices for improved propulsive efficiency*" Transactions of Institute of marine engineers, vol. 99 (paper 31), pp.23-9
- Google (2008) "*Google Earth v.4.2.0205.5730*" IMAGE @ 2009 Terrametrics, 2008 Europa Technology
- Grigson, C. (1990) "*Screws working in behind and prediction of the performance of full ships*" Journal of Ship Research, Vol. 34, No. 4 pp.262-282
- Grønlie, Ø. (2004) "*Wave radars, A comparison of concepts and techniques*" Hydro International, 2004
- Grossman, G., and Kloster, Y. (1993) "*Matching ship, propeller and main engine for worldwide service*" ICMES 93. Marine System Design and Operation, pp. 91-104,
- Guedes Soares, C., Fonseca, N., and Ramos, J. (1998) "*Prediction of voyage duration with weather constraints*" Int. Conf. Ship motions and manoeuvrability,

-
- Gulev, S. K., and Hasse, L. (1998) "*North Atlantic wind waves and wind stress fields from voluntary observing data*" J. Phys. Oceanogr., vol. 28 pp. 1107-1130
- Gursoy, O. (2006) "*Propeller design and performance analysis of MAST R/V Bernicia*" Newcastle University, Newcastle upon Tyne
- Harvald, S. A. (1950) "*Wake of Merchant Ships*" The Danish technical press, Copenhagen,
- Harvald, S. A. (1983) "*Resistance and propulsion of ships*" Wiley-interscience, ISBN: 0471063533
- Hasselaar, T. W. F. (2005a) "*A note on the performance analysis of the SS AL ZUBARAH. (Confidential report to International Paint)*" Newcastle University, Newcastle Upon Tyne
- Hasselaar, T. W. F. (2005b) Personal Communication "*Statistical analysis on the performance of the SS. Al Zubarah (Confidential report to International Paint)*" with C. Anderson 04 November 2005 17:19
- Hasselaar, T. W. F. (2006) Personal Communication "*Remarks / Questions with respect to the Vessel performance analysis report of the SS. Al-Zubarah (report dated 2004-12-02) from M.O. Marine Consulting*" with C. Anderson 25-08-2006
- Hasselaar, T. W. F. (2007) "*PM&A User Manual & DAQ interface characteristics: Ship performance monitoring system: MT OVERSEAS TANABE*" No. MT-2007-033, Feb 2007, University of Newcastle upon Tyne, School of Marine Science and Technology, Emerson Cavitation Tunnel, Newcastle upon Tyne, UK
- Hasselaar, T. W. F. (2008) "*Performance monitoring on R.V. Bernicia: Sensor and instrument specifications. Amended edition April 2008 of November 2006*" No. MT-2008-021, Apr 2008, amended edition of Report No. MT-2006-057, Nov 2006, University of Newcastle upon Tyne, School of Marine Science and Technology, Emerson Cavitation Tunnel,
- Havelock, T. H. (1942) "*Drifting force on a ship among waves*" Philosophical Magazine, Vol. 33
- Heijde, M. v. d. (2008) Personal Communication "*Torque measurement*" with T. W. F. Hasselaar March 2008
- Hitachi-Zosen (2001) "*Test results of Shop Trial MAN-B&W 7S80MC MK6*" Hitachi Zosen Diesel & Engineering Co., Ltd. Production Department,
-

-
- Hitachi-Zosen (2002) "*Instruction book for Hitachi Zosen - MAN B&W Diesel Engine*"
MAN B&W,
- Holtrop, J. (1984) "*A statistical re-analysis of resistance and propulsion data*"
International Shipbuilding Progress, Vol. 28 (n. 363, november) pp.272-276
- HSVA (1997) "*Model tests for a 2400 TEU Container ship*" Report WP 8/97, HSVA,
Hamburg
- Hundley, L. L., and Tsai, S. (1992) "*The use of propulsion shaft torque and speed
measurements to improve the life cycle performance of U.S. Naval ships*" Naval
Engineers Journal, November 1992, v.104 pp.43
- Hylarides, S. (1974) "*Thrust measurement by strain gauge without the influence of
torque*" Shipping world & shipbuilder, December 1974 pp.1259-1260
- IAGS (2008) "*The Future of Oil*" [www. iags.org/futureofoil.html](http://www.iags.org/futureofoil.html) (accessed 09-05-2008)
- IMO (2005) "*Interim guidelines for voluntary ship CO2 emission indexing for use in
trials*" MEPC Circular 471, 29 July 2005, IMO, London, UK,
- IMO (2007) "*International Maritime Organization website*" [www. imo.org/](http://www.imo.org/) (accessed 3-
8-2007)
- IMO (2008) "*IMO environment meeting approves revised regulations on ship emissions*"
www.imo.org. London, (accessed on 4 april 2008)
- IMO (2009) "*Marine Environment Protection Commitee (MEPC) 59th session*" [www.
imo.org](http://www.imo.org) (accessed 16-10-2009)
- InCoreTec (2005) "*Ship Predictor System ("SPS")*" [www. incoretec.com](http://www.incoretec.com) (accessed 19-
09-2005)
- International (2004) "*Hull Roughness Penalty Calculator Brochure*" [www. international-
marine.com/newbuilding/brochures/HRPCFolder&Paper.pdf](http://www.international-marine.com/newbuilding/brochures/HRPCFolder&Paper.pdf) (accessed 1-5-2008)
- International (2005) "*Hull Roughness Penalty Calculator Brochure*"
[http://www.international-
marine.com/newbuilding/brochures/HRPCFolder&Paper.pdf](http://www.international-marine.com/newbuilding/brochures/HRPCFolder&Paper.pdf) (accessed 1-2-2005)
- Inukai, Y., and Ochi, F. (2009) "*A study on the characteristics of self-propulsion factors
for a ship equipped with Contra-Rotating Propeller*" First International
Symposium on Marine Propulsors, smp'09, Trondheim, Norway, June 2009
- ISO15016 (2002) "*Ships and marine technology - Guidelines for the assessment of speed
and power performance by analysis of speed trial data*" I. Standard. International
Standard organisation. 15016, 2002-06-15, first edition
-

-
- ISO-9875 (2001) "*Ships and marine technology — Marine echo-sounding equipment*" I. Standard. International Standard organisation. EN ISO 9875:2001
- ITTC (1972) "*Technical decisions and recommendations of the seakeeping committee*" 12th and 13th ITTC, Rome, 1969 and Berlin, 1972
- ITTC (1978) "*Report of Performance committee*" proceedings of the 15th ITTC, the Hague, The Netherlands
- ITTC (1981) "*Reports of the Seakeeping and Power performance committees*" 16th ITTC, Leningrad, Russia
- ITTC (1999a) "*22th ITTC – Recommended Procedures: Appendix 4: 1. Sample DTMB ISO 9000 Work instruction: Thrustmeter Calibration*" ITTC,
- ITTC (1999b) "*Added resistance*" 22nd ITTC, Chapter 9 page 34, Seoul, Shanghai
- ITTC (1999c) "*The specialist committee on Trials and Monitoring, Final report*" 22nd ITTC, Seoul, Shanghai
- ITTC (2002a) "*Full Scale Measurements: Speed and Power Trials: Instrumentation, Installation and Calibration*" 23rd ITTC, Venice
- ITTC (2002b) "*The specialist Committee on Waves*" 23rd International Towing Tank Conference, pp. 497-543, Venice, Italy
- ITTC (2002c) "*The specialist Committee on Speed and Powering Trials*" Proceedings of the 23rd ITTC, Vol. II pp. 341- 367
- Jensen, S. H. (2009) "*Marine Diesel Engines - Improvements on the Efficiency*" http://www.dtu.dk/upload/institutter/kt/nyheder/cccs_pres/man_diesel-soeren_h_jensen.pdf (accessed 9-11-2010)
- Jorgensen, H. D., and Prohaska, C. W. (1966) "*Report of performance committee, Appendix IV: Wind Resistance*" 11th ITTC, p.123, Tokyo
- Journée, J. M. J. (2003) "*Review of the 1979 and 1980 Full-Scale Experiments Onboard Containership m.v. Hollandia*" 1349, Ship Hydromechanics Laboratory, Delft University of Technology,
- Journée, J. M. J., Rijke, R. J., and Verleg, G. J. H. (1987) "*Marine Performance Surveillance with a Personal Computer*" Automation Days 87, Helsinki, Finland
- Kan, S., Shiba, H., Tsuchida, K., and Yokoo, K. (1958) "*Effect of fouling of a ship's hull and propeller upon propulsive performance*" International Shipbuilding Progress, Vol. 5 No. 41 pp.15-34

-
- Kanerva, M., and Salana, H. (2004) "*Elements for environmentally sustainable ship design*" Deltamarin Ltd., Raisio, Finland
- Kempf, G. (1937) "*On the effect of roughness on the resistance of ships*" Trans INA, vol. 79 pp. 109-119
- Kent, E. C., and Taylor, P. K. (1997) "*Choice of a Beaufort Equivalent Scale.*" J. Atmos. & Oceanic Tech., V14(2) pp. 228 - 242.
- Kim, E., Yoon, H. S., Hong, S. Y., and Choi, Y. (2001) "*Evaluation and computer program on the speed trial analysis method of the ongoing work in ISO/TC8*" Practical Design of Ships and Other Floating Structures: Eighth International Symposium - PRADS 2001, p. 525,
- Kim, S. Y., and Lewkowicz, A. K. (1992) "*Computation of the surface roughness effects on a slender ship-hull*" ISP, Vol. 39 pp 5-18
- KleinWoud, H., and Stapersma, D. (2002) "*Design of propulsion and electric power generation systems*" IMarEST,
- Knaggs, T. (2006) "*Trim optimisation for reduction of bunker costs*" The Naval Architect, april 2006 p.29
- KRAL (2005) "*KRAL Volumeter - Fuel consumption measurement for diesel engines*" www.kral.at/catalog/start2_en.htm (accessed 7-1-2005)
- Kresic, M., and Haskell, B. (1983) "*Effects of propeller design-point definition on the performance of a propeller/diesel engine system with regard to in-service roughness and weather conditions*" Trans. SNAME, Vol. 91 pp. 195-224
- Kubo, M., Mizui, S., and Uemura, K. (1997) "*Mooring Problems in Ports Facing to Open Sea*" Journal of the Japan Institute of Navigation, Vol. 96 pp. 9-15
- Kuiper, G., Grimm, M., McNeice, B., Noble, D., and Krikke, M. (2002) "*Propeller inflow at full scale during a manoeuvre*" 24th Symposium on Naval Hydrodynamics, Fukuoka, Japan
- Kwon, Y. J. (1981) "*The effect of weather, particularly short sea waves, on ship speed performance*" PhD thesis, University of Newcastle upon Tyne, UK,
- Kwon, Y. J. (2008) "*Speed loss due to added resistance in wind and waves*" Naval Architect, march 2008 p.14-16
- KYMA (2006) "*Kyma Ship Performance*" <http://www.kyma.no/products/kymashipperformance> (accessed 13-09-2008)

- Kyrtatos, N. P., Theotokatos, K., and Xiros, N. I. (2000) "*Main engine control for heavy weather conditions: The ACME project*" 6th international symposium on marine engineering, Tokyo, Japan
- Lackenby, H. (1961) "*Note on the effect of shallow water on ship resistance*" Report No. 377, British shipbuilding research association BSRA, London
- Lee, C.-S. (1983) "*Propeller in waves - state of art -*" PRADS 83 - The 2nd International Symposium on Practical design in shipbuilding, p.139, Tokyo & Seoul
- Lewthwaite, J., C., Molland, A. F., and Thomas, K. W. (1985) "*An investigation into the variation of ship skin frictional resistance with fouling*" Trans RINA, Vol. 127 (pp. 88-94),
- Lloyd, A. R. J. M. (1998) "*Seakeeping*" Lloyd, Gosport, Hampshire, UK, ISBN: 0953263401
- LloydsList (2009) "*Future of Shipping - Shipping and the Environment - December 2009 - IMO Targets Newbuilding Design Improvements*" www.lloydslist.com/ipi/futureofshipping/article.jsp?pageid=imo-targets-newbuilding-design-improvements (accessed 12-02-2010)
- Logan, K. P., Reid, R. E., and Williams, V. E. (1980) "*Considerations in establishing a speed performance monitoring system for merchant ships - Part 1. Techniques based on propeller relationships - Part 2*" Shipboard Energy Conservation Symposium, pp93-135, New York city
- LR (2007) "*Environmental protection*" www.lr.org/Industries/Marine/Services/Classification/Environmental+protection.htm (accessed 5-5-2007)
- MAN-Diesel (2008) "*Basic principles of ship propulsion*" MAN Diesel,
- MarineNorway (2008) "*Panama accepts electronic logbooks*" <http://marinenorway.com/sider/tekst.asp?side=2344> (accessed 19-6-2008)
- MARINTEK (2005) "*SOPRANweb (Ship Operation Analysis software)*" <https://raga4.marintek.sintef.no/sopran> (accessed 03-11-2006)
- McGillivray, J. (1997) "*The aging of diesel engine combustion components and their associated effect on performance and emissions*" 11th International Maritime and Shipping Conference IMAS 97, pp. 71-77,
- McMahon, T. (2009) "*Inflation Adjusted Oil Price Chart*" www.inflationdata.com (accessed 11-10-2009)

-
- MICAD (2008) "*Micad Marine Real time Marine information systems*" www.micadmarine.com (accessed 12-02-2010)
- Miemois, M. (2006) "*CIMAC – Power Wartsila*" CIMAC Circle, SMM 2006, Hamburg, Germany
- Miller, M. L. (1963) "*A note on sinkage and squat*" Bureau of ships journal,
- Mitsuyasu, H., and Mizuno, S. (1976) "*Directional spectra of ocean surface waves*" 15th Coastal engineering conference, pp.329-348, Honolulu, Hawaii
- Moat, B. I., Yelland, M. J., Pascal, R. W., and Molland, A. F. (2005) "*An Overview Of The Airflow Distortion At Anemometer Sites On Ships*" Southampton Oceanography Centre, UK,
- MOL (2003) "*TOMAS Analysis system - operational manual*" Mitsui O.S.K. Lines. Marine engineering group / marine division,
- Moller, C. E. (2008) "*Future emissions grossly underestimated*" Tanker Operator, May 2008 p.6
- Moor, D. I., and O'Connor, F. R. C. (1964) "*Resistance and propulsion factors of single-screw ships at fractional draught*" trans NECIES 1963, pp.185-202
- Mosaad, M. A. (1986) "*Marine propeller roughness penalties*" PhD Thesis, University of Newcastle upon Tyne, Newcastle upon Tyne
- Munk, T. (2006a) "*Evaluating Hull coatings for precise impact on vessel performance*" Paint and Coatings Expo Tampa PACE2006, Florida USA
- Munk, T. (2006b) "*Fuel conservation through managing hull resistance*" Motorship / BIMCO Propulsion Conference, Copenhagen, Denmark
- Musker, A. J. (1977) "*Turbulent shear-flows near irregularly rough surfaces with Particular reference to ship hulls*" PhD Thesis, University of Liverpool,
- Mutton, R. J. (2003) "*The effect of a foul release coating on the propeller of the research vessel 'Bernicia'*" MT-2003-048, School of Marine Science and Technology, Newcastle University, Newcastle upon Tyn
- Nakamura, S., and Fujii, H. (1977) "*Nomial speed loss of ships in waves*" PRADS- International symposium on practical design in shipbuilding, pp. 373-380, Tokyo
- Nakamura, S., and Naito, S. (1977) "*Propulsive performance of a container ship in waves*" Naval Architecture and Ocean Engineering, SNAJ, Vol. 15 (paper 3),
- NCS (2008) "*FuelTrax - real-time fuel monitoring system*" www.fueltrax.com (accessed 12-02-2010)
-

-
- NDBC (2005) "*Ocean Current Profile for Buoy*" www.ndbc.noaa.gov (accessed 20-04-2005)
- NGDC (2008) "*2-minute Gridded Global Relief*" NOAA, National Geophysical Data Center (NGDC),
- NI (2004) "*LabVIEW 7.1*" National Instruments corp.
- NOAA (2008a) "*Sea Surface Temperature (SST) Contour Charts - Global 50 km resolution (with ice)*" www.osdpd.noaa.gov/PSB/EPS/SST/contour.html (accessed 15-8-2008)
- NOAA (2008b) "*The WMO Voluntary Observing Ships (VOS) Scheme*" www.vos.noaa.gov/vos_scheme.shtml (accessed 12-06-2008)
- Nortek (2007) "*Vectrino Doppler log*" www.nortek-as.com (accessed
- O'Mahony, H. (2007) "*A very green Emerald*" The Naval Architect, August 2006
- OceanWaveS (2004) "*WaMoS II CFAV Quest Trial Q279*" Sea-Image Communications Ltd./ OceanWaveS GmbH,
- OCIMF (1977) "*Prediction of wind and current loads on VLCCs*" OCIMF London, England,
- OCIMF (1994) "*Prediction of wind and current loads on VLCCs*" OCIMF London, England,
- ODAC (2008) "*Peak Oil Primer*" www.odac-info.org/overview.htm (accessed 01-05-2008)
- Oosterveld, M. W. C., and Oossanen, P. v. (1975) "*Further Computer-Analyzed Data of Wageningen B-Screw Series*" Int. Shipbuilding Progress, Vol. 22, No. 251, July 1975
- Orton-Jones, C. (2007) "*Shipping forecast: as East Asian factories multiply and more ports worldwide reach capacity, Charles Orton-Jones spots a storm brewing. How will your business fare if it has to wait for its ship to come in?*" Financial Management (UK). (accessed on Nov. 2007)
- OSI (2010) "*Performance Monitoring and Analysis system*" www.ocean-systems.com/perform.htm (accessed 19-3-2010)
- Ostojic, B. J. (1990) "*MOTORMAAN - the engine performance monitoring / control computer aided system*" International Conference on modelling and control of marine craft, pp.136-147, Exeter UK

-
- Pierson, W. J., and Moskowitz, L. (1964) "*A proposed spectral form for fully developed wind seas based on the similarity theory of S.A. Kitaigorodskii.*" J. Geophysical Research, Vol. 69 pp. 5181–5190
- Richardson, P. L. (1997) "*Drifting in the wind: leeway error in shipdrift data*" Deep-Sea Research, Vol. 44, no. 1 pp.1877-1903
- RINA (2007) "*Green star design: additional class notation and logo*" http://marine.rina.org/_files/pdf/green_star_design.pdf (accessed 24-07-2008)
- Rocchi, R. (1994) "*Delivered power - trim and sinkage - ship hull forms: an analysis of the effects of the trim variations on the power performance of a class of modern container ships*" Fifth Int. Conf. on computer aided manufacturing and operation in the Marine, Offshore and Ice technology industries, pp265-274,
- Rodriguez, G., Guedes Soares, C., Pacheco, M., and Pérez-Martell, E. (2002) "*Wave Height Distribution in Mixed Sea States*" Journal of Offshore Mechanics and Arctic Engineering, Volume 124, Issue 1 pp. 34-40
- Ross, S. (2003) "*Peirce's Criterion for the Elimination of Suspect Experimental Data*" J. Engr. Technology, Fall, 2003
- SAM (1998) "*General Description Doppler log Atlas DOLOG 23*" Dolog 23, Atlas-Elektronik GmbH, Bremen,
- Sampson, R. (2004) "*Preliminary propeller analysis of the RV Bernicia propeller*" Emerson Cavitation Tunnel, School of Marine Science and Technology, Newcastle University UK, Newcastle upon Tyne
- Schmiechen, M. (1991a) "*Lecture notes of M. Schmiechen and Oral discussions*" 2nd international workshop on the rational theory of ship hull-propeller interaction and its applications, pp41, Berlin
- Schmiechen, M. (1991b) "*Propulsive performance of METEOR and her model identified from quasi-steady propulsion tests*" Proceedings 2nd INTERACTION Berlin '91, Berlin
- Schmiechen, M. (1998) "*Contribution concerning a proposed ISO Standard "guidelines for the assessment of ship speed and power performance by means of speed trials"*" <http://www.m-schmiechen.homepage.t-online.de/> (accessed 17-04-2007)
- Schoenherr, K. E. (1931) "*On the analysis of ship trial data*" Transactions of the Society of Naval Architects & Marine Engineers, pp.281-301

-
- Schultz, M. P. (2007) "*Effects of coating roughness and biofouling on ship resistance and powering*" *Biofouling*, 23(5) 331-341
- Scott, J. R. (1971) "*Voyage performance of M.V. Protesilaus*" *Trans. Rina* 1971, p.287
- Skipper (2009) "*SKIPPER DL850 2-Axis Doppler Log. Operation and Installation Manual*" 20030401Bsw3.26, Skipper Electronics AS, Oslo, Norway
- SNAME (1989a) "*Guide for Sea trials*" Ships machinery committee, Panel M-19 (Ship Trials), Technical & Research bulletin 3-47,
- SNAME (1989b) "*Principles of Naval Architecture Vol 3*" SNAME,
- SNAME (1989c) "*Principles of Naval Architecture Vol. 2*" SNAME,
- Stapersma, D. (2003) "*Diesel engines B. Lecture Notes course WB4408b*" Delft University of Technology,
- Stapersma, D. (2005) "*Marine fuel oils. Chapter 11 from lecture notes Professor Stapersma. Course wb4408b TUDelft*" Delft University of Technology,
- Steier, S. (2009) Personal Communication "*Personal correspondence regarding operation of Doppler and EM logs*" with T. Hasselaar october 2009
- Strom-Tejsen, J., Yeh, H. Y. H., and Moran, D. D. (1973) "*Added resistance in waves*" *Trans. SNAME*, Vol. 81 p.109
- Suzuki, T., Nakato, M., Uchida, M., and Lewkowicz, A. (1992) "*Thrust measurement techniques in sea trial conditions: assessment and new developments*" PRADS '92, pp1.403, Newcastle upon Tyne
- Svensen, T. E. (1983) "*The economics of hull and propeller maintenance examined in the face of uncertainty*" *Trans NECIES*, okt. 1983 p.11
- Svensen, T. E., and Medhurst, J. S. (1984) "*A simplified method for the assessment of propeller roughness penalties*" *Marine Technology*, Vol. 21. No.1 Jan. 1984 pp. 41-48
- Swaan, W. A., and Rijken, H. (1964) "*Speed loss at sea as a function of longitudinal weight distribution*" *Trans NECIES*,
- Szantyr, J. A., and Glover, E. J. (1990) "*UPCA91 - The lifting surface program for unsteady propeller cavitation analysis. Instructions for the User.*" Emerson Tunnel report No. 3/90, Department of Marine Technology, Newcastle University, UK

-
- Takahishi, M., Umeno, M., and Higasa, N. (1984) "*An analysis on Variation of Propeller Immersion*" Bulletin of Marine Engineering Society of Japan (MESJ), Vol 12, no. 1 pp13-20
- Taniguchi, K., and Tamura, K. (1966) "*Appendix XI: On a new method of correction for wind resistance relating to the analysis of speed trial results*" 11th ITTC, pp. 144-149, Tokyo
- Taylor, P. K., and Kent, E. (1999) "*The Accuracy Of Meteorological Observations From Voluntary Observing Ships - Present Status And Future Requirements.*" James Rennell Division for Ocean Circulation and Climate, Southampton Oceanography Centre, UK,
- Taylor, P. K., Kent, E., Yelland, M., and Moat, B. (1994) "*The Accuracy of Wind Observations from Ships*" International COADS Winds Workshop, Institut für Meereskunde in Kiel, Germany.
- Telfer, E. V. (1926) "*The practical analysis of merchant ship trials and service performance*" trans NECIES 1926-1927, Vol. 43
- Telfer, E. V. (1972) "*Some Loose ends in Retrospect*" trans NECIES, Vol. 89 1972-1973
- Thomson, G. R. (1978) "*BSRA Standard Method of speed trial analysis*" Report NS466-1978, British Ship Research Association,
- Toki, N. (2005) "*Monitoring of Service Performance of a ROPAX Ferry*" 24th ITTC Group discussion on Full Scale Trial, Japan
- Townsin, R. I., Medhurst, J. S., Hamlin, N. A., and Sedat, B. S. (1984) "*Progress in calculating the resistance of ships with homogeneous or distributed roughness*" NEC 100: NECIES Century Conference on Marine Propulsion, Newcastle upon Tyne, UK
- Townsin, R. L. (2002) "*Discussions on proceedings of the specialist committee on procedures for Resistance, POW Tests*" 23rd International Towing Tank Conference, p700
- Townsin, R. L. (2003) "*The ship hull fouling penalty*" Biofouling 2003, Vol 19 (supplement) pp9-15
- Townsin, R. L., Byrne, D., Svensen, T. E., and Milne, A. (1986) "*Fuel Economy due to Improvements in Ships Hull Surface Condition* " International Shipbuilding Progress, Vol. 33 p.383

- Townsin, R. L., Byrne, D., T., S., and A., M. (1981) "*Estimating the technical and economic penalties of hull and propeller roughness*" trans SNAME, vol. 89 pp295-318
- Townsin, R. L., Moss, B., Wynne, J. B., and Whyte, I. M. (1975) "*Monitoring the speed performance of ships*" NECIES transactions, vol. 91, 1974-1975 pp.159
- Townsin, R. L., Spencer, D. S., Mosaad, M. A., and Patience, G. (1985) "*Rough propeller penalties*" SNAME transactions 1985, Vol. 93 pp.165-187
- Townsin, R. L., and Svensen, T. (1980) "*Monitoring speed and power for fuel economy*" Shipboard Energy Conservation Symposium, pp135-150, New York City
- Tsuda, N. (2008) "*Towards a reality-based CO2 index*" The Naval Architect, June 2008 pp. 38
- Tsugane, M., and Kagoyashi, H. (1987) "*A study of optimum trim for energy saving (in Japanese)*" Journal of Japan institute of navigation, vol. 77 pp.163-173
- UCLA (2008) "*Temperature Density Salinity Conversion Chart*" UCLA Marine Science Center OceanGLOBE, Los Angeles, CA
- UPCA91 (2005) "*UPCA91 - the lifting surface program for unsteady propeller cavitation analysis*" report No. 3/90, Department of Marine Technology, Newcastle University, UK and Institute of fluid flow machinery, Polish academy of sciences, Gdansk, Poland,
- Wallentin, B. (2004) "*The smoothing effect of TBT-free antifoulings*" www .jotun.com (accessed 12-06-2008)
- Wan, B., Nishikawa, E., and M., U. (2002) "*The Experiment And Numerical Calculation Of Propeller Performance With Surface Roughness Effects*" Journal of the Kansai Society of Naval Architects, Japan (KSNAJ), No.238, (Sep., 2002) pp49-54
- Wang, D. (2007) Personal Communication "*Personal correspondence regarding the design of an open water diagram for the RV Bernicia using propeller geometry measurements*" with
- Warkman, D. C. (1983) "*Performance monitoring based on an MIP calculator*" Marine Engineers Review, April 1983 pp. 88-11
- Wärtsilä (2004) "*Trial Report 7 RTA 72 U-B*" Wärtsilä Italia S.p.A,
- Watanabe, S., Nagamatsu, N., and Yokoo, K. (1969) "*The augmentation in frictional resistance due to slime*" J. Kansai Soc. Naval Architecture of Japan, March, No. 131 1969 p. 45

- Woodyard, D. (1998) "*Pounder's Marine Diesel Engines*" Butterworth Heinemann, 0 7506 2583 X
- Xiros, N. I., and Kyrtatos, N. P. (2000) "*A neural predictor of propeller load demand for improved control of diesel ship propulsion*" 15th IEEE International symposium on Intelligent control (ISIC 2000), Rio, Patras, Greece
- Yelland, M. J., Moat, B. I., and Taylor, P. K. (1998) "*Air-flow distortion around voluntary observing ships*" Contract report for AES and BIO, Southampton, UK, Southampton Oceanography Centre, 32pp.,
- Yoshino, I., and Matsumura, T. (1997) "*Application of speed correction method against waves at speed trial*" NAV 97, Intl Conf on Ship and Shipping Research, pp3.15, Sorrento, Italy
- Zin, C. T. (2008) "*Bunker costs threaten global box traffic*" portworld.com. (accessed on 05-05-2008)

APPENDIX A: DESIGN CHECKLIST PM&A SYSTEM

The following checklist describes practical requirements for the design and implementation of a PM&A system. The theoretical rationale behind the requirements, and the algorithms describing data conditioning, filtering and analysis are not described here, but follow from chapters 3 and 4 of this thesis. The design requirements are split into data collection and performance indication.

Data collection

Table A-1 lists, in order of importance, the parameters that must be logged continuously (at 1Hz) (●), or periodically (○). The periodical measurements may be done manually. However, this requires an unambiguous and intuitive user interface so that no confusion is possible where and how the information should be obtained from. Moreover, because each variable requires logging at different intervals, a function should be included that reminds the user when input is required by means of a visual and audible warning. To avoid hindrance of the system in periods where all attention should go to ship operation, e.g. during manoeuvring or in passages in narrow waterways, the warnings should be ceased until a more suitable period has occurred. Depending on ship operation, periods where the system should not request user input may be identified by monitoring position, engine speed, water depth, time, course deviations etc.

To be able to correct ship performance to standard conditions, a number of ship specific hydrostatic and hydrodynamic characteristics are required. They are available during the design of each ship and may be obtained from the yard the ship is build. Table A-1 lists the data required. Because the static data is for each ship different, the performance monitoring system build for one vessel cannot be implemented directly in other vessels. Apart from the static data, the data collection system should be adjusted for the characteristics and availability of sensors. Performance filtering characteristics may need re-adjustment and user interfaces for manual data entry need to be redesigned to guarantee clarity and unambiguosity.

The calibration of the torque sensor is one of the most important aspects of performance monitoring. Even if a system is installed, that claims not to drift over time, a procedure to periodically validate this claim is necessary. Torque calibration is a time consuming task that cannot be automated. It requires the use of the turning gear, which is manually operated and restricts the maintenance on the main engine during use. To get full cooperation of the crew, the reasoning behind doing periodical calibrations, even if the sensor has not shown any significant drift in a long time, should be clear. By giving insight in the long-term condition monitoring, the uncertainty margin of the output from the torque sensor, added resistance components and hull fouling can be made clear. The importance of being able to isolate the errors caused by the torque sensor can then be understood by the crew themselves. This increases their feeling of responsibility and challenges to execute the calibrations as good as possible.

At low revolutions, the torque is less stable and when the propeller is not rotating, currents cause a propeller load which may cause confusion. In many power measurement systems, the readings are automatically forced to zero when the RPM drops under a certain limit. This avoids however the user to get an insight into the possible offset. The torque sensor should therefore be configured so that even at low RPM the torque is displayed.

Table A-1: Variables required for PM&A, in order of importance

Dynamic data	Static data
<ul style="list-style-type: none"> • Ship speed through water • Torque • Engine speed • Wind speed & direction • Wave parameters ○ Draft and trim • Fuel consumption • Course and Heading • Speed over ground • Water depth • Fuel characteristics • Air density ○ Water temperature ○ Propeller roughness • Rudder angle • (Ship motion) 	<ul style="list-style-type: none"> • Propeller characteristics (offset) • Propeller open water diagram • Sea trial results (standard condition) • Wind resistance coefficient C_x • Windage area • Hull offset data or seakeeping characteristics • Thrust deduction fraction for range of loading conditions • Ship's hydrostatics • Self propulsion model test results for range of loading conditions

Most data is collected with a sampling frequency of 1Hz. The PM&A system uses this information directly to calculate a single or few performance indicators, which are saved to disc periodically. The raw, unconditioned data forms however a valuable source of information to other, non performance monitoring related systems, such as training, simulation, and development of performance optimisation systems. With data storage becoming cheap and practically without size limitation, the raw data can be stored on removable media (e.g. DVD) in an easy to read format (e.g. txt format) with clear, unambiguous headings.

System implementation

The human-machine system interaction for performance monitoring systems is the most important aspect for successful implementation. On merchant ships, crew changes are frequent. As a result, the amount of time available for familiarisation of any new KPI's used for vessel operation is limited. The user interface should therefore be intuitive to use by non-computer experts and show as little new information as possible to make familiarisation simple. The KPIs for performance indication are new to the user and are obtained mathematically. To increase trustworthiness of the system and generated KPIs, the following features should be included in the user interface:

- All steps in the conditioning process should be traceable to the source and shown real-time so that a trained user is able to trace uncertainties and develop and understanding of the system
- The ship and engine performance during a manoeuvre or speed increase is complex and difficult to understand. For an officer to get a feeling of understanding, direct performance indication is required. Any pre-processing such as averaging, filtering etc. intervenes in the process of learning and causes the user to lose control over what is exactly happening. Data should be displayed over a time period of e.g. 1 hour so that before and after conditions can be compared
- If instantaneous information is displayed that is a repeat from any existing display, e.g. speed over ground or wind speed, the difference should be made clear (e.g. the data is averaged/not averaged, calculated/measured etc.) to avoid confusion
- The KPIs for performance indication are new to the user. In order to increase the trustworthiness and interpretation of KPIs, the uncertainty ranges should be included. Furthermore, the derivation of the KPI should be traceable real-time by interested parties or experts
- A full describing, easy to understand help file should be available to allow the officer to gain basic understanding into ship performance analysis and the complications involved
- Reliability is of paramount importance for trustworthiness. Ill-defined KPIs caused by errors in input parameters should therefore be identified directly and

shown in the form of a warning on the user interface. It is better to display no information rather than information that cannot be validated

- To increase usability of the system, the officer should be able to print out a time history of the instantaneous performance. This can for example be used to compare different passages of a voyage or the effect of certain operational decision (change of trim, change of speed in shallow water areas etc.).
- Analysed ship performance data, in the form of KPIs for hull, propeller and engine condition, should be available to the operator at any time. Output in the form of an HTML document that can be downloaded from the PM&A computer at any time provides transparency to the captain about the information that is send ashore, and can be send electronically to shore.
- The main user interface shows only that information that is direct usable, in the form of easy to understand performance indicators. If the interface shows too many variables, the officer must interact too much with the system and will consequently not use it.

APPENDIX B: PM&A SYSTEM RV BERNICIA

B.1: Description data logs Bernicia

The PM&A system of the *Bernicia* is developed such that four data files are written simultaneously:

- ‘*Raw data XXX.xls*’; unconditioned data in raw format (units in volts or Hz), written every second
- ‘*Data in units XXX.xls*’; unconditioned data, but converted in direct readable units (knots, Newton, RPM, meter, degree etc.), written every second
- ‘*Conditioned data XXX.xls*’; Data filtered for transient periods together with the conditioned data and the KPI $\Delta P_{D,corr}$. To reduce file size, data is written every 10 seconds
- ‘*Global variables XXX.xls*’; A data file listing the averaging constants that have been used in the conditioning algorithm

The logged performance data is written in text format, tab separated. In Table B-1 a description is given for each column in the files ‘Raw data XXX.xls, where XXX represents the time and date of measurement.

Table B-1: Description of performance logs ‘Raw data XXX.xls’

Heading	Description	Unit
Position	Position of ship in lat/long WGS84 notation	deg.decmin
GPS-head	course over ground from DGPS	degree
Vs	ship speed through water from Walker EM log	kn
GPS-long	Ship speed over ground from DGPS	kn
GPS-trans	Transverse Ship speed over ground from DGPS	kn
time	UCS time from GPS satellite	hhmmss
date	UCS date from GPS satellite	ddmmyyyy
ROT	Rate of turn from DGPS	deg/min
heave	Heave from DGPS	m
pitch	pitch from DGPS	degree
roll	Roll from DGPS	degree

c-dir	relative wind direction from anemometer	degree
c	relative wind speed from anemometer	kn
depth	water depth under keel from echo sounder	m
Draft AFT P	aft portside pressure from draft pressure gauge	Volt
Draft AFT SB	aft starboard pressure from draft pressure gauge	Volt
Draft FWD P	Bow portside pressure from draft pressure gauge	Volt
Draft FWD SB	Bow starboard pressure from draft pressure gauge	Volt
Torque	torque from torque sensor	Nm
Fuel flow	fuel flow from flow sensor, converted from Hz to V	Volt
rudder	rudder angle from rudder sensor	Volt
rpm	alternator shaft speed from pickup sensor	Hz

In March 2007, an adjustment was made in the sensor transmission from the torque sensor. Where previous a DA converter converted the torque in volts, in March 2007 a serial interface was made to send the torque from the shaft directly in Nm to the data acquisitioning interface. In the files created after March 2007, the torque is listed in Nm.

A description of the data in the files ‘Data in units XXX.xls’, where XXX represents the time and date of the trial, is included in Table B-2.

Table B-2: Description of performance logs ‘Data in Units XXX.xls’

Heading	Description	Unit
Position	Position Coordinates	Lat, long
Comp.time	Time on datalogging computer	UK time
GPS-head	Ship’s heading from DGPS	degrees
c-dir	relative wind direction from anemometer	degrees
c	relative wind speed from anemometer	knots
Vs	ship speed through water from Walker EM log	knots
GPS-long	Ship speed over ground from DGPS	knots
GPS-trans	Transverse Ship speed over ground from DGPS	knots
time	UCS time from GPS satellite	hhmmss
date	UCS date from GPS satellite	ddmmyyyy
ROT	rate of turn from DGPS	deg/min
depth	Depth under keel from echo sounder	m
heave	Heave from DGPS	m
pitch	Pitch from DGPS	deg
roll	roll from DGPS	deg

Taft P	Draft aft port side, from pressure sensor	m
Taft SB	Draft aft star board side, from pressure sensor	m
Tfwd P	Draft forward port side, from pressure sensor	m
Tfwd SB	Draft forward starboard side, from pressure sensor	m
Tmean	Mean draft, calculated from pressure sensors	m
Trim	Mean trim, calculated from pressure sensors	m
List	List, calculated from pressure sensors	degrees
torque	Torque, from strain gauges on propeller shaft	Nm
fuel flow	Fuel flow from flow meter	liter/min
Rudder	Rudder angle, from rudder indicator	degrees
rpm	propeller speed, from engine pick-up	rpm
waveh	wave heading (if entered)	degrees
H13	significant wave height (if entered)	m
period	wave period (if entered)	sec
spectr	spectrum selection (0 = 1 parameter ITTC, 1 = 2-parameter ITTC)	
spread	sea spreading (0=cos ² , 1 = cos ⁴ , 2 = long crested) (if entered)	
swellh	Swell heading (if entered)	degrees
Sw-H13	Swell significant height (if entered)	m
Sw-T	Swell period (if entered)	sec
Sw-spec	Swell spectrum (Not in use)	
Sw-spr	Swell spreading (0=cos ² , 1 = cos ⁴ , 2 = long crested, 3 = cos ¹⁰⁰ , 4 = cos ¹⁵⁰) (if entered)	
w-comp	Absolute wave direction (compass direction) (if entered)	
Sw-comp	absolute swell direction (compass direction) (if entered)	

An example of the unconditioned speed through water is shown in Figure B-1. The bottom figure shows the data filtered for outliers, transient conditions and averaged.

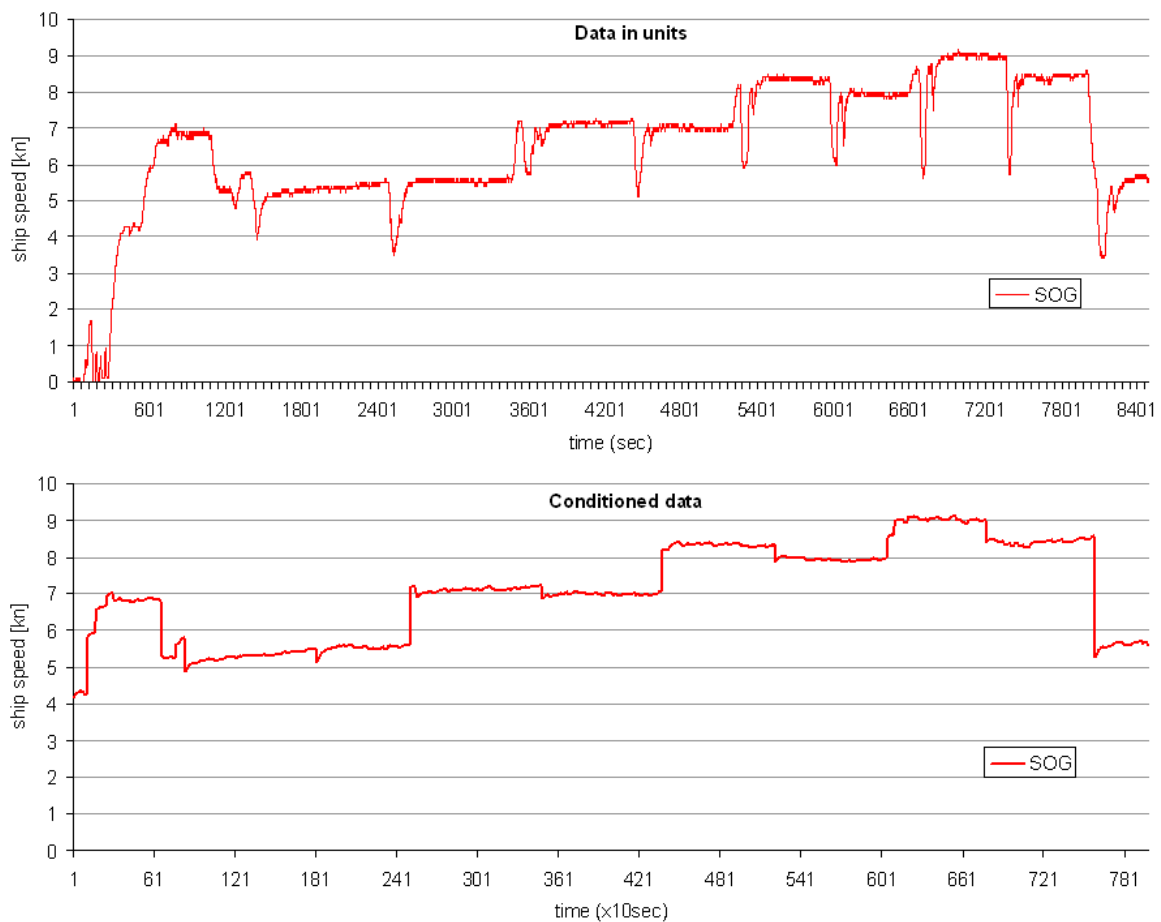


Figure B-1: Example of unconditioned and conditioned shaft torque

B.2: Software description

The PM&A system of the *Bernicia* is written using LabVIEW 7.1 from National Instruments (NI 2004). LabVIEW is a graphical programming language originally designed for data acquisition and visualising data in an intuitive manner. The source code cannot easily be printed and is therefore available on DVD with this thesis. A screen shot of part of the source code of the main interface panel (Figure B-2) is shown in Figure B-3. From this panel, 117 sub-programs, called ‘subvi’s, are controlled. The subprograms are filed in sub-folders Data collection, Data to units, Data writing, Data conditioning, Added resistance, Calculate standard performance, User interface and Warnings. Data files are automatically generated and stored each time the program is stopped by the user.

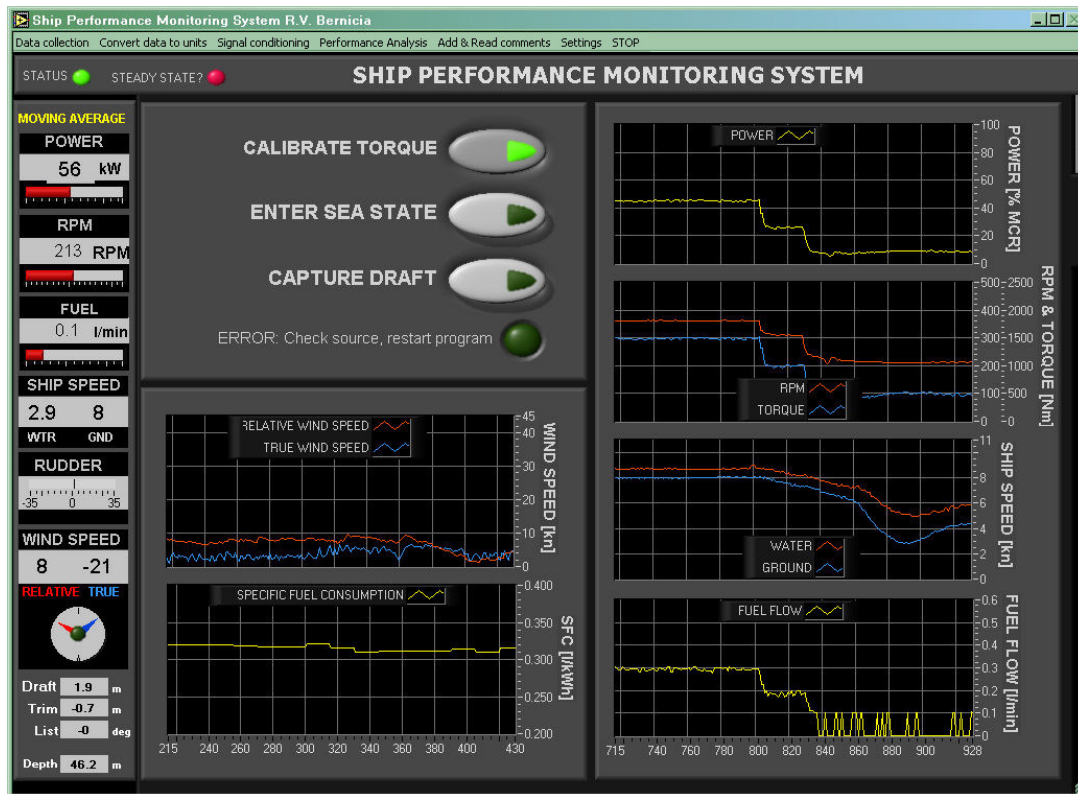


Figure B-2: Main interface panel of PM&A system Bernicia

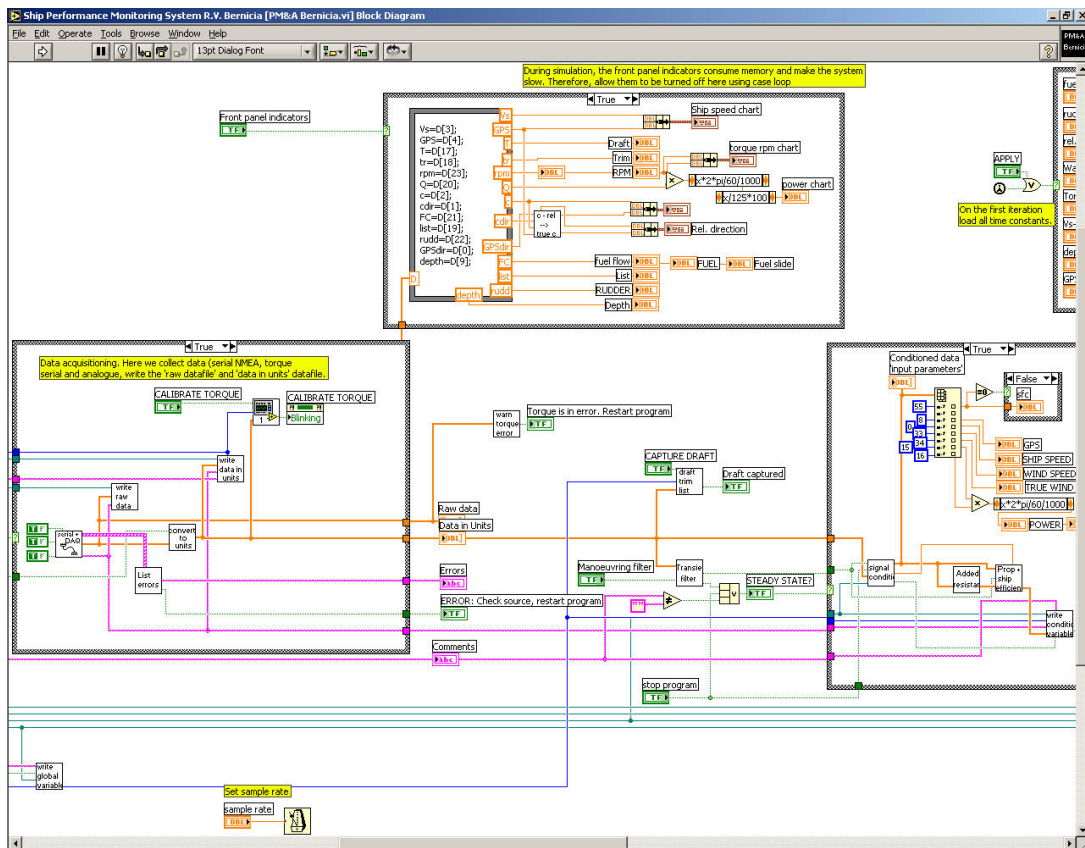


Figure B-3: Example of source code PM&A system Bernicia

The PM&A system for the *Bernicia* can easily be altered for other types but similar size of vessels. Most vessel and propeller characteristics, and added wave resistance parameters are entered using separate text files.

The moment the software is turned on, the user is asked to enter the voyage name, calibrate the torque sensor and capture the draft (all automatically done). A menu structure on the top of the screen allows the user to select and open information screens indicating how data is captured, converted, conditioned and used in the calculation of standard conditions. The following figures show the interface panels of the PM&A system, excluding the interface for long-term KPIs. Figure B-4 shows the interface for the data acquisition. All data is real-time visualised and information is given from which sensor the data is received. Figure B-5 and the top right picture in Figure B-6 show the interfaces for the conversion of raw data to units. All steps in the conversion are shown, including calibration constants (where applicable) and pictures of the sensors to clarify which sensor output is dealt with.

The transients filter and input fields of wave parameters and propeller roughness is included in Figure B-6. The way parameters are conditioned (filtered and averaged) is shown for each parameter in Figure B-7 and Figure B-8. Finally, Figure B-9 shows the interfaces of the calculation of wind, wave and shallow water resistance and the conversion from in-service performance to standard conditions.

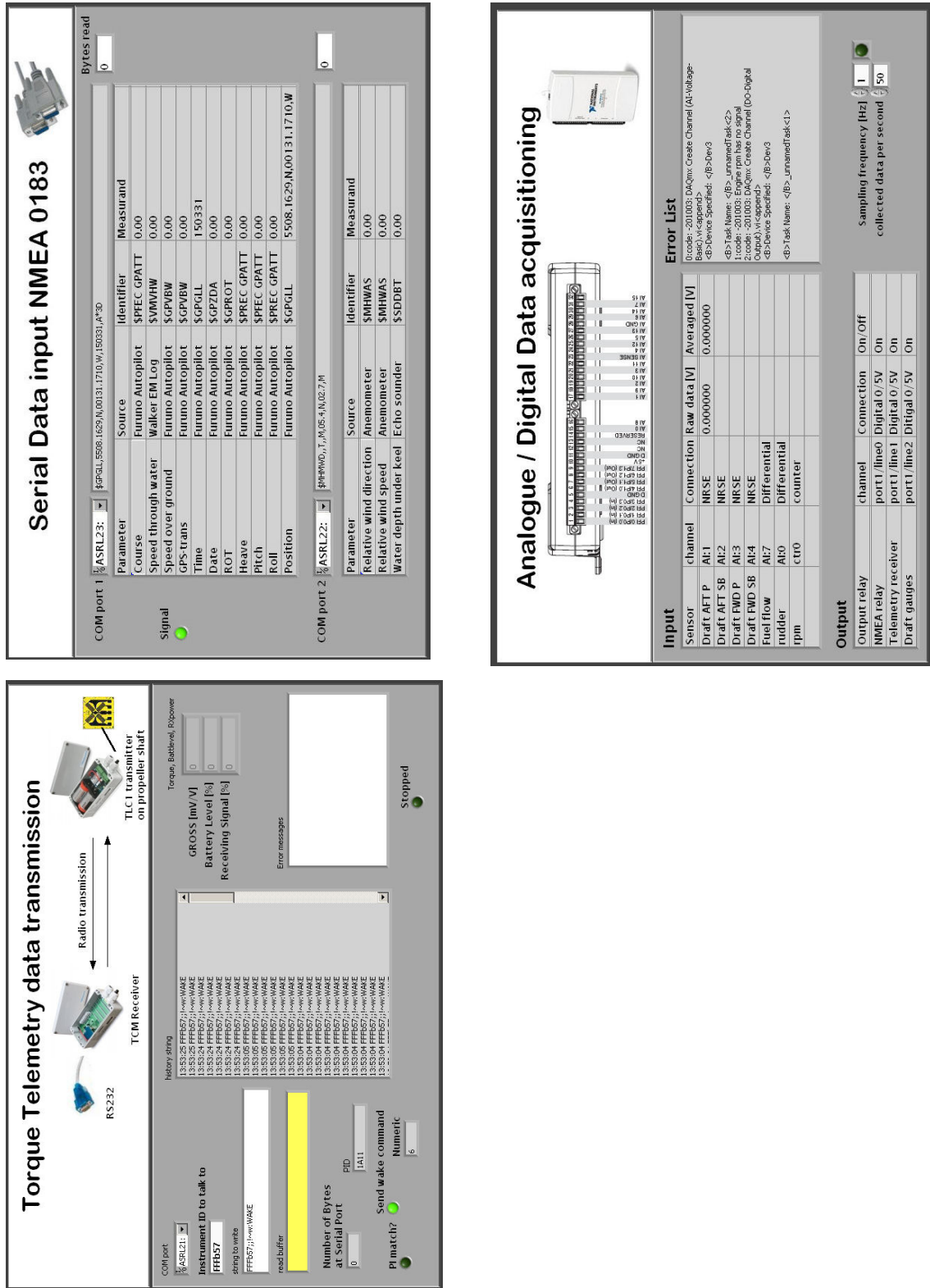


Figure B-4: Interface panels for data collection on PM&A system Bernicia

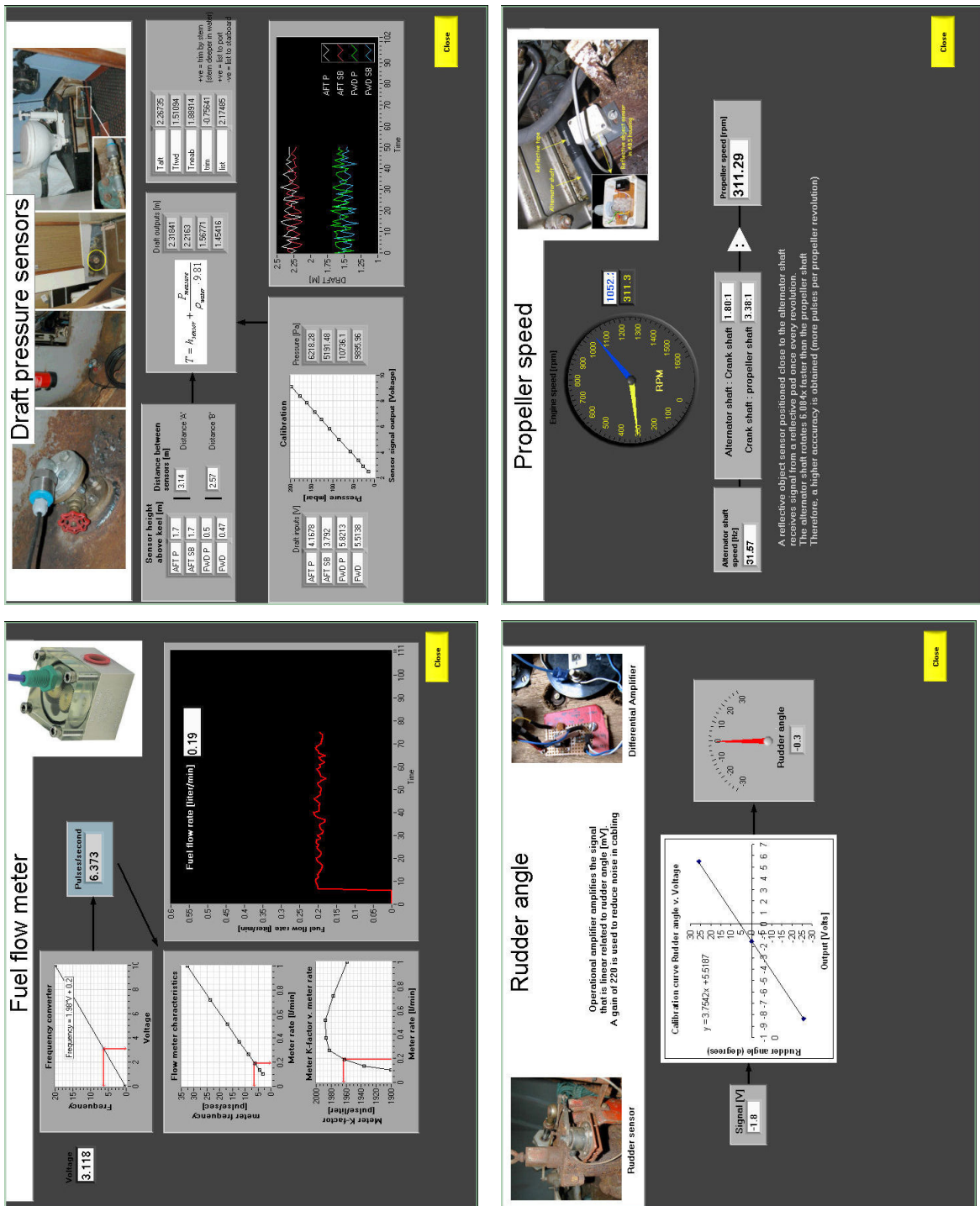


Figure B-5: Interface panels ‘conversion to units’ on PM&A system Bernicia for fuel flow, draft, rudder and engine speed

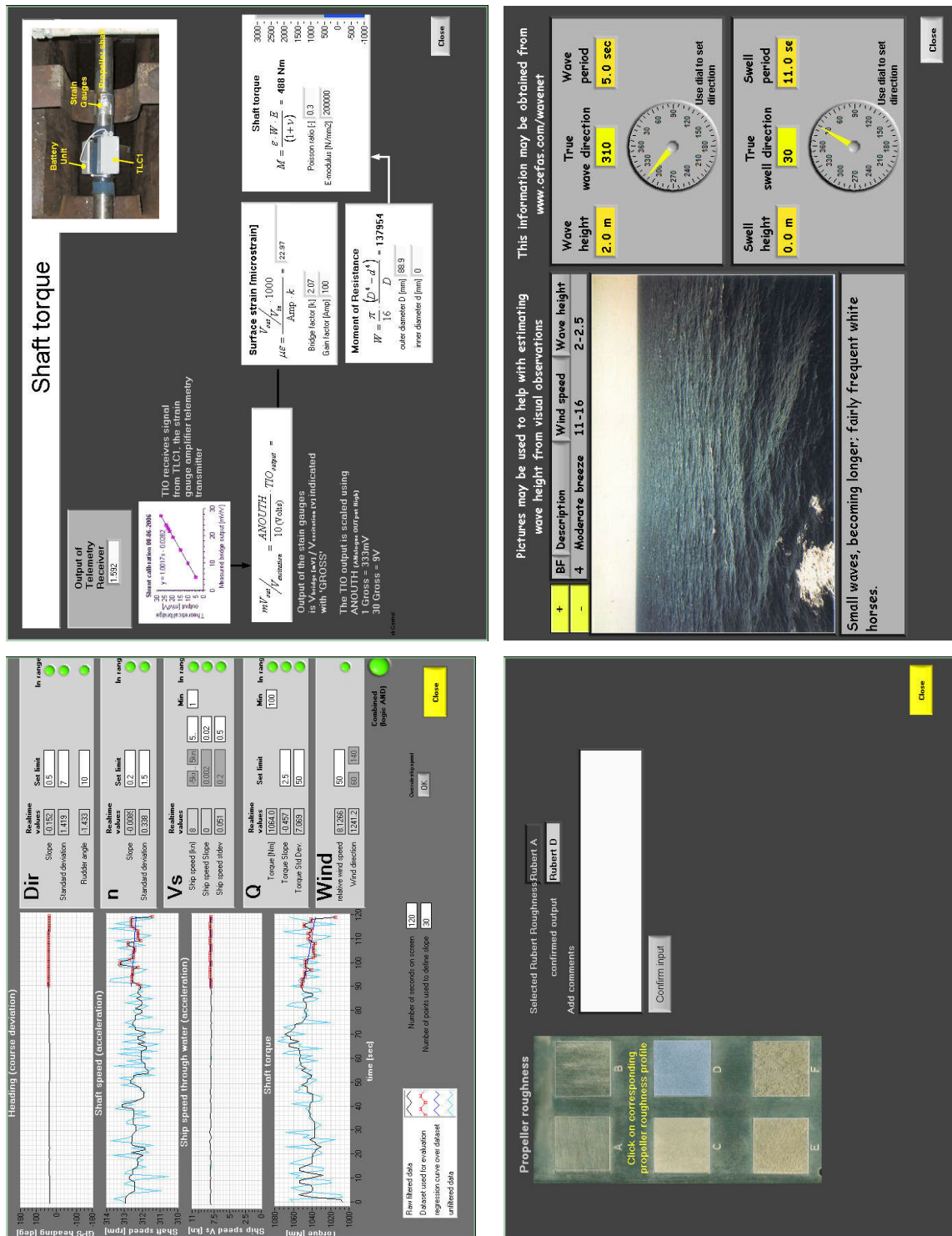


Figure B-6: Interface panels on PM&A system Bernicia for the Transients filter, torque conditioning to units, propeller roughness and wave conditions

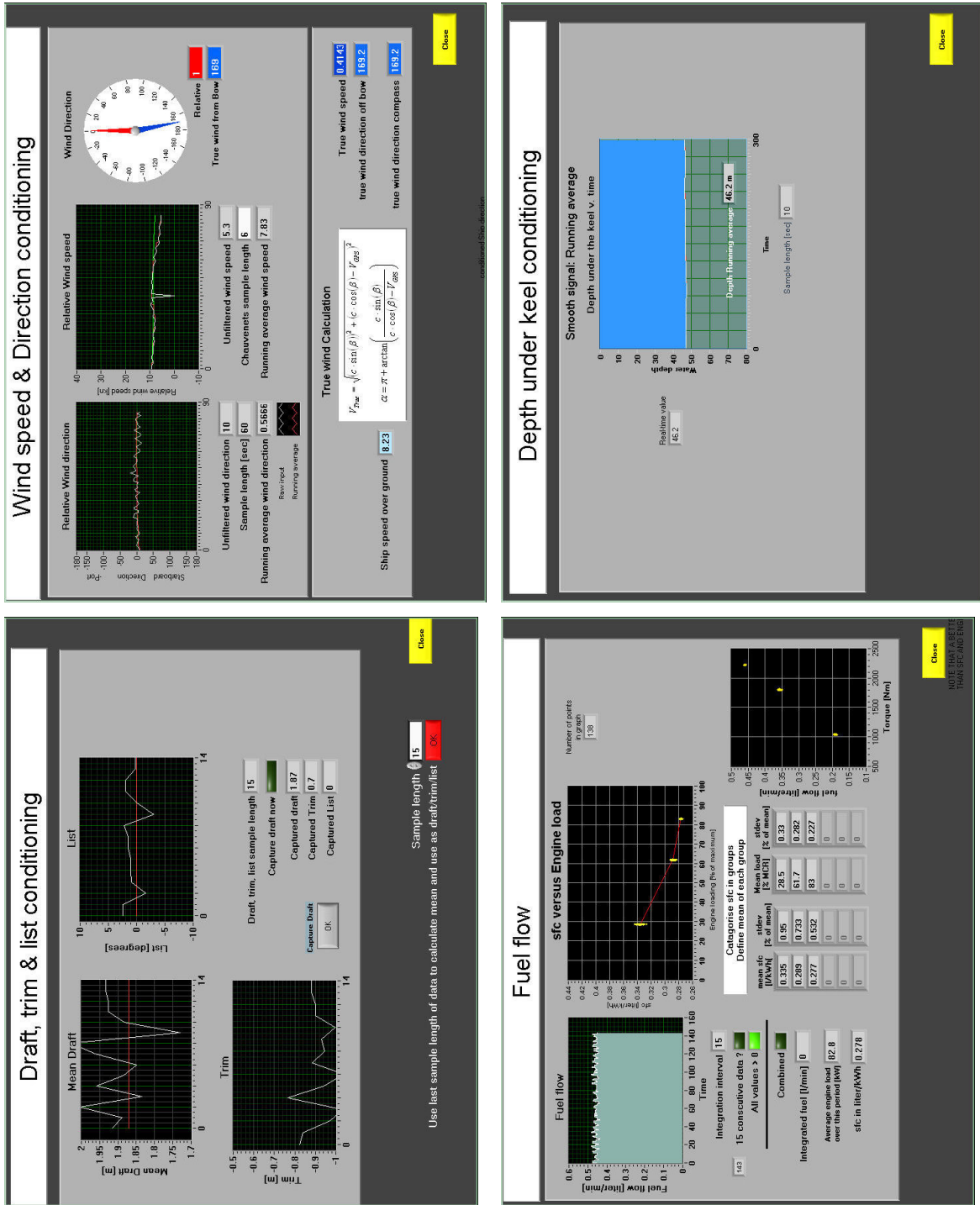


Figure B-7: Interface panels of data conditioning on PM&A system Bernicia for the draft, wind speed, fuel flow and water depth

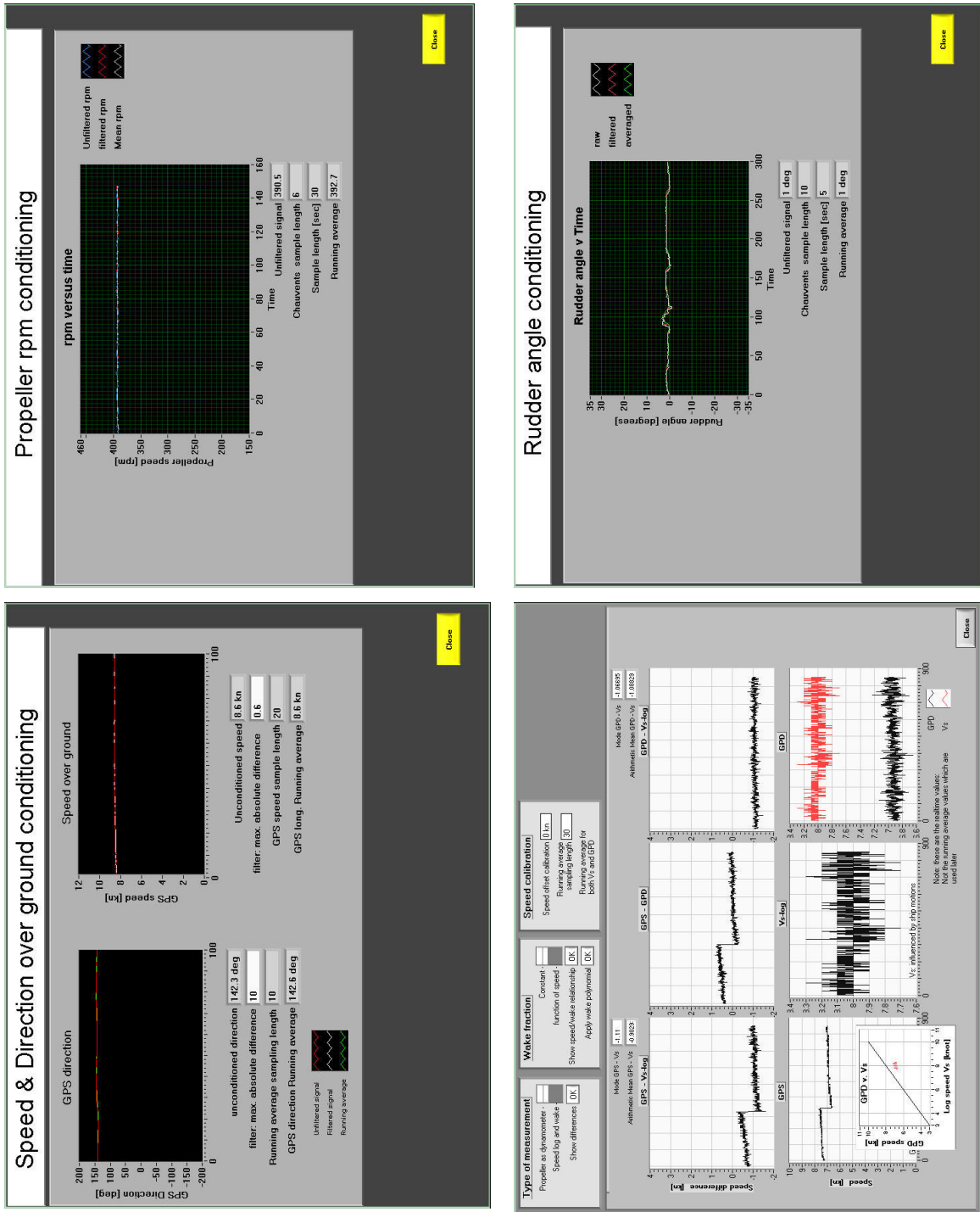


Figure B-8: Interface panels for data conditioning on PM&A Bernicia for speed over ground, course, propeller rpm, ship speed through water and rudder angle

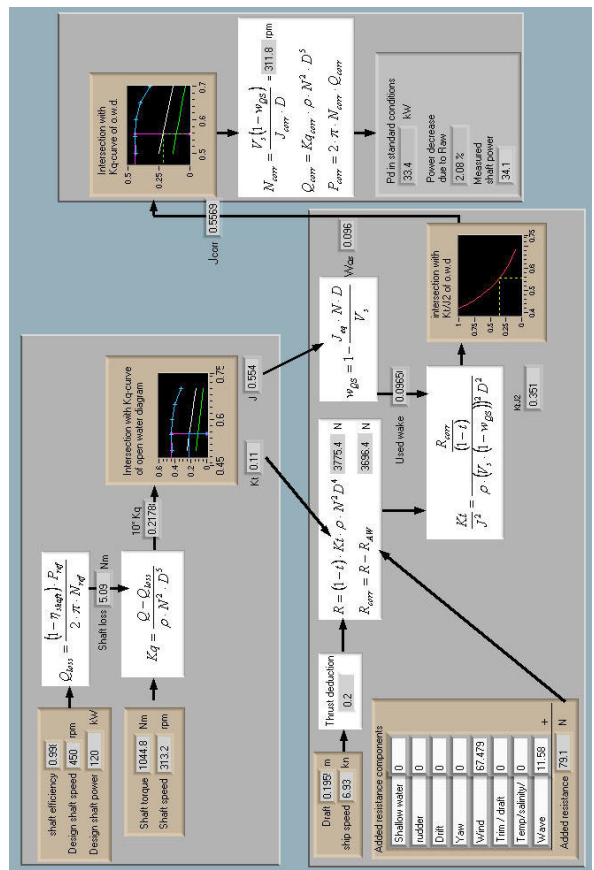
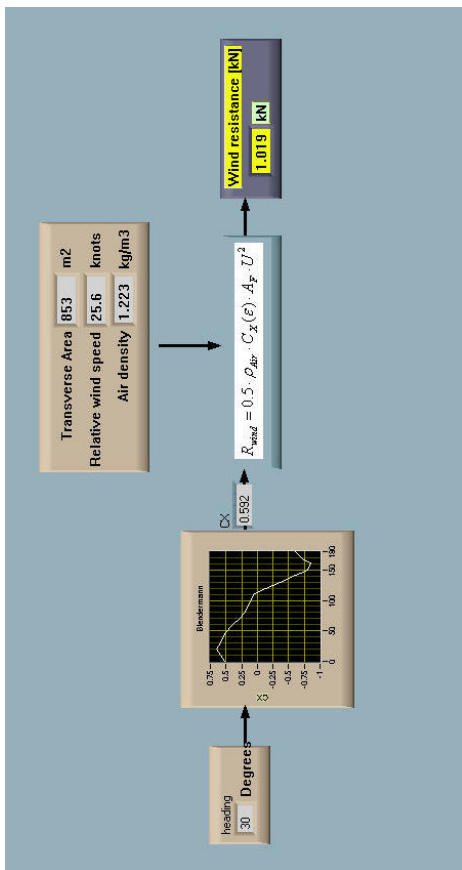
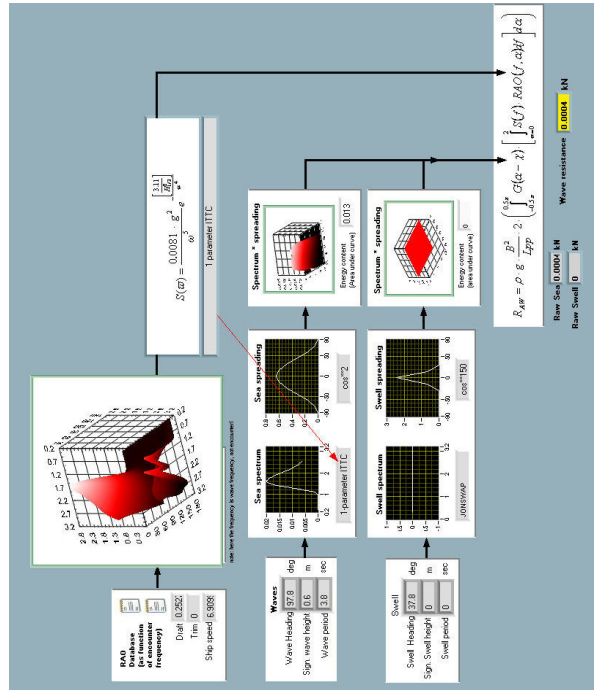
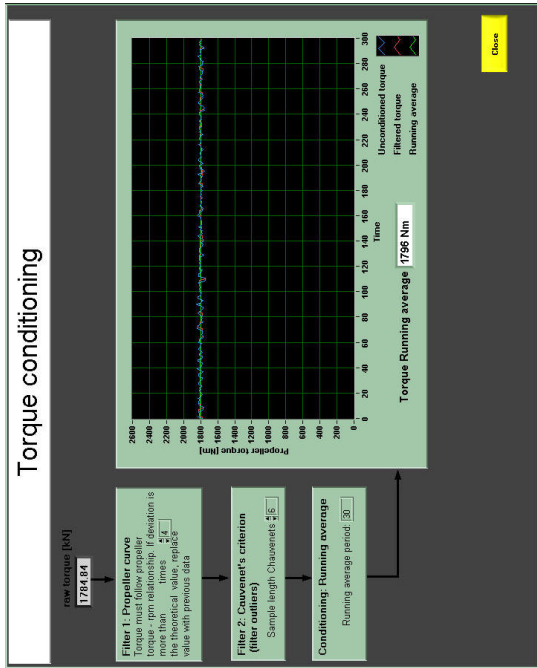


Figure B-9: Interface panels for calculation of standard performance

APPENDIX C: PM&A SYSTEM MT OVERSEAS TANABE

C.1: PM&A system on bridge



Figure C-1: Data acquisition system installed on the bridge of the Overseas Tanabe



Figure C-2: Performance monitoring system on the bridge of the Overseas Tanabe

C.2: Description performance logs

The PM&A system of the *Overseas Tanabe* is similar to the PM&A system of the *Bernicia*. Data is written every second in a text file (tab separated). A new file is automatically created every 24h to keep file size limited to approx. 24MB. No data is written when the engine speed is below 10rpm. 10 DVDs are available with data collected over the period March 2007 – July 2009.

Table C-1: Description performance logs ‘Raw data XXX.xls’

Header	Description	Unit
Filter	Manoeuvring filter that determines whether the conditioned data is written to file or not.	0=False, 1=True
Position	Position of the ship from GPS navigator (Long, Lat in degrees, minutes and decimals)	
Comp. date	Computer time (GMT) in 24h	ddmmyyyy
Comp. time	Computer date (GMT)	hhmmss
Date	Ship’s date, from GPS and corrected to local ship time. A nine in the beginning should be read as a 0	ddmmyyyy
Time	Ship’s time in 24h. GMT time comes from GPS navigator, time difference is manually entered by officer on duty. A nine in the beginning should be read as a 0	hhmmss
GPS-course	GPS course from GPS navigator. 180.01 to 359.99 degrees is converted to -179.99 to -0.01 degrees	degrees
GPS-spд	Speed over ground from GPS navigator. Accuracy depends on GPS quality.	knots
Bot-long	Bottom speed from Doppler log (= speed over ground). Only if water depth < 600m, otherwise it gives ‘99’	knots
Bot-trans	Transverse bottom speed from Doppler log (= sideways speed over ground). Only when depth <600m, otherwise it is ‘99’	knots
wind-dir	Relative wind direction from anemometer signal converter	degrees
wind-spд	Relative wind speed from anemometer signal converter. No calibration needed	knots
Wat-long	Longitudinal speed through the water from Doppler log	knots
Wat-trans	Transverse speed through the water from Doppler log. -ve is port, +ve is starboard	knots
GPS qual	GPS quality from GPS navigator. 0 = no GPS fix, 1 = fix with GPS mode, 2 = fix with DGPS mode	-

HDOP	Horizontal Dilution Of Precision. Positioning accuracy of horizontal plane for signals received from GPS satellites. 1=Good, >1=bad	-
Torque	Propeller shaft Torque measured by the Metapower torque sensor, based on shaft twist	kNm
rpm	propeller speed of rotation, measured by the Metapower system	rpm
Twist [D]	Shaft twist measured by the Metapower Torque sensor. Unit unknown	?
Twist [o]	Shaft twist between a distance of 1854mm of shaft length, measured by the Metapower torque sensor	1/1000 degree
fuel flow	Fuel flow measured by the fuel flow sensor of the main engine alone	liters/hour
LCV	Net Calorific Value of the fuel currently used, Manually entered by chief engineer. Default is 40.46	MJ/kg
density	Fuel density of fuel currently in use at 15degC, Manually entered by chief engineer. Default is 0.9684	grams/liter
Tfore	Foreward draft, Manually entered by Officer on Duty	meter
Taft	Aft draft, Manually entered by Officer on Duty	meter
TmiddP	Midship draft Port side, manually entered by Officer on duty	meter
TmiddS	Midship draft Starboard side, manually entered by Officer on duty	meter
New draft	Indicator showing when the officer pressed the button 'Draft/Fuel', in other words, when he was asked to fill in the new draft/fuel.	0=False, 1=True
Seastate	Seastate indicator. 0 = Beaufort 0, 1=BF1 etc.	BF
H13	Significant wave height, entered manually. By default the seastate indicator fills in this field, but the user is asked to change it	meter
waveh	Wave direction. Direction from where the waves come from. 0-360 degrees	degrees
Sw-H13	Swell wave height. 1 = 0..2m, 3 = 2..4m, 6 = over 4 (listbox selection)	meter
Sw-length	Swell length. 25 = 0..50, 77 = 50..100, 75 = 100..200, 150 = 200..300, 99 = confused swell (listbox selection)	meter
roll angle	Roll amplitude of the ship. Default is 0	degrees
pitch angle	Pitch amplitude of the ship. Default is 0	degrees
vision	Vision outside at the moment of entering wave parameters. 0 = Good, 1 = difficult, 2 = Bad(night) (listbox selection)	-
New sea	Indicator showing when the officer pressed the button 'Wave', in other words, when he was asked to fill in the Wave parameters.	0=False, 1=True
Comments	Any comments that the user has entered in the program	-

C.3: Software description

The PM&A system of the Overseas Tanabe is written using LabVIEW 7.1 from National Instruments. The PM&A system as installed onboard is only used for logging and data conditioning. It can be expanded with a data analysis module in the same architecture of the program. However, due to time restrictions, this could not be completed within the time frame of the project. The source code is however available on DVD with this thesis. Figure C-3 shows a screen dump of the main interface panel. From this panel, all other interface screens can be called using the menu structure on the top of the page.

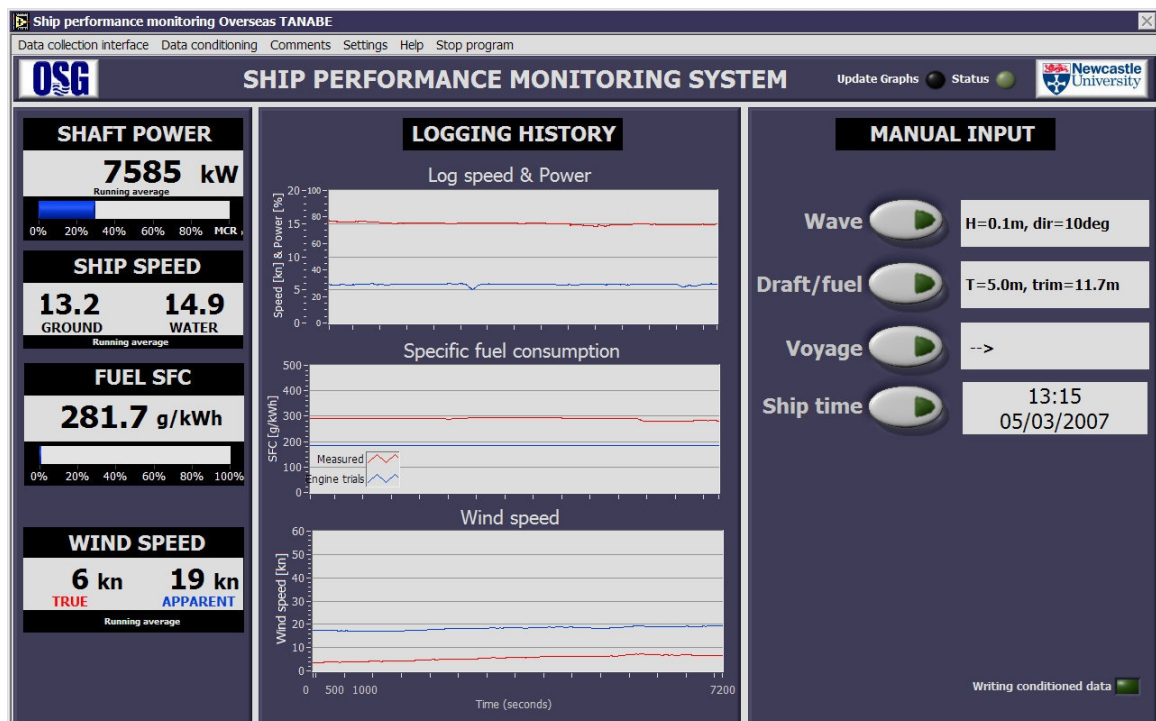


Figure C-3: Main interface panel of PM&A system Overseas Tanabe

A user manual of the software can be found in (Hasselaar 2007). The following screen dumps give an impression of the user interfaces of the system. Figure C-4 shows the interface screens describing how signals are collected in the data acquisition system for the fuel flow (digital pulse), GPS, wind and doppler log (via NMEA) and torque and rpm (binary). Figure C-5 and Figure C-6 indicate the interface screens of the data conditioning (filtering, averaging and/or conversion). Finally, Figure C-7 and Figure C-8 show the interfaces used to collect manual data such as sea characteristics, draft, fuel characteristics, voyage name, comments related to ship performance and ship's time.

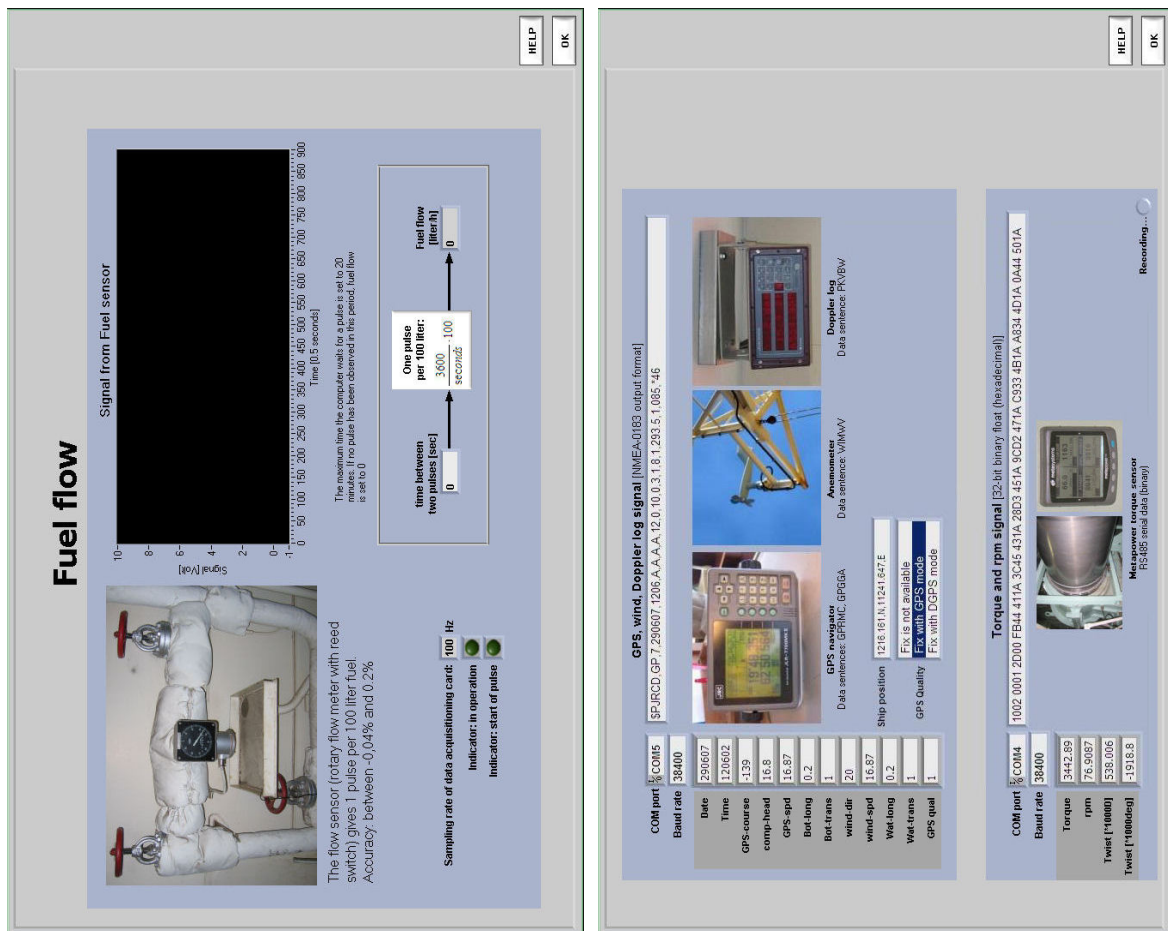


Figure C-4: Interface panels for data collection on PM&A system Overseas Tanabe

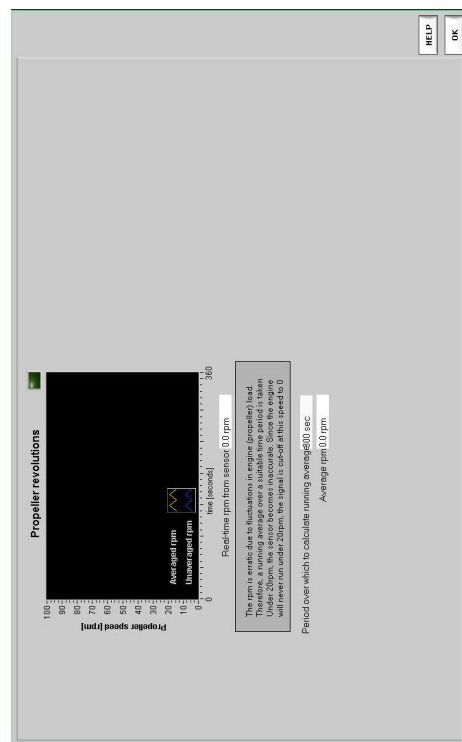
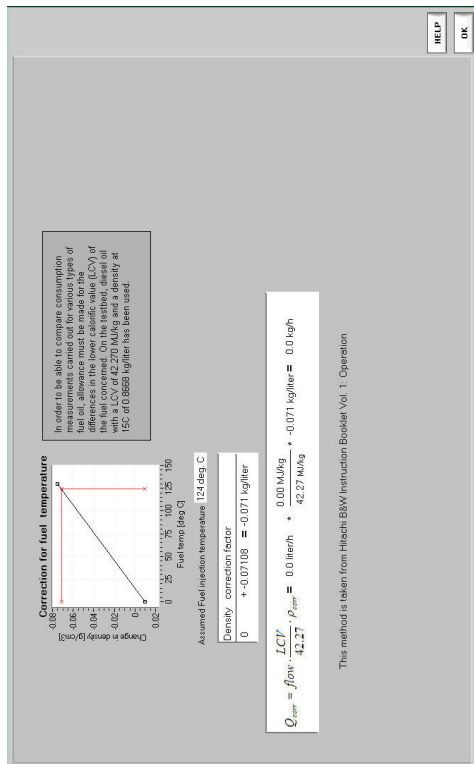
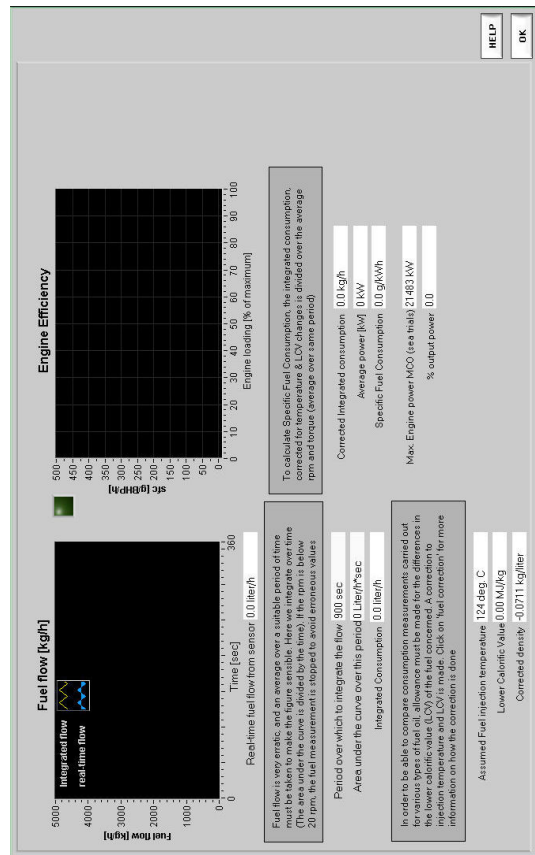
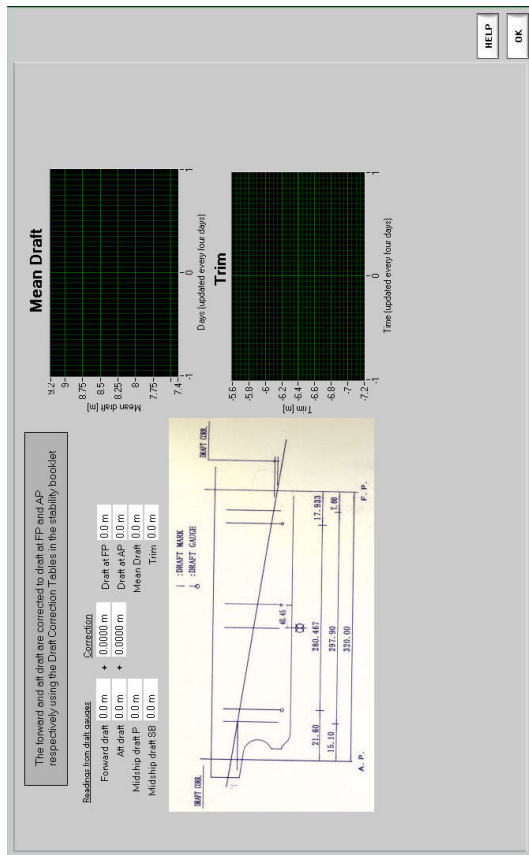


Figure C-5: Interface panels for ‘data conditioning’ on PM&A system Overseas Tanabe for fuel LCV, draft, propeller revolutions and fuel flow

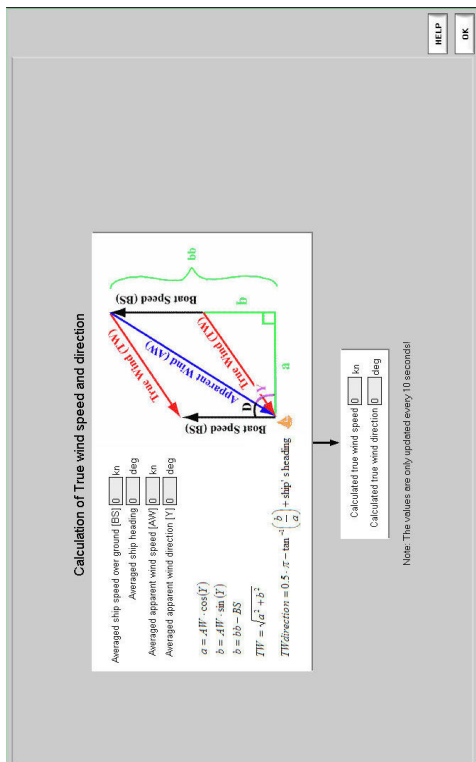
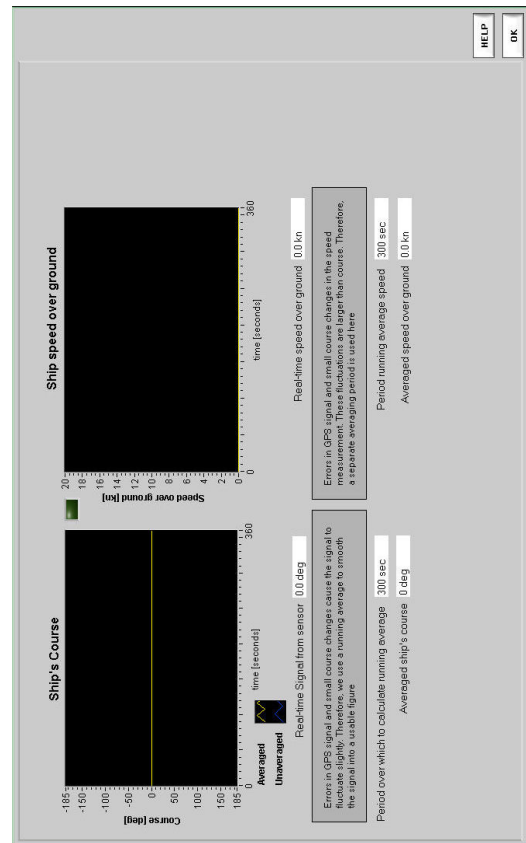
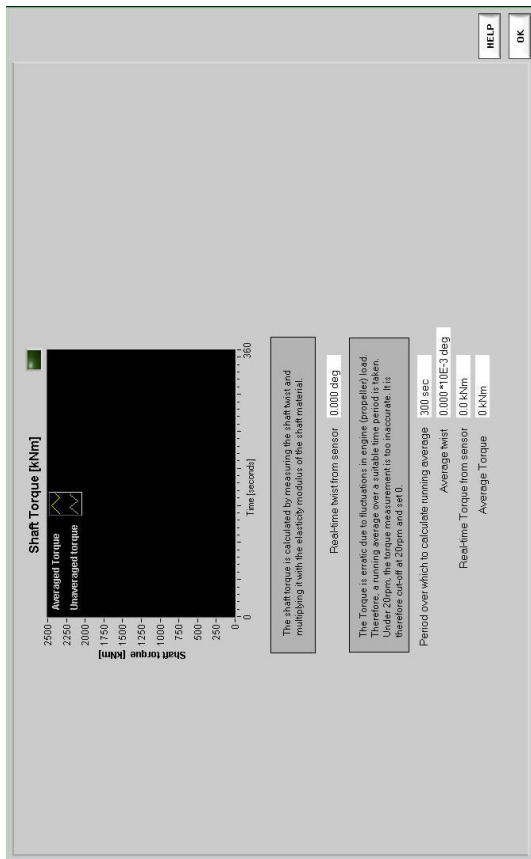


Figure C-6: Interface panels for ‘data conditioning’ on PM&A system Overseas Tanabe for wind speed, shaft torque, course and speed over ground

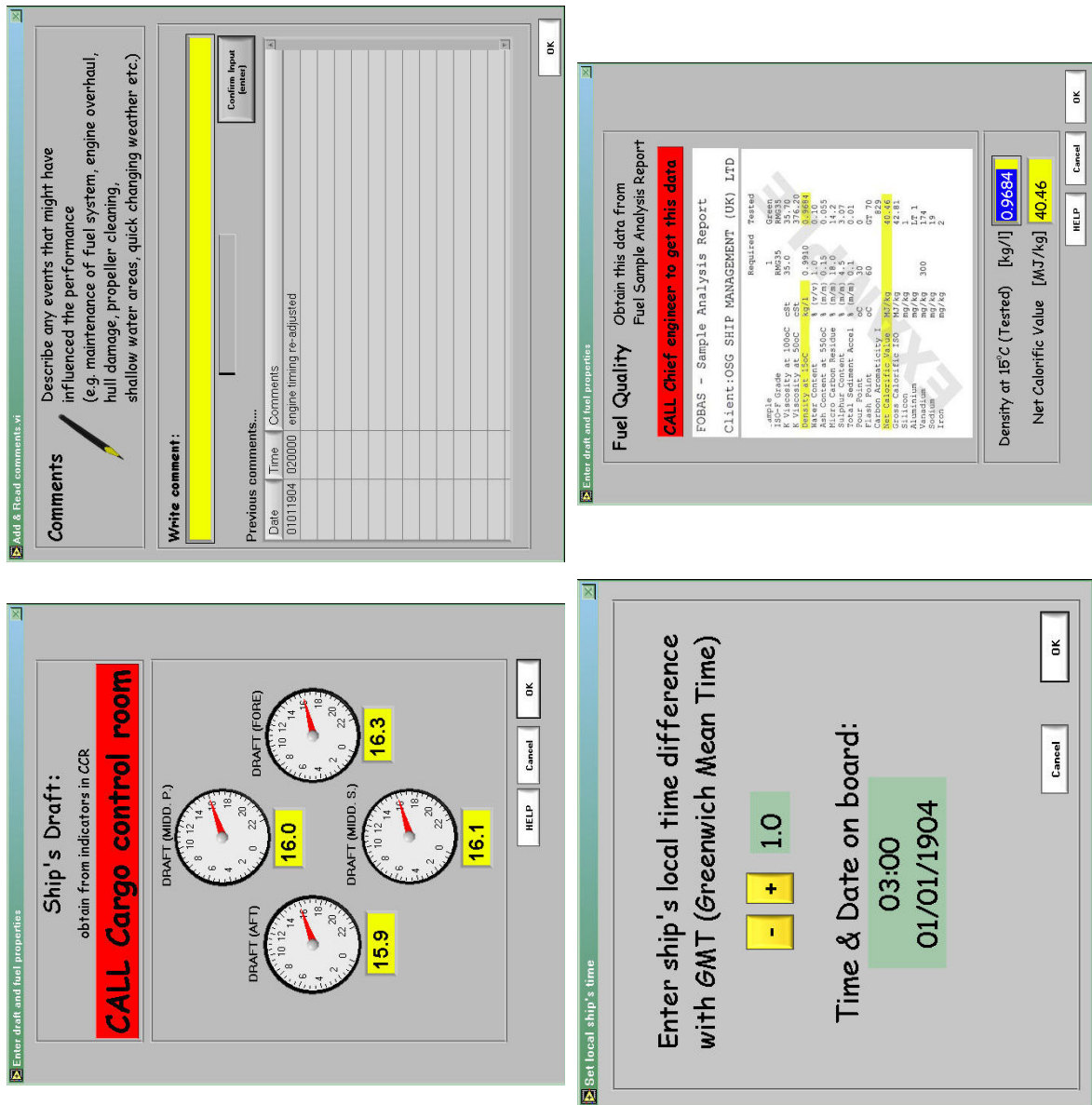


Figure C-7: Interface panels for manual data entry on PM&A system Overseas Tanabe for the ship's draft, comments, ship time and fuel quality

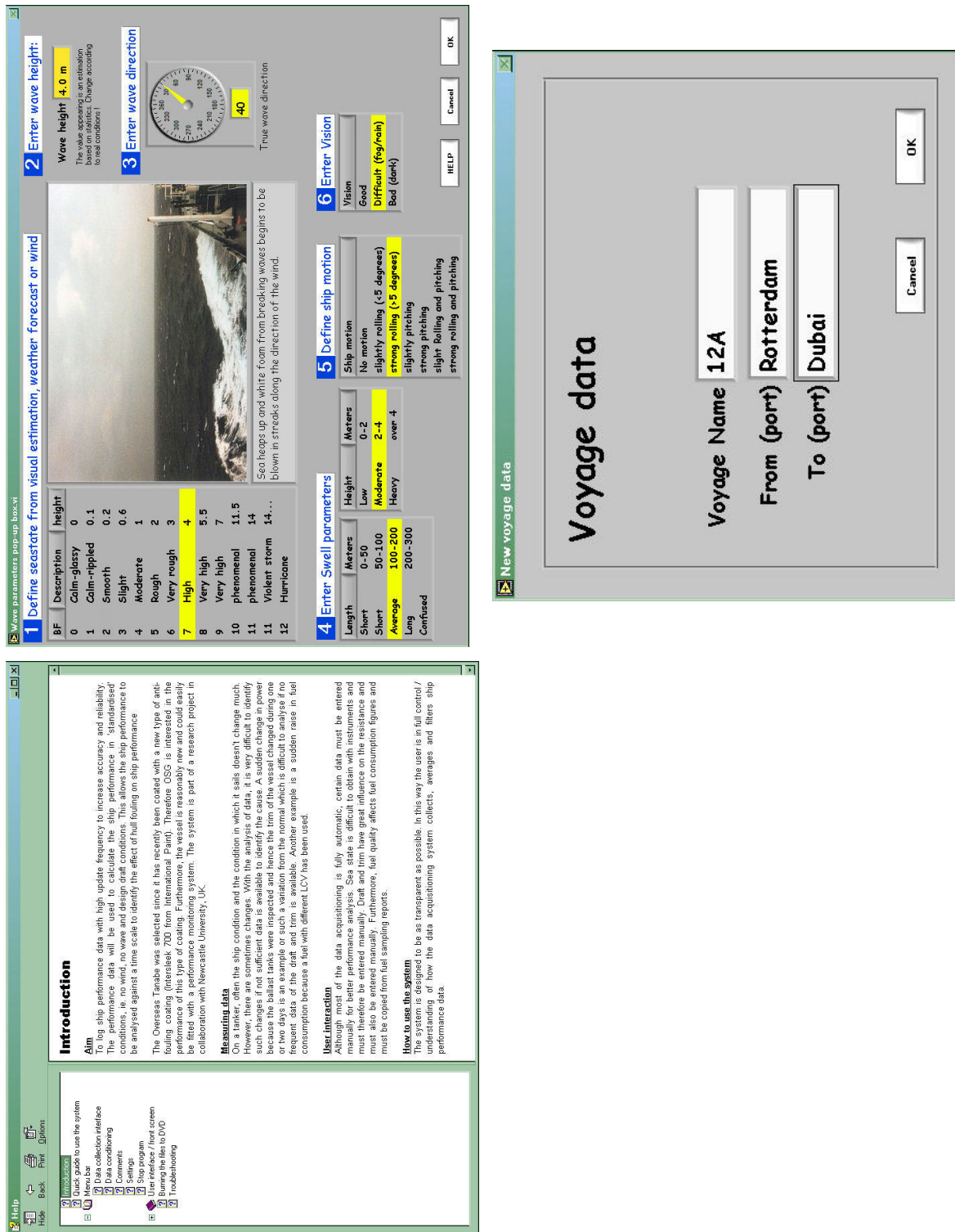


Figure C-8: Interface panels for manual data entry on PM&A system Overseas Tanabe for the sea state and voyage data and help function

